Author:
Leach, Edward Stephen Hardy

Title:
Stability and gelation of non-aqueous clay suspensions

Stability and Gelation of Non-Aqueous Clay Suspensions

Edward Stephen Hardy Leach

University of BRISTOL

A thesis submitted to the University of Bristol in accordance with the requirements for the degree of Doctor of Philosophy, Faculty of Science

School of Chemistry, February 2004

47 075 words

Abstract

The formation of gels in non-aqueous solvents can be achieved at a relatively low concentration by the addition of clay platelets treated with a long chain cationic surfactant. For these systems under good solvent conditions gelation is inevitable. Novel routes to effective dispersion and stabilisation have been explored using sedimentation, rheological and scattering studies.

Previous work has shown an alternative route to stabilise clay platelets in non-aqueous solvents is possible by adsorption of a low molecular weight poly isobutylene polymer to the surface. These dispersions were truly stable and could be taken to a relatively high concentration without the onset of gelation.

By combining the surfactant treatment, poly isobutylene polymer treatment and a careful choice of organic solvent stable dispersions of clay have been made in toluene. The samples displayed vivid flow birefringence and by exchanging the solvent displayed an original thermoreversible gelling transition. The driving force for the transition was determined from rheology, differential scanning calorimetry, and small angle X-ray scattering as the crystallisation of the alkyl chains of the cationic surfactant as the temperature dropped.

Acknowledgements

My deepest gratitude goes to my academic supervisor, Dr. Jeroen van Duijneveldt for his tireless assistance throughout the course of this project. I thank Dr. Andrew Hopkinson and Dr. Kevin Franklin at Unilever for some very insightful suggestions and helpful discussions regarding the behavioural subtleties of the particles and intricacies of the dispersions. I must thank Unilever and EPSRC for the funding of the project.

For the massive amount of support and encouragement in helping me complete this study I have to thank Dr. Susanne Klein at Hewlett Packard who focussed my attention with supreme skill and determination.

I thank Professor Richardson for the help with the SAXS experiment and Claire Pizzey for help with the SAXS data analysis, Cheryl Flynn and Roy Hughes for the assistance with the rheology, Les Corbin for help with the BET measurements, Rachel Owen for carrying out the AFM work, Sean Davis and Steve Bodiley for help with the electron microscopy and Annela and Gait for showing me the TGA.

Thank you everybody for the very interesting time I had in the Colloid section of the University of Bristol with special mention to Robin Mogford, Paul Seymour, David Voisin, Yves Hennequin, Pierre Starck, Alex Routh, Pete Dowding, Elaine Wightman, Patricia Marr and Darby Kozak.

Lastly and by no means leastly, a very special thank you to Manon Phillips for keeping me under control and bringing a very large smile to my face.

AUTHORS DECLARATION

I declare that the work in this thesis was carried out in accordance with the regulations of the University of Bristol. The work is original except where indicated by special reference in the text and no part of the thesis has been submitted for any other degree.

Any views expressed in the thesis are those of the author and in no way represent those of the University of Bristol. The thesis has not been presented in any other University for examination either in the United Kingdom or overseas.

Signed 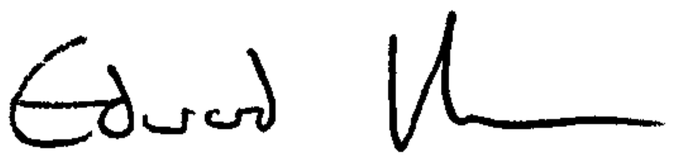

Edward Stephen Hardy LEACH

Date: 05 MAR 2004

Table of Contents

List of Figures

Chapter One Introduction

Chapter Two Materials

Chapter Three Methods

Figure Number Page

Chapter Four Characterisation of the Clay Surface

Figure Number Page

Chapter Five Optical Inspection

Figure Number Page

Chapter Six Electron Microscopy and atomic force microscopy

Chapter Seven Thermoreversible Gelation

Chapter Eight Small Angle X-Ray Scattering

Appendix III

Appendix IV

List of Tables

Chapter 2

Chapter 3

Chapter 4

Chapter 5

Chapter 7

Appendix I

Appendix II

Dedicated to

Richard Michael Leach

1 Introduction

1.1 Summary

The aim of this project was to prepare an original stable dispersion of plate-shaped colloidal particles dispersed in an organic solvent and to achieve a novel thermoreversible gelling transition by controlling the stability of the particles.

Thermoreversible processes are very desirable for many widespread applications. Such a system is gelatin in water. Gelatin is a protein manufactured by the partial hydrolysis of collagen and is used in the food and photographic industries [1]. In the photographic industry layers of light-sensitive chemicals are deposited on photographic film at an elevated temperature and these chemicals set as the temperature drops.

For many applications plate-shaped particle dispersions are desired since they display distinct behavioural characteristics such as shear thinning. Also the gelation of plate-shaped particles can be achieved at lower concentration than with spherical particle dispersions as they posses a high effective particle volume. Plate-shaped particle dispersions in organic solvents have a wide variety of uses from anti-settling agents in anti-perspirant sprays, fillers to make impact resistant plastics and rheological modifiers in nail varnish [2-4]. For cosmetic applications the constancy of the product is very important to the customer and shear thinning of the material is often desirable as it gives a rich texture.

Clay dispersions treated with a cationic surfactant dispersed in organic solvents have been studied for more than half a century, [5-7] are commercially available made by a number of companies [4, 8] and sold as rheological modifiers. There are a lots of different grades of these modifiers given names depending on the type of clay used and surface treatment, Claytone AF, Gelwhite, and Bentone to name but a few. The rheological modifiers are sold as dry powders that are often added near the end of industrial processes being dispersed using both physical and chemical methods but once dispersed the products form a gel that persists at all temperatures and is not thermoreversible.

Three types of clay have been used in this study, a synthetic clay Laponite, a naturally occurring Wyoming bentonite, and a commercially available dimethyl dialkyl ammonium cationic surfactant treated montmorillonite called Claytone AF. The types of clay used were similar in chemical make up but very different in size with the bentonite and Claytone AF particles being much larger than the Laponite particles. All particles were treated in a number of ways in order to stabilise them in organic solvents. The behaviour of the particles and the nature of the dispersions were investigated using simple observations, optical, electron, and atomic force microscopy, small angle X-ray scattering, and rheology.

A stable dispersion of synthetic clay Laponite in toluene was made by treating the particles with a short-chain polymer stable in toluene. By changing the solvent conditions with the addition of polar but miscible ethanol to the dispersion, instability could be induced and it was hoped a temperature effect would be evident. However, the treated Laponite particles were difficult to make in any quantity and experiments such as rheology proved irreproducible as the high volatility of the solvent was problematic.

Therefore we attempted instead to exploit the plentiful supply of Claytone AF and attempt to make stable dispersion of it in an organic solvent by adsorbing polar organic molecules amongst the cationic surfactant molecules to the clay surface. This was carried out to reduce bare clay surface/solvent contact and promote particle stability. A short-chain polymer was adsorbed to the surface of the Claytone AF and rendered the particles colloidally stable in toluene. No thermoreversible gelation was found for this system in toluene even with addition of ethanol to marginalise the solvent. A single solvent was sought that was marginal, non-volatile, non-toxic and capable of showing thermoreversible gelation. A solvent used in the cosmetic industry, polydecene 364NF, made from oligomerised decene molecules was shown to possess all the required characteristics including thermoreversible gelation.

1.2 Colloidal systems

Colloidal systems are made up of one material dispersed in a continuous phase of another material [9]. The behaviour and control of colloidal systems is a concern to a wide range of scientific disciplines including physics, biology, materials science, geology, electrical and mechanical engineering. Industrially, a vast array of processes from oil recovery, heterogeneous catalysis, and the manufacture of cosmetics involve such dispersions. Even the human body consists of colloidal dispersions and particles, such as blood. For a colloidal dispersion, the size of the dispersed material (in at least one of the material's dimensions), must be in the range 1-1000 nm [10, 11]. Perhaps the most important implication of the colloidal size range is that it is small enough to make thermal motion significant compared to sedimentation, it is the response to thermal motion that provides the closest guide to the upper size limit of colloids. Also, the colloidal size range is at least an order of magnitude larger than the surrounding solvent molecules, which can be treated as a continuum [12].

1.3 Forces acting on colloids

Colloidal dispersions, just like atoms and molecules experience interparticle forces of attraction and repulsion from a number of effects depending on the type of particles and their environment. The particles also have thermal energy keeping them in a constant state of random motion.

1.3.1 Thermal Motion

The thermal energy of atoms and molecules is actually the translational kinetic energy of those particles [11].

$$k_E = \frac{1}{2}mv^2 \qquad [1.1]$$

where k_E is kinetic energy, m is mass, and v is velocity. Atoms and molecules in a gas of known temperature have a Boltzmann distribution of energy with a mean energy of $\frac{3}{2}kT$, where k is the Boltzmann constant ($1.38\text{x}10^{-23}$ JK^{-1}) and T is the absolute temperature [9]. The thermal energy of a collection of colloidal particles in a

dispersion is also subjected to the Boltzmann distribution of energy promoting mixing of the particles in the dispersion. Just like with atoms and molecules the mean energy of the colloidal particles is $\frac{3}{2}kT$ and the average particle velocity increases with temperature and decreasing particle mass [11]. The consequence of thermal energy is the particles are continually moving and well mixed in the dispersion. This process of continual random motion is called Brownian motion.

1.3.2 Van der Waals attractions

Ubiquitous van der Waals forces arise from electrostatic dipoles between atoms and molecules. Molecules may possess permanent dipoles but non-polar molecules and atoms are still subjected to the van der Waals interactions, which are always attractive and occur instantaneously arising from fluctuations in electron density. The van der Waals forces act between all colloidal particles inducing dipole-dipole attractions. There are three types of dipole-dipole interactions: permanent dipole/permanent dipole interactions known as Keesom forces, permanent dipole/induced dipole interactions known as Debye forces, and induced dipole/ induced dipole interactions (London forces). For atoms, the magnitude of the interactions diminishes with the sixth power of their separation distance. $V_a(h) \sim -h^{-6}$

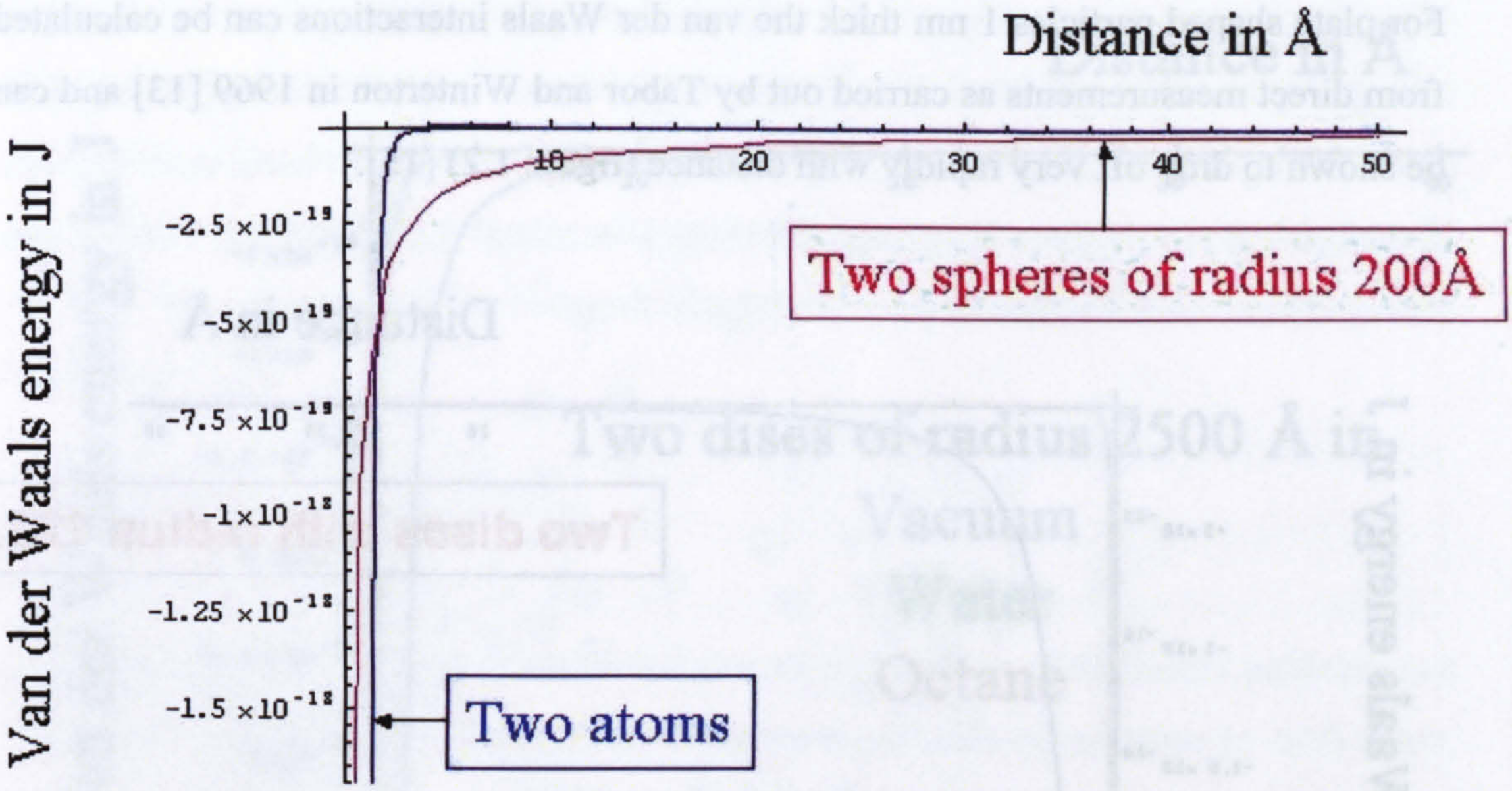

Figure 1.1. The van der Waals attraction between two atoms and two spheres in a vacuum. As reported by Tabor and Winterton [13].

Hamaker considered the interactions between two colloidal particles, made up of many atoms. Hamaker assumed all the atoms in the first particle were all able to interact with all the atoms in the second and the effect was attractive. As a result, the interactions between colloidal particles are more long range and the magnitude of interactions decreases inversely proportionally to the particle separation, ($V_a(h) \sim -h^{-1}$).

The Hamaker expression for two spherical particles (with radius a and separation h) in close proximity to each other ($h<<2a$), is given by:

$$V_a(h) = -\frac{A_{eff}a}{12h} \qquad [1.2]$$

Where A_{eff} is the effective Hamaker constant given by $A_{eff} = (A_p^{0.5} - A_m^{0.5})^2$ subscripts p and m refer to the particle and the suspending medium respectively. The magnitude of the Hamaker constant is very often in the range of 10^{-20} J but the magnitude of the attractions can be reduced by refractive index matching of the particles with the solvent [14].

For plate shaped particles 1 nm thick the van der Waals interactions can be calculated from direct measurements as carried out by Tabor and Winterton in 1969 [13] and can be shown to drop off very rapidly with distance (figure 1.2) [15].

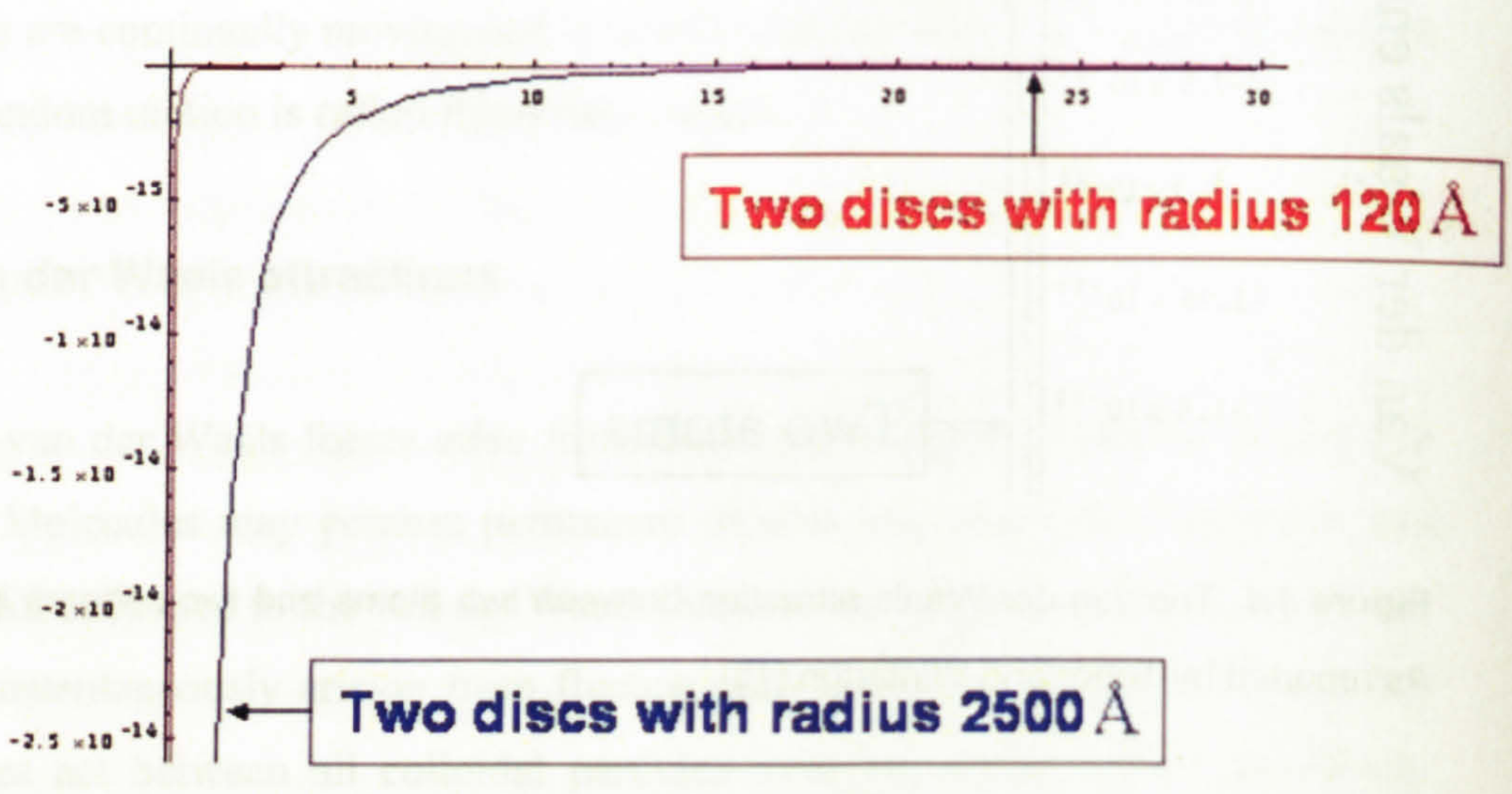

Figure 1.2. The van der Waals attraction between two discs of different radius in a vacuum. As reported by Tabor and Winterton [13].

Suspension of the 1 nm thick plates in solvents also has a dramatic effect on the magnitude and the range of the van der Waals forces (figure 1.3). The implication is that if particles are suspended in a solvent of the same Hamaker constant as the particles there will be no attraction.

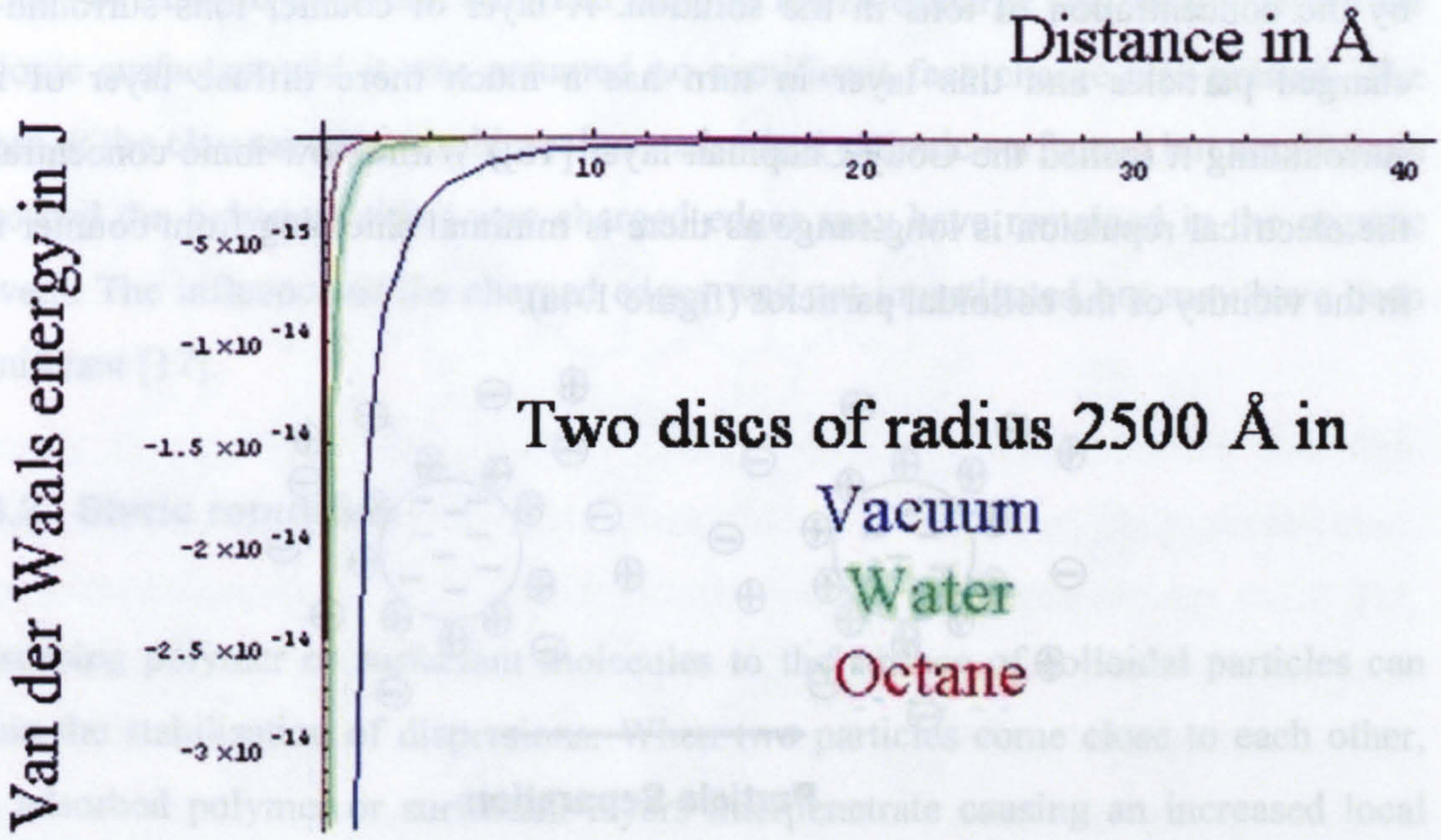

Figure 1.3. Van der Waals attraction between two large discs in a vacuum, in water and in octane. After Tabor and Winterton [13].

1.4 Colloidal stability

Colloidal particles dispersed in a solvent are in a state of constant Brownian motion and even if the particles are at very low concentration they will sooner or later collide with other particles in the dispersion. Under the influence of the long-range van der Waals forces alone the particles will stick together (aggregate) irreversibly [10]. To counteract these forces, equally long-range repulsive forces are required. Electrostatic repulsion from like-charged particles and steric repulsion provided by adsorbed polymer layers on the surface of the particle can give highly effective repulsive forces [11].

1.4.1 Electrostatic repulsion

Many aqueous colloidal dispersions are stabilised by long range electrostatic repulsion. The like-charged particles are stabilised, as the energy required for them to approach closely enough for the Van der Waals attractions to outweigh the electrostatic repulsion is much greater than the thermal energy of the particles. The picture is not simple in reality as the range of the electrostatic repulsion is governed

by the concentration of ions in the solution. A layer of counter ions surround the charged particles and this layer in turn has a much more diffuse layer of ions surrounding it (called the Gouy-Chapman layer [16]) With a low ionic concentration the electrical repulsion is long-range as there is minimal shielding from counter ions in the vicinity of the colloidal particles (figure 1.4a).

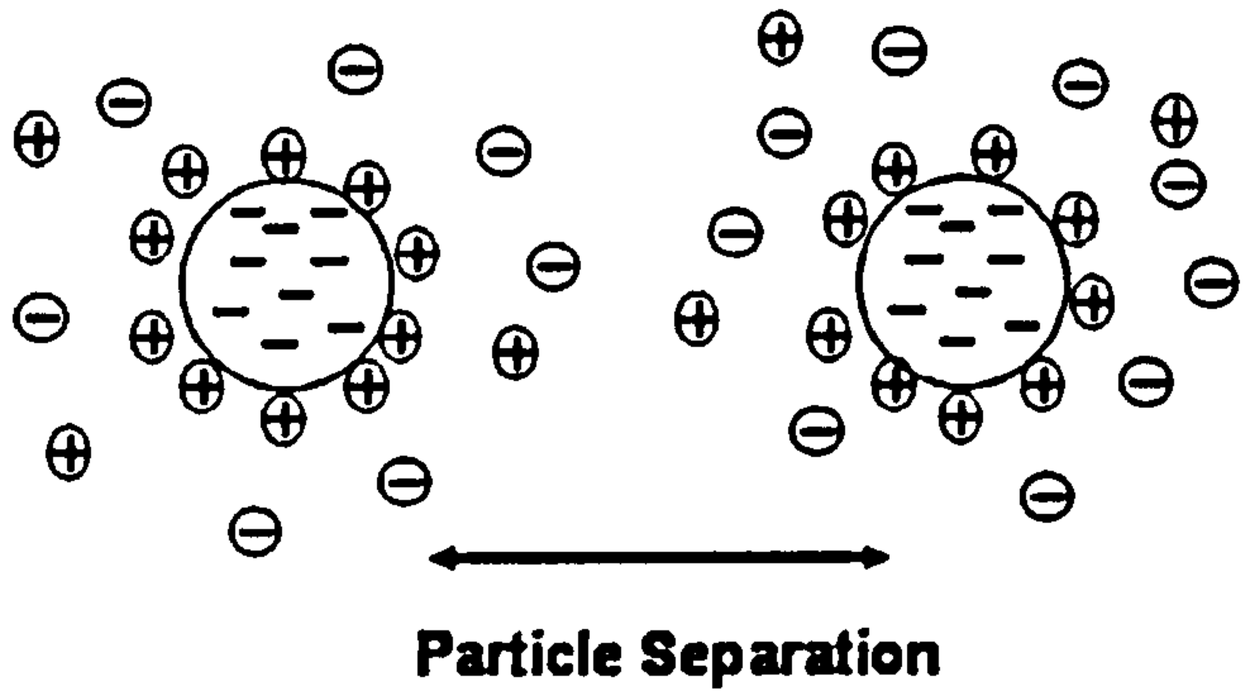

Figure 1.4a. Charged Colloidal Particle in an aqueous dispersion at low ionic strength. The range of the repulsive electrostatic energy barrier is long.

If the ionic strength is high enough the counter ions shield the like-charge repulsion from the colloidal particles to such an extent they can approach so closely that the van der Waals force of attraction will dominate and cause them to aggregate (figure 1.4b).

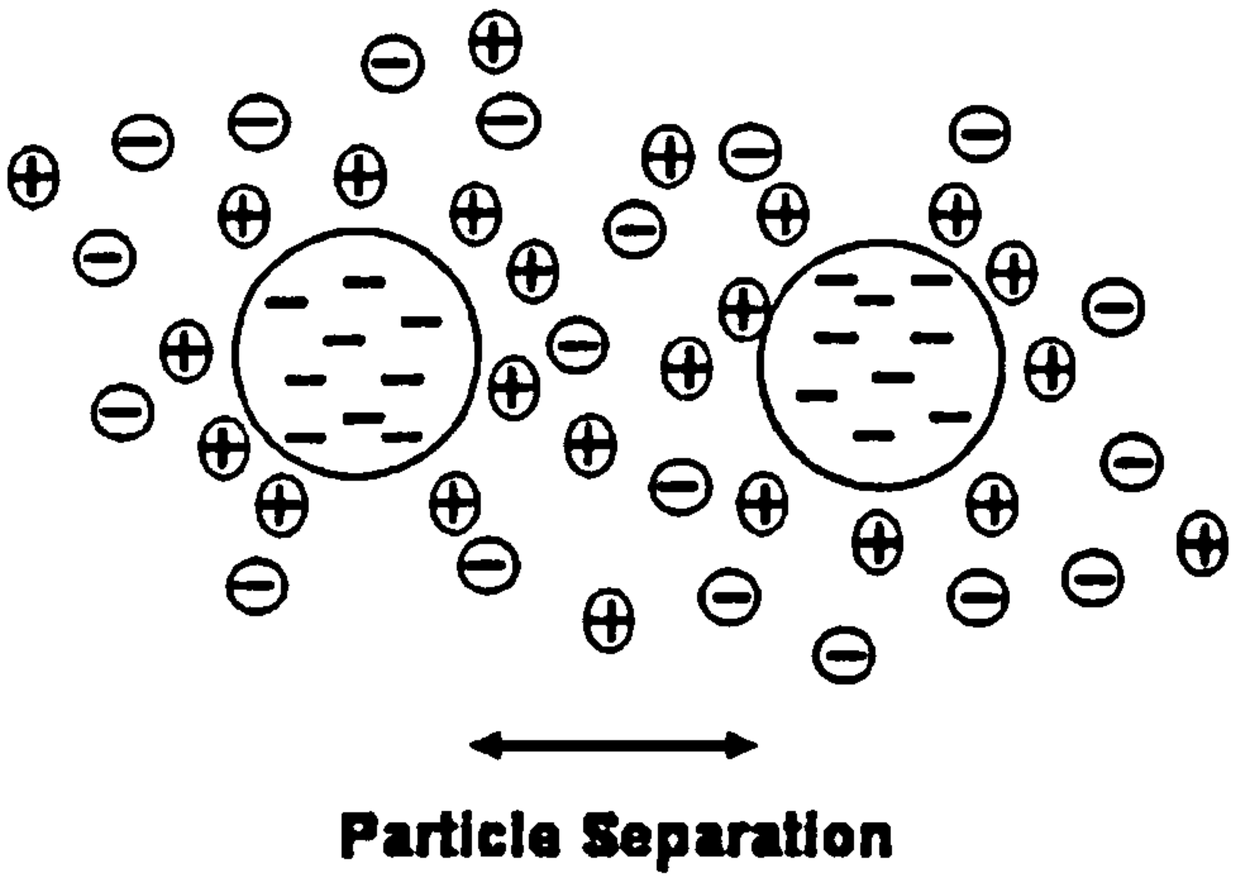

Figure 1.4b. Charged Colloidal Particle in an aqueous dispersion at high ionic strength. The repulsive electrostatic energy barrier is shielded by counter ions allowing for the particles to approach closely.

Non-aqueous solvents have a low relative dielectric permittivity (dielectric constant) and as a result the electrostatic repulsion for dispersed particles was considered insignificant. Clay particles treated with an uncharged short-chain polymer were considered neutral as displacement of the sodium counter ions was not assumed to

occur. For cationic surfactant adsorbed samples the face charge was neutralised by the cationic surfactant and it was assumed no significant face charge was present. The edges of the clay samples would not have adsorbed cationic surfactant but would have adsorbed the polymer, either way charged edges may have remained in the organic solvent. The influence of the charged edges was not investigated but may have been significant [17].

1.4.2 Steric repulsion

Adsorbing polymer or surfactant molecules to the surface of colloidal particles can attain the stabilisation of dispersions. When two particles come close to each other, the adsorbed polymer or surfactant layers interpenetrate causing an increased local concentration of the surface layer. The number of chain-chain contacts is increased at the expense of chain-solvent interactions and in a good solvent osmotic effects cause solvent molecules to migrate into the region of high polymer or surfactant chain concentration driving the particles apart [18]. Also, if the adsorbed polymer or surfactant layers on adjacent colloidal particles overlap to a great extent the number of degrees of freedom of the polymer or surfactant chains will be reduced. This reduction in entropy is thermodynamically unfavourable and gives rise to an elastic (entropic) repulsion [10]. Both of these repulsive effects prevent particles from approaching close enough for the van der Waals force to take over causing aggregation.

1.4.3 Solvency

A bad solvent for the polymer coating on the surface of the particles is one where polymer-solvent interactions are minimised as the polymer contracts [19] as this is thermodynamically more favourable. Marginalising the solvent, by addition of a poor but miscible solvent, attractions between the polymer or surfactant coating of the particles can be induced and this has two effects. The first effect is the thickness of the adsorbed layer decreases which allows the particles to approach more closely and possibly succumb to the van der Waals attractions and aggregate. However, the particles must approach very closely for this to happen so the adsorbed layer must collapse on the surface of the particles. The second effect is the adsorbed layers on

neighbouring particles stick upon meeting, reducing the contact between adsorbed layer and the solvent. This effect is reversible on addition of good solvent to the sample and often can be induced by a change in temperature [10, 20].

1.5 Spherical particles

Spherical particles make very good models to study because preparation methods have advanced giving control of overall particle size and reducing polydispersity [21, 22]. Silica spheres coated with steryl alcohol ($C_{18}H_{37}OH$) and dispersed in benzene have been shown to display temperature dependent gelling [23, 24] due to very short ranged polymer-polymer attraction induced on lowering temperature. Anisotropic particles (plates and rods) although abundant in nature have attracted less interest primarily due their high polydispersity and their less well defined chemical composition. More recently the rheological and phase behaviour of synthesised particles with lower polydispersity and known chemical composition have been studied [25-30].

1.6 Clay minerals

Clay minerals belong to the phyllosilicates [15]. The basic building blocks of the clay minerals are two-dimensional arrays of silicon oxygen tetrahedra and two-dimensional arrays of aluminium or magnesium oxygen-hydroxyl octahedra (figure 1.5). In most clay minerals, such sheets of tetrahedra and octahedra are superimposed in different fashions.

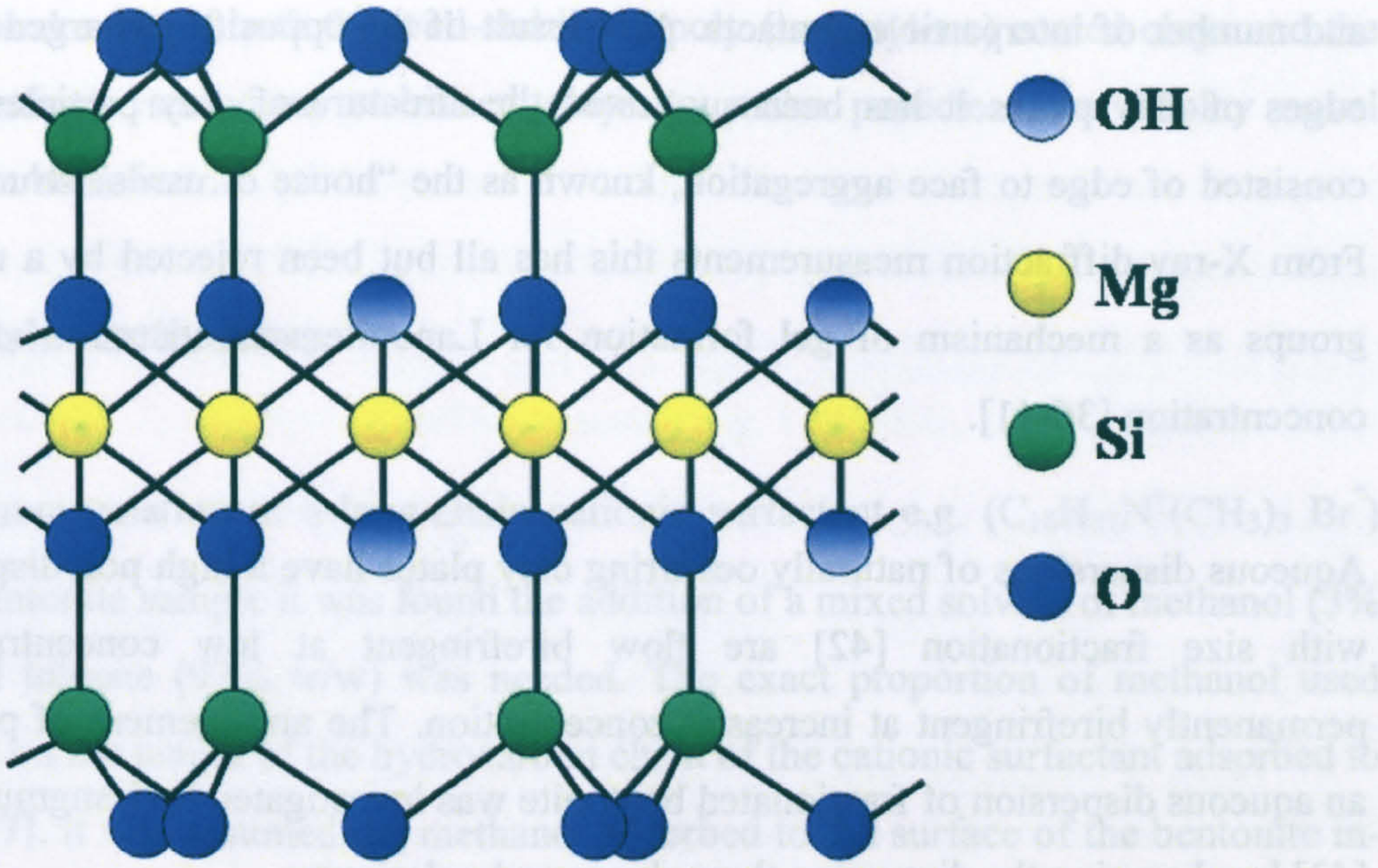

Figure 1.5. Structure of the mineral talc made up of a layer of magnesium-oxygen octahedra sandwiched between two silicon oxygen tetrahedra. The structure has no overall charge.

The mineral talc is a tri-octahedral clay with no overall charge since all the octahedral sites are occupied. This mineral is neutral but for a clay such as Laponite a few of the octahedral positions are occupied by lower valence lithium yet surrounded by the same number of oxygen atoms and it therefore adopts a negative charge. This feature is called isomorphous substitution and the charge can only be balanced by a positive ion, usually sodium, which sits on the face of the clay above and below the silica tetrahedra. These ions neutralise the whole structure but are relatively weakly bonded and can be exchanged for other positive ions such as cationic surfactant ions.

In addition to the permanently negatively charged faces of Laponite or bentonite, the edges of the particles are also charged due to the presence of ionisable hydroxyl groups. The sign and magnitude of the charge is pH and ionic strength dependent being positive at neutral to low pH and negative under alkaline conditions [31].

The behaviour of aqueous clay dispersions has received a lot of attention from a number of groups over the years [25, 32, 33]. The formation of a gel has been found for dispersions of bentonite clay at low concentration [34] and Laponite dispersions are a common model gelling system to study [31, 35]. A gel has a homogeneous appearance and displays some solid-like character; its rigidity comes from the strength

and number of interparticle contacts. As a result of the oppositely charged faces and edges of clay plates it has been suggested the structure of clay particles in a gel consisted of edge to face aggregation, known as the "house of cards" structure [15]. From X-ray diffraction measurements this has all but been rejected by a number of groups as a mechanism of gel formation for Laponite and bentonite at low salt concentration [36-41].

Aqueous dispersions of naturally occurring clay plates have a high polydispersity but with size fractionation [42] are flow birefringent at low concentration and permanently birefringent at increased concentration. The arrangement of particles in an aqueous dispersion of fractionated bentonite was investigated by Langmuir in 1938 [43] by observing the dispersion through crossed polarisers.

1.7 Clays dispersed in organic solvents

In recent work carried out in The Netherlands, van der Kooij [12] synthesised gibbsite platelets with a low polydispersity. The particles produced in the aqueous phase were then coated in a short-chain poly (isobutylene) polymer and transferred to toluene. The colloidally stable particles that showed "hard interactions", i.e. short range, strong repulsions, and rich phase behaviour which was mapped out and compared to the long standing theoretical work of Onsager [44].

The adsorption of cationic surfactants to the surface of bentonite clay has been investigated for over 50 years [6, 7]. After preparation the samples were dispersed in a variety of organic solvents and the plate separation was investigated using X-ray diffraction. The dispersions of bentonite coated with higher molecular weight cationic surfactants had a greater tendency to gel than the samples of bentonite treated with a lower molecular weight cationic surfactant. This was because of the greater area occupied by the longer chain surfactants was required for the development of the gels. Throughout these samples a stable colloidal dispersion was not found.

Here we make use of both the well-stabilised poly (isobutylene) coated clays and the gelling cationic surfactant stabilised clays to make particles that display novel switchable behaviour.

1.7.1 Polar activators

For optimum gelation of a long-chain cationic surfactant e.g. ($C_{18}H_{37}N^{+}(CH_3)_3$ Br^{-}) treated bentonite sample it was found the addition of a mixed solvent of methanol (3% w/w) and toluene (97% w/w) was needed. The exact proportion of methanol used depended on the length of the hydrocarbon chain of the cationic surfactant adsorbed to the clay [7]. It was assumed the methanol adsorbed to the surface of the bentonite in-between the surfactant molecules and increased the clay particle separation aiding dispersion in toluene. The polar organic molecules added to the dispersion (polar activators) have a dramatic effect causing rapid gelation. Alcohols, ketones, propylene carbonate, and even traces amounts of water have all been used as polar activators.

The role of trace amounts of water in dispersions of cationic surfactant treated clay in organic solvents has been debated for long time. It was noted from infra-red absorption measurements that after dehydration gels were converted to viscous liquids without the presence of small amounts of water [45]. The water was suggested to form hydrogen bonding bridges between clay plates leading to a gelling network.

1.8 Thesis layout

The aim of this work was to find thermoreversible gelation for anisotropic particles dispersed in a non-aqueous solvent. The first part of the thesis concerns the materials used during the study, how the dispersions were made, and the experimental techniques used to investigate their behaviour (chapters 2 and 3). In chapter 4, particle characterisation is described in terms of the amounts of materials adsorbed to the surface of the different clays. Simple observations and light microscopy of the behaviour of the samples, dried down and as dispersions in organic solvents are described in chapter 5. Closer examination of the individual dried down particles using atomic force microscopy and electron microscopy can be found in chapter 6.

The behaviour of dispersions that show thermoreversible gelation is investigated using rheological techniques and differential scanning calorimetry is reported in chapter 7. Small angle X-ray scattering from a variety of dry samples and dispersions has been used to find the separation and organisation of the particles in chapter 8. Finally, overall conclusions and suggestions for further work are given in chapter 9.

1.9 References

1. Ward, A.G. and A. Courts, eds. *The Science and Technology of Gelatin*. First ed. 1977, Academic Press: London. UK.
2. Hanley, H.J.M., C.D. Muzny, and B.D. Butler, *Surfactant adsorption on a clay mineral: Application of radiation scattering*. Langmuir, 1997. **13**(20): p. 5276-5282.
3. Bongiovanni, R., *Small Angle Neutron Studies on Clay Systems*. PhD. Thesis. School of Chemistry University of Bristol, Bristol. UK, 1997.
4. *Rheox Incoporated*. P.O.Box 700. Hightstown, NJ 08520, USA.
5. Hendricks, S.B. *Base exchange of the mineral montmorillonite for organic cations and its dependence upon adsorption due to van der Waals forces*. in *Seventeenth Colloidal Symposium*. 1940. Ann Arbor, Michigan: p. 65-81.
6. Jordan, J.W., *Organophilic Bentonites I*. Journal of Physical and Colloidal Chemistry, 1949. **53**: p. 294-306.
7. Jordan, J.W., B.J. Hook, and C.M. Finlayson, *Organophilic Bentonites II*. Journal of Physical and Colloidal Chemistry, 1950. **54**: p. 1196-1208.
8. *Southern Clay Products*. 1212 Church Street, Gonzales, Texas, 78629, USA.
9. Atkins, P.W. and J. de Paula, *Atkins' Physical Chemistry*. Seventh Edition ed. 2002, Oxford: Oxford University Press.
10. Hunter, R.J., *Foundations of Colloid Science*. Second Edition ed. 2001, Oxford: Oxford University Press.
11. Shaw, D.J., *Colloid and Surface Chemistry*. Fourth Edition ed. 1992, Oxford: Butterworth-Heinemann.
12. van der Kooij, F.M., *Phase behaviour and dynamics of suspensions of hard colloidal platelets*. PhD. Thesis, 2000. Van't Hoff Laboratrory. University of Utrecht. Utrecht. The Netherlands.
13. Tabor, D. and R. Winterton, *The direct measurement of Normal and Retarded van der Waals Forces*. Proceedings of the Royal Society A, 1969. **312**: p. 435-450.
14. Larson, R.G., ed. *The structure and rheology of complex fluids*. Topics in Chemical Engineering, ed. K.E. Gubbins. 1999, Oxford University Press: New York.
15. van Olphen, H., *An Introduction to Clay Colloid Chemistry: For Clay Technologists, Geologists, and Soil Scientists*. 2nd Edition ed. 1977: John Wiley & Sons, Inc.
16. Israelachvili, J.N., *Intermolecular & Surface Forces*. Second ed. 1991, London: Academic Press. 450.
17. Vissers, J.P.C., et al., *Sedimentation behaviour and colloidal properties of porous, chemically modified silicas in non-aqueous solvents*. Colloids and Surfaces A: Physicochemical and Engineering Aspects, 1997. **126**: p. 33-44.
18. Nelson, A.J.R., *Neutron and Light Scattering Studies of Polymer Adsorbed on Laponite*. PhD. Thesis. School of Chemistry, University of Bristol, Bristol, UK, 2002.
19. Hamley, I.W., *Introduction to Soft Matter. Polymer, Colloids, Amphiphiles and Liquid Crystals*. First ed. 2000, Oxford: John Wiley and sons, Ltd. 342.

20. Grant, M.C. and W.B. Russel, *Volume-Fraction Dependence of Elastic-Moduli and Transition- Temperatures for Colloidal Silica-Gels.* Physical Review E, 1993. **47**(4): p. 2606-2614.
21. Pusey, P.N. and W. Vanmegen, *Phase-Behavior of Concentrated Suspensions of Nearly Hard Colloidal Spheres.* Nature, 1986. **320**(6060): p. 340-342.
22. Penders, M.H.G.M. and A. Vrij, *A Small-Angle Neutron-Scattering Study on Polydisperse Silica Spheres Coated with Polyisobutene.* Colloid and Polymer Science, 1990. **268**(9): p. 823-831.
23. Vliegenthart, G.A., J.S. van Duijneveldt, and B. Vincent, *Phase transitions and gelation of silica-polystyrene mixtures in benzene.* Faraday Discussions, 2003. **123**: p. 65-74.
24. Verduin, H. and J.K.G. Dhont, *Phase-Diagram of a Model Adhesive Hard-Sphere Dispersion.* Journal of Colloid and Interface Science, 1995. **172**(2): p. 425-437.
25. Ramsay, J.D.F., *Colloidal Properties of Synthetic Hectorite Clay Dispersions .1. Rheology.* Journal of Colloid and Interface Science, 1986. **109**(2): p. 441-447.
26. Mourchid, A., et al., *On viscoelastic, birefringent, and swelling properties of Laponite clay suspensions: Revisited phase diagram.* Langmuir, 1998. **14**(17): p. 4718-4723.
27. Kroon, M., W.L. Vos, and G. Wegdam, *Structure and Formation of a gel of Colloidal discs.* International Journal of Thermophysics, 1998. **19**(3): p. 887-893.
28. Brown, A.B.D., S.M. Clarke, and A.R. Rennie, *Preparation of mono dispersed plate-like particles of tungstic acid.* Colloid and Polymer Science, 1998. **276**: p. 549-552.
29. Buining, P.A., et al., *Preparation of a Nonaqueous Dispersion of Sterically Stabilized Boehmite Rods.* Colloids and Surfaces, 1992. **64**(1): p. 47-55.
30. van der Kooij, F.M. and H.N.W. Lekkerkerker, *Formation of nematic liquid crystals in suspensions of hard colloidal platelets.* Journal of Physical Chemistry B, 1998. **102**(40): p. 7829-7832.
31. Saunders, J., *An investigation of the Structure and Interactions in Aqueous Dispersions of Novel Laponite Clays.* PhD Thesis. School of Chemistry, University of Bristol, Bristol, UK, 1998.
32. Duran, J.D.G., et al., *Rheological and electrokinetic properties of sodium montmorillonite suspensions - I. Rheological properties and interparticle energy of interaction.* Journal of Colloid and Interface Science, 2000. **229**(1): p. 107-117.
33. Abend, S. and G. Lagaly, *Sol-gel transitions of sodium montmorillonite dispersions.* Applied Clay Science, 2000. **16**(3-4): p. 201-227.
34. Fripiat, J., et al., *Thermodynamic and Microdynamic Behavior of Water in Clay Suspensions and Gels.* Journal of Colloid and Interface Science, 1982. **89**(2): p. 378-400.
35. Kroon, M., W.L. Vos, and G.H. Wegdam, *Structure and formation of a gel of colloidal disks.* Physical Review E, 1998. **57**(2): p. 1962-1970.
36. Norrish, K., *The Swelling of Montmorillonite.* Discussions of the Faraday Society, 1954. **18**: p. 120.
37. Callaghan, I.C. and R.H. Ottewill, *Interparticle Forces in Montmorillonite Gels.* Faraday Discussions of the Chemical Society, 1974. **57**: p. 110-118.

38. Morvan, M., et al., *Ultrasmall and Small angle X-ray scattering of smectite clay suspensions.* Colloids and Surfaces A: Physicochemical and Engineering Aspects, 1994. **82**: p. 193-203.
39. Ramsay, J.D.F., S.W. Swanton, and J. Bunce, *Swelling and Dispersion of Smectite Clay Colloids - Determination of Structure by Neutron-Diffraction and Small- Angle Neutron-Scattering.* Journal of the Chemical Society-Faraday Transactions, 1990. **86**(23): p. 3919-3926.
40. Bonn, D., et al., *Laponite: What is the difference between a gel and a glass?* Langmuir, 1999. **15**(22): p. 7534-7536.
41. Saunders, J.M., et al., *A small-angle X-ray scattering study of the structure of aqueous laponite dispersions.* Journal of Physical Chemistry B, 1999. **103**(43): p. 9211-9218.
42. Hauser, E.A. and C.E. Reed, *Studies in Thixotropy, I. Development of a new method for measuring Particle-size Distribution in colloidal systems.* The Journal of Physical Chemistry, 1936. **40**: p. 1169-1182.
43. Langmuir, I., *The role of Attractive and Repulsive forces in the Formation of Tactoids, Thixotropic gels, Protein Crystals and Coacervates.* Journal of Chemical Physics, 1938. **6**: p. 873-896.
44. Onsager, L., *The Effects of Shape on the Interaction of Colloidal Particles.* The Annals of the New York Academy of Science, 1949. **51**: p. 627-659.
45. Damerell, V.R. and E. Milberger, *Organophilic Montmorillonite Gels.* Nature, 1956. **178**: p. 200.

2 Materials

2.1 Introduction

Attempts to stabilise the clays in an organic solvent involved treatment with a short chain polymer [1], a cationic surfactant [2, 3], and a mixture of both. The types of clay used for this study were synthetic **Laponite RD**, naturally occurring **Wyoming Bentonite** and an industrially processed and purified bentonite called **Claytone AF.** The Claytone AF was received treated with an excess amount of a polydisperse cationic surfactant, making it readily gel in organic solvents.

2.2 Laponite RD

A sample of Laponite RD, the RD standing for rapid dispersion, (hereafter referred to as Laponite) made by Laporte plc (PO Box 2, Moorfield Road, Widnes, Cheshire WA8 0JU), was received as a fine dry white powder that was dried under vacuum overnight at 100°C to remove adsorbed water and was then transferred to an airtight container.

A description of Laponite is given by the manufacturer, Laporte, [4] as an entirely synthetic material which closely resembles the naturally occurring clay mineral hectorite in both structure and composition. There are a number of grades of Laponite made for specific applications, and RD is described as a gel-forming grade ideal for rapid dispersion in water for general and industrial use. Laponite has a high chemical purity and consistency free from quartz impurities making it suitable as a thickener for aqueous based dispersions such as toothpaste and a wide variety of cosmetic formulations. Laponite rapidly disperses without the need for high shear and imparts no colour on the dispersion, which is also desirable for the cosmetics industry. Laponite forms gels at low concentration and is highly thixotropic, that is, the viscosity of suspensions decrease if the gel is rapidly stirred, and increases when allowed to stand.

Laponite (figure 2.1) was chosen as a model clay to study because it was of known chemical composition, well characterised and of high purity.

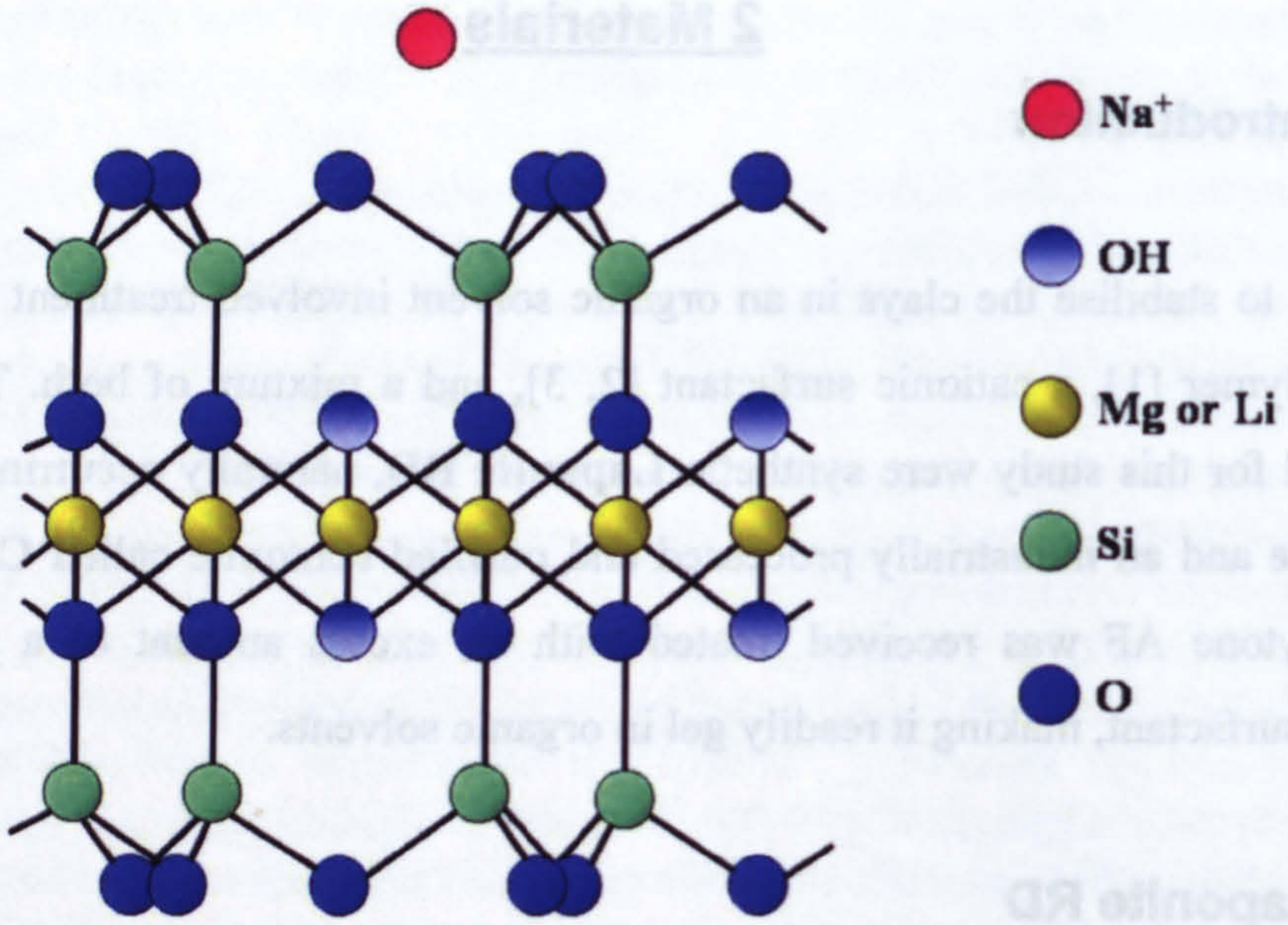

Figure 2.1. The structure of Laponite RD [4].

Laponite is a tri-octahedral clay as all the octahedral positions of the central metal atom are occupied, (figure 2.1). It is very close in composition to the mineral talc and belongs to the montmorillonoid (smectite) group of clays and has the chemical formula $Na^{+}_{0.7}([Si_8Mg_{5.5}Li_{0.3}O_{20}(OH)_4]^{0.7-})$ [5]. The small but fundamental difference between talc and Laponite arises from the composition of the central metal atoms, which in talc is divalent magnesium giving rise to a neutral structure. In Laponite a proportion of the metal atoms are monovalent lithium giving rise to an overall negative charge in the structure of the clay. This effect is called isomorphous substitution [6] and is balanced out by the adsorption of counter ions, usually sodium, to the surface of the mineral. Single Laponite plates consist of a disc with a diameter of ~30 nm, a thickness of 1 nm, (30:1 aspect ratio [5]), and a surface area of 800 m^2g^{-1} [7]. From the above formula, the cationic exchange capacity of the clay can be calculated as 92 millimols per 100 g. Values in the literature vary depending on pH and grade of Laponite but experimental results vary from 70 millimols per 100 g [8, 9] to 160 millimols per 100 g [10, 11].

The units of cationic exchange capacity are often quoted in the literature as milli equivalents/100 g (meq/100 g). This is equal to millimols per 100g of clay.

2.3 Bentonite

The montmorillonite sample used was bentonite (American Petroleum Institute 25.) from Upton, Wyoming prepared for the Petroleum Institute Clay Mineral Standard, project number 49 [12]. This standard is important because it contains information about the exact location where the sample of clay was extracted and this has a bearing on their properties [13, 14]. The raw bentonite was received in the form of a light grey powder with some large lumps that were easily crushed using an agate pestle and mortar. The chemical structure of bentonite is shown below (figure 2.2).

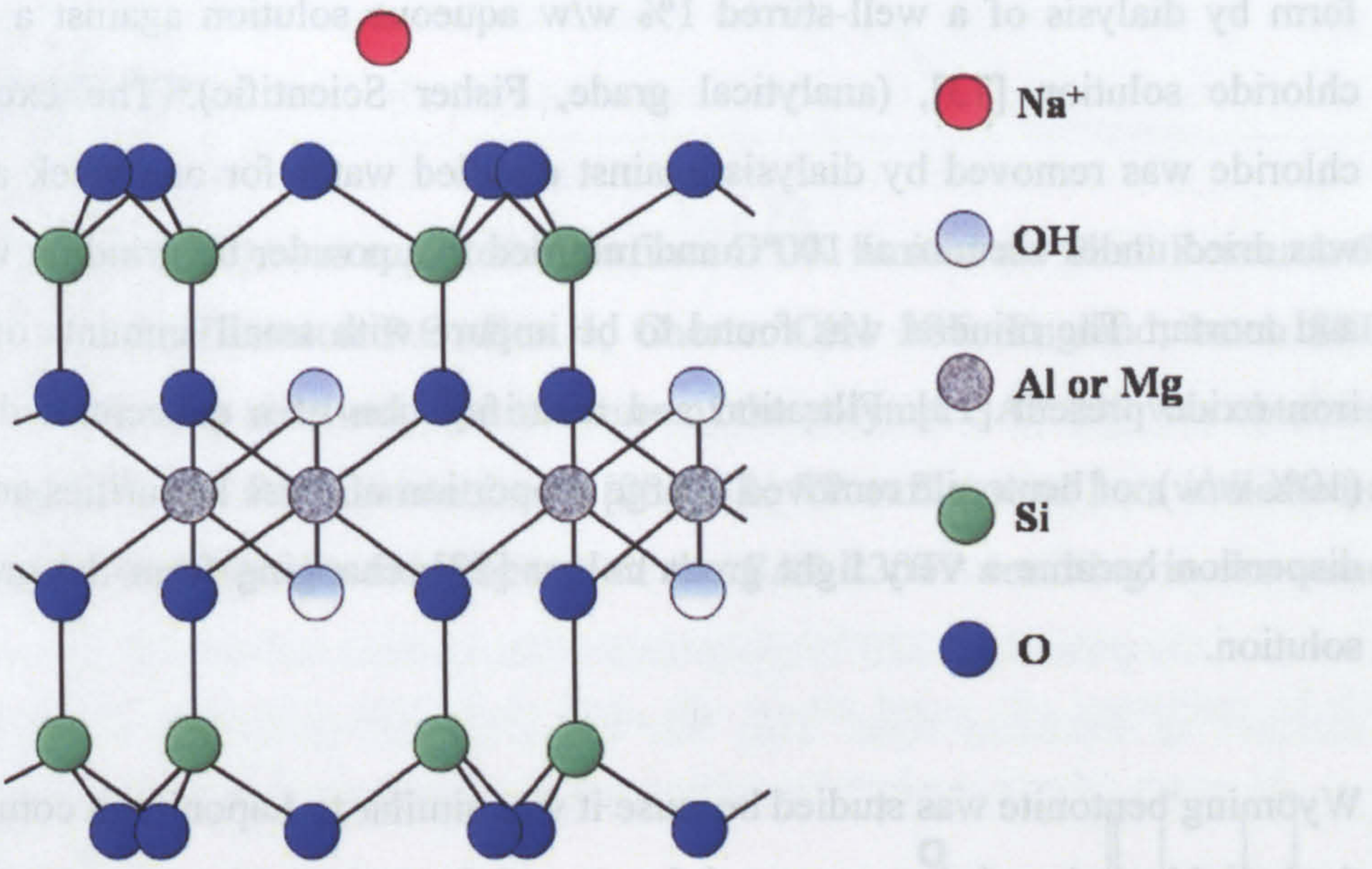

Figure 2.2. The idealised structure of bentonite [15].

Like Laponite, the bentonite clay has a charge due to isomorphous substitution but unlike Laponite the substitution is magnesium for aluminium. The mineral is di-octahedral due to the higher valency of the central metal atoms with the formula of $Na^{+}_{0.33}[(Al_{1.67}Mg_{0.33})Si_4O_{10}(OH)_2]nH_2O$ [16]. Single clay particles have a similar thickness to Laponite plates (1 nm), but the diameter is much greater, from 100 to 1000 nm. The calculated surface area of the plates is 750 m^2g^{-1} [15, 16] and an aspect ratio of up to 1000:1, but with a very high polydispersity. The cationic exchange capacity of bentonite from the above formula is 90 millimols per 100 g and literature values corroborate this [15, 17].

Colloidally dispersed bentonite has many commercial uses from oil well drilling fluids, ceramics, paints, pesticide formulations, cosmetic and pharmaceutical preparations, and as a reinforcement additive in polymers [13, 18-21]. The behavioural properties of the bentonite depend on sufficient particle disaggregation which is required to form a uniform dispersion [18].

Organic material was removed from the surface of the clay by treatment with hydrogen peroxide, the excess hydrogen peroxide removed by slowly heating the solution to 70°C for one hour. The bentonite sample was converted to the pure sodium form by dialysis of a well-stirred 1% w/w aqueous solution against a 2M sodium chloride solution [13], (analytical grade, Fisher Scientific). The excess sodium chloride was removed by dialysis against distilled water for one week and the clay was dried under vacuum at 100°C and returned to a powder by grinding with a pestle and mortar. The mineral was found to be impure with small amounts of quartz and iron oxide present [13]. Filtration and centrifugation of a concentrated dispersion, (10% w/w), of bentonite removed a large proportion of these impurities and a purified dispersion became a very light green colour [22], changing from the grey raw clay solution.

Wyoming bentonite was studied because it was similar to Laponite in composition but the individual clay plates were much larger and the aspect ratio was much higher.

2.4 Claytone AF

Claytone AF was supplied by Southern Clay Products Inc., 1212 Church Street, Gonzales, Texas 78629, lot number 990917N-225. Claytone is essentially a montmorillonite [16] type clay with a polydisperse cationic di-chain surfactant, dihydrogenated tallow (2HT) adsorbed to the surface. Tallow is animal fat and primarily exists as C_{18} chains (65%), with a lesser amount of C_{16}, (30%) and C_{14}, (5%), chains, [16, 23-25]. The Claytone was supplied as a very fine beige powder and used without further purification. The fully hydrogenated surfactant chains had a greater tendency to crystallise than less mobile unsaturated chains.

The manufacturers report Claytone AF is suitable for use in systems containing aliphatic solvents that display low to medium polarity. Upon addition of Claytone AF reproducible viscosity and thixotropic development of the sample occurs [26]. Claytone AF has been added to paints, adhesives, and cosmetics because of this strongly thixotropic behaviour. The AF grade of Claytone is "activator free" and can be gelled with the addition of a so-called polar activator under mixing at any desired point of the process. Claytone AF is described hereafter as Claytone.

2.5 Clay treatments.

2.5.1 SAP 230 TP

SAP 230TP, (figure 2.3), was supplied by Infineum UK limited c/o Shell Research & Technology Centre, Thornton P.O. Box 1, Chester CH1 3SE, England, batch SPL 1564/97. It was used as received. The structure of the polymer SAP 230 was obtained from Buining [27] and Pathmamanoharan [28]. The TP suffix used here indicated a thermal process used for the manufacture of the SAP 230TP resulting in the same product.

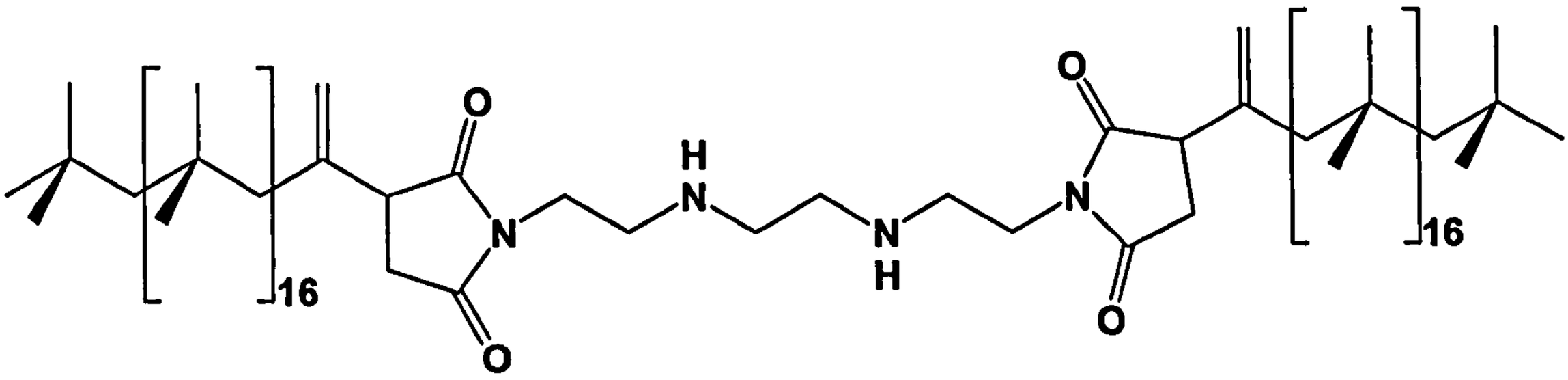

Figure 2.3. The structural formula of SAP 230 TP

SAP 230TP was developed as a steric stabiliser for use in engine oil to prevent the build up of sooty deposits reducing performance and efficiency of petrol engines. It also found an application as a stabiliser in model suspensions of silica spheres in toluene [28, 29], boehmite rods [27], and gibbsite plates [1].

Laponite and bentonite were treated with SAP 230TP stabiliser as was cationic surfactant treated Laponite, bentonite, and Claytone during the course of this study.

Owing to the industrial scale of manufacture the SAP 230 TP was expected to have a high polydispersity, (table 2.1) and this was found by gel permeation chromatography (GPC) carried out by Rapra Technology Limited, Shawbury, Shrewsbury, Shropshire, SY4 4NR, UK under the supervision of Dr. Steve Holding.

The GPC technique involves forcing the polymer, dissolved in an appropriate solvent, tetrahydrofuran, through a chromatographic column, 30 cm in length, filled with 5 μm cross-linked divinyl benzene and polystyrene beads with a range of morphologies. The separation occurred as the larger polymer molecules are size-excluded from the pores in the beads, so stay on the column for a shorter time. The smaller polymer molecules can explore the pores and consequently pass through the column less rapidly. Detection of the eluded polymer was achieved by a refractive index/(differential pressure) analysis system. The molecular weight of the polymer given is in polystyrene equivalents since the molecular weight standards are polystyrene polymers with very narrow, known, size distributions. The columns contain some residual polarity, generally aromatic rings from the polystyrene and / or remaining unsaturation from the divinyl benzene, this means that physical interaction between the polar SAP 230 TP polymer and the column will take place resulting in an increase in retention time. This has the effect of producing a molecular mass distribution that has a lower statistical value than in reality [30] but can still be applied comparatively (figure 2.4).

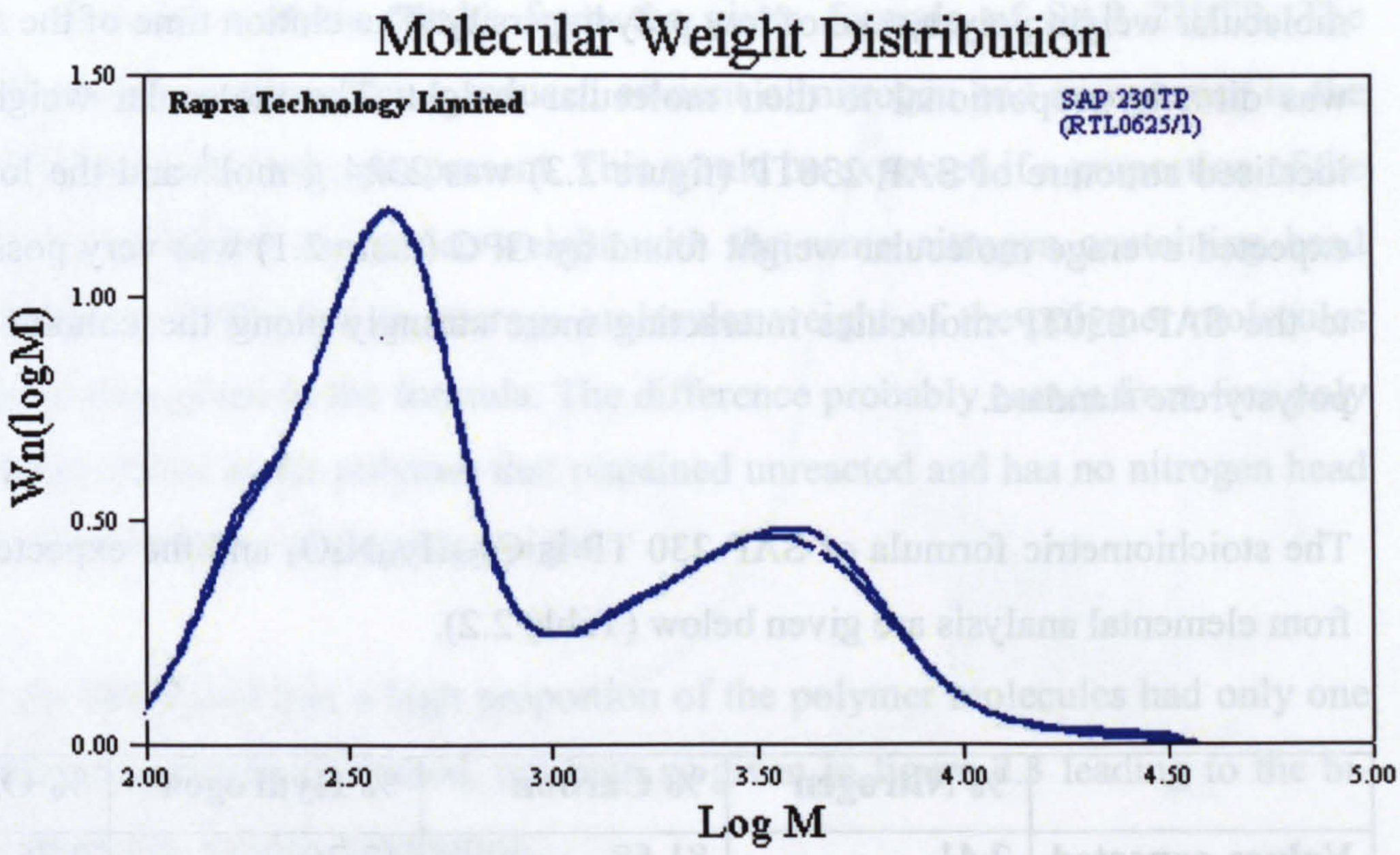

Figure 2.4. Plot showing the computed molecular weight distributions for duplicate runs of a sample of SAP 230TP showing both high and low molecular weight components constituting the polymer sample.

The plot is normalised with respect to area, the x-axis being the logarithm of the molecular weight, M and the y-axis being the number of molecules with mass, M.

Sample	Mw (g mol^{-1})	Mn (g mol^{-1})	Polydispersity
SAP 230TP run 1.	1,750	450	3.9
SAP 230TP run 2.	1,700	450	3.8

Table 2.1. Molecular weight average, (Mw), and number average, (Mn), for duplicate runs of SAP 230 TP measured by GPC.

Polydispersity is the distribution of masses of polymer molecules and is defined as the ratio of the mass of polymer and the number of polymer molecules with that mass.

$$\text{Degree of polydispersity} = \frac{Mw}{Mn} \qquad [2.1]$$

The standard polymers run to find the column characteristics were samples of known molecular weight polystyrene of low polydispersity. The elution time of the standards was directly proportional to their molecular weight. The molecular weight of the idealised structure of SAP 230TP (figure 2.3) was 2324 g mol^{-1} and the lower than expected average molecular weight found by GPC (table 2.1) was very possibly due to the SAP 230TP molecules interacting more strongly along the column than the polystyrene standard.

The stoichiometric formula of SAP 230 TP is $C_{158}H_{306}N_4O_4$ and the expected results from elemental analysis are given below (Table 2.2).

	% Nitrogen	% Carbon	% Hydrogen	% Oxygen
Values expected from structure given in fig. 2.3	2.41	81.58	13.26	2.75
Expected values normalised	1.00	33.85	5.50	1.14

Table 2.2. Expected elemental analysis results for SAP 230 TP.

Elemental analysis gives results for the nitrogen, carbon, and hydrogen content in a sample of SAP 230 TP. There is good agreement between the expected values of Table 2.2 and the experimental results, (Table 2.3).

	%. Nitrogen (±0.3%)	%. Carbon (±0.3%)	% Hydrogen (±0.3%)
Neat SAP 230 TP	2.24	81.88	15.09
Neat SAP 230 TP	2.25	82.88	15.08
Average Values	**2.25**	**82.38**	**15.09**
Normalised neat SAP	1.00	36.61	06.71

Table 2.3. Elemental analysis results for SAP 230TP. The elemental analysis only gave percentage masses for carbon, nitrogen and hydrogen.

There was a difference between the experimental elemental analysis results and the expected elemental analysis results from the given formula of SAP 230TP. The elemental analysis results show a reduced amount of nitrogen and an increase in the amount of carbon and hydrogen present. This would be expected if a proportion of the polymer was of higher molecular weight with the same nitrogen containing head group. However, GPC gave an average molecular weight of the polymer molecules that is lower than given in the formula. The difference probably comes from free poly (isobutylene) chains in the polymer that remained unreacted and has no nitrogen head group but are of a lower molecular weight.

There is the likelihood that a high proportion of the polymer molecules had only one poly (isobutylene) chains attached, not both as given in figure 2.3 leading to the bi-disperse molecular weight distribution.

The absorption maximum of SAP 230TP (figure 2.5) is at 284 nm with a broad peak tailing off into the visible region giving the yellow colour. Absorption at this wavelength is due to an electronic transition from the substituted succinimide ring within the molecule [31, 32]. A big contribution to the absorption below 280 nm was from the toluene solvent.

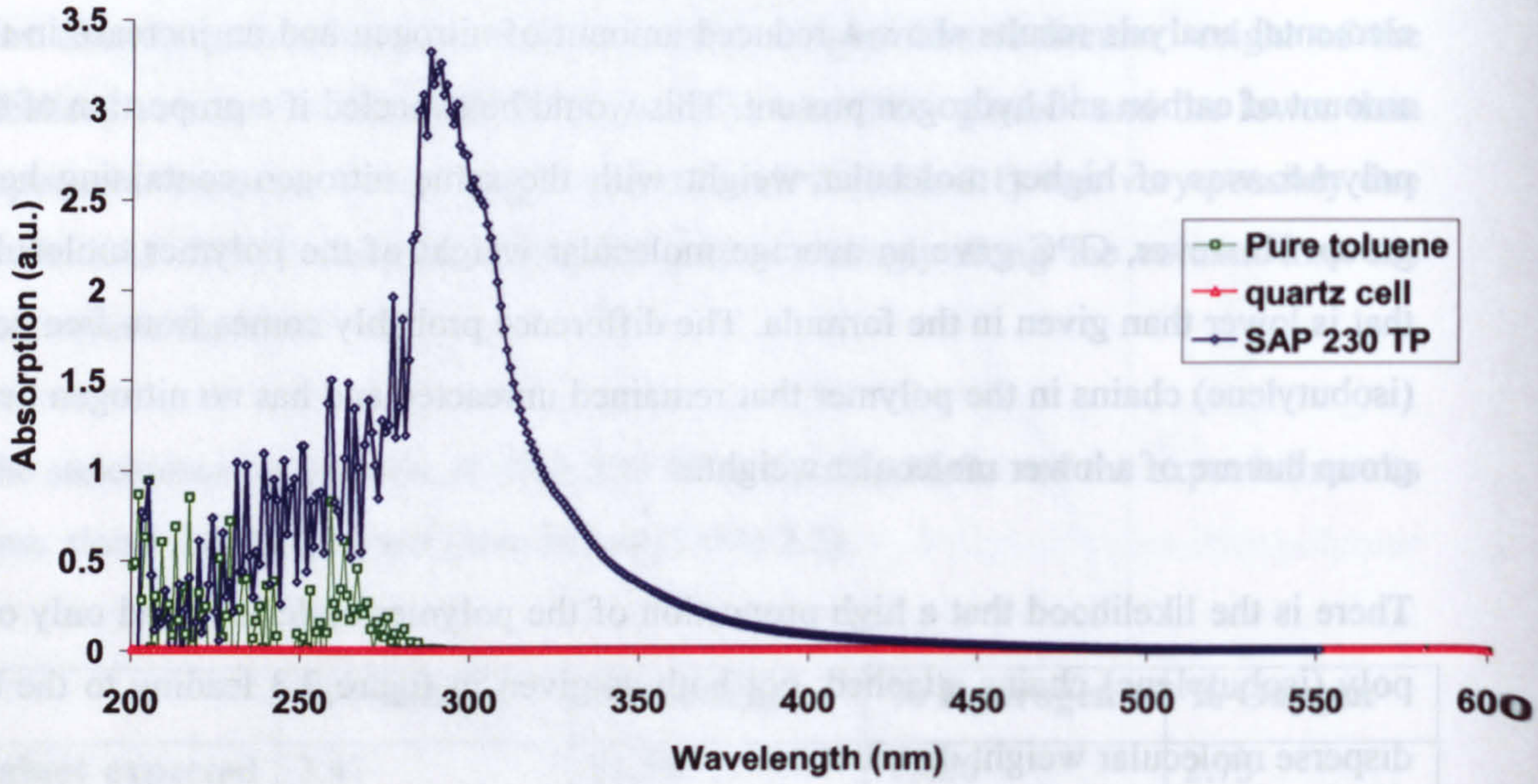

Figure 2.5. UV spectrum of SAP 230 TP showing the maximum absorbance at a wavelength of 284 nm. The SAP sample was 1% w/w dispersed in toluene.

The SAP 230TP polymer is hereafter referred to as SAP.

2.5.2 Dimethyldioctadecyl ammonium bromide (DODAB).

DODAB is a di-chain cationic surfactant with a molecular weight of 630.96 g mol^{-1} (figure 2.6). The cationic ammonium group adsorbs to the negatively charged faces of the clays stabilising the particles in a non-aqueous solvent. It was obtained from Acros Chemicals, Fisher Scientific UK. The DODAB molecule is a pure version of the dihydrogenated tallow found on the surface of the Claytone (section 2.4).

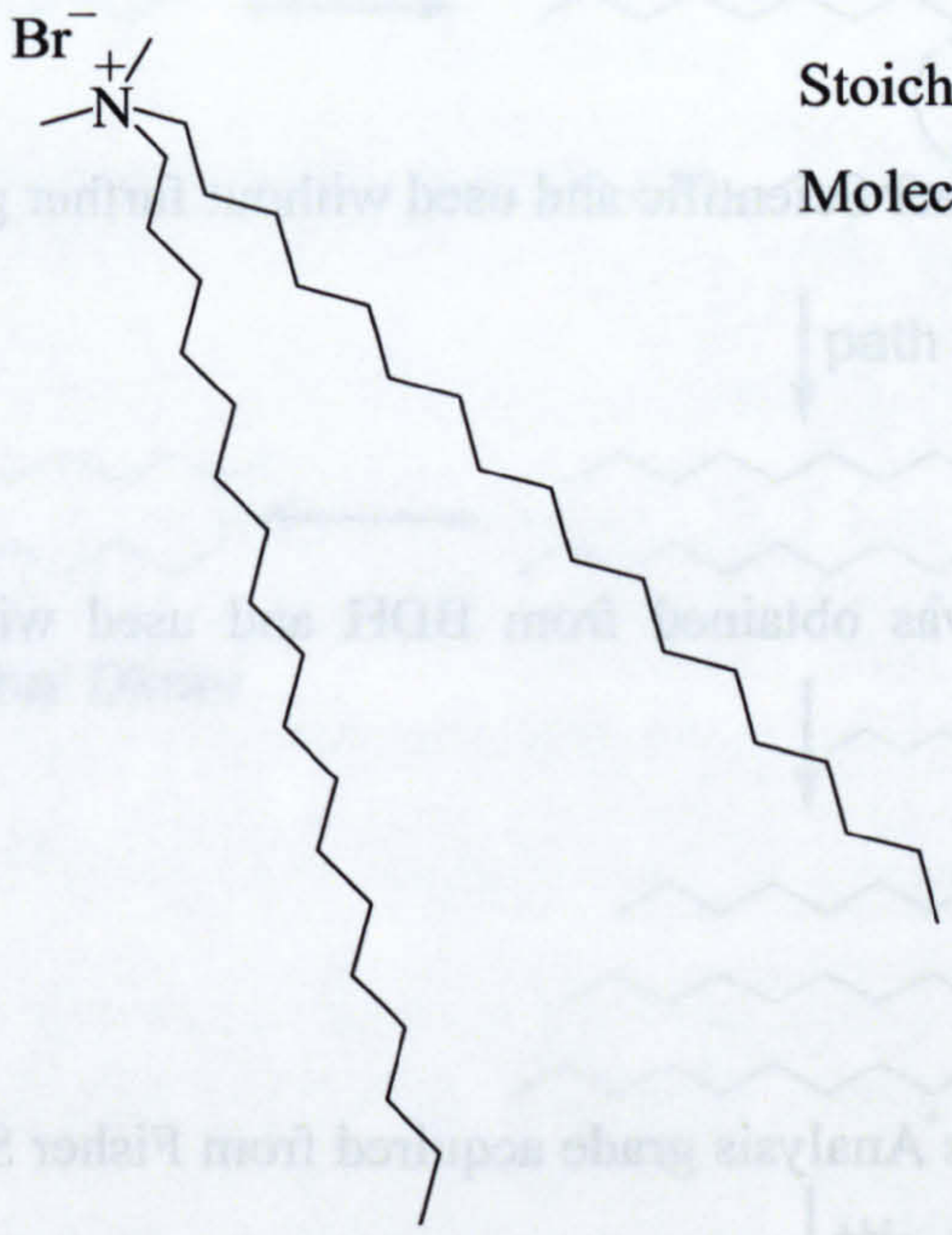

Stoichiometric formula = $C_{38}H_{80}N^{+}Br^{-}$

Molecular Weight = 630.96 $gmol^{-1}$

Figure 2.6. The structural formula for the cationic surfactant Dimethyldioctadecyl ammonium Bromide, (DODAB).

2.6 Chemicals and Solvents used

2.6.1 Water

The water used throughout the study was purified using a Milli-Q plus water purifier fitted with a 0.22 μm filter. Before contact with the air the water had a resistivity of 18.2MΩ cm^{-1}.

2.6.2 Hydrogen Peroxide

Specified reagent for general laboratory work (SLR) grade (30%w/v) hydrogen peroxide was obtained from Fisher Scientific and was used as received.

2.6.3 Tetrabutyl ammonium hydroxide

40-weight percent solution of tetrabutly ammonium hydroxide dispersed in water was obtained from Acros Organics and was used as received.

2.6.4 Propan-1-ol

SLR grade was obtained from Fisher Scientific and used without further purification.

2.6.5 Tetrahydrofuran

AnalaR Grade tetrahydrofuran was obtained from BDH and used without further purification.

2.6.6 Toluene

The toluene used for the work was Analysis grade acquired from Fisher Scientific and was used without further purification.

2.6.7 Silkflo 364 NF polydecene

Silkflo 364NF polydecene (referred to throughout as polydecene) was supplied by Lipo Chemicals Inc., 207 Nineteenth Avenue, Paterson, New Jersey 07504.

Silkflo 364 NF polydecene, (hereafter referred to as polydecene) is a non-polar, non-volatile, colourless, non-toxic branched chain hydrocarbon solvent made from the oligomerisation of 1-decene, [20, 33, 34]. Polydecene was initially developed as a polymeric emollient for use in colour cosmetics, creams, lotions, sunscreens, shave gels, anti-perspirants, and hair products. Due to the highly branched nature of polydecene it remains as a liquid over a very wide temperature range with a pour point of below -50 °C and a flash point of above 150 °C. Representative structures of the molecules in polydecene are shown below, (figure 2.7).

The structures of the molecules found in the polydecene solvent come from the following catalyst initiated reactions.

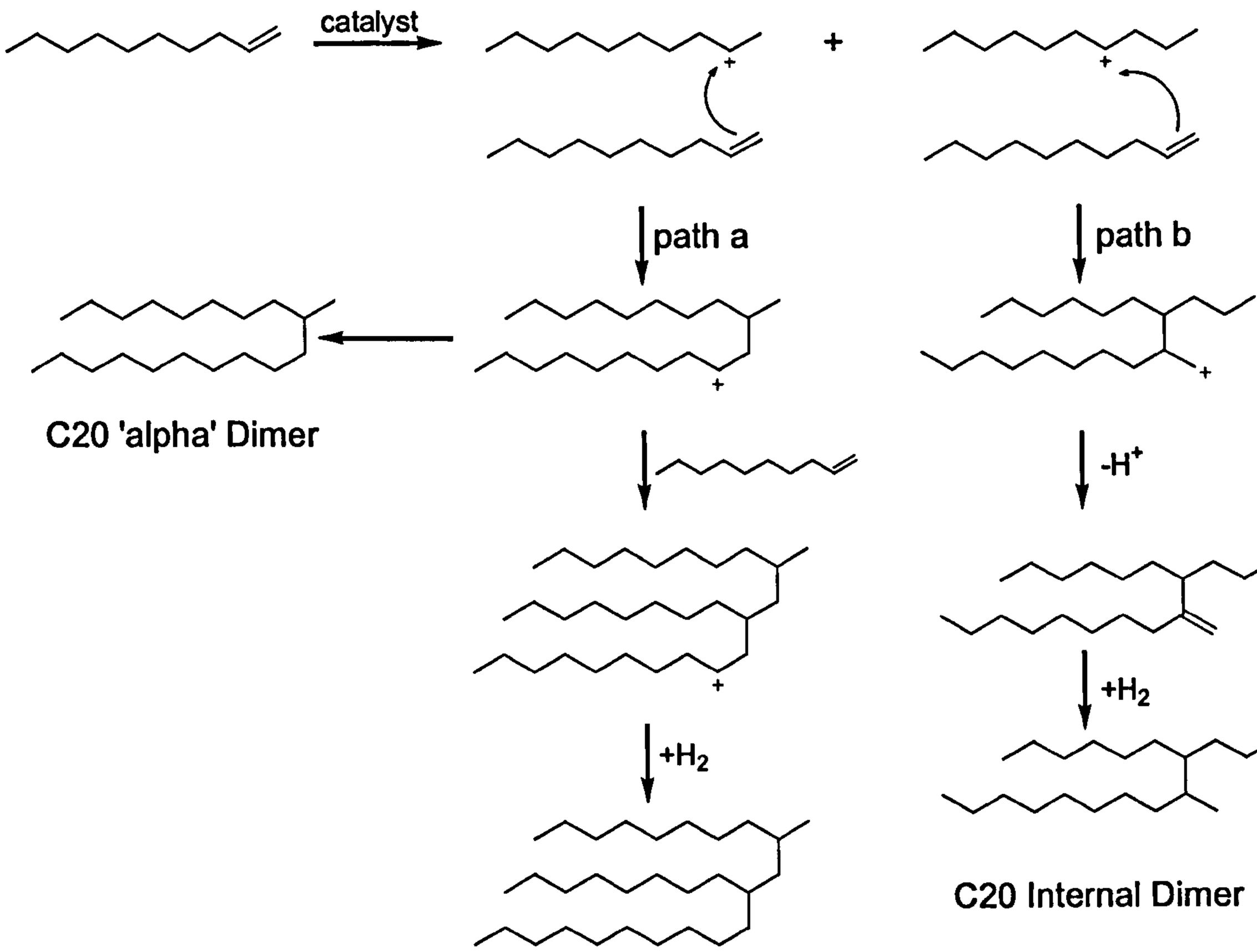

Figure 2.7. Scheme depicting the formation of common structures found in Silkflo 364 NF polydecene [33].

2.7 References

1. van der Kooij, F.M. and H.N.W. Lekkerkerker, *Formation of nematic liquid crystals in suspensions of hard colloidal platelets.* Journal of Physical Chemistry B, 1998. **102**(40): p. 7829-7832.
2. Jordan, J.W., *Organophilic Bentonites I.* Journal of Physical and Colloidal Chemistry, 1949. **53**: p. 294-306.
3. Jordan, J.W., B.J. Hook, and C.M. Finlayson, *Organophilic Bentonites II.* Journal of Physical and Colloidal Chemistry, 1950. **54**: p. 1196-1208.
4. http://www.Laponite.com. 2002, Laporte Inc.
5. Bonn, D., et al., *Laponite: What is the difference between a gel and a glass?* Langmuir, 1999. **15**(22): p. 7534-7536.
6. Theng, B.K.G., *The Chemistry of Clay-Organic Reactions.* 1974, London: Rank Precision Industries.
7. Grillo, I., P. Levitz, and T. Zemb, *Insertion of small anisotropic clay particles in swollen lamellar or sponge phases of nonionic surfactant.* European Physical Journal E, 2001. **5**(3): p. 377-386.
8. Esumi, K., Y. Takeda, and Y. Koide, *Competitive adsorption of cationic surfactant and pesticide on laponite.* Colloids and Surfaces A: Physicochemical and Engineering Aspects, 1998. **135**(1-3): p. 59-62.
9. Morvan, M., et al., *Ultrasmall and Small angle x-ray scattering of smectite clay suspensions.* Colloids and Surfaces A: Physicochemical and Engineering Aspects, 1994. **82**: p. 193-203.
10. Saunders, J.M., et al., *A small-angle X-ray scattering study of the structure of aqueous laponite dispersions.* Journal of Physical Chemistry B, 1999. **103**(43): p. 9211-9218.
11. Thompson, D.W. and J.T. Butterworth, *The Nature of Laponite and Its Aqueous Dispersions.* Journal of Colloid and Interface Science, 1992. **151**(1): p. 236-243.
12. *Reference Clay Minerals*, American Petroleum Institute, Project 49, Columbia University, New York, USA. 1951.
13. Howarth, L.G., *Rheological Studies of Bentonite Dispersions.* PhD. Thesis, School of Chemistry, University of Bristol, Bristol U.K, 1986.
14. Williams, F.J., B.C. Elsley, and D.J. Weintritt. *The Variation of Wyoming Bentonite Beds as a Function of the Overburden.* in *Second National Conference on Clay and Clay Minerals.* 1952. Columbia, Missouri, USA: The Clay Mineral Society.
15. van Olphen, H., *An Introduction to Clay Colloid Chemistry: For Clay Technologists, Geologists, and Soil Scientists.* 2nd Edition ed. 1977: John Wiley & Sons, Inc.
16. Ho, D.L., R.M. Briber, and C.J. Glinka, *Characterization of organically modified clays using scattering and microscopy techniques.* Chemistry of Materials, 2001. **13**(5): p. 1923-1931.
17. Bongiovanni, R., *Small Angle Neutron Studies on Clay Systems.* PhD. Thesis. School of Chemistry, 1997. University of Bristol, UK.
18. Luckham, P.F. and S. Rossi, *The colloidal and rheological properties of bentonite suspensions.* Advances in Colloid and Interface Science, 1999. **82**(1-3): p. 43-92.

19. Khandal, R.K. and T.F. Tadros, *Applicationof Viscoelastic Measurements to the Investigation of the Swelling of Sodium Montmorillonite Suspensions.* Journal of Colloid and Interface Science, 1988. **125**(1): p. 122-128.
20. Abend, S. and G. Lagaly, *Sol-gel transitions of sodium montmorillonite dispersions.* Applied Clay Science, 2000. **16**(3-4): p. 201-227.
21. Biswas, M. and S.S. Ray, *Recent progress in synthesis and evaluation of polymer- montmorillonite nanocomposites*, in *New Polymerization Techniques and Synthetic Methodologies*. 2001. p. 167-221.
22. Hauser, E.A. and H.K. Scahachman, *Particle size determination of colloidal systems by the supercentrifuge.* The Journal of Physical Chemistry, 1940. **44**: p. 584-591.
23. Fasman, G.D., ed. *Practical Handbook of Biochemistry and Molecular Biology*. Third ed. 1976, CRC Press: New York.
24. Xie, W., et al., *Thermal Degradation Chemistry of Alkyl Quaternary Ammonium Montmorillonite.* Chemistry of Materials, 2001. **13**: p. 2979-2990.
25. Ho, D.L. and C.J. Glinka, *Effects of solvent solubility parameters on organoclay dispersions.* Chemistry of Materials, 2003. **15**(6): p. 1309-1312.
26. http://www.scprod.com/europe/claytoneseurope.htm, *Claytone AF Safety Data Sheet*. 2002, Southern Clay Products.
27. Buining, P.A., et al., *Preparation of a Nonaqueous Dispersion of Sterically Stabilized Boehmite Rods.* Colloids and Surfaces, 1992. **64**(1): p. 47-55.
28. Pathmamanoharan, C., *Preparation of Monodisperse Polyisobutene Grafted Silica Dispersion.* Colloids and Surfaces, 1988. **34**(1): p. 81-88.
29. Smits, C., et al., *Influence of the stabilizing coating on the rate of crystalization of colloidal systems.* Progress in colloidal and polymer science, 1989. **79**: p. 287-292.
30. Holding, S., *Personal Communication*. 15th May 2000.
31. Williams, D.H. and I. Fleming, *Spectroscopic Methods in Organic Chemistry.* Fourth Edition ed. 1989, Miadenhead: McGraw-Hall Book Company (UK) Limited.
32. Lee, C. and W. Kumler, *The dipole moment and Structure of the Imide Group. 1. Five- and Six-membered Cyclic Imides.* Journal of the American Chemical Society, 1961. **83**(22): p. 4586-4590.
33. Lee, B., *The physical properties of polydecene and its use in personal care products.* 1994, Amoco Chemical Company: Chicago.
34. Lipo, *Material Safety Data Sheet*. 1996, Lipo Chemicals Inc. 207 Nineteenth Avenue, Paterson, New Jersey 07504 USA.

3 Methods

3.1 Introduction

Untreated Laponite and bentonite clay are both hydrophilic due to their surface charge [1-3] and do not suspend in organic solvents. In order to disperse clay particles in an organic solvent treatment methods with cationic surfactants [4, 5] have been used giving rise to gels. Treatment with a short chain polymer acting as a steric barrier has been developed to give stable colloidal dispersions [6, 7] in toluene.

Attaching a short chain polymer, cationic surfactant, and a combination of both was performed to treat the clay particles and in this chapter a detailed description of the treatment and dispersion procedure is given.

A wide range of observations and experiments was undertaken in order to investigate the macroscopic and microscopic composition, behaviour, and interactions of treated clay particles and dispersions. Simple qualitative observations over time showed the stability of the dispersions and experiments such as small angle X-ray scattering, (SAXS) gave specific information regarding particle separation and agglomeration of the clay plates. Rheology and calorimetery were used to determine the gelling behaviour for some specific samples and polarisation microscopy was used to examine how samples aggregated and settled.

Examinations of dry samples of treated clay were carried out using electron microscopy and atomic force microscopy giving particle size and shape information. The surface treatment was inspected by elemental analysis and X-ray photoelectron spectroscopy to find the amount of surfactant and polymer adsorbed to the different types of clay.

Adsorption isotherms were carried out to find the amount of polymer that became adsorbed to surfactant treated clays. Elemental analysis was inconclusive as some surfactant desorbed during the process of polymer adsorption.

3.2 Clay treatment procedures

A number of methods were used to treat clay particles in order to disperse them in an organic solvent.

3.2.1 Adsorption of short chain polymer to the surface of the clay

This procedure (table 3.1) has been followed to adsorb a short chain polymer to the surface of silica spheres, boehmite rods, and gibbsite plates [7-9]. The polymer gave the treated particles a hydrophobic steric barrier and was carried out at very low concentration to reduce the possibility of particle aggregation during the solvent transfer steps.

1.	1 litre of 0.7% w/w untreated Laponite and bentonite plates were dialysed against deionised water for 1 week with 5 changes a day.
2.	600 ml of 0.7% w/w particle suspension (dry weight analysis) was added to a 5-litre RB flask.
3.	Over 30 minutes 2.5 litres of propan-1-ol was added to the aqueous particle suspension via a dropping funnel whilst under sonication at room temperature.
4.	The dispersion was placed on a heating mantle with the solvent level marked and mechanically stirred whilst an azeotropic distillation occurred. Propan-1-ol was added to the flask, via a dropping funnel at the same rate as the water propan-1-ol mixture distilled over.
5.	After about 10 litres of distilled propan-1-ol and water were removed and the same amount of pure propan-1-ol was added the boiling point returned to 97 °C and the refractive index of the distilled solvent returned to that of pure propan-1-ol (1.385) [10].
6.	25 g of SAP 230TP was added to 2 litres of tetrahydrofuran and warmed to 40 °C for 1 hour to disperse.
7.	The SAP solution was added over 30 minutes via a dropping funnel to the particles in the propan-1-ol solution at room temperature under sonication.

8.	The dispersion was returned to the heating mantle, stirred, and gently boiled. 1 litre was distilled before the addition of 250 ml of toluene. Then another 500 ml was distilled before the addition of the next 250 ml of toluene. This slow decrease of the reaction volume continued until the volume in the flask reached 2.5 litres.
9.	The refractive index of the distillate was measured and further additions of pure toluene were made until the refractive index and boiling point of the distillate reached that of toluene (1.496 and 110 °C) [10].
10.	The solution was allowed to cool to room temperature and centrifuged for 1 hour at 10,000 rpm causing the particles to sediment.
11.	The free polymer rich supernatant was removed and replaced with pure toluene and the particles were redispersed under sonication. The centrifuging and redispersing was repeated until no free polymer remained in the supernatant, (4 times).

Table 3.1. Procedure carried out to adsorb short chain polymer SAP to the surface of Laponite and bentonite clay and stabilise the particles in toluene.

During the dialysis of the Laponite the concentration of the particles in the dispersion increased to nearly 1% w/w and as a result the concentration was determined using dry weight analysis and adjusted accordingly before addition to the round bottomed flask.

The adsorption of SAP to Laponite and bentonite required large volumes of solvents and at best produced 6 g of stabilised particles. The particles produced were very interesting to study despite the considerable effort required and problems with particle aggregation before the addition of the stabiliser.

3.2.2 Determination of the clay cationic exchange capacity

The cationic exchange capacity (CEC) of the Laponite and bentonite was determined by the adsorption of tetrabutyl ammonium hydroxide, 40 wt. % solution in water, (Acros Organics), to the surface (table 3.2). The ammonium ion exchanged for the sodium cation at the same overall concentration. Heavier molecular weight cationic surfactants were not used to measure the CEC because they have been shown to

associate strongly with the cationic surfactant molecules attached to the surface giving a spurious value for the CEC [1].

1.	5 cm^3 of 40% w/w solution of tetrabutyl ammonium hydroxide was added to 250ml of deionised water and the solution was stirred at room temperature for 5 minutes.
2.	0.5 g of finely ground clay was slowly added to the stirred solution of tetrabutyl ammonium hydroxide it quickly flocculated but was stirred overnight to make sure equilibrium adsorption had been reached.
3.	The flocculated clay was filtered out and redispersed in 250 cm^3 deionised water. The sample was redispersed and filtered again 4 times to remove all the unabsorbed surfactant.
4.	The clay was collected and dried in a vacuum oven at 100 °C overnight and a sample was submitted for elemental analysis.

Table 3.2. Procedure for the measurement of the cationic exchange capacity for Laponite and bentonite.

The CEC was not measured for the sample of Claytone as it was received with an excess of cationic surfactant adsorbed to the surface [11].

The calculations can be found in appendix 1.

3.2.3 Adsorption of dimethyldioctadecyl ammonium bromide (DODAB) to clay

Cationic surfactants adsorb to the surface of clays with a high affinity and as a result there have been a number of different methods employed to carry out the reaction, [1, 12, 13]. For this study the method chosen was the simple addition of the stoichiometric amount of powdered clay to a solution of cationic surfactant (table 3.3).

1.	To 800 ml water 5.0 g of DODAB, (ACROS Organics), was added, stirred and heated to 80 °C. Carefully 200 ml of propan-1-ol was added to the solution to dissolve the DODAB whilst still stirring. The DODAB dissolved on the addition of the alcohol to the water leaving a colourless solution.
2.	The stoichiometric amount of clay was added carefully to the hot surfactant solution and stirred, forming flocs immediately. The stirring solution was covered and cooled to room temperature overnight.
3.	The flocs were filtered and redispersed in 250 ml 50/50 water/propan-1-ol mixture for 1 hour and filtered again. This process was repeated 4 times to remove any free surfactant.
4.	The filtered treated clay was dried at 100 °C in a vacuum oven overnight, then crushed with a pestle and mortar and returned to the vacuum oven for one hour at 100 °C.
5.	The dry clay was placed in an airtight container until use.

Table 3.3. Procedure for addition of dioctadecyl dimethyl ammonium bromide to Laponite and bentonite.

The treatment of Laponite and bentonite with the cationic surfactant DODAB was relatively quick and easy and large amounts of treated particles were made. A sample from each batch was submitted for elemental analysis to ensure consistency.

3.2.4 DODAB adsorbed clay dispersions in organic solvents

Clay particles that have a cationic surfactant adsorbed to the surface are described as organophilic. This does not mean they spontaneously disagglomerate when added to an organic solvent. The main problem was the dry clay particles are made up of large numbers of tightly bound platelets and organic solvent molecules cannot easily penetrate the layers. This can be overcome with the addition of a small amount of a polar organic liquid [12] or very vigorous mixing of the sample (section 5.3) [14]. It was decided to shake the solution to get the particles as well dispersed as possible rather than add a polar activator (table 3.4).

1.	Cleaned and dried DODAB adsorbed clay was weighed into a sample bottle.
2.	Organic solvent was added by weight to the sample bottle and the lid was tightened to make an airtight seal. PTFE tape was wrapped around the base of the lid to stop the possibility of water from getting into the sample.
3.	The samples was placed on a spin mixer for 1 minute to remove the powder stuck on the bottom of the sample tube and begin the dispersing process.
4.	The sample was then placed in a beaker of water at 80 °C and left to stand in an ultrasonic bath for 1 hour.
5.	The temperature of the ultrasonic bath was set at 60 °C and the sample was sonicated and shaken by hand every minute for an hour.
6.	For a further two hours the dispersing sample was left to stand in the ultrasonic bath at 60 °C with occasional shaking by hand.
7.	Finally, the sample was sonicated for three hours at room temperature.

Table 3.4. Method used to disperse samples of cationic surfactant adsorbed Laponite, bentonite, and Claytone in organic solvents.

Contamination of the samples by water was a problem as they stood for a number of hours in a beaker of very hot water and in the ultrasonic bath. With small additions of water to the samples they quickly became turbid and large flocs were seen. To reduce the risk of contamination it was very important to wrap a layer of PTFE tape around the thread of the sample holder before screwing on the lid to seal.

3.2.5 Combined surfactant and polymer treatment.

The method used to prepare samples with both surfactant and polymer adsorbed to the surface was the straightforward addition of free polymer to a sample of dispersed surfactant-adsorbed clay particles in toluene (table 3.5). However, for ease of handling, the highly viscous neat SAP was diluted in toluene to a 10% w/w solution.

1.	A suspension of the surfactant-adsorbed clay particles in toluene was prepared according to the method above (section 3.2.4). 5 g of 10% w/w SAP 230TP solution in toluene per gram of surfactant-adsorbed clay was added giving a large excess of polymer.

2.	The sample was spin mixed for 1 minute and tumbled at room temperature overnight.
3.	The excess polymer was removed by centrifugation at 5,000 rpm for 1 hour and exchange of the supernatant with fresh toluene. The sample was redispersed by sonication and centrifuged three times to remove all excess toluene.
4.	The sample was redispersed in toluene and dry weight analysis was carried out to find the exact concentration.

Table 3.5 Procedure for the addition of SAP polymer to DODAB Laponite, DODAB bentonite and Claytone in toluene.

The SAP adsorbed DODAB bentonite and Claytone formed almost clear yellow fluids after the treatment and showed no sign of settling after one week. The SAP DODAB Laponite sample appeared granular and rapidly sedimented in toluene and did not flow over time if the sample holder was tilted.

3.2.6 Solvent transfer from toluene to polydecene

Transfer of dispersed samples from toluene to polydecene was carried out without drying the particles in order to reduce the possibility of irreversible aggregation. The concentration of the dispersion in polydecene could not be increased because polydecene was non-volatile. The simple method used is described below (table 3.6).

1.	A weighed sample of SAP surfactant treated clay in toluene (no more than 20 cm^3) at known concentration was added to a round bottom flask.
2.	Polydecene was added of known weight to the round-bottomed flask containing the SAP treated sample.
3.	The toluene was evaporated from the mixed solvent sample in the rotary evaporator under vacuum (water aspirator) at 40 °C and 120 revolutions per minute.

Table 3.6. Solvent transfer procedure of SAP DODAB Laponite, SAP DODAB bentonite and SAP Claytone from toluene to polydecene.

The maximum concentration of the SAP surfactant treated particles in polydecene attempted was 10.1% w/w as the dispersions became very viscous above this strength.

Evaporation of the polydecene during rotary evaporation was considered negligible as a control sample of pure polydecene were placed in a vacuum oven at 80 °C overnight and the weight loss was recorded at less than 4%. Dry weight analysis was not attempted on the polydecene dispersions for the same reason.

3.3 Sample preparation

3.3.1 Spin mixer

The first step to disperse clay samples in an organic solvent was to spin mix them for several seconds to break up the large dry powder agglomerate at the bottom of the sample tube. This was carried out using a Clifton cyclone bench top vortex spin mixer from Fisher Scientific (figure 3.1). Spin mixing samples several times throughout the dispersing stage was necessary to break up small particle aggregates.

Figure 3.1. Bench top spin mixer used to break up large clay powder aggregates.

3.3.2 Ultrasonic bath

Using the ultrasonic bath, wetted clay aggregates were rapidly broken down forming a dispersion that appeared homogeneous to the eye. The ultrasonic bath was a vigorous and highly effective method of dispersion and no evidence from microscopy was found of individual clay plates being destroyed by its action. However, it would be hard to tell if the ultrasonic waves caused anything but total destruction of the bentonite plates as they had a very broad distribution of size and shape. The much smaller Laponite plates appeared not to suffer under ultrasonic action as from atomic force microscopy they were of the expected size range.

A 5 litre capacity 280-Watt U500D Ultrawave sonic bath (figure 3.2) with an operating frequency of 30-40 kHz, fitted with 2 pillar type transducers was used throughout the study (figure 3.2).

Figure 3.2. Ultrasonic bath used to homogenise the clay dispersions.

3.3.3 Centrifuge

Removal of unadsorbed polymer and surfactant and concentration of the particles was achieved by centrifugation and redispersion of the particle sediment at the bottom of the tubes in clean solvent. The speed and duration of the centrifugation process depended entirely on the type of sample. The particles were redispersed in fresh clean solvent with the aid of the spin mixer and ultrasonic bath. The centrifuge used for all of the work carried out for this study was a Sorvall RC-5B Plus Superspeed Centrifuge (figure 3.3) fitted with a Sorvall SA-600 rotor with a maximum diameter of 12.96cm.

Figure 3.3. Sorvall RC-5B Plus Superspeed Centrifuge and rotor.

3.4 Experiments undertaken

The experiments and techniques used at any point during the course of this project are described below.

3.4.1 Electron Microscopy

Beams of electrons accelerated in a vacuum can have wavelengths shorter than X-rays, below 0.01 nm [15] and can be very finely focussed using electro-magnetic lenses. In order to see an image the sample must absorb or scatter the electron beam and it is the way the beam changes that is what is detected. Samples examined using electron microscopy are examined under vacuum as air molecules can deflect and scatter the electron beam therefore volatile samples may not be suitable. This means clean dried samples must be used for standard electron microscopy. The resolving power of electron microscopes is nowhere near 0.01 nm due to difficulties with keeping the magnetic lenses perfectly stable [16]. There are two types of electron microscope, the transmission electron microscope (TEM) with resolution down to the nanometer scale and the scanning electron microscope (SEM) with resolution down to tens of nanometers.

3.4.1.1 Transmission Electron Microscopy (TEM).

In the TEM microscope (figure 3.4) electrons are accelerated by a potential difference of 50 thousand to 200 thousand volts and pass through the sample. The image is formed as a result of the interaction of electrons with the sample and local variations in the structure of sample affecting the proportion of electrons deflected. However the sample must be very thin for any electrons to pass through without deflection and form the image but the sample must be thick enough to give good electron contrast. Clay samples have been examined using the TEM as the thin plates can easily be deposited from dilute suspensions on to sample grids. However, the untreated clay plates are 1 nm thick and do not give good electron contrast making the exact size and shape difficult to see [17].

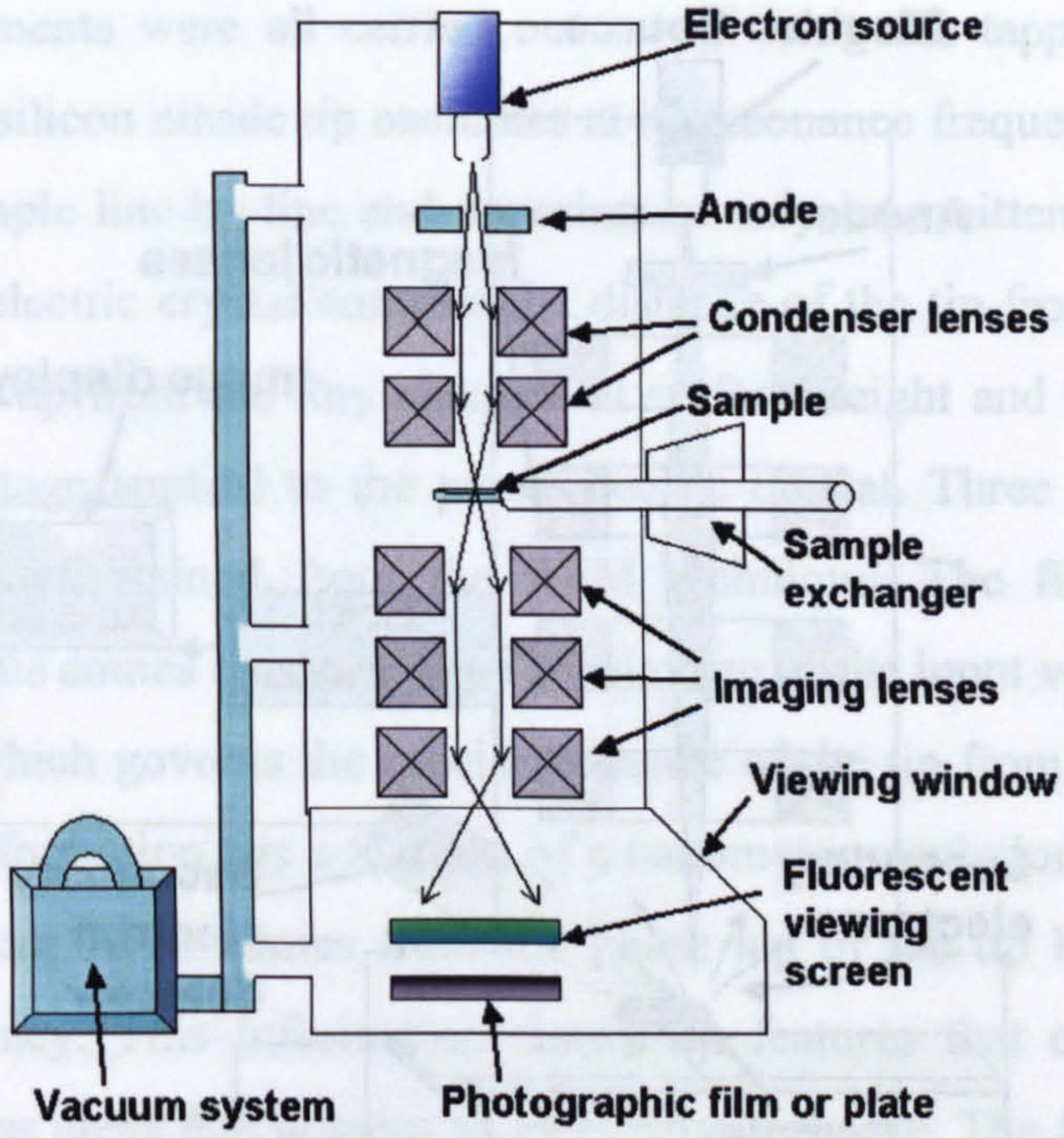

Figure 3.4. Schematic diagram of a transmission electron microscope.

The Transmission Electron Microscope used was a JEOL JEM 1200EX

3.4.1.2 Scanning Electron Microscopy (SEM).

In the SEM (figure 3.5) an electron beam is accelerated by a potential difference of up to 30 kV giving a wavelength of 0.04 nm and focussed on a spot of about 3 nm in diameter. Large and thick samples can be easily imaged in the SEM as it gives an image of the surface of the sample. Like the TEM the samples are placed in an evacuated chamber and the electron beam is scanned across the sample. Some electrons are backscattered and some secondary electrons are displaced from the sample surface and a very sensitive collector detects these [18]. The image is built up line by line from the intensity of the backscattered and secondary electrons falling on the detector producing a two dimensional image.

Non-conducting samples submitted for analysis using the SEM must be coated with a thin conducting metal layer to stop the samples from charging up and giving bright spots on the corners and edges.

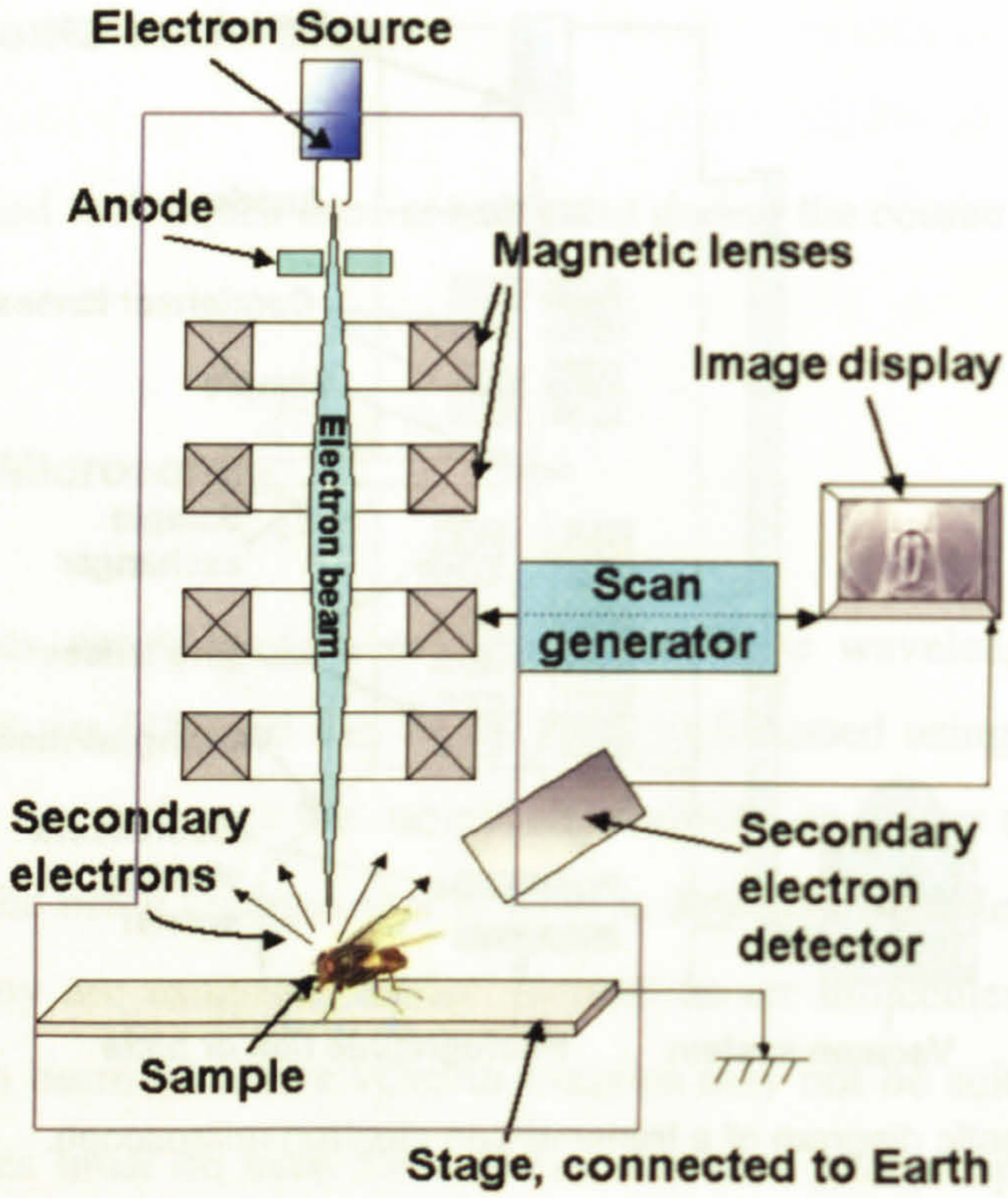

Figure 3.5. Schematic diagram of a scanning electron microscope.

The Scanning Electron Microscope was a JEOL JSM 6330F fitted with a high intensity Field emission electron gun.

SEM is less often used to image clay samples as the fine detail cannot be seen for the very thin plates. However, SEM studies have been carried out on clay samples showing detail of plate aggregates [19].

3.4.2 Atomic Force Microscopy (AFM).

Samples submitted for analysis under the AFM were dried from very low concentration solutions on a molecularly flat mica substrate. The technique involved measuring the deflection (attraction or repulsion) of a fine silicon nitride stylus as it approached the surface of the sample [20]. To identify the tiny changes of position of the stylus as it was rastered across the sample a laser light was reflected off the back of the stylus to a position sensitive detector. The AFM set up is shown in figure 3.6.

The AFM experiments were all carried out in air using the tapping mode. In the tapping mode the silicon nitride tip oscillates at its resonance frequency as it scans the surface of the sample line-by-line and experiences only intermittent contact with the surface. A piezo electric crystal controls the distance of the tip from the surface and the image is built up from the tiny changes in surface height and the corresponding change in the voltage applied to the piezo electric crystal. Three different types of information can be obtained from the AFM technique. The first is topological information and this comes from sensitive monitoring of the input voltage to the piezo electric scanner which governs the precise distance of the tip from the surface of the sample. Height information has a fraction of a nanometer resolution. The second type of information from AFM comes from the phase lag of the tip behind the driving oscillating frequency. This information shows up features that exhibit long range interactions such as areas that possess an electrostatic charge. The final type of signal received from the AFM tip is amplitude information. If the tip passes over an area that is unusually spongy such as a polymer molecule the tip oscillation becomes damped.

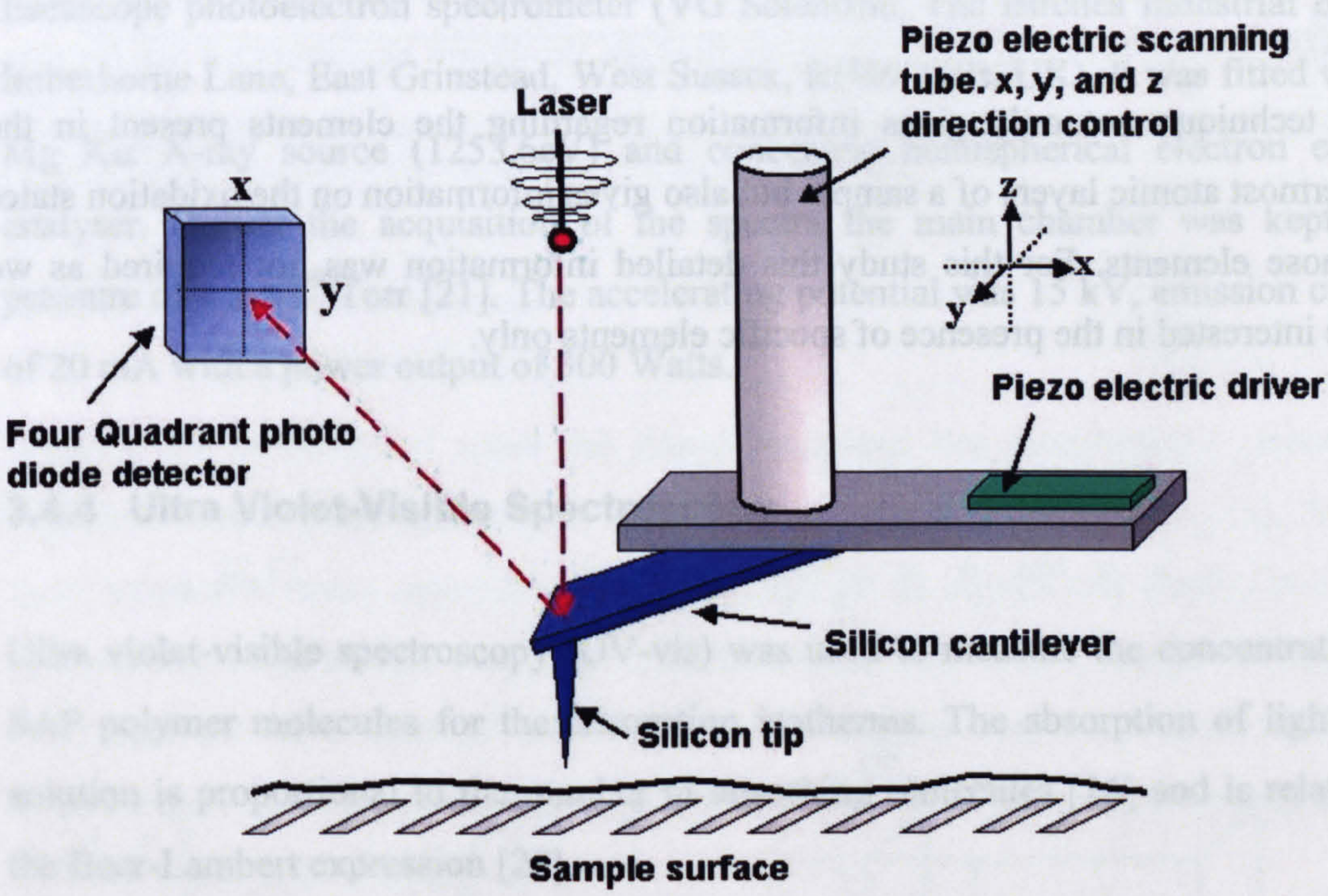

Figure 3.6. Schematic diagram of an AFM.

The microscope used in these experiments was a Multimode run from a Nanoscope IIIa controller (Digital Instruments/Veeco, Santa Barbara, CA). Olympus silicon cantilevers with a nominal spring constant of 42 Nm^{-1} were used for imaging in air.

The samples were prepared diluted to ~0.001% w/w in toluene and a drop of the solution was applied to a mica surface that was cleaned by the removal of the uppermost layer using a sharp blade. The solution was allowed to dry under a dust cover in air. The mica was attached to a steel stub with superglue.

3.4.3 X-ray Photoelectron Spectroscopy (XPS)

The XPS phenomenon is based on the photoelectric effect where the concept of the photon was used to describe the ejection of electrons from a surface when photons impinged upon it [20]. Monochromated magnesium Kα X-rays of 1254eV were fired at the sample under ultra high vacuum conditions and the ejected electrons were directed into a hemispherical energy analyser. The kinetic energy of the photoelectrons was so low that only those that escape from the uppermost layers of the sample, (1-5 nm), did so without interaction with the sample and made their way to the energy analyser [21-23]. A schematic representation of the XPS machine is shown in figure 3.7.

The technique not only gives information regarding the elements present in the uppermost atomic layers of a sample but also gives information on the oxidation states of those elements. For this study this detailed information was not required as we were interested in the presence of specific elements only.

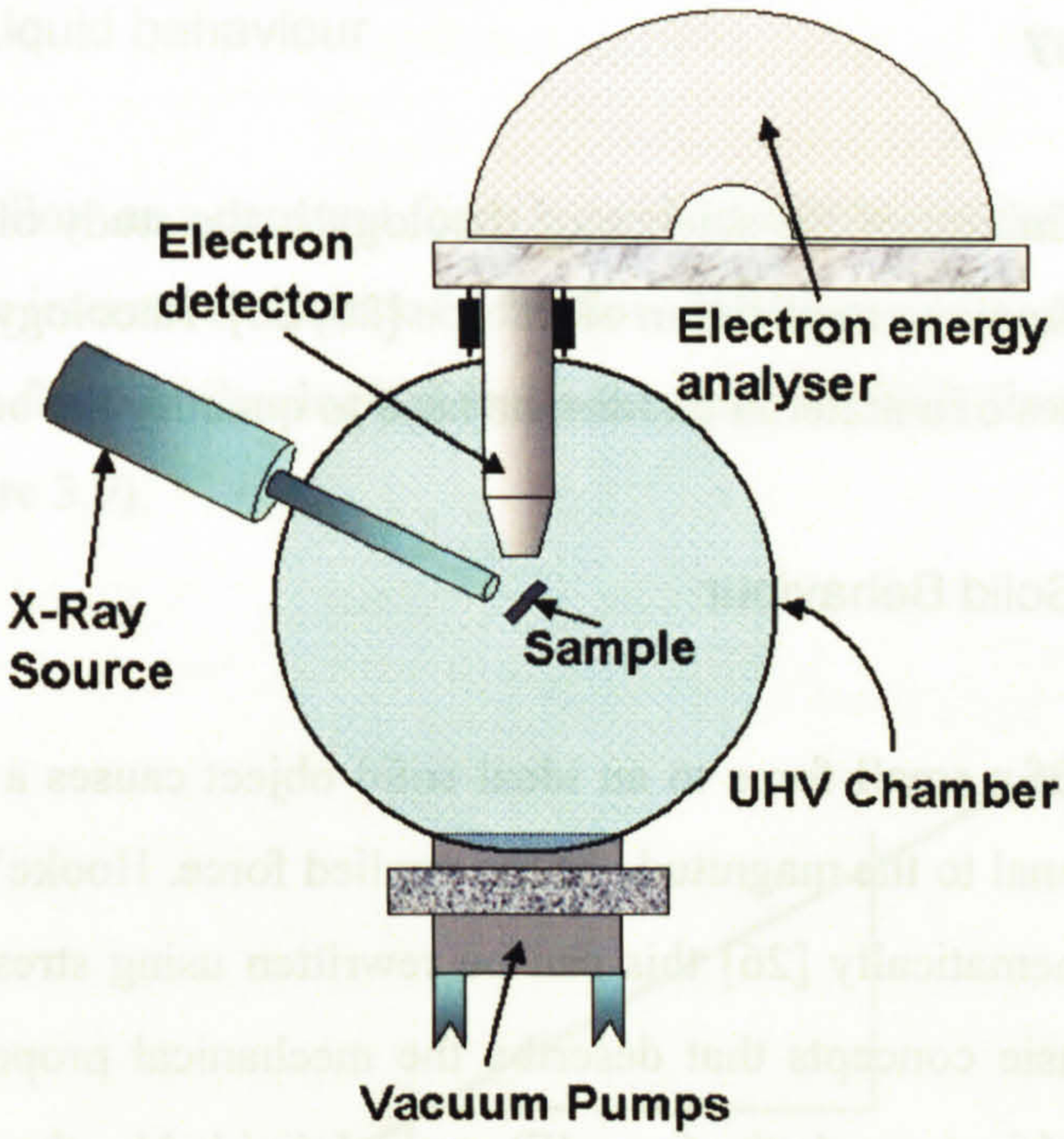

Figure 3.7. Schematic diagram of an XPS spectrometer.

The X-ray photoelectron spectrometer was manufactured by VG scientific as an Escascope photoelectron spectrometer (VG Scientific, The Birches Industrial Estate, Imberhorne Lane, East Grinstead, West Sussex, RH19 1UB, UK). It was fitted with a Mg Kα X-ray source (1253.6eV) and concentric hemispherical electron energy analyser. During the acquisition of the spectra the main chamber was kept at a pressure of 8×10^{-9} Torr [21]. The accelerating potential was 15 kV, emission current of 20 mA with a power output of 300 Watts.

3.4.4 Ultra Violet-Visible Spectroscopy

Ultra violet-visible spectroscopy (UV-vis) was used to measure the concentration of SAP polymer molecules for the adsorption isotherms. The absorption of light by a solution is proportional to the number of absorbing molecules [24] and is related by the Beer-Lambert expression [20].

A Hewlett Packard Diode Array Ultra Violet-Visible spectrometer Model 8453 with built-in Hewlett Packard software was used throughout.

3.4.5 Rheology

The classical definition of the science of rheology is the study of the deformation of matter resulting from the application of a force [25, 26]. Rheology is a measure of the handling properties of a material and can be used to quantify the behaviour [27].

3.4.5.1 Elastic Solid Behaviour

The application of a small force to an ideal solid object causes a deformation that is directly proportional to the magnitude of the applied force. Hooke's law describes this relationship mathematically [26] this can be rewritten using stress and strain. Stress and strain are basic concepts that describe the mechanical properties of a material. Stress (σ) on an object equals the force (F) applied divided by the area over which the force acts (A) (equation 3.1) and the strain (γ) is a measure of the relative deformation of the object under the stress (equation 3.2) [20]. A rheometer measures the rheological properties as a function of rate or frequency of deformation. For liquids the simplest devices impose a shearing flow on the liquid and measure the resulting stresses, or alternatively, impose a shearing stress and measure the resulting shearing rate [29].

$$\sigma = \frac{F}{A} \qquad [3.1]$$

$$\gamma = \alpha \approx \tan \alpha = \frac{\delta x}{y} \text{ (for small } \alpha) \qquad [3.2]$$

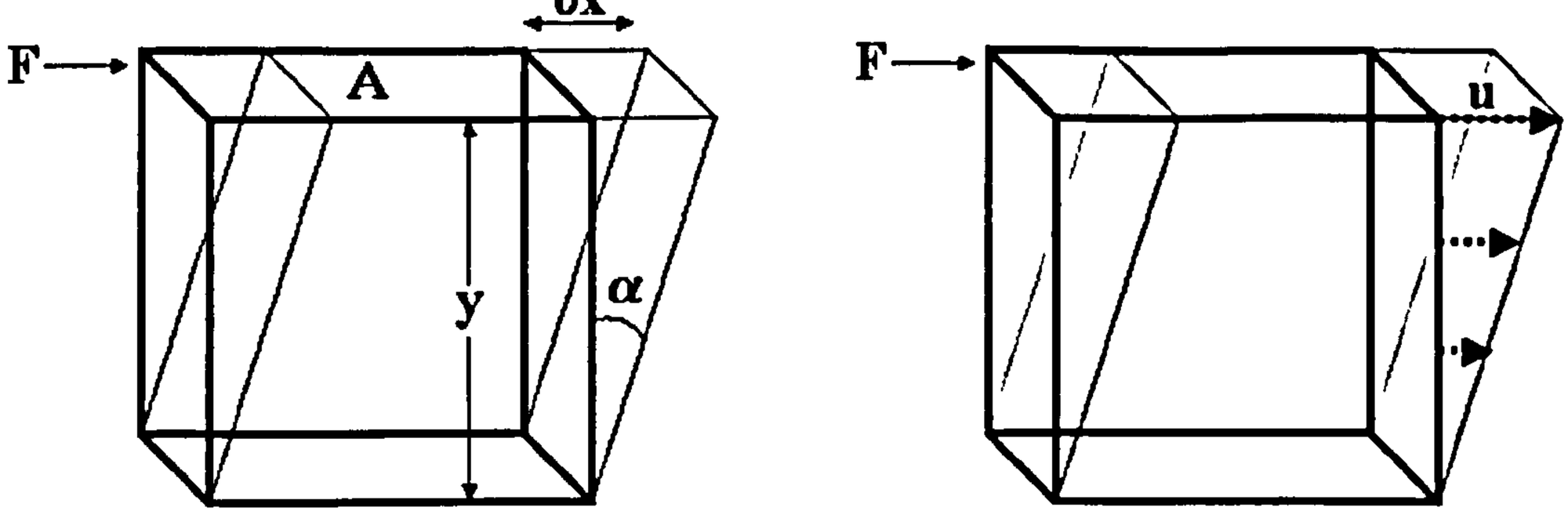

Figure 3.8. Response of a cube to an applied force.

3.4.5.2 Viscous Liquid behaviour

Ideal simple fluids flow as a constant force is applied with a constant rate proportional to the force with an internal resistance to the flow called viscosity, such fluids are in a state of Newtonian flow. In rheological terms the shear stress is linearly dependent on the shear rate (figure 3.9).

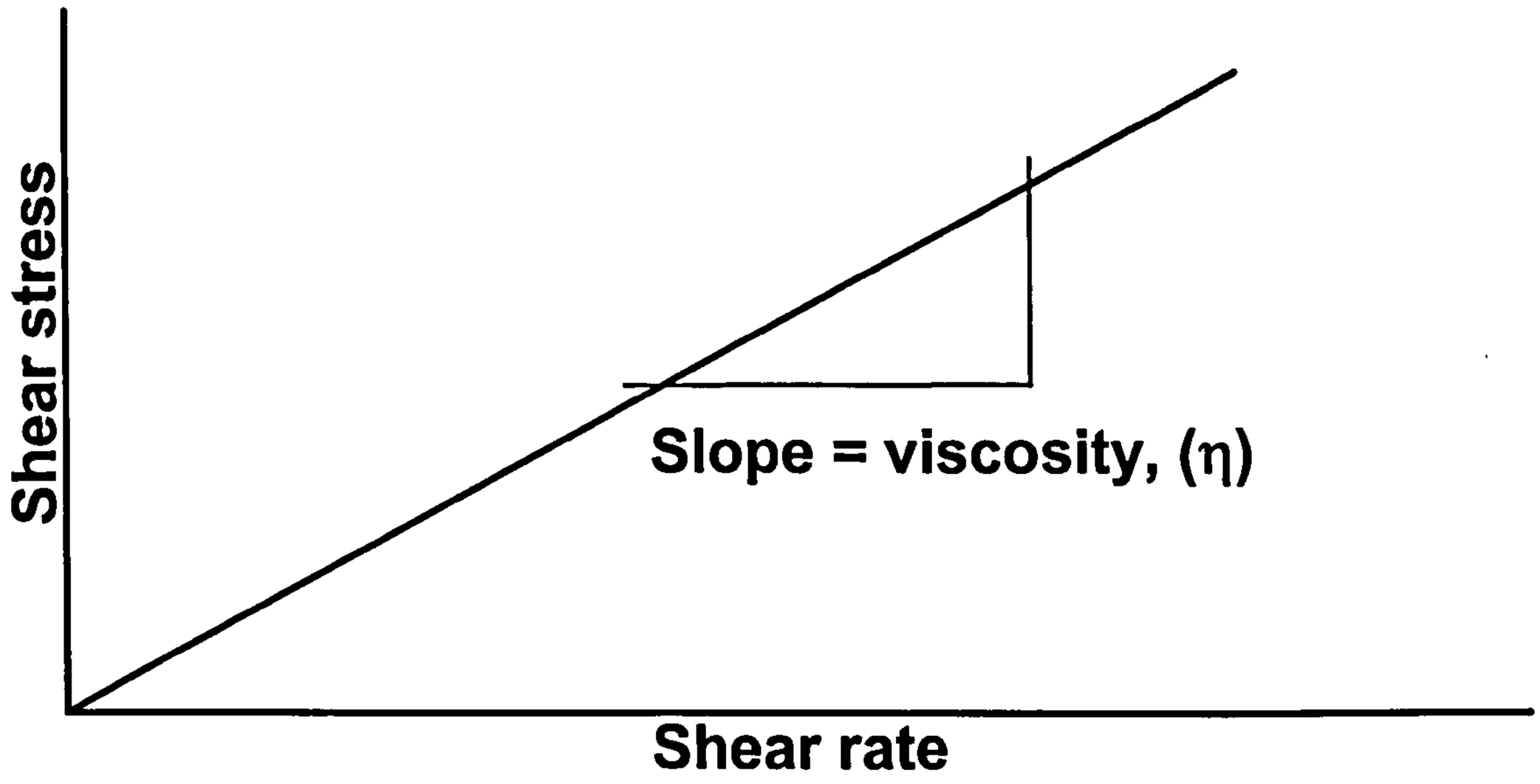

Figure 3.9. Schematic of the behaviour of a Newtonian fluid.

3.4.5.3 Viscoelastic behaviour

Between the extremes of solid and liquid behaviour lies intermediary viscoelastic behaviour where materials possess both viscous and elastic properties [25]. At very short timescales many materials that are thought of as liquids can display solid-like characteristics and at very long timescales solids can behave like liquids. "Silly putty" is an example of a material that behaves like a solid over very short timescales (it bounces when dropped on the floor) but behaves like a fluid over longer timescales (it flows if left to stand) [26].

The issue of timescales is very important when undertaking rheological experiments because the sample behaviour is dependent on the timescale of the observation. A simple test can be performed to measure the relaxation time of a sample (table 3.7) [28].

1.	Apply a strain (deformation) to a sample and the sample will become stressed.
2.	Energy is stored in the sample.
3.	Internal rearrangements within the sample cause the stress to relax with a characteristic relaxation time (τ_r).

Table 3.7. Simple measurement of the relaxation time.

The Deborah Number (*De*) is defined as the ratio of the relaxation time (τ_r) to the experimental timescale (t_{expt}) of the sample.

$$De = \frac{\tau_r}{t_{expt}} \qquad [3.3]$$

At high Deborah number the measurement is fast compared to the fluids ability to relax giving a solid-like response and at low Deborah number the sample will relax more rapidly than the timescale of the measurement [29]. Samples that show a time dependent response in their behaviour are termed viscoelastic [27] and include a wide range of colloid and polymer dispersions.

$De \rightarrow 0$	$De \rightarrow \infty$	$De \approx 1$
Viscous fluid behaviour.	Elastic solid behaviour.	Viscoelastic behaviour

The range of behaviour that dispersions can show is as varied as the range of dispersions themselves. Typical rheograms are shown below (figure 3.10).

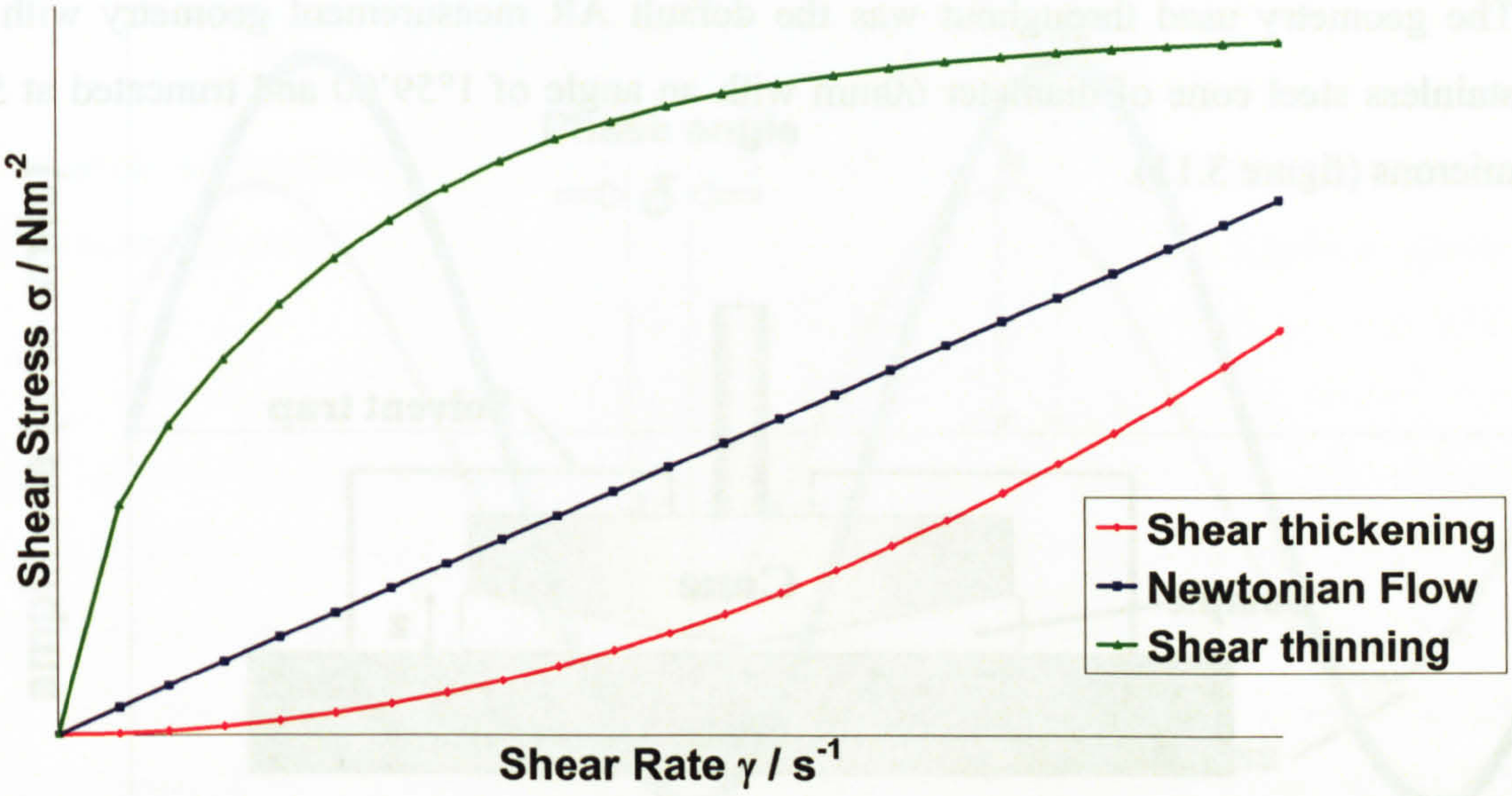

Figure 3.10. Examples of the flow curves for Newtonian and non-Newtonian fluids.

Shear-thinning is defined as the reduction of viscosity with increasing rate of shear in a steady shear flow [25]. Lipstick is a good example of a material that shear thins as it is applied to the lips leaving the bulk of the material undeformed.

Shear-thickening is defined as the increase of viscosity with increasing rate of shear in a steady shear flow [25]. Concentrated corn flour in water behaves like this, as it does not yield if struck with a spoon but can be poured from a cup.

Aqueous and non-aqueous clay dispersions display some very interesting rheological properties and have been studied by many groups [30-33]. One very common feature of clay dispersions is shear thinning behaviour where the viscosity of the sample decreases as the shear rate increases. Shear thinning occurs as the anisotropic clay particles align as the shear rate increases and aggregates start to break down in the dispersion.

3.4.5.4 Rheological measurements

The rheological measurements were made by placing a sample with all bubbles removed between a flat plate and a truncated cone of a known diameter and profile (the geometry). The cone was oscillated at a chosen frequency and the complex response of the sample was measured.

The geometry used throughout was the default AR measurement geometry with a stainless steel cone of diameter 60mm with an angle of 1°59'00 and truncated at 58 microns (figure 3.11).

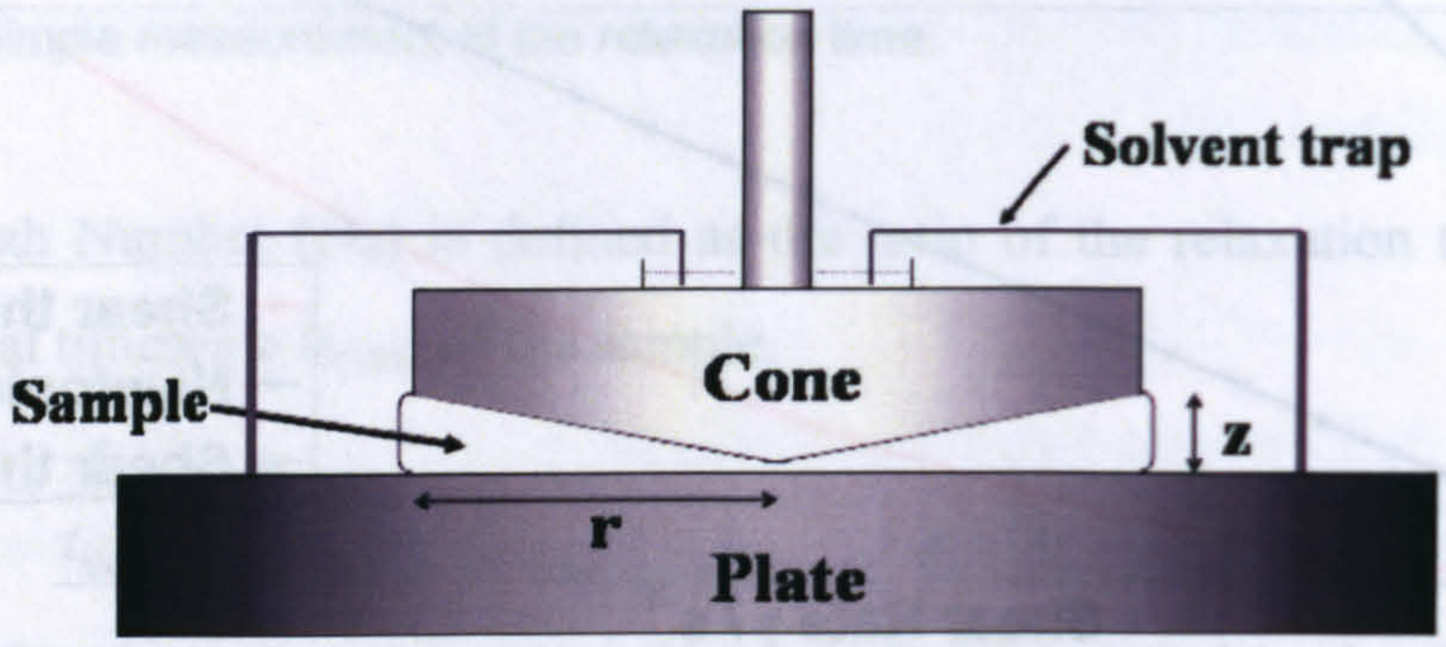

Figure 3.11. Cone and plate geometry used for the rheological measurements.

3.4.5.5 Phase angle

If an oscillating strain at a given frequency is applied to a sample an oscillating stress in direct response will quickly develop due to transient sample and instrumental responses. If the strain has an oscillating response with time then the stress will also be oscillating with time [26] (figure 3.12). The phase difference (δ) is the difference between the peak value of the stress and the peak value of the strain in radians at a given value of the radial frequency, ω (units of radians per second). If the sample consists of an elastic solid when a tangential displacement is applied a strain in the sample is produced and the displacement is transmitted straight through the sample. This response is in phase with the strain so the phase angle will be zero. If a Newtonian liquid is placed between the cone and plate the peak stress is out of phase by π /2 radians because the peak stress is proportional to the rate of strain [26]. For viscoelastic materials it follows that the response will be in-between the two extremes.

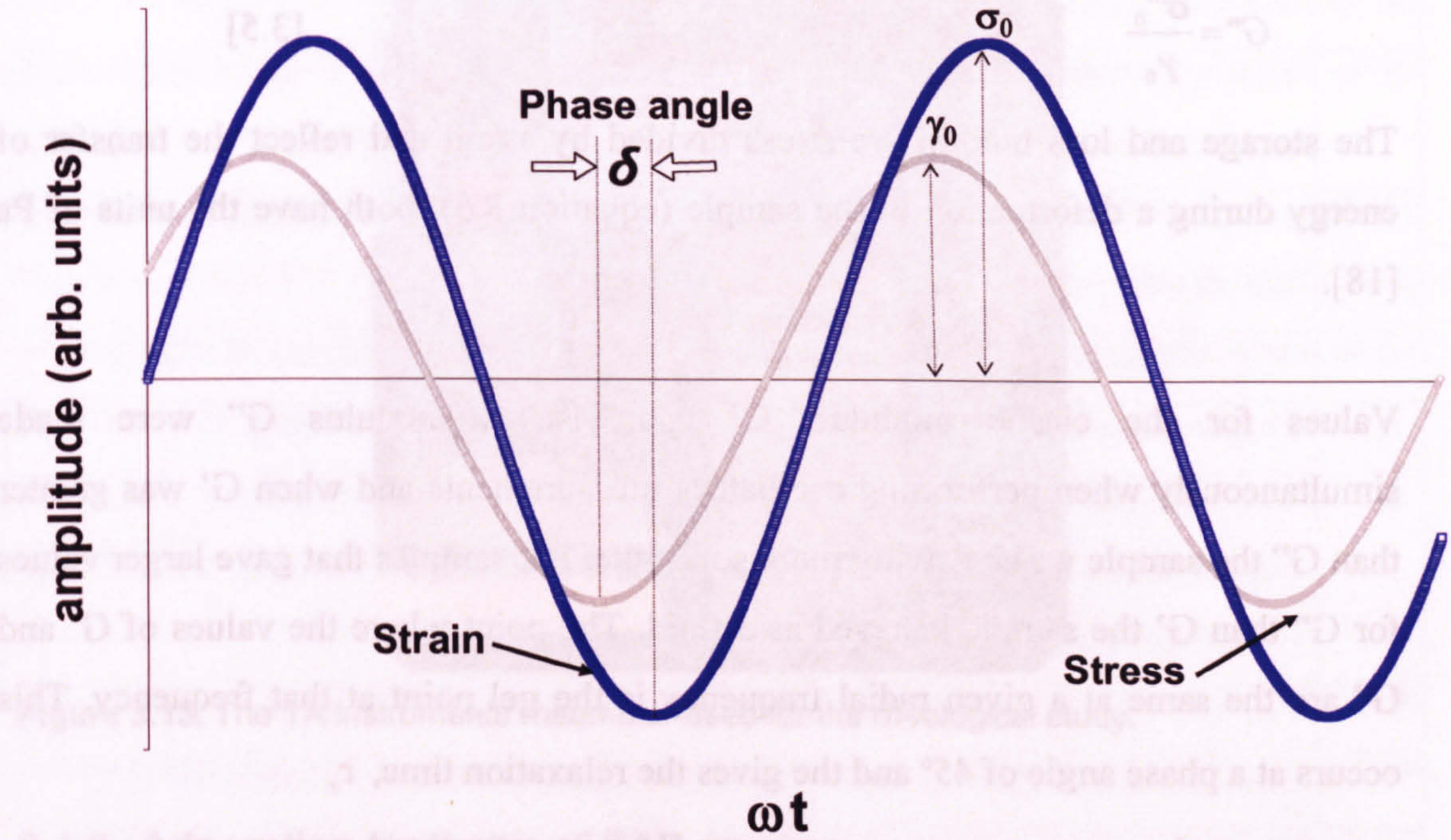

Figure 3.12. An oscillating strain and stress response for a viscoelastic material [26].

3.4.5.6 Gelation

A gel has the properties of a solid but comprises mainly of a fluid. There is no universally recognised strict definition because the concept of gelation covers such a wide range of scientific disciplines [34]. The features common to most definitions are that gelation occurs in a colloidal dispersion of particles as a result of the formation of a giant network when the concentration and inter-particle interactions are sufficiently high [1, 35, 36]. The solvent in most gels has freedom to move (bicontinuous) but remains within the network due to capillary forces [29]. A gel is made up of two main constituents: a fluid phase and a "solid" component that provides the building blocks of the structure which can store elastic energy.

We can define a quantity (G') as the storage or elastic modulus, (the in-phase shear modulus) given in equation 3.4 [18].

$$G' = \frac{\sigma'_0}{\gamma_0} \qquad [3.4]$$

and G" as the loss or viscous modulus, (the out of phase shear modulus) given in the equation

$$G''=\frac{\sigma''_0}{\gamma_0} \qquad [3.5]$$

The storage and loss moduli are stress divided by strain and reflect the transfer of energy during a deformation in the sample (equation 3.5), both have the units of Pa [18].

Values for the elastic modulus, G' and viscous modulus G" were made simultaneously when performing oscillatory measurements and when G' was greater than G" the sample was behaving more solid-like. For samples that gave larger values for G" than G' the sample behaved as a fluid. The point where the values of G' and G" are the same at a given radial frequency is the gel point at that frequency. This occurs at a phase angle of 45° and the gives the relaxation time, τ_r

$$\tau_r = \frac{1}{\omega} \qquad [3.6]$$

If the particles have a high affinity for the dispersing medium (solvent) but a weak long range interparticle interaction and short range repulsion then the suspension will behave as a fluid and is referred to as a "sol" [15].

3.4.5.7 Rheometer

The rheometer used for all experiments was a Thermal Advantage AR 1000-N made by TA Instruments Ltd. Europe House, Leatherhead, Surrey KT22 7UQ (figure 3.13).

The instrument was fitted with a TA Instruments extended temperature range Peltier plate for temperature control with a half and half mixture of ethylene glycol and water for cooling to below 0 °C.

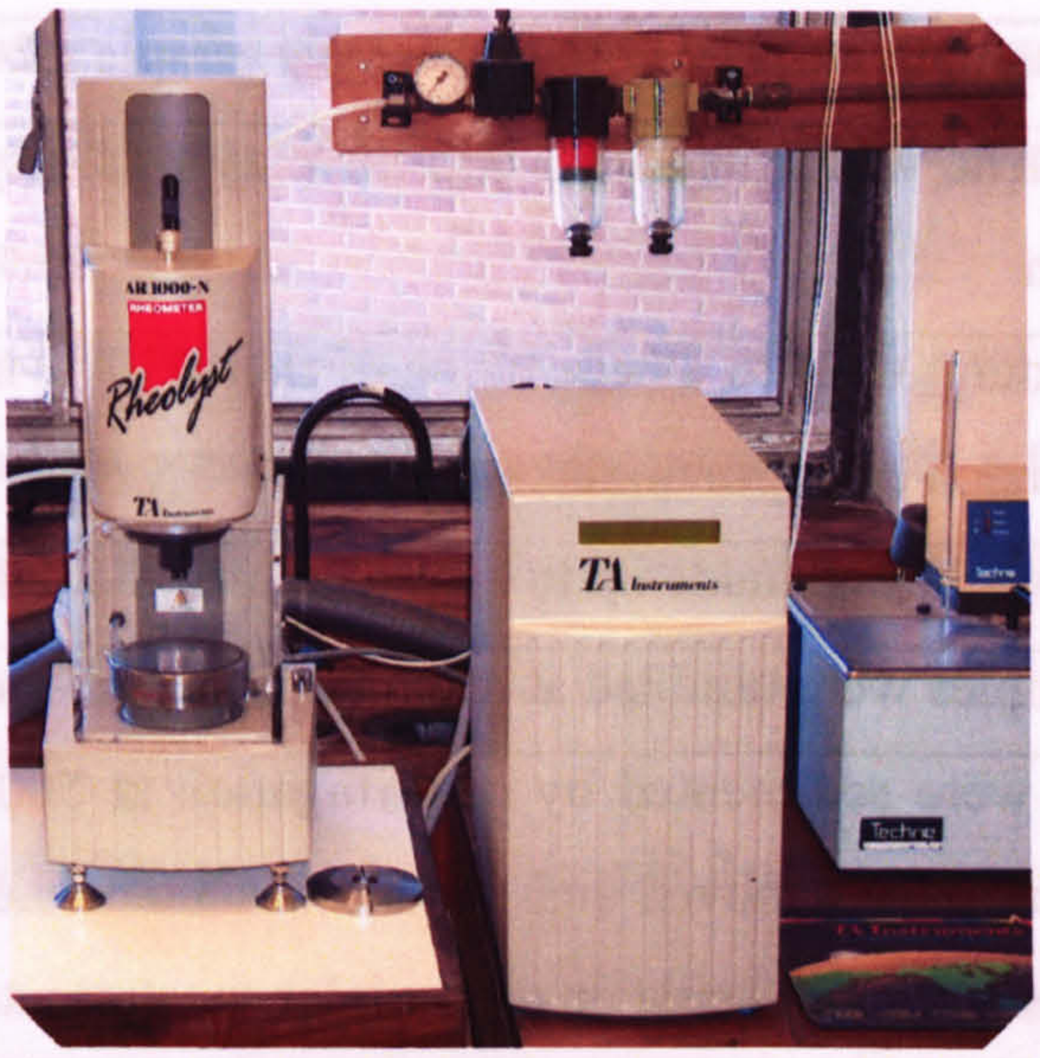

Figure 3.13. The TA instruments rheometer used for the rheological study.

3.4.6 Adsorption Isotherm of SAP on clay

With addition of SAP 230TP to a dispersion of surfactant treated clay in toluene, a dramatic decrease in the viscosity was observed indicative of particle stabilisation or destabilisation [6]. The colour of purified particles changed from light brown to the colour of the polymer, yellow suggesting the polymer had adsorbed to the surface of the clay. The amount of polymer adsorbed was measured by adding a known amount of free polymer to a solution of surfactant treated clay dispersed in toluene, allowing to mix thoroughly, and measuring by ultra-violet visible spectroscopy the amount of polymer left in the solution after the clay was removed by centrifugation. The measurements were repeated to reduce the magnitude of the errors. The procedure undertaken to carry out the adsorption isotherms is shown in table 3.8.

1.	0.5 g of clay sample was added to a clean dry sample tube.
2.	10.0 g of toluene was then added and the clay was dispersed by spin mixing and sonication
3.	Measured amounts of 10% w/w solution of SAP 230TP in toluene was added to the clay dispersion and spin mixed.
4.	The sample weight was made up to 20 g with a further addition of toluene.
5.	Dispersed samples were tumbled at room temperature overnight.
6.	The particles were sedimented by centrifugation at 5000 rpm for 1 hour, the supernatant carefully removed and the absorbance of the SAP at a wavelength of 284 nm was measured using an ultra-violet spectrometer.
7.	For the more concentrated polymer solutions the supernatant was carefully diluted and the dilution factor was taken into account for the analysis.

Table 3.8. Protocol followed for SAP addition to surfactant treated clay adsorption isotherms.

3.4.7 Elemental Analysis

Elemental analysis was a very useful technique to determine the amount of nitrogen and carbon adsorbed to the surface of the clay samples as these elements were present only in the adsorbed species (quaternary ammonium surfactant or SAP stabiliser).

The elemental analysis was carried out using a Carlo Erba elemental analyser model EA1108 with an estimated accuracy of ±0.3% of the measured mass per measurement. The elements analysed were nitrogen, carbon, and hydrogen and at least two measurements were made for each sample to reduce errors.

3.4.8 Small Angle X-ray Scattering (SAXS)

Small angle X-ray scattering (SAXS) is a technique well suited for studying structural features in samples of colloidal dispersions. SAXS was performed by focusing a narrow X-ray beam on a sample and observing the coherent scattering pattern that arose from electron density inhomogeneities within the sample.

Due to the wavelength of the X-rays used for the scattering experiments, 1.54 Å, it was possible to see very small features in the samples. The X-rays are scattered by

electrons so a distribution in the electron density, [18], was required, provided by the high electron density of the clay surface compared to the lower electron density of the adsorbed layer and the solvent.

The samples were placed in the path of the X-ray beam for up to two hours and the resulting scattering pattern was averaged over this time with information on the rates of processes being lost. The features that stood out were periodic distances such as the distance apart of clay platelets.

3.4.8.1 The Scattering Vector and Reciprocal Space

Figure 3.14 is a schematic of a beam of radiation scattered at an angle of 2θ by inhomogeneities in the medium. If the scattering is elastic the wavelength of the incoming and outgoing beams are the same [29]. The scalar wavenumber k is defined as $2\pi n/\lambda$, where n is the index of refraction of the medium and n/λ is the wavelength in the scattering medium.The incoming wavevector ki is $2\pi n/\lambda$ times the unit vector in the direction of the propagation; the outgoing beam is defined analogously. If two rays are scattered at the same angle from points in the medium separated by a distance vector x' then there is a difference in the path length of the two rays given by $l2 - l1$. From trigonometry $kl2 = ks\ x'$ and $kl1 = ki\ x'$. The difference in the phase of the two beams is $\Delta\delta = kl2 - kl1 = ks\ x' - ki\ x' = q\ x'$

Where q is the scattering vector defined by

$$q = ks - ki, \qquad |q| = \frac{4\pi n}{\lambda}(\sin\theta) \qquad [3.7]$$

If the scattering is caused by tiny particles separated from each other by a periodic distance of x' then there will be a peak in the scattering at an angle at 2θ for which the phase difference is 2π. This corresponds to a q vector of magnitude $\frac{2\pi}{x'}$. This can be written as

$$d = \frac{2\pi}{q} \qquad [3.8]$$

where d is the separation distance.

There is an inverse relationship between the scattering vector (or angle) and the structural length scale producing the scattering [37].

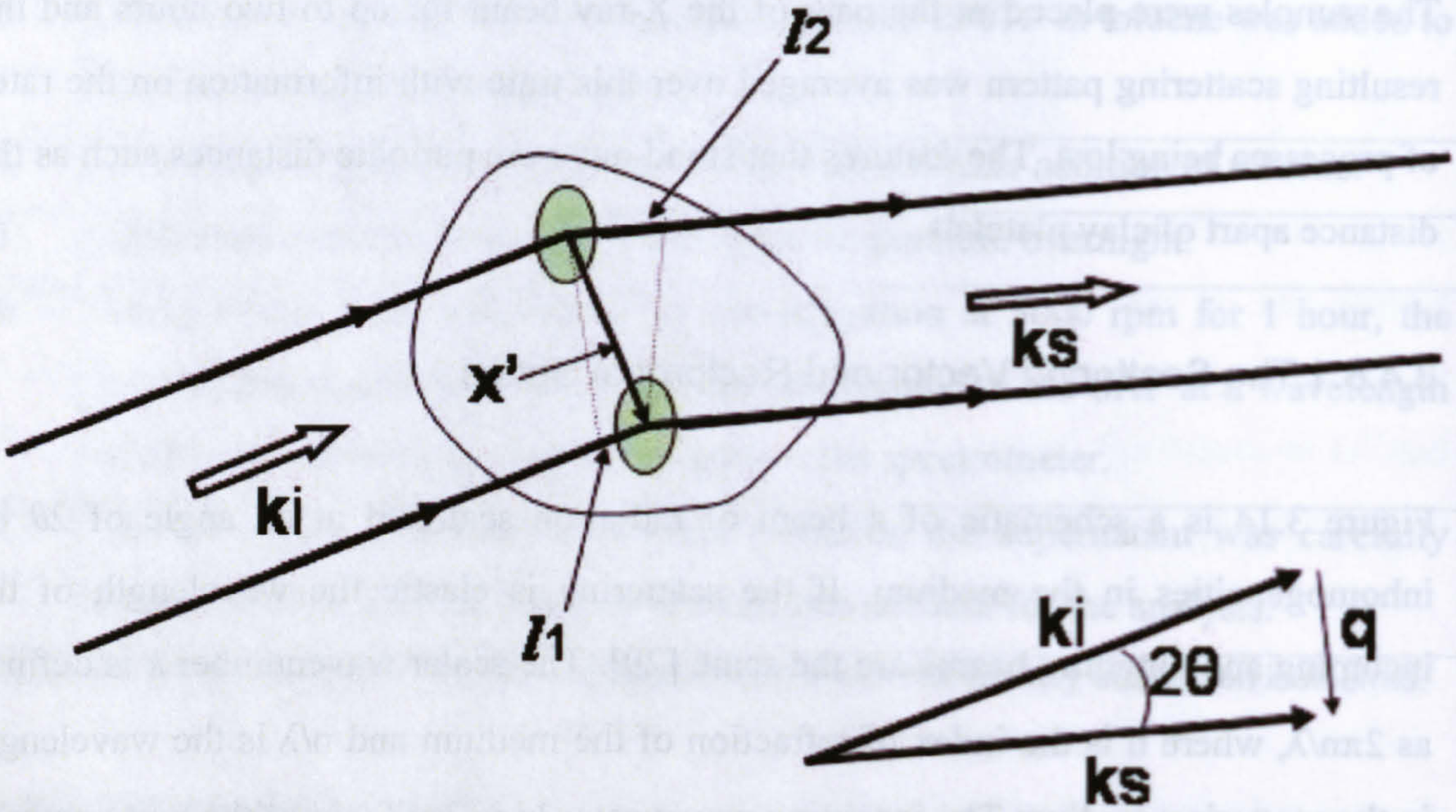

Figure 3.14. Constructive interference between two waves originating at two scattering centres.

Small angle X-ray scattering (SAXS) (figure 3.15) was carried out at room temperature, (21-23°C) using equipment constructed in the Physics Department of the University of Bristol. The measurements were carried out using copper Kα, (1.54Å wavelength), radiation from a sealed tube with other wavelengths excluded using a nickel filter and a carbon graphite monochromator. The scattering pattern was identified using a multi-wire area detector placed 840mm from the sample through an evacuated path giving a Q (scattering vector) range of 0.03 $Å^{-1}$ to 0.5 $Å^{-1}$. The sample to detector distance was calibrated using a silver behenate standard and the scattering data were averaged over the whole detector.

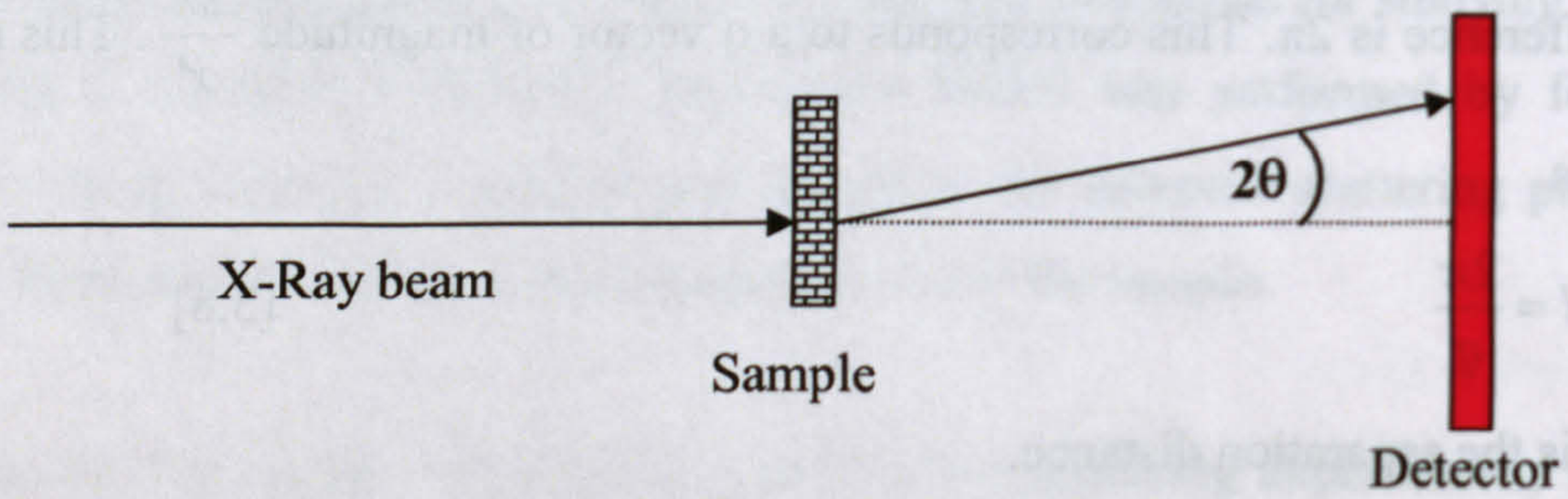

Figure 3.15. Schematic diagram of the SAXS instrument.

3.4.8.2 Lindemann Tubes

All the samples examined using the SAXS technique were placed in Lindemann tubes with a sample depth of 1.0 mm made from 0.16mm thick, high silica glass slightly flattened by heating, sealed with quick setting Araldite glue and held in a brass sample holder (figure 3.16).

Figure 3.16. Lindemann tube placed in the brass sample holder.

3.4.9 Surface Area Determination using the Brunauer, Emmett, and Teller (BET) isotherm

A direct method for determination of the surface area of a powdered solid was developed by Brunauer, Emmett, and Teller [38] from the physisorption of a vapour or gas on the solid surface. Nitrogen is most commonly employed as the adsorbate with a cross-sectional area taken as 0.162 nm^2 [15] but a number of gasses and vapours such as water vapour and ammonia have been used to determine powder surface area [39].

The adsorbed gas molecules are in dynamic equilibrium and the fractional coverage of the surface depends on the pressure of the overlying gas [40]. The variation of surface coverage with pressure at a given temperature is called the adsorption isotherm and the BET equation is derived by balancing the rates of evaporation and condensation for the various adsorbed molecular layers, and is based on the simplifying assumption that a characteristic heat of adsorption applies to the first molecular layer, while the

heat of liquefaction of the vapour or gas in question applies to adsorption in the second and subsequent molecular layers [15].

The BET equation is [41]:

$$\frac{P}{V_S(P_0-P)}=\frac{1}{V_M C}+\frac{(C-1)P}{V_M C P_0} \qquad [3.9]$$

Where P = equilibrium pressure, V_S = volume at standard temperature and pressure of gas adsorbed P_0 = vapour pressure of adsorbate at temperature of adsorbent, V_M = volume at standard temperature and pressure of gas required to form a monolayer, C = a constant involving the heat of adsorption.

For most cases of physisorption a graph of $\frac{P}{V_S(P_0-P)}$ against $\frac{P}{P_0}$ is linear in the relative pressure region of 0.05 to 0.35.

From the equation (x) the slope, $S=\frac{C-1}{V_M C}$ and the intercept, $I=\frac{1}{V_M C}$

$$S+I=\frac{C-1}{V_M C}+\frac{1}{V_M C}=\frac{1}{V_M} \qquad [3.10]$$

$$V_M=\frac{1}{S+I} \qquad [3.11]$$

From the V_M value the specific surface area of the solid can be calculated thus:

$$\text{Specific Surface Area}=\frac{V_M K}{Sample\ Weight\ in\ grams}$$

where $K=\frac{NA}{M_V}$ where $N=$ Avogadro's number, $A=$ area per adsorbate molecule, M_V = molar gas volume.

For the experimental measurements ideal behaviour of the gas is assumed $PV=nRT$ where $P=$ pressure, $V=$ volume of gas, $n=$ number of moles, $R=$ Universal gas constant, and $T=$ absolute temperature.

Since all the measurements are carried out at constant temperature then $PV \propto n$.
The BET method worked by holding a carefully weighed sample in a vacuum at 105 °C to desorb all gas and water vapour from the surface and then cooling in liquid nitrogen. Nitrogen gas at low pressure was passed over the cool sample and it was warmed back to room temperature to desorb the nitrogen from the surface of the clay. The increased pressure due to the desorbing gas was measured and was used to calculate the amount of nitrogen that had been adsorbed to the sample, assuming complete and uniform monolayer coverage and knowing the surface area of the nitrogen molecules was 0.162 nm^2. Despite the simplification the BET method is commonly used in surface area determination and the approximations involved are largely self-cancelling [15].

The crystallographic determined surface area of Laponite is 800 m^2g^{-1} [42] and bentonite is 752 m^2g^{-1} [39] but published BET surface areas are much less than this [19, 43, 44] due to aggregation of the clay plates. The plates aggregate and much of the surface area becomes inaccessible to the non-polar nitrogen adsorbate [39] so just the external surface is measured. By comparing the crystallographic data with the nitrogen BET data a value for the average number of clay plates in a grain of powder was estimated.

The estimate of the number of plates in a stack assumes all the plates are flat monodisperse discs with an edge area that can be neglected when compared to the face area. For bentonite plates with a diameter of 200 nm and a thickness of 1 nm the face area per plate is $2\Pi r^2$ (62800 nm^2) where r is the radius, and the area of the plate edge is Πdh (628 nm^2) where d is the diameter and h is the thickness of the plate. When 2 plates aggregate face to face they were assumed to lie perfectly on top of each other making 2 faces unavailable for nitrogen adsorption and reducing the surface area by a factor of two. If three plates aggregate on top of each other the reduction in the surface area is by a factor of three. The ratio of surface area calculated from plate thickness given by crystallographic measurements to the BET surface area measurements gives the average number of plates in a stack. This calculation when applied to Laponite becomes less valid as the assumption that the edges do not contribute to the overall surface area of aggregates is less valid.

3.4.10 Birefringence box

For the observations of samples through crossed polarisers a home-made "birefringence box" was used (figure 3.17). This consisted of a light, a diffuser and crossed polarisers with a big gap between to hold a sample tube to see permanent or flow birefringence.

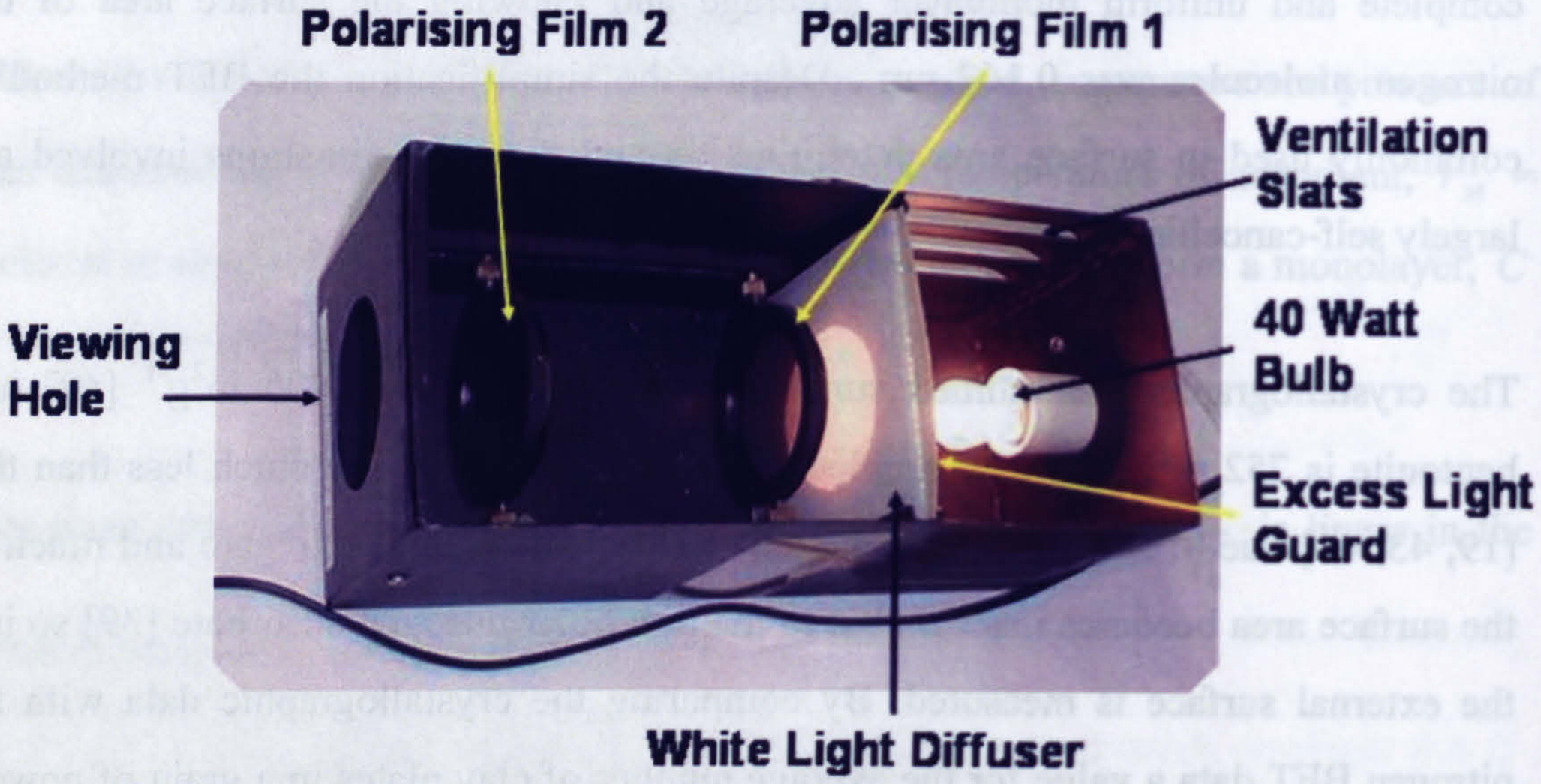

Figure 3.17. The birefringence box with the lid removed.

The lid of the birefringence box had an 80mm by 80mm square cut hole to hold the samples by hand between the crossed polarisers. The samples could be shaken to check for flow birefringence or left to stand to check for static birefringence. To keep the samples motionless for the photographs they were either fastened between the polarisers with sticky tape or placed on a stage between the polarisers.

The occurrence of birefringence originates from particles with orientationally dependent refractive indices [33, 45, 46]. Plate and rod shaped colloidal particles often display birefringence.

3.4.11 Polarising microscopy

The polarising microscope used to examine birefringent features in the samples was a desktop Leica DM LP polarising optical microscope fitted with a circular stage and a digital camera.

3.4.12 Differential Scanning Calorimetry (DSC)

Differential scanning calorimetry (DSC) was a technique for used to measure the energy necessary to keep the sample and an inert reference material at the same temperature, as the two specimens were heated at a controlled rate on a metal stage. There are many processes that have an effect on the energy required to heat a sample at a constant rate such as phase changes and decomposition and these showed up as peaks and troughs depending on the exothermic or endothermic nature of the changes [47] (figure 3.18).

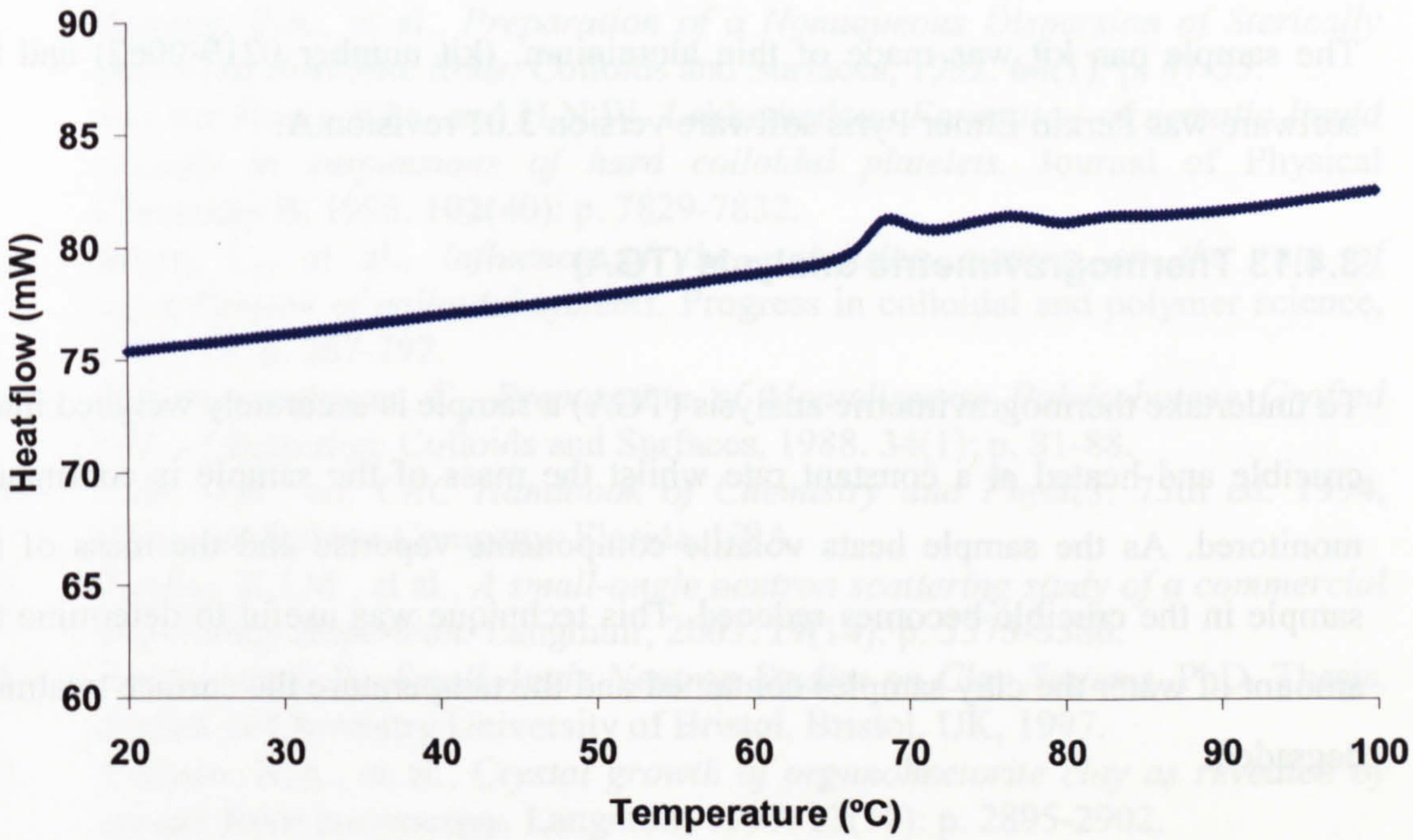

Figure 3.18. Model DSC data showing the peak as a surfactant goes into solution.

The peak seen in the DSC trace (figure 3.18) was endothermic as an increase in heat flow was required to keep the sample heating at constant rate. The area under the peak was equal to the total amount of energy required for the transition and by knowing the exact mass of the sample a molar value was possible.

By following a protocol all samples were subjected to the same heating and cooling rates enabling direct comparisons to be made.

1.	Weigh out 20-30 mg of sample in aluminium sample holder on microbalance.
2.	Place sample in calorimeter with empty reference in adjacent holder and place cover over the sample and reference to stop water vapour freezing to the metal.
3.	Cool samples to -30 °C and hold for 5 minutes.
4.	Heat samples at 10 °Cmin^{-1} up to 110 °C and hold for 2 minutes.
5.	Cool samples at 20 °C min^{-1} to -30 °C.

Table 3.9. DSC protocol used for all samples.

The DSC measurements were carried out on a Perkin Elmer DSC-7 fitted with a Perkin-Elmer TAC 7/3 instrument controller.

The sample pan kit was made of thin aluminium, (kit number 0219-0062) and the software was Perkin Elmer Pyris software version 3.01 revision A.

3.4.13 Thermogravimetric analysis (TGA)

To undertake thermogravimetric analysis (TGA) a sample is accurately weighed into a crucible and heated at a constant rate whilst the mass of the sample is continually monitored. As the sample heats volatile components vaporise and the mass of the sample in the crucible becomes reduced. This technique was useful to determine the amount of water the clay samples contained and the temperature the surface treatment degraded.

The instrument used was a STA 409 EP and the heating rate was kept at 5 °C min^{-1} up to 500 °C and the 30 mg samples were kept in a dry air atmosphere during the heating process.

3.4.14 Digital Camera

The camera used to take the digital photographs of the samples was an Olympus model C-860L with 1.3 million pixels. The images were downloaded using Camedia software.

3.5 References

1. van Olphen, H., *An Introduction to Clay Colloid Chemistry: For Clay Technologists, Geologists, and Soil Scientists*. 2nd Edition ed. 1977: John Wiley & Sons, Inc.
2. Levitz, P., et al., *Liquid-solid transition of Laponite suspensions at very low ionic strength: Long-range electrostatic stabilisation of anisotropic colloids.* Europhysics Letters, 2000. **49**(5): p. 672-677.
3. Langmuir, I., *The role of Attractive and Repulsive forces in the Formation of Tactoids, Thixotropic gels, Protein Crystals and Coacervates.* Journal of Chemical Physics, 1938. **6**: p. 873-896.
4. Jordan, J.W., *Organophilic Bentonites I.* Journal of Physical and Colloidal Chemistry, 1949. **53**: p. 294-306.
5. Theng, B.K.G., *The Chemistry of Clay-Organic Reactions*. 1974, London: Rank Precision Industries.
6. Buining, P.A., et al., *Preparation of a Nonaqueous Dispersion of Sterically Stabilized Boehmite Rods.* Colloids and Surfaces, 1992. **64**(1): p. 47-55.
7. van der Kooij, F.M. and H.N.W. Lekkerkerker, *Formation of nematic liquid crystals in suspensions of hard colloidal platelets.* Journal of Physical Chemistry B, 1998. **102**(40): p. 7829-7832.
8. Smits, C., et al., *Influence of the stabilizing coating on the rate of crystalization of colloidal systems.* Progress in colloidal and polymer science, 1989. **79**: p. 287-292.
9. Pathmamanoharan, C., *Preparation of Monodisperse Polyisobutene Grafted Silica Dispersion.* Colloids and Surfaces, 1988. **34**(1): p. 81-88.
10. Lide, D.R., ed. *CRC Handbook of Chemistry and Physics*. 75th ed. 1994, Chemical Rubber Company: Florida, USA.
11. Hanley, H.J.M., et al., *A small-angle neutron scattering study of a commercial organoclay dispersion.* Langmuir, 2003. **19**(14): p. 5575-5580.
12. Bongiovanni, R., *Small Angle Neutron Studies on Clay Systems.* PhD. Thesis. School of Chemistry University of Bristol, Bristol. UK, 1997.
13. Carrado, K.A., et al., *Crystal growth of organohectorite clay as revealed by atomic force microscopy.* Langmuir, 1997. **13**(10): p. 2895-2902.
14. Lewkowicz, N.M., *An Investigation into the Structuring of an Hydrophobic Clay in Silicone Fluid.* PhD. Thesis. Faculty of Medicine, University of London, London. UK, 2000.
15. Shaw, D.J., *Colloid and Surface Chemistry*. Fourth Edition ed. 1992, Oxford: Butterworth-Heinemann.
16. Hunter, R.J., *Introduction to Modern Colloid Science.* 1993, Oxford: Oxford University Press.
17. Thompson, D.W. and J.T. Butterworth, *The Nature of Laponite and Its Aqueous Dispersions.* Journal of Colloid and Interface Science, 1992. **151**(1): p. 236-243.
18. Hamley, I.W., *Introduction to Soft Matter. Polymer, Colloids, Amphiphiles and Liquid Crystals*. First ed. 2000, Oxford: John Wiley and sons, Ltd. 342.
19. Zou, J. and A.C. Pierre, *Scanning electron microscopy observations of "card-house" structures in montmorillonite gels.* Journal of Materials Science Letters, 1992. **11**: p. 664-665.

20. Atkins, P.W. and J. de Paula, *Atkins' Physical Chemistry*. Seventh Edition ed. 2002, Oxford: Oxford University Press.
21. Graveling, G.J., *A Study into the Adsorption of partially hydrolysed polyacrylamide on Kaolinite, Feldspar, and Quartz*. PhD. Thesis, Geology, 1997. University of Bristol, Bristol, UK.
22. Allen, G.C., et al., *Mineral/reagent interactions: an X-ray photoelectron spectroscopic study of adsorption of reagents onto mixtures of minerals*. Clay Minerals, 1999. 34(1): p. 51-56.
23. Allen, G.C., et al., *XPS analysis of polyacrylamide adsorption to kaolinite, quartz and feldspar*. Surface and Interface Analysis, 1998. 26(7): p. 518-+.
24. Williams, D.H. and I. Fleming, *Spectroscopic Methods in Organic Chemistry*. Fourth Edition ed. 1989, Maidenhead: McGraw-Hall Book Company (UK) Limited.
25. Barnes, H.A., J.F. Hutton, and K. Walters, *An Introduction to Rheology*. First Edition ed. Rheology Series, 3. 1989, Amsterdam: Elsevier.
26. Goodwin, J.W. and R.W. Hughes, *Rheology for Chemists*. 2000, Cambridge: The Royal Society of Chemistry. 290.
27. Macosko, C.W., *Rheology :principles, measurements, and applications*. First ed. 1994, New York: Wiley-VCH. 550.
28. Hughes, R.W., *Rheology*, in *the taught MSc. course . Colloid and Interface Science and Technology*. 1999: Bristol.
29. Larson, R.G., ed. *The structure and rheology of complex fluids*. Topics in Chemical Engineering, ed. K.E. Gubbins. 1999, Oxford University Press: New York.
30. Luckham, P.F. and S. Rossi, *The colloidal and rheological properties of bentonite suspensions*. Advances in Colloid and Interface Science, 1999. 82(1-3): p. 43-92.
31. Ramsay, J.D.F., *Colloidal Properties of Synthetic Hectorite Clay Dispersions .1. Rheology*. Journal of Colloid and Interface Science, 1986. 109(2): p. 441-447.
32. de Kretser, R.G., P.J. Scales, and D.V. Boger, *Surface chemistry-rheology inter-relationships in clay suspensions*. Colloids and Surfaces A: Physicochemical and Engineering Aspects, 1998. 137(1-3): p. 307-318.
33. Schmidt, G., A.I. Nakatani, and C.C. Han, *Rheology and flow-birefringence from viscoelastic polymer-clay solutions*. Rheologica Acta, 2002. 41(1-2): p. 45-54.
34. Kavanagh, G.M. and S.B. Ross-Murphy, *Rheological characterisation of polymer gels*. Progress in Polymer Science, 1998. 23(3): p. 533-562.
35. Weeks, J.R., J.S. van Duijneveldt, and B. Vincent, *Formation and collapse of gels of sterically stabilized colloidal particles*. Journal of Physics-Condensed Matter, 2000. 12(46): p. 9599-9606.
36. Abend, S. and G. Lagaly, *Sol-gel transitions of sodium montmorillonite dispersions*. Applied Clay Science, 2000. 16(3-4): p. 201-227.
37. Guinier, A., *X-Ray Diffraction In Crystals, Imperfect Crystals, and Amorphous Bodies*. 1994, New York: Dover Publcations, Inc.
38. Brunauer, S., P.H. Emmett, and E. Teller, *Adsorption of Gases in Multimolecular Layers*. Journal of the American Chemical Society, 1938. 60: p. 309-319.

39. van Olphen, H. *Determination of Surface Areas of Clays-Evaluation of Methods*. in *The International Symposium on Surface Area Determination*. 1969. IUPAC. Held at the School of Chemistry, University of Bristol, UK: Butterworths.
40. Mogford, R., *The Effect of Polymer Chain Architecture on the Adsorption and Dispersion Properties of Functionalised Oligomers*. PhD. Thesis. School of Chemistry, University of Bristol, Bristol, UK, 2002.
41. *MSc. Taught course: Surface and Colloid Science and Technology: Experiment 3*. 1993: Surface Area Determination by Nitrogen Adsorption. School of Chemistry, University of Bristol, Bristol, UK.
42. Grillo, I., P. Levitz, and T. Zemb, *Insertion of small anisotropic clay particles in swollen lamellar or sponge phases of nonionic surfactant*. European Physical Journal E, 2001. **5**(3): p. 377-386.
43. http://www.Laponite.com. 2002, Laporte Inc.
44. Rossi, S., et al., *Influence of low molecular weight polymers on the rheology of bentonite suspensions*. Revue De L Institut Francais Du Petrole, 1997. **52**(2): p. 199-206.
45. Decruppe, J.P., R. Hocquart, and R. Cressely, *Experimental-Study of the Induced Flow Birefringence of a Suspension of Rigid Particles at the Transition from Couette- Flow to Taylor Vortex Flow*. Rheologica Acta, 1991. **30**(6): p. 575-580.
46. Schmidt, G., et al., *Shear orientation of viscoelastic polymer-clay solutions probed by flow birefringence and SANS*. Macromolecules, 2000. **33**(20): p. 7219-7222.
47. Xie, W., et al., *Thermal Degradation Chemistry of Alkyl Quaternary Ammonium Montmorillonite*. Chemistry of Materials, 2001. **13**: p. 2979-2990.

4 Characterisation of the Clay Surface

4.1 Introduction.

In order to understand the behaviour and stability of the treated clay dispersions it was crucial to gain information about the clay and the surface treatment. A number of experiments were carried out on dry samples and dispersions of the untreated and treated clays to characterise the particles. Descriptions of the experiments can be found in chapter 3. The clay types used were Laponite RD, Wyoming bentonite and commercially available Claytone AF. The Claytone was described as montmorillonite [1], a major constituent of bentonite rock [2] and the structure was compared to a sample of Wyoming bentonite by X-ray diffraction.

The surface area per gram of the clay samples has been determined previously from crystallographic data [3, 4] and this was compared to direct surface area analysis undertaken with the BET adsorption isotherm method.

The amount of surfactant and polymer present in the washed and thoroughly dried treated clay powder was determined from the elemental analysis in terms of percentage values of nitrogen, carbon, and hydrogen. Nitrogen and carbon only exist in the pure clay samples as contaminants and a comparison of the elements present in the uppermost surface layers of the samples was carried out using X-ray photoelectron spectroscopy.

Thermogravimetric analysis was performed to obtain a value for the amount of water adsorbed to the surface of the treated and untreated particles and to find the temperature the surface treatment decomposed.

The amount of polymer adsorbed to surfactant treated clay particles was established by undertaking adsorption isotherms and unlike elemental analysis; this method was used to distinguished between the surfactant and polymer molecules.

4.2 Determination of Claytone clay type by X-ray Diffraction (XRD)

The X-ray diffraction technique was very similar to the small angle X-ray scattering SAXS technique (section 3.4.9) but was carried out at much higher angle and looked at intramolecular periodic features rather than the longer range intermolecular features seen using SAXS. The diffracted X-rays are given in terms of angle 2θ rather than the Q range.

The clay used for Claytone is described as montmorillonite [5, 6] and this was confirmed by comparison of XRD data with a sample of untreated Wyoming bentonite and DODAB Laponite (figure 4.1). The peak positions for the untreated bentonite and Claytone overlap exactly at high angle showing the internal structure of the clay particles were the same. The low angle peaks do not match exactly and this was due to the cationic surfactant coating of the Claytone. The diffraction pattern of DODAB Laponite sample was close to the Claytone but not exact showing small differences in the internal structures of Laponite and Claytone.

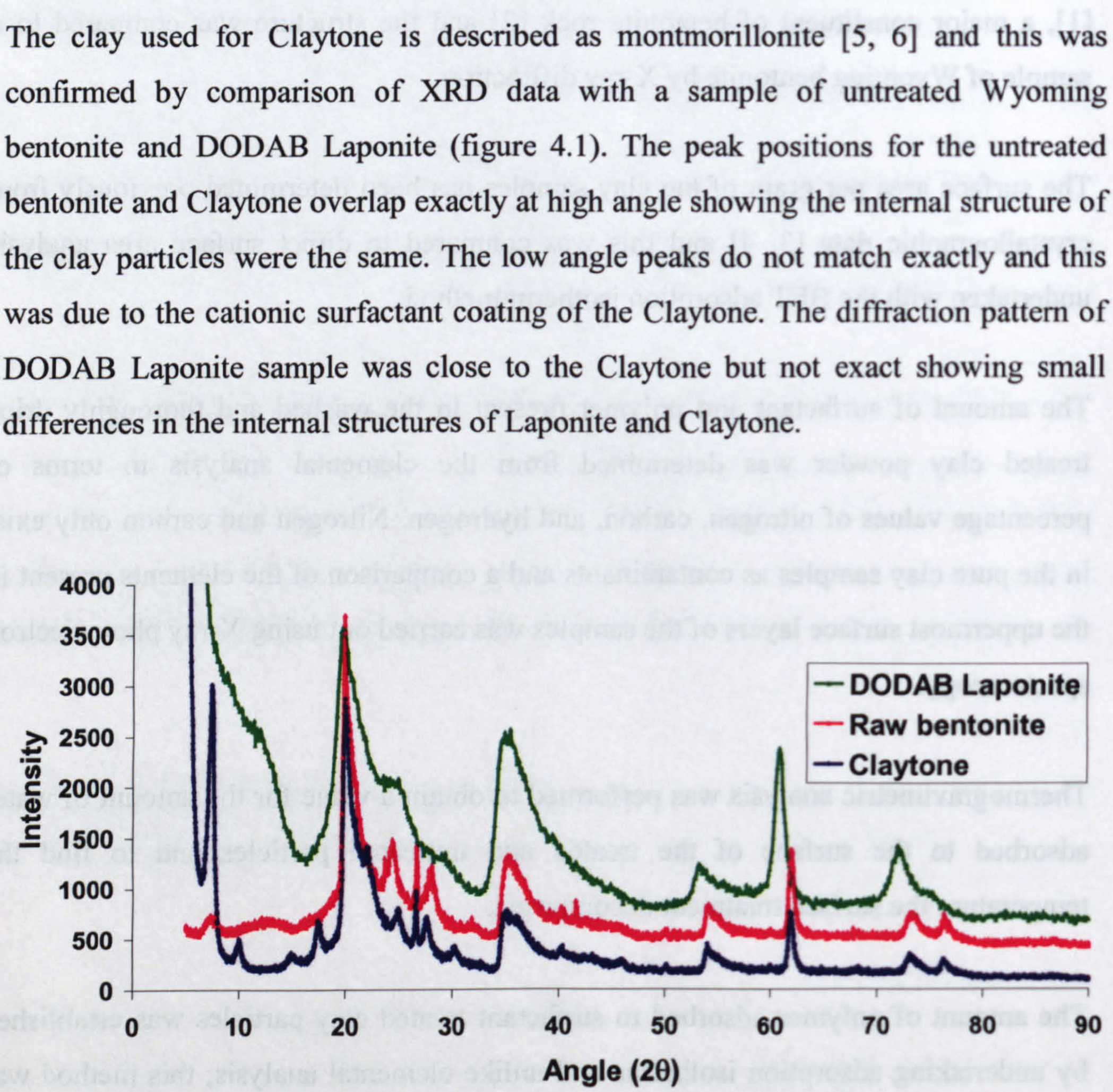

Figure 4.1. X-ray diffraction pattern of Claytone, untreated bentonite and DODAB Laponite showing the clay types are very similar.

4.3 Untreated clay samples

A sample of bentonite from Upton, Wyoming was obtained from Professor Ottewill (Bristol University) and was supplied with documentation from the American Petroleum Institute giving the origin of the sample (Petroleum Institute Clay Mineral Standard, project number 49). The bentonite was a fine light beige coloured powder. A sample of Laponite RD was obtained from Laporte as a fine white powder.

4.3.1 Water adsorption measured by Thermal Gravimetric Analysis (TGA) and oven drying of untreated clays

The clay samples if left open to the atmosphere for any length of time adsorb water and this can be a significant proportion of the mass of the sample (figure 4.2). The amount of water adsorbed on the surface of the untreated Laponite and bentonite samples was measured by thermal gravimetric analysis (section 3.4.13) under an argon atmosphere.

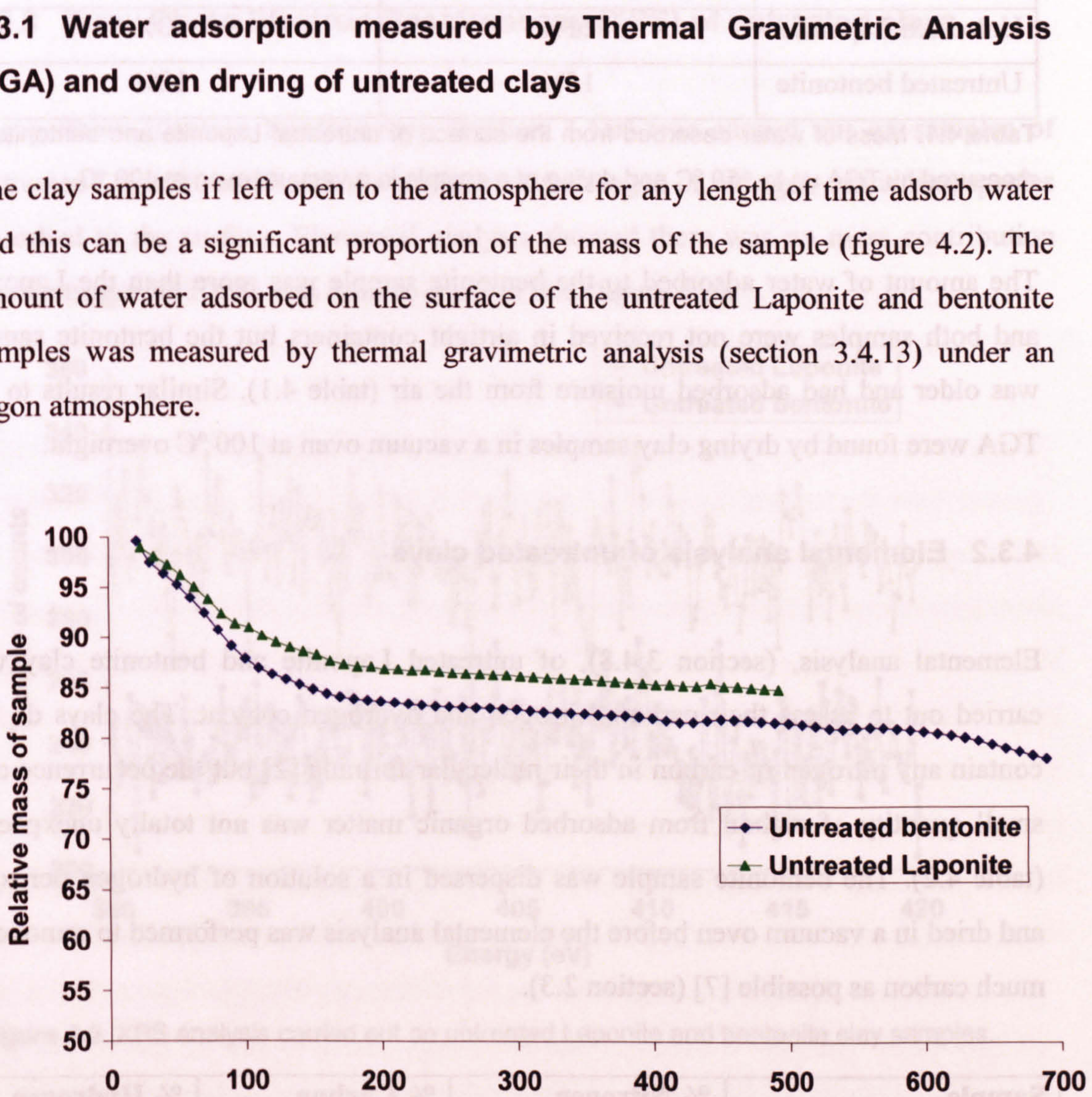

Figure 4.2. Thermo gravimetric analysis of untreated Laponite and bentonite.

The thermo gravimetric analysis gave sample weight loss as a function of temperature and the loss of mass up to 150 °C was attributed to evaporation of water from the

exposed surface of the clay. The graph shows a slow but steady loss of mass at temperatures above 150 ºC and this may also be due to desorption of water from between the layers of clay as structural changes in the clay such as dehydroxylation do not occur until 450 ºC [6].

Sample	**Mass of water desorbed from clay surface by TGA.**	**Mass of water lost from drying in a vacuum oven at 100 ºC**
Untreated Laponite	11%	10%
Untreated bentonite	15%	12%

Table 4.1. Mass of water desorbed from the surface of untreated Laponite and bentonite as measured by TGA up to 150 ºC and drying of a sample in a vacuum oven at 100 ºC.

The amount of water adsorbed to the bentonite sample was more than the Laponite and both samples were not received in airtight containers but the bentonite sample was older and had adsorbed moisture from the air (table 4.1). Similar results to the TGA were found by drying clay samples in a vacuum oven at 100 ºC overnight.

4.3.2 Elemental analysis of untreated clays

Elemental analysis, (section 3.4.8), of untreated Laponite and bentonite clay was carried out to assess their carbon, nitrogen and hydrogen content. The clays do not contain any nitrogen or carbon in their molecular formula [2] but the occurrence of a small quantity of carbon from adsorbed organic matter was not totally unexpected (table 4.2). The bentonite sample was dispersed in a solution of hydrogen peroxide and dried in a vacuum oven before the elemental analysis was performed to remove as much carbon as possible [7] (section 2.3).

Sample	**% Nitrogen**	**% Carbon**	**% Hydrogen**
Untreated Laponite	0.0	0.1	1.5
Untreated bentonite	0.0	0.2	0.8

Table 4.2. Elemental analysis of untreated vacuum oven dried Laponite and bentonite. Only nitrogen was completely absent from the samples.

Some organic material, of unknown origin, was found between the closely packed layers of clay. It was hard to remove all trace of the carbon despite treatment with the concentrated hydrogen peroxide solution. Hydrogen in the form of hydroxyl groups in the structure of the clay made up 0.5% of the weight of the untreated sample. The majority of the hydrogen content came from water adsorbed between the layers of clay surviving heat treatment in a vacuum oven overnight or water vapour becoming adsorbed to the sample as it was being prepared for the elemental analysis.

4.3.3 X-ray Photo Electron Spectroscopy (XPS) of untreated clays

X-ray Photo Electron Spectroscopy (section 3.4.3) was carried out on samples of untreated Laponite and bentonite to detect any nitrogen or nitrogen containing species adsorbed to the surface. Elemental analysis showed there was no mass contribution from nitrogen and XPS was used to confirm this (figure 4.3).

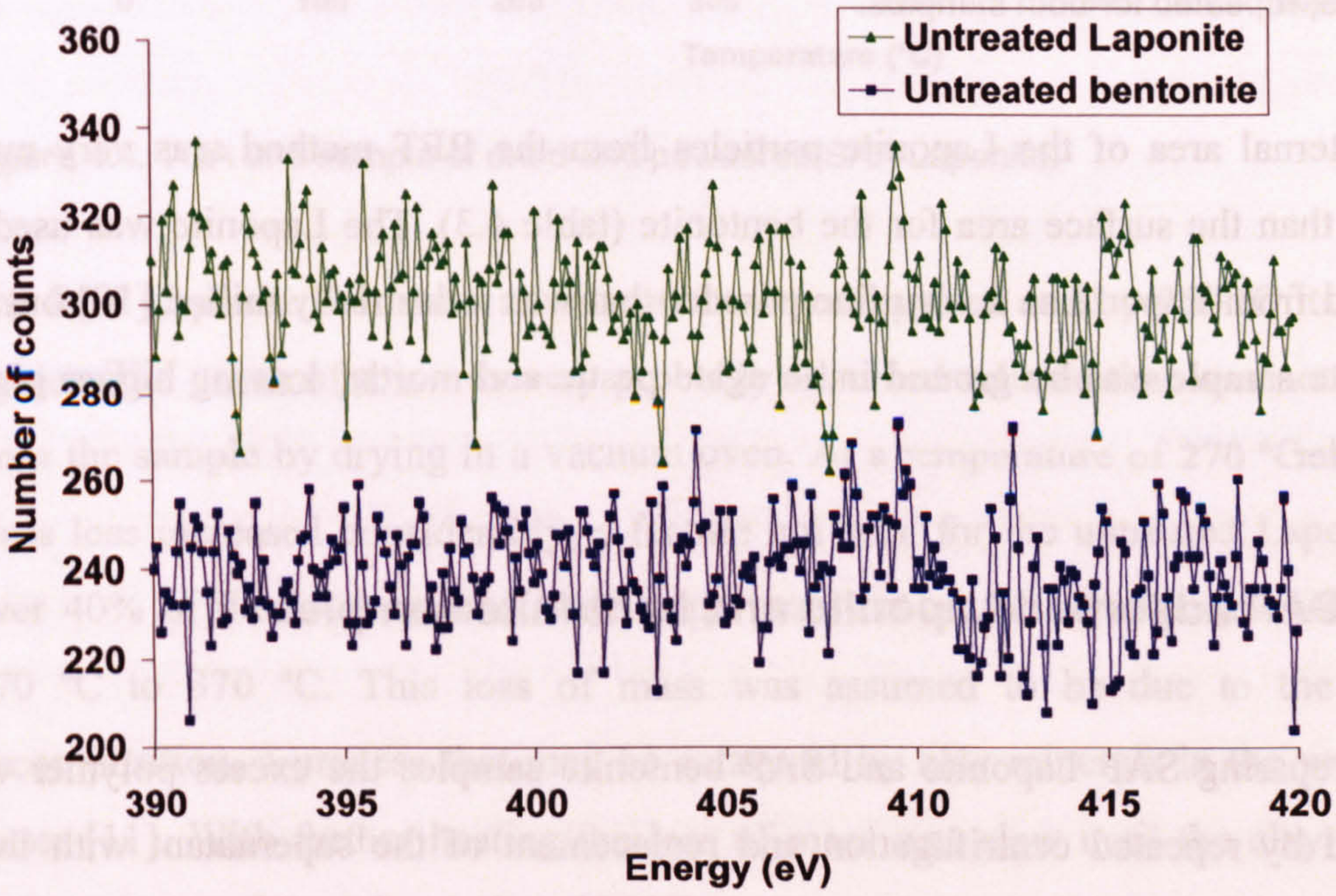

Figure 4.3. XPS analysis carried out on untreated Laponite and bentonite clay samples.

The XPS showed that no nitrogen was present on the surface of the Laponite or bentonite particles. The uneven trace was due to noise; the sample was scanned 20 times to reduce the noise level as far as possible.

4.3.4 BET adsorption isotherm of untreated clays

The external area found using the BET method (section 3.4.10) was smaller than the crystallographic surface area because not all of the surface area of the clay plates was available for adsorption of nitrogen [2]. The data was in agreement with published BET surface areas for bentonite (30-100 m^2g^{-1}) [2, 8, 9] and Laponite (350-400 m^2g^{-1}) [10].

Sample	BET surface area (m^2g^{-1})	Average (m^2g^{-1})
Untreated Laponite i	352	
Untreated Laponite ii	428	**390**
Untreated bentonite i	42.2	
Untreated bentonite ii	43.3	**42. 7**

Table 4.3. BET surface area determination for powdered untreated Laponite and untreated bentonite, repeated for both samples.

The external area of the Laponite particles from the BET method was very much greater than the surface area for the bentonite (table 4.3). The Laponite was used as received from Laporte as a very fine powder that was industrially milled [10] but the bentonite sample was by ground in an agate pestle and mortar, leaving bigger grains of powder.

4.4 SAP adsorbed Laponite and bentonite samples

After preparing SAP Laponite and SAP bentonite samples the excess polymer was removed by repeated centrifugation and replacement of the supernatant with fresh toluene (section 3.2.1). Examination of the supernatant by UV-Vis absorption showed no SAP peak. The SAP treated samples were then heated to 100 °C and sonicated as they cooled to room temperature. The samples were then centrifuged and the supernatant was analysed by UV-Vis absorption and no SAP absorption maxima were found indicating no SAP was desorbed from the clay particles. A small portion of the dispersions was dried in a vacuum oven at 100 °C overnight and characterised using TGA, elemental analysis and XPS.

4.4.1 Thermal Gravimetric Analysis of SAP Laponite

The thermal stability of a sample of dried SAP Laponite was tested using TGA and the sample was powdered in a pestle and mortar before the TGA was carried out in an argon atmosphere.

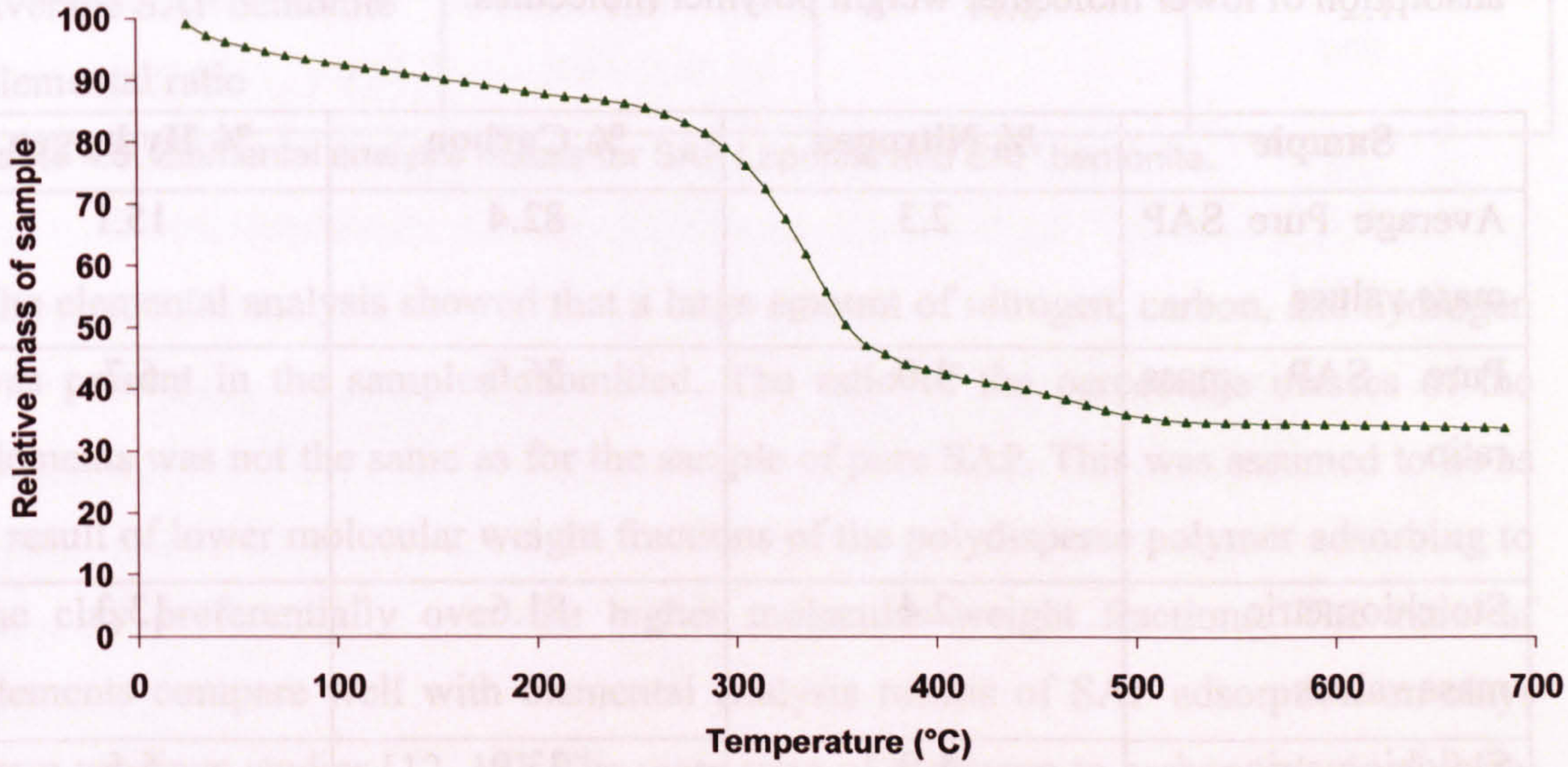

Figure 4.4. TGA of a sample of dried and powdered SAP Laponite.

The SAP Laponite lost mass as soon as heat was applied and by 250 ºC it was 14% lighter. The cause of this was very probably adsorbed toluene that was not removed from the sample by drying in a vacuum oven. At a temperature of 270 ºC the rate of mass loss increased considerably, a feature not seen for the untreated Laponite, and over 40% of the total mass of the sample was lost as the sample was heated from 270 ºC to 370 ºC. This loss of mass was assumed to be due to the polymer decomposition, a process that may be catalysed by clay minerals in the presence of water [11]. With further heating the loss of mass was slow until the clay structural hydroxyls were lost at just below 500 ºC.

4.4.2 Elemental analysis for SAP Laponite and SAP bentonite

Carrying out an adsorption isotherm on the samples of Laponite and bentonite treated exclusively with SAP polymer was impractical as the process was complex. Elemental analysis on cleaned samples of SAP Laponite and SAP bentonite was used as the primary method to find the amount of polymer adsorbed. Although it was

known from GPC (figure 2.4) that the SAP was polydisperse, it was assumed the anchoring group was always constant with 4 nitrogen atoms.

Dividing the percentage mass of each element by the percentage mass of nitrogen made the elemental mass ratio and it was very useful as a method to find preferential adsorption of lower molecular weight polymer molecules.

Sample	% Nitrogen	% Carbon	% Hydrogen
Average Pure SAP mass values	2.3	82.4	15.1
Pure SAP mass ratio	1.0	36.6	6.7
Stoichiometric mass values	2.4	81.6	13.3
Stoichiometric mass ratio	1.0	33.9	5.5

Table 4.4. Elemental analysis of SAP polymer and expected values from the stoichiometric formula.

The stoichiometric percentage mass of nitrogen, carbon, and hydrogen agree well with the values obtained from the elemental analysis (table 4.4). The percentage values do not add up to 100% as oxygen was also present in the molecule. The mass ratios show an increased amount of carbon and hydrogen present indicating polymer molecules on average had longer chains than the stoichiometric formula indicated, or alternatively the difference can be due to presence of some chains without headgroups.

After the treatment of Laponite and bentonite with SAP and thorough washing in toluene the small amounts of the samples were dried in a vacuum oven overnight at 100 °C then powdered and submitted for elemental analysis (table 4.5).

Sample	% Nitrogen	% Carbon	% Hydrogen
Average SAP Laponite	2.9	41.5	7.2
Average SAP Laponite Elemental ratio	1.0	14.3	2.5
Average SAP bentonite	2. 5	28. 8	5.1
Average SAP bentonite Elemental ratio	1.0	11.8	2.1

Table 4.5. Elemental analysis results for SAP Laponite and SAP bentonite.

The elemental analysis showed that a large amount of nitrogen, carbon, and hydrogen was present in the samples submitted. The ratio of the percentage masses of the elements was not the same as for the sample of pure SAP. This was assumed to be as a result of lower molecular weight fractions of the polydisperse polymer adsorbing to the clay preferentially over the higher molecular weight fractions. The ratio of elements compare well with elemental analysis results of SAP adsorption on clays from previous studies [12, 13]. The mass ratio of hydrogen to carbon remained fairly constant across the samples of adsorbed and pure SAP but all slightly lower than the stoichiometric mass value.

The amount of polymer adsorbed to the clay was estimated from the elemental analysis results for nitrogen and it was assumed every polymer molecule possessed 4 nitrogen atoms (the calculations can be found in appendix 2). The average area of each SAP molecule adsorbed to the surface of the Laponite was 1.2 nm^2 per molecule and for the bentonite 1.8 nm^2 per molecule. This assumes even adsorption over the whole surface including plate edges and also no aggregation occurring to block adsorption sites for the SAP. A literature value of 1.4 nm^2 per SAP molecule adsorbed to the surface of gibbsite [14] compares well with the values obtained here.

4.4.3 X-ray photoelectron spectroscopy of SAP Laponite and SAP bentonite

X-ray Photoelectron Spectroscopy, (XPS), was carried out on samples of SAP adsorbed bentonite and compared to SAP adsorbed Laponite. This type of experiment

has been used to determine the polymer adsorption on minerals and is semi-quantitative [15-17].

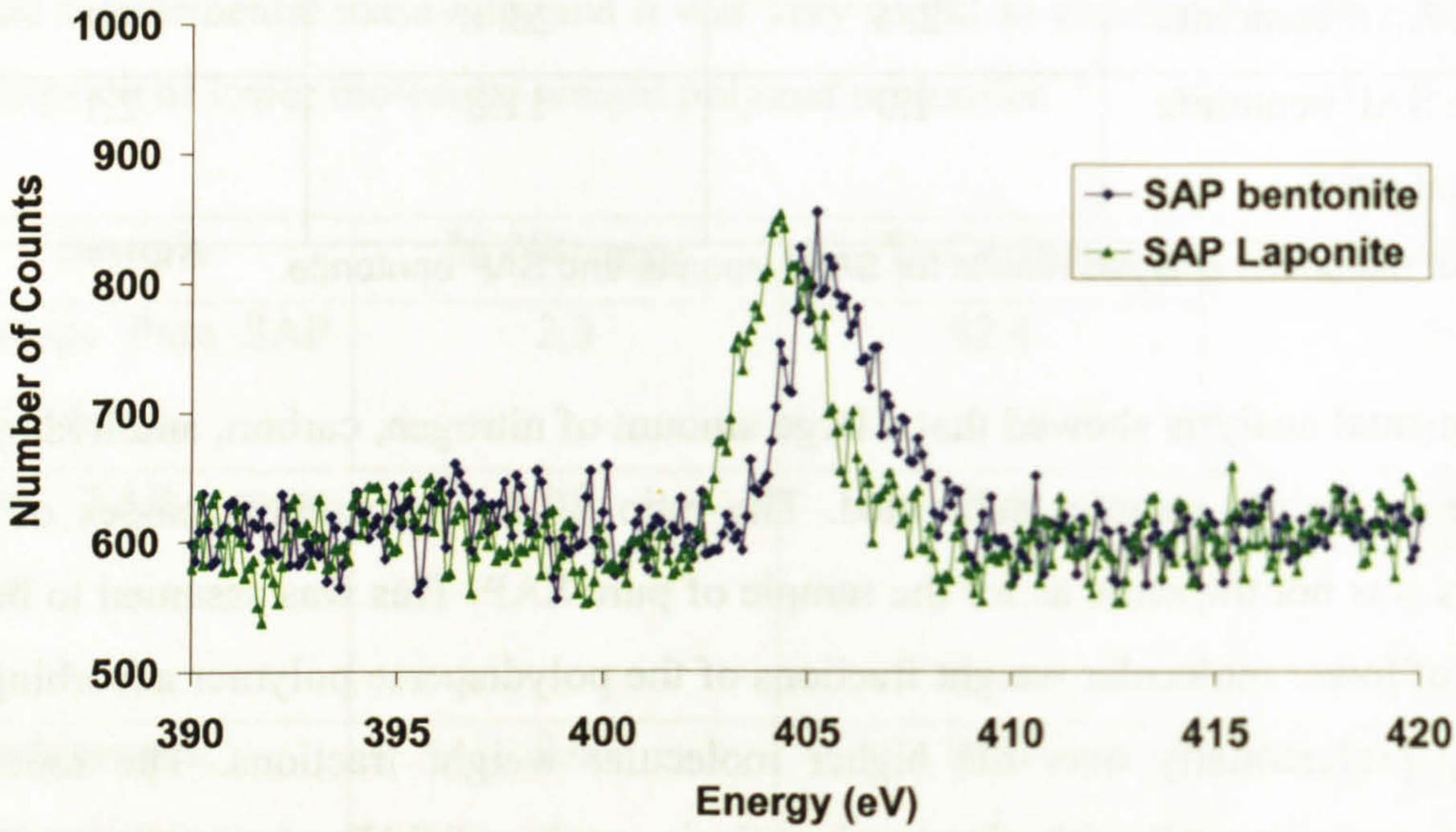

Figure 4.5. XPS analysis of SAP bentonite and SAP Laponite nitrogen 1s peak.

The absolute intensity from a sample does not depend on the concentration of the of the element alone but direct comparisons between the intensities of elements from different samples in the same environment can be made (figure 4.5) [18]. However, only electrons expelled from the uppermost layers contribute to the signal so the technique is blind to multilayer adsorption. It was assumed no multilayer adsorption had occurred for the polymer-clay particles and the particles were cleaned well to remove the free polymer.

SAP 230TP Laponite			SAP 230TP bentonite		
Element identity	Relative peak area	Centre (eV)	Element identity	Relative peak area	Centre (eV)
Nitrogen 1s	4.139	404.30	Nitrogen 1s	3.319	405.20

Table 4.6. Peak area analysis of nitrogen 1s peak for SAP Laponite and SAP bentonite. The values can be directly compared giving a relative concentration of the polymer.

The SAP Laponite peak was 1.25 times bigger than the SAP bentonite peak (table 4.6). Therefore the concentration of SAP on the surface is 1.25 times larger for the Laponite sample. From elemental analysis, assuming well-dispersed single plates, the concentration of the SAP on Laponite was 1.5 times larger, a potentially significant result as it indicates the surface area of the bentonite sample available for SAP adsorption was not as large as the crystallographic surface area and therefore aggregation of the plates may have occurred.

4.5 Determination of the Cationic Exchange Capacity (CEC) by elemental analysis

Determination of the CEC was carried out using elemental analysis results of a short-chain cationic surfactant adsorbed to the surface of the clays. Other methods have been used to determine the CEC [11] but this was a very simple method that was reliable.

Previous studies have also shown cationic surfactants with long chain lengths, such as DODAB, carry on adsorbing beyond the cationic exchange capacity. This is due to the attraction between the long hydrocarbon chains of the surfactant molecules in aqueous solution [2]. For the CEC measurements a short chain water soluble surfactant, tetrabutyl ammonium hydroxide, $(C_4H_9)_4N^+OH^-$, was chosen as all unadsorbed surfactant could be thoroughly washed off with water (table 4.7). Also no surfactant aggregates would be present on the surface of the clay and the quaternary ammonium ions occupied a small space, reducing the chance of obscuring adjacent cationic exchange sites. The procedure is outlined in section 3.2.2.

The CEC for the clays were measured and the elemental mass ratio was noted in order to have an idea about the amount of excess organic material and water present.

Sample	% Nitrogen	% Carbon	% Hydrogen
Stoichiometric mass value for tetrabutyl ammonium hydroxide.	5.8	79.3	14.9
Elemental mass ratio	1.0	13.7	2.6

Table 4.7. The expected elemental analysis for tetrabutyl ammonium ion. Expected results and mass ratio.

A comparison of the elemental mass ratio showed the amount of carbon and hydrogen to be higher than expected (table 4.8).

Sample	% Nitrogen	% Carbon	% Hydrogen
Laponite average	0.7	11.3	2.8
Elemental mass ratio	1.0	15. 5	3.9

Table 4.8. The amount of tetrabutyl ammonium adsorbed to the surface of the Laponite

The excess hydrogen in the DODAB Laponite sample was assumed to have come from adsorbed water in the sample. Polydispersity in the surfactant was suspected for the excess carbon in the sample.

The value for the CEC of the Laponite clay provided by the percentage nitrogen data from was 61 +/- 10 mmol/100g clay, (calculation is in appendix 1). Values for the CEC in the literature for Laponite were slightly higher at 75 mmol/100g clay [19, 20] and the average area per surfactant molecule on the clay surface was 2.2 nm^2.

For bentonite in particular there are many values given for the CEC from sources around the world [21-25] however the value is specific to the exact location from where the sample was obtained and samples from the same quarry can vary depending on the area within the quarry the bentonite was extracted [26].

Sample	% Nitrogen	% Carbon	% Hydrogen
Bentonite Average	0. 8	11.2	2.9
Elemental mass ratio	1.0	14.4	3.7

Table 4.9. Elemental analysis results for well-rinsed and vacuum dried tetrabutyl ammonium adsorbed bentonite.

The CEC for the sample of tetrabutyl ammonium adsorbed bentonite was 73 ± 10 mmol/100g clay (table 4.9). The literature values are higher (80-100 mmol/100g clay). For exactly the same sample of bentonite used in this study a value of 82 mmol/100g clay was reported [27].

4.6 Cationic Surfactant treated Clays

The preparation of the dioctadecyl dimethyl ammonium bromide (DODAB) treated clays was straightforward and quick. Any excess surfactant was washed off and the samples were dried in a vacuum oven overnight at 100 °C. The sample of Claytone was used as received but it was known to contain cationic surfactant 30% above the CEC of the clay [5].

4.6.1 Thermal Gravimetric Analysis of DODAB Laponite, DODAB bentonite, and Claytone

The thermal stability of a sample of dried SAP Laponite was tested using TGA and the sample was powdered in a pestle and mortar before the TGA was carried out in an argon atmosphere (figure 4.6).

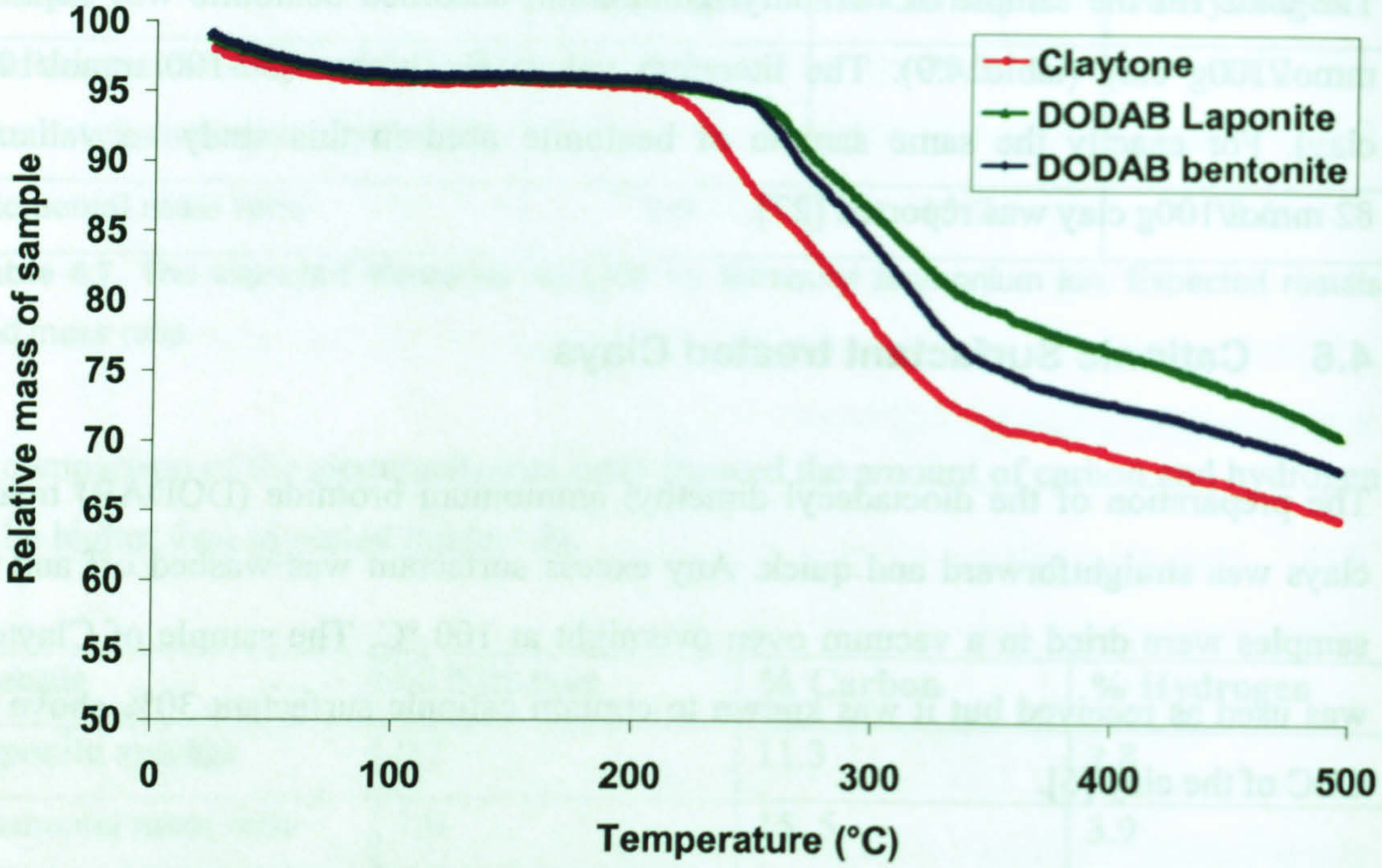

Figure 4.6. TGA of samples of DODAB Laponite, DODAB bentonite, and Claytone under an argon atmosphere.

For all of the samples about 4% of the mass was made up of water adsorbed to the plates (figure 4.6). The temperature at which the water was desorbed was up to 100 °C (the temperature of the samples in the vacuum oven). This water must have adsorbed when the samples were transferred at room temperature to the airtight sample containers and on exposure to the atmosphere before carrying out the TGA. It has been reported that the chains of the adsorbed surfactants on the surface of the clay displace the adsorbed water molecules [2] but clearly space for water to adsorb still exists.

After the water was desorbed there was little loss of mass until the samples were heated to 205 °C where the Claytone sample started to rapidly loose mass. The loss of mass was assumed to be due to the surfactant thermally degrading. This did not happen to the DODAB Laponite and DODAB bentonite samples until a temperature of 245 °C was reached. The reason for the difference between the DODAB samples and the Claytone was put down to the polydisperse cationic surfactant at higher concentration used for the Claytone. A number of processes have been suggested for

the thermal decomposition of the cationic surfactant adsorbed to clay samples [6, 11] but it was impossible to tell without analysing the products of the decomposition.

The data showed the dry samples very readily adsorbed water if exposed to the atmosphere and could be heated to well in excess of 100 ºC without degrading the surfactant on the surface of the clay.

4.6.2 Elemental analysis for DODAB Laponite and DODAB bentonite

The addition of DODAB to the samples of Laponite and bentonite was carried out at the calculated CEC to ensure that no excess surfactant became adsorbed. The measurements of the adsorbed amount were carried out in the same way as before, using elemental analysis (table 4.10).

Sample	% Nitrogen	% Carbon	% Hydrogen
Pure DODAB	2.31	73.06	14.87
Elemental mass ratio	1.00	31.63	6.44
Stochiometric mass value	2.55	82.91	14.55
Elemental mass ratio	1.00	32.51	5.71

Table 4.10. Elemental analysis results for pure DODAB and the expected mass values from the stoichiometric formula of the DODAB ion.

The measured DODAB values were different from the expected values because the expected values were of the DODAB ion, (leaving out the bromide). This was done because the bromide was removed in the sodium bromide salt when the DODAB became adsorbed to the clay.

Sample	% Nitrogen	% Carbon	% Hydrogen
DODAB Laponite Average	0.7	24.0	5.0
Elemental mass ratio	1.0	32.4	6.8
DODAB bentonite Average	0.9	26.8	6.0
Elemental mass ratio	1.0	30.8	6.8

Table 4.11. The elemental analysis results for DODAB Laponite and DODAB bentonite.

The amount of DODAB adsorbed to the surface of the Laponite clay was calculated from the mass of nitrogen in the sample (figure 4.11) as 75.3 mmol/100g clay and the DODAB bentonite at 94 mmol/100g clay. These values were above the CEC determined from the tetra butyl ammonium hydroxide preparation but within the range of values quoted in the literature (75 mmol/100g clay for Laponite and 80-100 mmol/100g clay for bentonite) The samples were prepared at the correct stoichiometric ratio and the increased amount of surfactant adsorbed was thought to be due to a non uniform distribution of the surfactant on the surface of the clay powders. Clay that did not have surfactant adsorbed may have been washed through the filter paper (Whatman number 5 paper circles, 2.5 μm retention).

4.6.3 Elemental analysis of Claytone

It was known that the amount of surfactant adsorbed to the surface of the Claytone was in excess of the CEC [5, 28] of the clay. Elemental analysis was carried out to find the value of the excess surfactant adsorbed (table 4.12). For this calculation the assumption was made that all the cationic surfactant adsorbed to the Claytone was dihydrogenated tallow (2HT), [29] and had one nitrogen atom per molecule. Two samples were prepared, one straight from the sample supplied and the other washed in a 50:50 mixture of water and propan-1-ol. The washed sample caused the solvent to foam indicating free surfactant was present and took 3 solvent exchanges before the foaming ceased.

Sample	% Nitrogen	% Carbon	% Hydrogen
Average as received Claytone	1.1	34.7	7.0
Elemental mass ratio	1.0	31.6	6.4
Average washed Claytone	1.0	29.6	6.0
Elemental mass ratio	1.0	28.4	5.8

Table 4.12. The elemental analysis results for Claytone.

The amount of surfactant adsorbed to the surface of the clay in a sample of Claytone was in excess of the CEC for montmorillonite with a value of 137 mmol/100g clay (table4.12). The correct CEC was 92 mmol/100g clay for the Claytone sample [1]. From the simple observation of foaming when the Claytone was rinsed in water/propan-1-ol mixtures some excess surfactant was washed off. After washing, the amount of surfactant adsorbed to the surface of the Claytone reduced to 117 mmol/100g clay. The reduction was not as low as the literature values for the CEC for montmorillonite and it was assumed that a small excess of cationic surfactant remained adsorbed to the surface of the Claytone [11, 24]. For this reason all of the samples of Claytone AF used for experiments were not repeatedly washed in an attempt to clean the particles. The difference made by the excess surfactant to the behaviour of the Claytone sample was assessed by comparison with the control DODAB bentonite samples.

4.6.4 Surface coverage by surfactant

If monolayer coverage of the cationic surfactant molecules on the clay surface is assumed the average area per surfactant molecule can be estimated from the elemental analysis data and adsorbed amount of surfactant.

Type of Clay	Surface area of clay (m^2g^{-1})	mmol of surfactant g^{-1} of clay	Number of surfactant molecules g^{-1} clay	Area per surfactant molecule (nm^2)
Laponite	800	0.8	$4.5x10^{20}$	1.8
Bentonite	752	1.1	$6.6x10^{20}$	1.3
Claytone	752	1.4	$8.2x10^{20}$	0.9

Table 4.13. Area per surfactant molecule based on percentage mass of nitrogen from elemental analysis data.

4.6.5 X-ray photoelectron spectroscopy of DODAB Laponite, DODAB bentonite and Claytone

From elemental analysis it was shown that Claytone AF had a larger amount of cationic surfactant adsorbed to the surface than DODAB Laponite and DODAB bentonite. The XPS of the nitrogen 1s peak from the surfactant was used to confirm this (figure4.7).

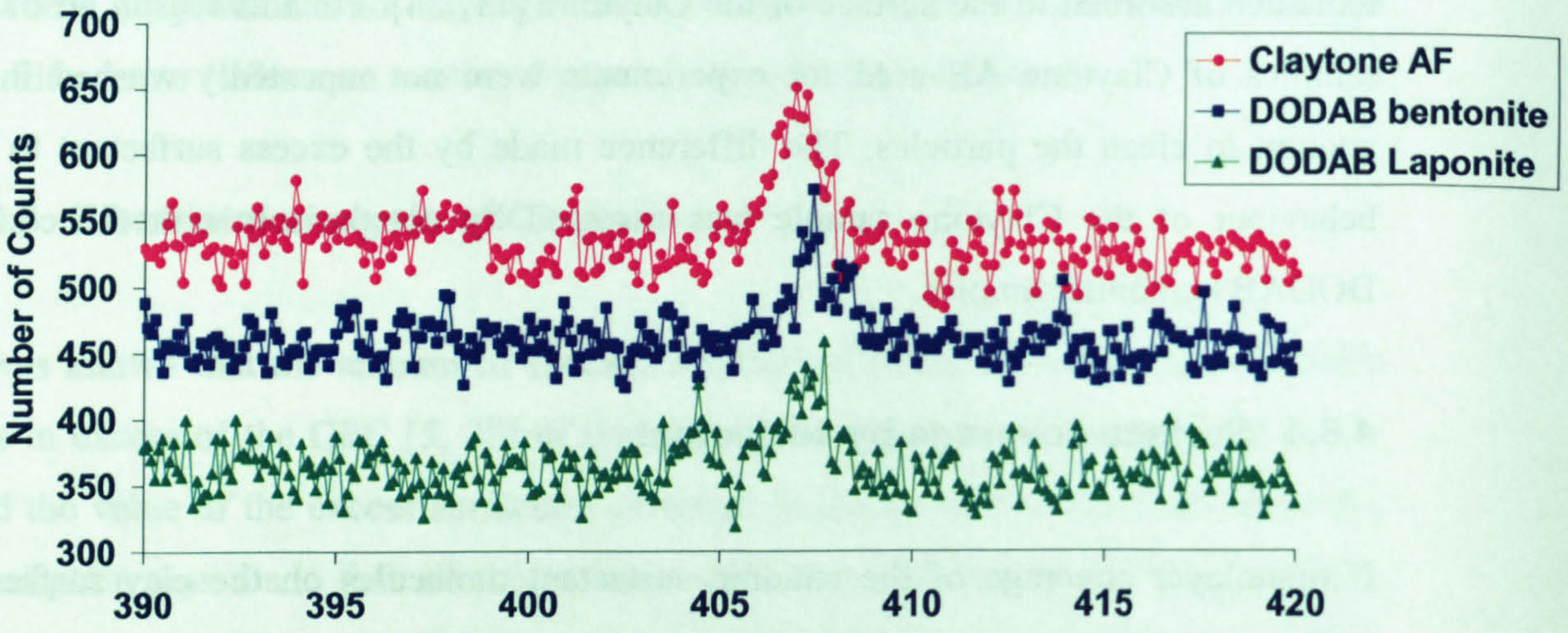

Figure 4.7. XPS of the nitrogen 1s peak from dry DODAB Laponite, dry DODAB bentonite, and dry Claytone all carried out at room temperature under ultra high vacuum conditions. To reduce the noise levels 20 scans averaged.

XPS was a highly surface sensitive technique and the nitrogen cation may have been partially covered by neighbouring surfactant tails [30]. This led to small and noisy nitrogen 1s peaks, the data from which was less reliable, however, the peak area (table 4.14) was in broad agreement with the elemental analysis result.

DODAB Laponite		**DODAB bentonite**		**Claytone**	
Relative peak area	Centre (eV)	Relative peak area	Centre (eV)	Relative peak area	Centre (eV)
1.028	407.70	1.095	407.40	1.396	406.90

Table 4.14. Area analysis of XPS nitrogen 1s peak for DODAB Laponite, DODAB bentonite and Claytone. A comparison between the values gives the relative amounts of nitrogen adsorbed to the surface.

The nitrogen 1s relative peak area of the Claytone sample was 1.3 times as large as the DODAB bentonite and 1.4 times as large as the DODAB Laponite peak. From elemental analysis the Claytone had 1.3 times the amount of surfactant adsorbed to the surface as DODAB bentonite and 1.5 times the amount of surfactant adsorbed to the surface as DODAB Laponite. This was in close agreement and supported the idea that even though the Claytone had above the CEC amount of surfactant adsorbed to the surface multilayer adsorption did not occur. Schematics of the surfactant molecules lie on the plates, [2, 23, 31], show monolayer adsorption and swelling from surfactant overlap from adjacent plates. This description was supported by the XPS data, however electrons from a few atoms deep were likely to escape without their energies becoming affected by layers above, [32].

4.6.6 BET surface area measurement of DODAB Laponite, DODAB bentonite, and Claytone

The BET results gave the external area of the sample (table 4.15) and this value was used as a measurement of the average number of plates stacked together per grain of powder.

Sample	BET surface area (m^2g^{-1})	Average (m^2g^{-1})
DODAB Laponite i	1.92	
DODAB Laponite ii	2.31	**2.1**
DODAB bentonite i	8. 91	
DODAB bentonite ii	6.42	**7.7**
Claytone AF i	4.63	
Claytone AF ii	4.59	**4.6**

Table 4.15. BET surface area determination for powdered DODAB Laponite, DODAB bentonite and Claytone repeated for all samples.

After treatment with DODAB the BET surface area was reduced to 7.7 m^2g^{-1} a ratio of 98:1 from the completely dispersed single plates and 98 plates were on average stuck together. For the Claytone sample the external area of single plates was assumed to be the same as for the bentonite clay but the external surface area of the Claytone was only 4.6 m^2g^{-1}. The ratio of the single plate surface area and the BET surface area was 163:1 giving the average number of plates in a stack as 163.

The diameter of the Laponite plates was 30 nm with a thickness of 1 nm [33] and as a result the assumption that the area of the plate edge was negligible when compared to the area of the face was harder to justify. The ratio of face area to edge area was 15:1 but the plates had a lower polydispersity than the natural bentonite. If the assumption that the edge area can be ignored is made the average number of particles of untreated Laponite stuck together in stacks was. $\frac{800m^2g^{-1}}{390m^2g^{-1}} = 2.05$

For the DODAB treated Laponite particles this increased to 377 particles per stack.

From this very crude analysis of the Laponite, bentonite, and Claytone data the conclusion that can be drawn is the particles formed large agglomerates that did not allow nitrogen molecules to penetrate. The untreated Laponite sample had a much higher external surface area per gram than the untreated bentonite and this was assumed to be due to the industrial methods employed to powder the material. The Claytone sample did not show a similarly high surface area per gram despite being industrially prepared.

4.7 Combined Cationic surfactant polymer treated clays

Samples of surfactant treated clay dispersed in toluene adsorbed SAP polymer rapidly (section 3.2.5) and the samples went from a gel to a low viscosity fluid. Adsorption of the SAP polymer was assumed from the colour change of the particles to that of the polymer when centrifuged.

4.7.1 Elemental analysis for SAP DODAB Laponite, SAP DODAB bentonite, and SAP Claytone

With the excess polymer removed by centrifugation and redispersion in fresh toluene the samples were dried under vacuum at 100 °C and submitted for elemental analysis.

Sample	% Nitrogen	% Carbon	% Hydrogen
Stochiometric mass value for DODAB	2.55	82.91	14.55
Elemental mass ratio for DODAB	1.00	32.51	5.71
Stochiometric mass value for SAP	2.41	81.58	13.26
Elemental mass ratio for SAP	1.00	33.85	5.50

Table 4.16. Elemental composition of adsorbed DODAB surfactant (without the bromide ion) and elemental composition of SAP polymer.

The elemental ratios for DODAB and SAP were very similar (table 4.16) therefore no difference between the samples was obvious from the elemental analysis results. As a further complication, lower molecular weights of SAP were thought to preferentially adsorb. However, it was known that the surfactant adsorbed very strongly to all the clays and it was thought that the SAP would just add and not exchange for surfactant molecules. However, this was not found to be the case (table 4.16).

Sample	% Nitrogen	% Carbon	% Hydrogen
Average DODAB Laponite	0.74	23.99	5.03
SAP DODAB Laponite	1.73	36.21	7.12
Change in values	**+0.99**	**+12.22**	**+2.09**
Average DODAB bentonite	0.87	26.79	5.95
SAP DODAB bentonite	1.24	33.56	6.38
Change in values	**+0.37**	**+6.77**	**+0.43**
Average Claytone AF	1.10	34.72	7.03
SAP Claytone	1.20	32.38	6.34
Change in values	**+0.10**	**-2.34**	**-0.69**

Table 4.17. Elemental analysis of SAP DODAB Laponite, SAP DODAB bentonite, and SAP Claytone compared to the surfactant treated samples.

For all of the samples there was an increase in the amount of nitrogen adsorbed to the surface (table 4.17) however, the Claytone showed a decrease in the amount of carbon and hydrogen after the treatment with the SAP. This may have been due to surfactant molecules becoming desorbed in the toluene solvent or because the SAP exchanged with the surfactant. The Claytone sample also pointed to the fact that lower molecular weight SAP molecules adsorbed preferentially as the overall nitrogen mass went up whilst the carbon and hydrogen reduced. The SAP DODAB Laponite and SAP DODAB bentonite samples showed an increase in material adsorbed over their DODAB precursors but it was not possible to tell if any exchange of DODAB surfactant for SAP had taken place, however it was assumed no DODAB was exchanged as it was close to the CEC.

4.7.2 Adsorption isotherm for SAP DODAB Laponite, SAP DODAB bentonite and Claytone

The calculations carried out for the adsorption isotherms can be found in appendix 3.

The treatment of surfactant-adsorbed clay with SAP polymer was suitable for carrying out an adsorption isotherm as the addition of SAP was a rapid, single step process. The measurements were all carried out at room temperature in filtered toluene solvent. The concentration of unadsorbed SAP was monitored with a series of ultraviolet-visible (UV-Vis.) measurements on the supernatant of centrifuged samples. It was shown from elemental analysis that surfactant became desorbed from the samples of Claytone but the desorbed surfactant showed no absorption in the UV-Vis. that could interfere with the strong SAP absorption at 284 nm.

The shape of the adsorption isotherms for all clay samples showed strong adsorption at low concentration of added SAP and rapidly reached a slightly inclined plateau (figure 4.8). This could indicate that at increased concentration of added SAP further adsorption of SAP may occur.

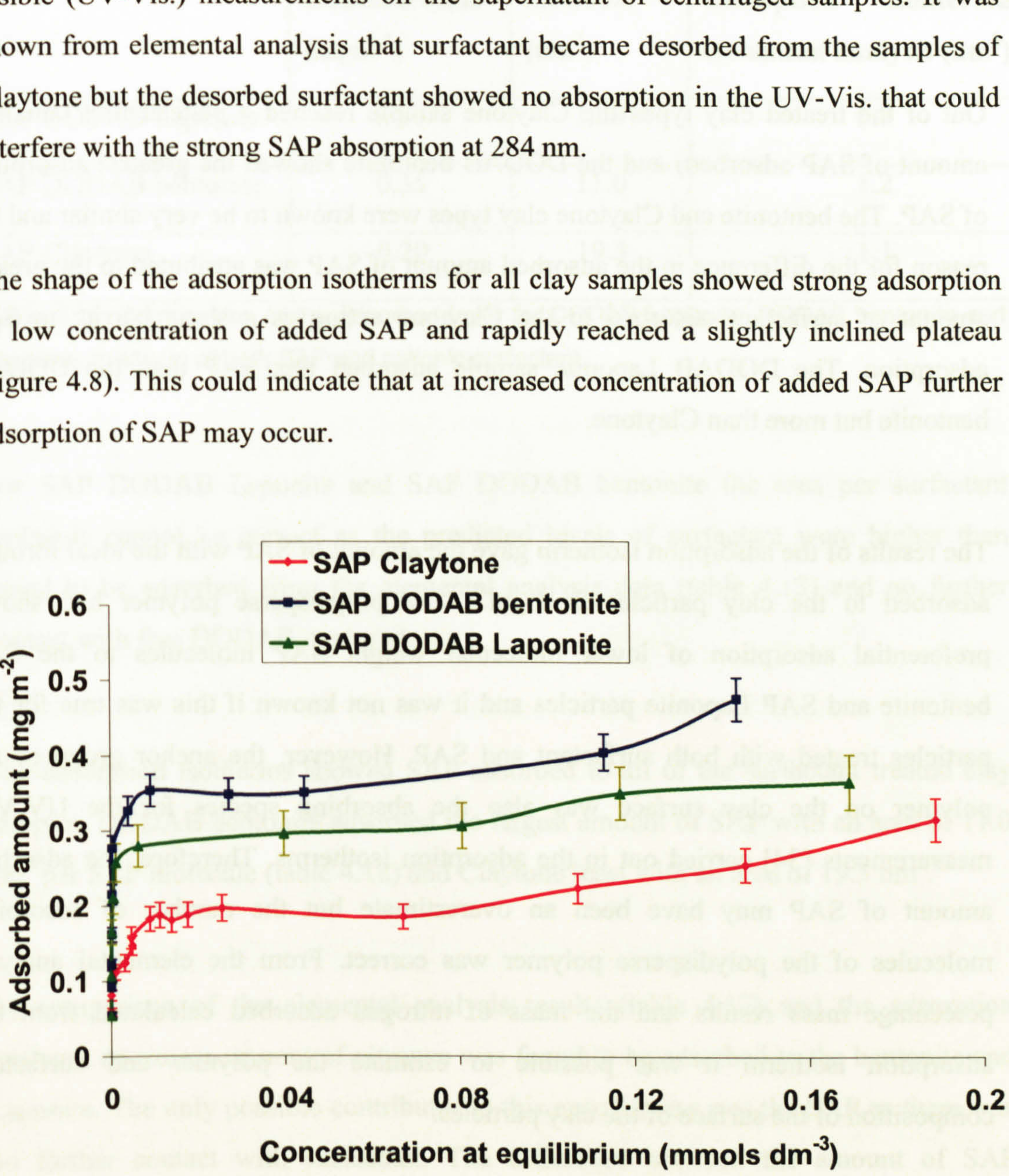

Figure 4.8. Adsorption of SAP to the surface of DODAB Laponite, DODAB bentonite, and Claytone at room temperature in toluene.

In order to get a value of the adsorbed amount in terms of milligrams per metre^2 the molecular weight of the adsorbing polymer was required. This was given as the molecular weight of the ideal SAP molecule but elemental analysis suggested that preferential adsorption of low molecular weight polymer occurred. The significance of this problem arose when the adsorption isotherm data was used in conjunction with the mass dependent elemental analysis data to obtain the composition of the surface of the clays. Also a value for the surface area of the clay was taken that assumed no clay aggregation occurred to reduce the area available for adsorption of the SAP. This value was the crystallographically determined area (table 4.13).

Out of the treated clay types the Claytone sample reached a plateau first (smallest amount of SAP adsorbed) and the DODAB bentonite showed the greatest adsorption of SAP. The bentonite and Claytone clay types were known to be very similar and the reason for the difference in the adsorbed amount of SAP was attributed to the greater amount of surfactant adsorbed to the Claytone acting as a steric barrier to SAP adsorption. The DODAB Laponite sample adsorbed less SAP than the DODAB bentonite but more than Claytone.

The results of the adsorption isotherm gave the amount of SAP with the ideal formula adsorbed to the clay particles in mgm^{-2}. The polydisperse polymer had shown preferential adsorption of lower molecular weight SAP molecules to the SAP bentonite and SAP Laponite particles and it was not known if this was true for the particles treated with both surfactant and SAP. However, the anchor group of the polymer on the clay surface was also the absorbing species for the UV-Vis. measurements [34] carried out in the adsorption isotherms. Therefore, the adsorbed amount of SAP may have been an overestimate but the number of adsorbing molecules of the polydisperse polymer was correct. From the elemental analysis percentage mass results and the mass of nitrogen adsorbed calculated from the adsorption isotherm it was possible to estimate the polymer and surfactant composition of the surface of the clay particles.

The amount of SAP added to the samples of surfactant treated clay for the experiments and elemental analysis was far in excess of the amount added for the adsorption isotherms and the assumption was made that the amount of SAP adsorbed to these samples did not exceed the plateau value as found from the adsorption isotherm.

Sample	Equilibrium SAP Concentration (mgm^{-2})	Area of SAP molecule (nm^2)	Area of DODAB moleculetaken from adsorption isothermand elemantal analysis (nm^2)
SAP DODAB Laponite	0.30	12.9	0.7
SAP DODAB bentonite	0.35	11.0	1.2
SAP Claytone	0.20	19.3	1.1

Table 4.18. Composition of the adsorbed layer for DODAB Laponite, DODAB bentonite and Claytone, made up of both SAP and cationic surfactant.

For SAP DODAB Laponite and SAP DODAB bentonite the area per surfactant molecule cannot be correct as the predicted levels of surfactant were higher than found to be adsorbed from the elemental analysis data (table 4.13) and no further contact with free DODAB occurred.

The adsorption isotherms showed SAP adsorbed to all of the surfactant treated clay samples. DODAB bentonite adsorbed the largest amount of SAP with an area of 11.0 nm^2 per SAP molecule (table 4.18) and Claytone least with an area of 19.3 nm^2.

By comparison of the elemental analysis results (table 4.17) and the adsorption isotherm an excess amount of nitrogen was found to be adsorbed to the bentonite and Laponite. The only possible contributor to this excess mass was the SAP as there was no further contact with surfactant. The difference between the amount of SAP adsorbed given by the adsorption isotherm and the amount found from the elemental

analysis was due to the much greater amount of SAP added to the samples that were centrifuged and dried for the elemental analysis measurement. The excess SAP was strongly adsorbed as it remained attached to the clay samples throughout the redispersion process of sonication and heating.

4.7.3 X-ray photoelectron spectroscopy of SAP DODAB Laponite, SAP DODAB bentonite, and SAP Claytone

Centrifuged samples of SAP DODAB Laponite, SAP DODAB bentonite and SAP Claytone were dried under vacuum at a temperature of 100 °C overnight and crushed in a pestle and mortar to a fine powder. The powder dried in a vacuum oven at 100 °C for 1 hour and was examined using the XPS technique (figure 4.9). The overall nitrogen content was given even though the polymer nitrogen atoms were in a different chemical environment as the surfactant nitrogen atoms.

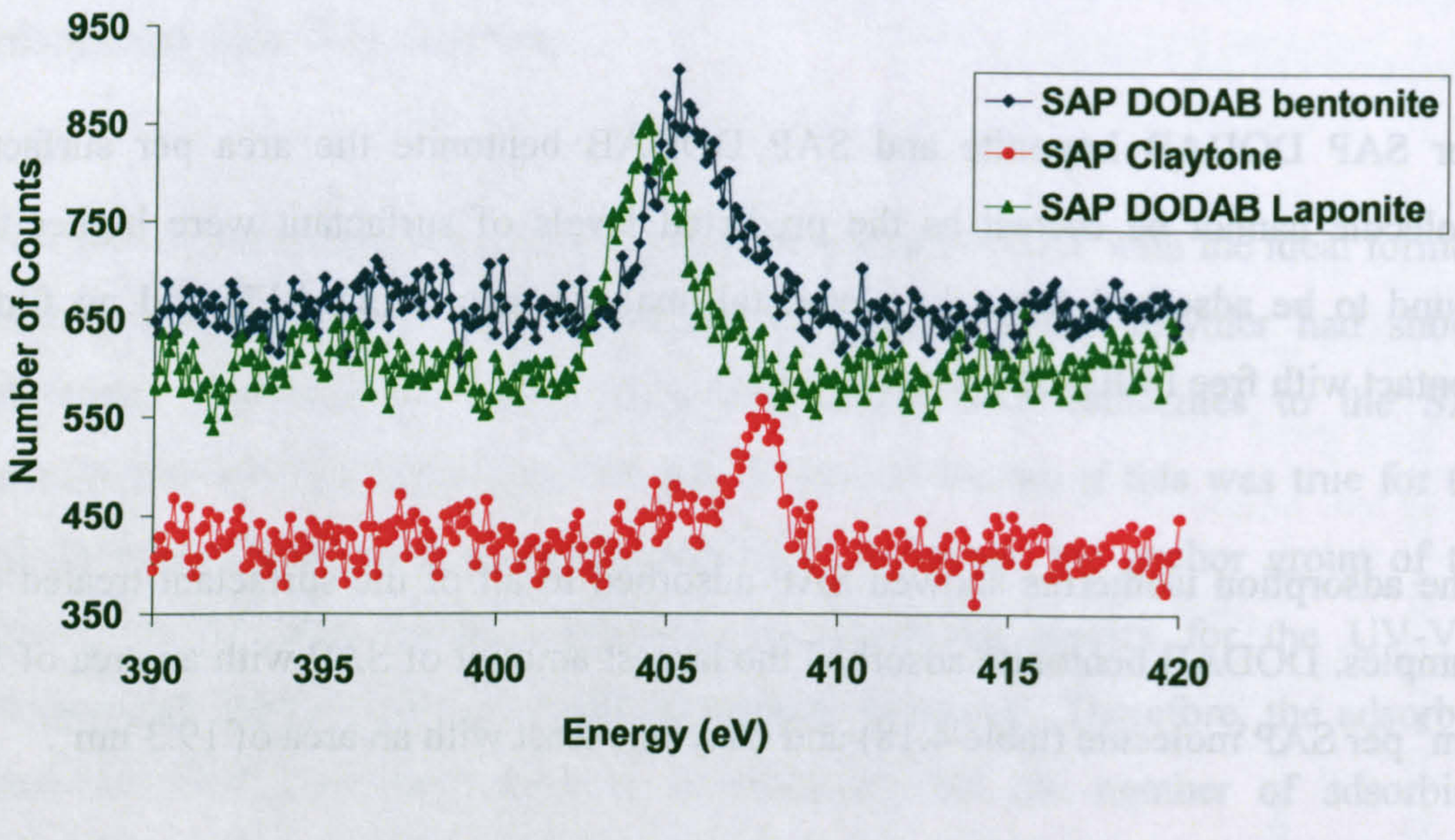

Figure 4.9. XPS plot from the nitrogen 1s peak of dried SAP DODAB Laponite, SAP DODAB bentonite and SAP Claytone. The energy difference is due to charging of the samples.

The SAP DODAB bentonite sample gave the peak with the largest area that was 1.4 times as big as the SAP DODAB Laponite peak and 1.7 times as big as the SAP Claytone peak (table 4.19). This did not agree with the elemental analysis results

where the SAP DODAB bentonite sample contained 0.7 times the overall percentage mass of nitrogen as the SAP DODAB Laponite sample and about the same percentage mass of nitrogen as the SAP Claytone. The reason for the big difference was thought to be due to the polymer chains covering up the nitrogen on the SAP DODAB Laponite and SAP Claytone samples.

SAP DODAB Laponite		**SAP DODAB bentonite**		**SAP Claytone**	
Relative peak area	Centre (eV)	Relative peak area	Centre (eV)	Relative peak area	Centre (eV)
1.760	404.30	2.386	405.20	1.384	407.70

Table 4.19. The area analysis of XPS nitrogen 1s peak for SAP DODAB Laponite, SAP DODAB bentonite, and SAP Claytone.

The reason why the polymer and surfactant chains obscured the nitrogen for the SAP Claytone sample and not for the SAP DODAB bentonite sample was not known especially as the clay types and overall percentage mass of nitrogen were so alike. The difference may have been due to the exact ratio of surfactant and polymer adsorbed to the surface.

From the elemental analysis the overall the amount of polymer and surfactant adsorbed to the surface of the SAP bentonite and SAP Claytone samples was comparable.

It appears there is twice the SAP or surfactant adsorbed to the bentonite; however from elemental analysis the total amount of nitrogen adsorbed to both clay samples is similar.

4.8 Conclusions

Experiments have been performed on samples of untreated and treated Laponite and bentonite in order to characterise the surface of the samples. Adsorption of water has been shown to occur on powdered samples if exposed to the atmosphere for any length of time. For untreated clays the mass of water can be in excess of 10% of the overall mass. Treated clays adsorb less water but still a significant amount to their surfaces. For all samples most of the water can removed with heat treatment in a vacuum.

A poly (isobutylene) polymer has been shown to adsorb strongly to the surface of Laponite and bentonite with the lower molecular weight polymer molecules adsorbing preferentially. Differences between the samples in the amount of polymer adsorbed and concentration on the surface suggest the SAP bentonite particles form aggregates.

DODAB, a cationic surfactant, was successfully adsorbed to the clays but the samples did not form stable dispersions in toluene and polydecene and formed gels. The Laponite sample adsorbed a lower amount of DODAB to the surface than the bentonite sample and the Claytone had the highest proportion of surfactant adsorbed, however the CEC was not determined for the Claytone but the surfactant adsorption was found to be in excess of the CEC.

The DODAB treated clay samples and Claytone adsorbed SAP, a short-chain poly (isobutylene) polymer, to the surface. The DODAB bentonite and Claytone formed stable dispersions after polymer treatment in toluene but the DODAB Laponite sample flocculated very quickly. The amount of the polymer adsorbed to all clay samples was determined from adsorption isotherms that assumed the clays became completely delaminated exposing all surfaces.

4.9 References

1. Hanley, H.J.M., et al., *A small-angle neutron scattering study of a commercial organoclay dispersion.* Langmuir, 2003. 19(14): p. 5575-5580.
2. van Olphen, H., *An Introduction to Clay Colloid Chemistry: For Clay Technologists, Geologists, and Soil Scientists.* 2nd Edition ed. 1977: John Wiley & Sons, Inc.
3. van Olphen, H. *Determination of Surface Areas of Clays-Evaluation of Methods.* in *The International Symposium on Surface Area Determination.* 1969. IUPAC. Held at the School of Chemistry, University of Bristol, UK: Butterworths.
4. Grillo, I., P. Levitz, and T. Zemb, *Insertion of small anisotropic clay particles in swollen lamellar or sponge phases of nonionic surfactant.* European Physical Journal E, 2001. 5(3): p. 377-386.
5. Hanley, H.J.M., et al., *A SANS study of organoclay dispersions.* International Journal of Thermophysics, 2001. 22(5): p. 1435-1448.
6. Xie, W., et al., *Thermal Degradation Chemistry of Alkyl Quaternary Ammonium Montmorillonite.* Chemistry of Materials, 2001. 13: p. 2979-2990.
7. Callaghan, I.C. and R.H. Ottewill, *Interparticle Forces in Montmorillonite Gels.* Faraday Discussions of the Chemical Society, 1974. 57: p. 110-118.
8. Zou, J. and A.C. Pierre, *Scanning electron microscopy observations of "card-house" structures in montmorillonite gels.* Journal of Materials Science Letters, 1992. 11: p. 664-665.
9. Rossi, S., et al., *Influence of low molecular weight polymers on the rheology of bentonite suspensions.* Revue De L Institut Francais Du Petrole, 1997. 52(2): p. 199-206.
10. http://www.Laponite.com. 2002, Laporte Inc.
11. Theng, B.K.G., *The Chemistry of Clay-Organic Reactions.* 1974, London: Rank Precision Industries.
12. Buining, P.A., et al., *Preparation of a Nonaqueous Dispersion of Sterically Stabilized Boehmite Rods.* Colloids and Surfaces, 1992. 64(1): p. 47-55.
13. van der Kooij, F.M. and H.N.W. Lekkerkerker, *Formation of nematic liquid crystals in suspensions of hard colloidal platelets.* Journal of Physical Chemistry B, 1998. 102(40): p. 7829-7832.
14. van der Kooij, F.M., E.S. Boek, and A.P. Philipse, *Rheology of dilute suspensions of hard platelike colloids.* Journal of Colloid and Interface Science, 2001. 235(2): p. 344-349.
15. Allen, G.C., et al., *Mineral/reagent interactions: an X-ray photoelectron spectroscopic study of adsorption of reagents onto mixtures of minerals.* Clay Minerals, 1999. 34(1): p. 51-56.
16. Allen, G.C., et al., *XPS analysis of polyacrylamide adsorption to kaolinite, quartz and feldspar.* Surface and Interface Analysis, 1998. 26(7): p. 518-+.
17. Graveling, G.J., et al., *Controls on polyacrylamide adsorption to quartz, kaolinite, and feldspar.* Geochimica Et Cosmochimica Acta, 1997. 61(17): p. 3515-3523.
18. Graveling, G.J., *A Study into the Adsorption of partially hydrolysed polyacrylamide on Kaolinite, Feldspar, and Quartz.* PhD. Thesis, Geology, 1997. University of Bristol, Bristol, UK.

19. Hanley, H.J.M., C.D. Muzny, and B.D. Butler, *Surface adsorption in a surfactant/clay mineral solution.* International Journal of Thermophysics, 1998. **19**(4): p. 1155-1164.
20. Levitz, P., et al., *Liquid-solid transition of Laponite suspensions at very low ionic strength: Long-range electrostatic stabilisation of anisotropic colloids.* Europhysics Letters, 2000. **49**(5): p. 672-677.
21. Slabaugh, W.H., *Cationic exchange properties of Bentonite.* The Journal of Physical Chemistry, 1954. **58**: p. 162-165.
22. Slabaugh, W.H. and F. Kupka, *Organic cationic exchange properties of calcium montmorillonite.* The Journal of Physical Chemistry, 1958. **62**: p. 599-601.
23. Jordan, J.W., *Organophilic Bentonites I.* Journal of Physical and Colloidal Chemistry, 1949. **53**: p. 294-306.
24. Jones, T.R., *The Properties and Uses of Clays Which Swell in Organic Solvents.* Clay Minerals, 1983. **18**(4): p. 399-410.
25. Lagaly, G., *Characterization of Clays by Organic-Compounds.* Clay Minerals, 1981. **16**(1): p. 1-21.
26. Williams, F.J., B.C. Elsley, and D.J. Weintritt. *The Variation of Wyoming Bentonite Beds as a Function of the Overburden.* in *Second National Conference on Clay and Clay Minerals.* 1952. Columbia, Missouri, USA: The Clay Mineral Society.
27. Bongiovanni, R., *Small Angle Neutron Studies on Clay Systems.* PhD. Thesis. School of Chemistry University of Bristol, Bristol. UK, 1997.
28. Ho, D.L., R.M. Briber, and C.J. Glinka, *Characterization of organically modified clays using scattering and microscopy techniques.* Chemistry of Materials, 2001. **13**(5): p. 1923-1931.
29. Fasman, G.D., ed. *Practical Handbook of Biochemistry and Molecular Biology.* Third ed. 1976, CRC Press: New York.
30. Weiss, A. *Mica-Type Layer Silicates With Alkylammonium Ions.* in *The Proceedings of the Tenth National Conference on Clay and Clay Minerals.* 1962. Ottawa, Canada: The Clay Mineral Society.
31. Jordan, J.W., B.J. Hook, and C.M. Finlayson, *Organophilic Bentonites II.* Journal of Physical and Colloidal Chemistry, 1950. **54**: p. 1196-1208.
32. Hunter, R.J., *Foundations of Colloid Science.* Second Edition ed. 2001, Oxford: Oxford University Press.
33. Mourchid, A., et al., *On viscoelastic, birefringent, and swelling properties of Laponite clay suspensions: Revisited phase diagram.* Langmuir, 1998. **14**(17): p. 4718-4723.
34. Lee, C. and W. Kumler, *The dipole moment and Structure of the Imide Group. 1. Five- and Six-membered Cyclic Imides.* Journal of the American Chemical Society, 1961. **83**(22): p. 4586-4590.

5 Optical Inspection

5.1 Introduction

After treating the Laponite and bentonite and dispersing them in an organic solvent the procedure was simply to observe their behaviour. This was done since broad qualitative observations clearly showed the range of behaviour of the treated clay samples. Toluene was chosen as the organic solvent for all the clay samples since they dispersed with least difficulty in this solvent and marginalisation experiments were easy to conduct with the addition of miscible ethanol. Solvent evaporation and toxicity were a problem using toluene and therefore polydecene, a non-volatile and much less toxic alternative, was employed for a number of experiments. It was also suggested that crystallisation of the octadecyl surfactant chains would occur at a higher temperature in polydecene and this was found to be the case.

A wide range of behaviour was found depending on the specific treatment and solvent; some samples remaining colloidally stable with low viscosity, some slowly sedimenting out and some forming gels. Also a wide range of turbidity in the samples was found. The differences in the behaviour of the different clays and treatments potentially have many causes. Sedimentation of the particles may have occurred as a result of incomplete disaggregation (exfoliation) of the clay particles, but this was minimised by repeated ultrasonication and heating. The use of polar activators is a well documented method for breaking up particle aggregates to produce a homogeneous dispersion [1-3] but was not employed during this study since the role of the polar activator is a matter of discussion [3-5]. For many samples gelation occurred even at low concentration and was characterised by the trapped bubbles observed within the sample. Some of the most interesting samples were colloidally stable and displayed flow and static birefringence depending on their concentrations.

This chapter is arranged according to treatment method to enable, where possible, direct comparison between the types of clay under the same conditions. The differences in behaviour between Laponite, bentonite and Claytone may be due to the

differences in the amount of surfactant and polymer adsorbed to the surface or due to a physical difference such as the size of the particles and polydispersity.

5.2 SAP Laponite and SAP Bentonite

The procedure of treating Laponite and bentonite clays with SAP is described in section 3.4 and was carried out following the method of van der Kooij [6] in exactly the same manner for both samples. The length of the SAP polymer chains had been determined as 4 nm from light scattering measurements carried out by Smits *et al* [7] in toluene. This gave an aspect ratio of SAP Laponite of ~3:1 and for the much larger and polydisperse SAP bentonite [8] from 10:1 to 100:1. The aspect ratios assume complete delamination of the particles in the organic solvent.

The Claytone was not treated with SAP in this way since it was supplied with a cationic surfactant adsorbed to the surface that could not be completely removed rendering a comparison with the SAP bentonite and SAP Laponite samples invalid.

The first difference between the SAP Laponite and SAP bentonite was noticed in the final stages of solvent transfer to toluene, where the swirled SAP Laponite remained as a clear yellow suspension (the colour of the polymer) and the swirled SAP bentonite was a yellow but cloudy dispersion showing a layered pattern throughout the sample giving it an inhomogeneous appearance (figure 5.1). This layering was caused by particles aligning in the velocity gradient of the moving fluid and was not thought to be a shear banding phenomenon [9]. The lines disappeared when the flow stopped leaving a much more homogeneous looking dispersion.

Figure 5.1. 3.2% w/w SAP bentonite dispersion swirled by hand at room temperature in toluene. A number of 2 mm wide dark bands are seen running parallel with the direction of flow. Scale bar represents 20 mm.

After the removal of excess polymer by centrifugation, the redispersed SAP bentonite remained cloudy (figure 5.2b) whereas the SAP Laponite dispersion was clear (Figure 5.2a). The colour of the dispersions was yellow, due to the presence of the adsorbed SAP on the clay particles. This was most noticeable as the samples were sedimented under centrifugation leaving a colourless supernatant. Both dispersions had low viscosities and flowed as the sample tubes were tilted slightly.

Figure 5.2a. SAP Laponite at 3.6% w/w dispersed in toluene with all excess SAP removed. The sample was clear yellow.

Figure 5.2b. SAP bentonite at 3.2% w/w dispersed in toluene with all excess SAP removed. The sample was turbid.

Scale bars represent 20 mm.

The reason for the turbidity of the SAP bentonite dispersion was that the larger size of the bentonite plates led to much greater scattering of light [10].

The SAP bentonite dispersion displayed vivid birefringence whilst under flow when the sample was swirled and observed through crossed polarisers (figure 5.3). This effect was due to alignment of the highly anisotropic SAP bentonite platelets and was not found for the much lower aspect ratio SAP Laponite particles. The flow birefringence was visible for samples that had never been allowed to settle and for sediments redispersed with vigorous shaking by hand, showing that extensive irreversible aggregation did not occur upon sedimentation of the SAP bentonite.

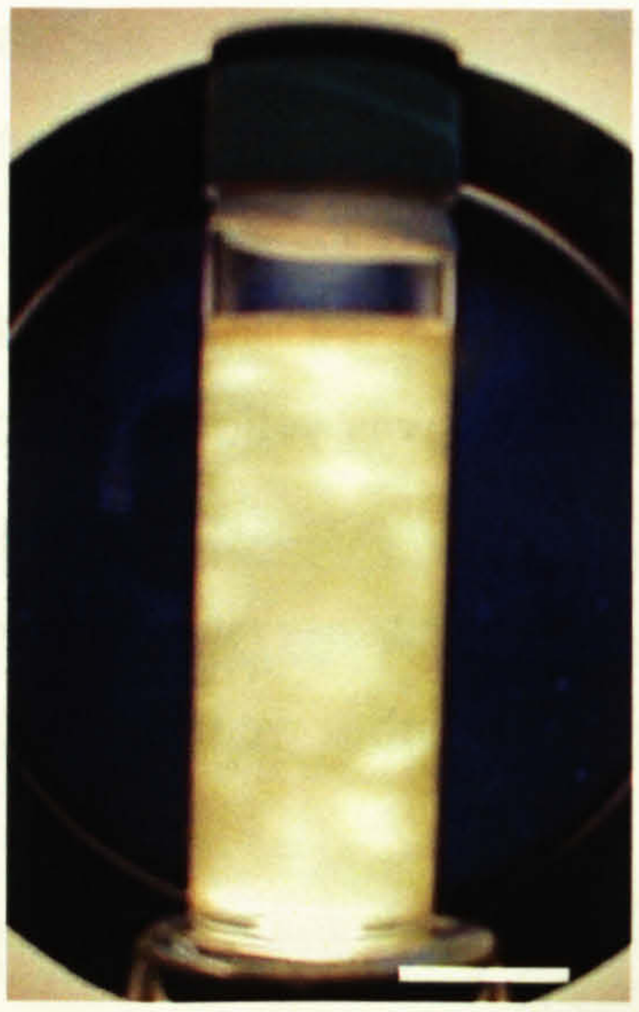

Figure 5.3. Flow birefringence of SAP bentonite. Sample concentration was 3.2% w/w in toluene. The sample was swirled by hand just before the photograph was taken. The birefringent domains were up to 4 mm by 2 mm depending on the rate of flow. The scale bar represents 10 mm.

At high rates of flow, the birefringent domains were small and rapidly changing but as the flow rate decreased, the domains grew larger until just prior to stopping the flow when the flow birefringence ceased. The shape and size of the birefringent domains in a sample tube of 22 mm diameter was not consistent but was not larger than 4 mm by 3 mm. The pattern caused by flow birefringence was quite different from the narrow stripes observed with the naked eye for swirled samples (see figure 5.1).

5.2.1 Settling of SAP Bentonite

On standing for a few hours the SAP Laponite particles remained well dispersed but the SAP bentonite particles started to settle out. SAP Laponite and SAP bentonite

particles are of similar densities, bare bentonite is 2.7 gcm^{-3} [11] and bare Laponite is 2.65 gcm^{-3} [12] and fairly similar overall surface coverage (see XPS and EA in section 4.4). Careful measurements were taken to find the rate of settling of the SAP bentonite sample by taking a 3.2% w/w dispersion in toluene and sealing it in a 28ml sample tube. Shaking in a spin mixer gave a well-dispersed solution that became clear from the top upon standing (figures 5.4). The rate of this sedimentation (i.e. the drop in level) was measured once every 24 hours (table 5.1).

Settling rate of SAP bentonite.	Drop from the top in 24 Hours (mm)	Drop from the top in 48 Hours (mm)
1	16	30
2	15	29

Table 5.1. Settling rate of 3.2% w/w SAP bentonite in toluene at room temperature. The settling quickly became very diffuse as the particles had a wide range of settling rates due to their high polydispersity.

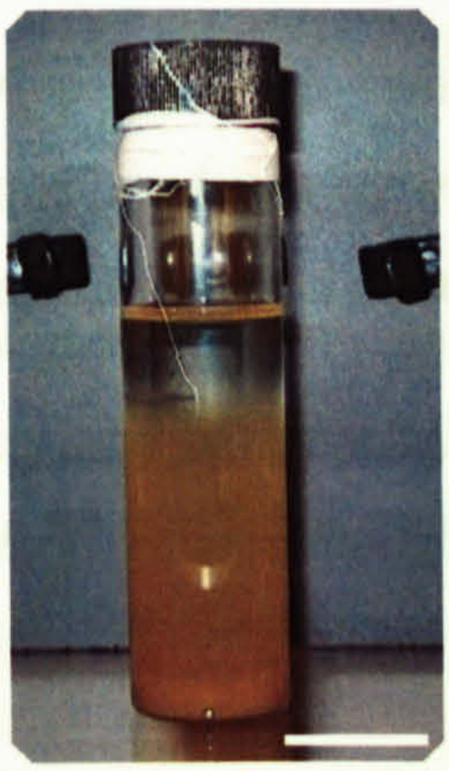

Figure 5.4a. 3.2% w/w SAP bentonite in toluene dispersion 24 hours after mixing. A dense sediment was visible at the bottom of the tube.

Figure 5.4b. 3.2% w/w SAP bentonite in toluene dispersion 48 hours after mixing. The settling layer was becoming more diffuse.

Figure 5.4c. 3.2% w/w SAP bentonite in toluene dispersion 72 hours after mixing. Almost all of the particles had settled out.

Scale bar represents 20 mm for all samples.

The concentration of the SAP bentonite particles in the sediment was measured at 23%w/w by dry weight analysis after letting a sample settle for one week and carefully removing the excess solvent. This compared well with a measurement of the sediment thickness in the sample tube, and knowing the overall SAP bentonite

concentration to be 3.2% w/w, the particle concentration in the sediment was estimated as 22% w/w.

If the SAP bentonite particles were non-aggregating, the rate of settling in a given solvent depended on their overall density, their size and their shape. The particles, regardless of size, were subjected to the force of gravity and as they were denser than the surrounding solvent the force attracted them towards the bottom of the sample tube causing settling if acted upon by no other force. In opposition to the gravitational force was the randomising effect of Brownian motion (thermal energy) promoting a more uniform dispersion [13]. Also, as the particles moved through the solvent a frictional force became important which retarded the settling rate.

5.2.1.1 Settling rate of SAP Bentonite

The viscosity of the solvent toluene is 0.560 mPa s at 25 °C.

Sedimentation rate measurements yield weight average values for the "equivalent spherical radius" by calculating the particle radius as if it were a sphere, applying Stokes' formula. The equivalent spherical radius is related to the *a* and *b* dimensions of ellipsoid of revolution by

$r_{eq} = (\frac{ab}{F})^{0.5}$ where *a* is diameter of the plates and *b* is thickness and F = 0.66 a form factor for thin discs [14].

For the bentonite samples of thickness 1 nm and diameter of 200 nm $r_{eq} = 17.41$ nm.

The sedimentation rate of an uncharged particle of mass m and specific volume v in a liquid of density ρ depends on the viscosity of the liquid. The driving force on the particle, which is independent of particle shape, is $m(1\text{-}v\rho)g$, where g is the acceleration due to gravity. The factor $(1\text{-}v\rho)$ allows for the buoyancy of the liquid [15].

As the particle settles it will reach its terminal velocity very quickly and the resistance of the liquid is $m(1\text{-}v\rho)g = f$ where f is the frictional coefficient of the particle in the given medium.

For spherical particles the frictional coefficient is given by Stokes' Law.

$$f = 6\Pi\eta \times r_{eq} \qquad [5.1]$$

where η is the viscosity of the medium and r_{eq} is the radius of the particle.

Therefore, if ρ_2 is the density of a spherical particle (in the dissolved or dispersed state).

(i.e. $\rho_2 = \frac{1}{v}$)), then $\frac{4}{3}\Pi r_{eq}^3(\rho_2 - \rho)g = 6\Pi\eta \times r_{eq}\frac{dx}{dt}$ or

$$\frac{dx}{dt} = \frac{2r_{eq}^2(\rho_2 - \rho)g}{9\eta} \qquad [5.2]$$

Throughout the calculation the dimensions of the particles have been taken as the dimensions of the clay cores. This is clearly inaccurate as the adsorbed layer of polymer reduces the overall density of the particles and has an effect on the rate of settling.

For the SAP bentonite samples settling in toluene the expected settling rate, based on plates with a radius of 100 nm, was $2.16\text{x}10^{-9}$ ms^{-1}. This translates to 0.2 mm in a 24 hour period. The actual sedimentation rate was 80 times as fast! Clearly aggregation of the SAP bentonite plates occurs.

From the measured sedimentation rate an estimate of the particle size was made

$$\sqrt{\frac{\frac{dx}{dt}\eta \times 9}{(\rho_2 - \rho)g \times 2}} = r_{eq} = 1.58\text{x}10^{-7}\text{m}.$$

Conversion back to radius from the effective radius gives

$$r_{eq} = (\frac{ab}{F})^{0.5} \quad \frac{r_{eq}{}^2 \times 0.66}{b} = a \ = 1.65\text{x}10^{-5} \text{ m.}$$

The radius of a plate of 1 nm thick to settle at the observed rate is 16.5 μm. Plates of this size would be easily visible through the optical microscope and no such large aggregates have been observed. Therefore, face to face aggregation was strongly suspected.

5.2.2 SAP bentonite birefringence

Permanent birefringence was seen in the sediment of the samples that were allowed to settle under gravity. The birefringence showed the plates had an ordered structure upon settling which implies that they settle as anisotropic species such as individual particles or as anisotropic aggregates (figure 5.5). It is well understood that bentonite plates are polydisperse and due to this polydispersity it was very unlikely that higher ordering such as a columnar phase would be found in the sediment [16].

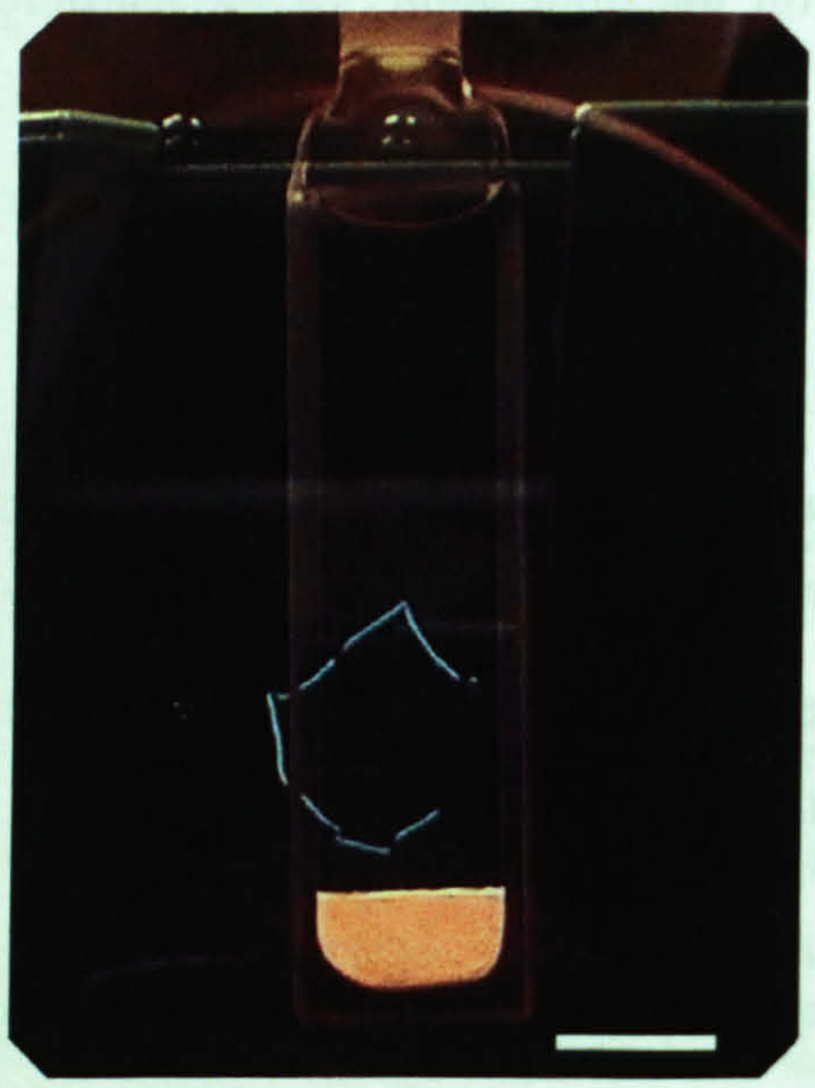

Figure 5.5. 3.2% w/w SAP bentonite sample settled in a 1mm thick, 9 mm wide glass cell over 7 days at room temperature showing a birefringent pattern. The picture was taken through the crossed polarisers of the birefringence box. The bright C-shape was from the filament of the bulb. Scale bar is 10 mm.

5.2.2.1 Polarising Microscopy of SAP samples

The polarising microscope pictures of the sedimented SAP bentonite were taken with the samples in a 1mm thick flat walled scattering tube and allowed to settle upright for one week at room temperature (figures 5.6). The sample was placed horizontally, with care, on the microscope stage, which disturbed the sediment slightly.

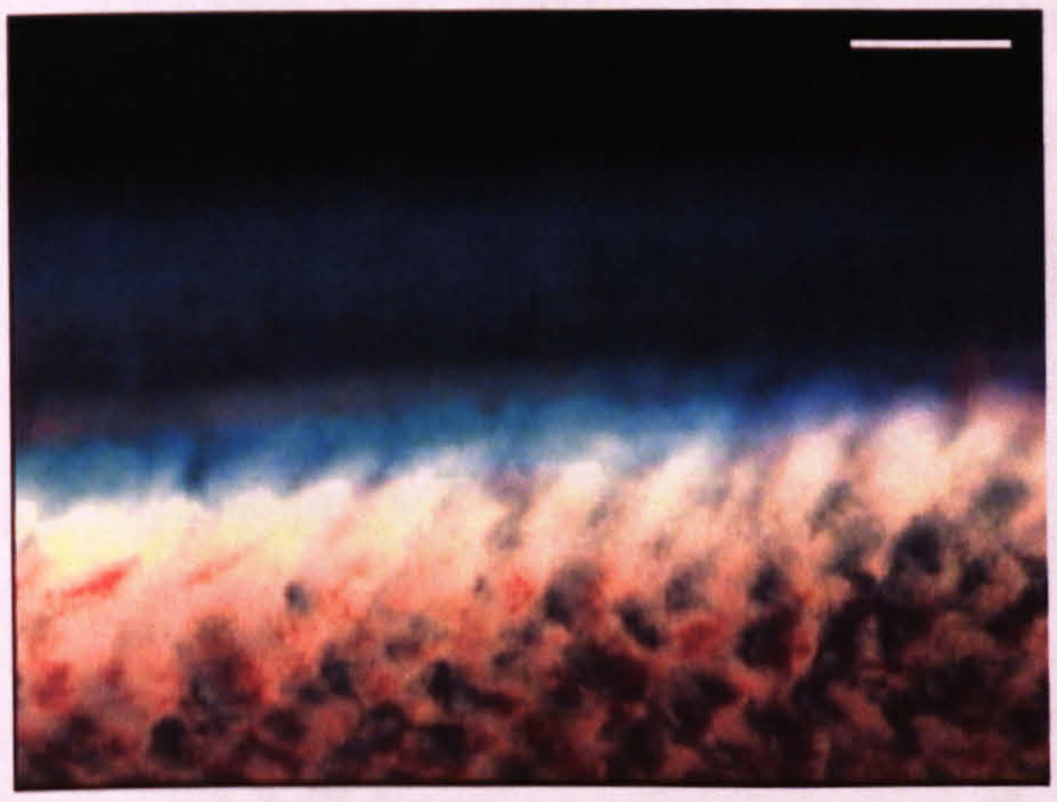

Figure 5.6a. Surface of the SAP bentonite sedimented layer. Tiger stripes and mottled patterns are seen with a haze of particles above the sediment.

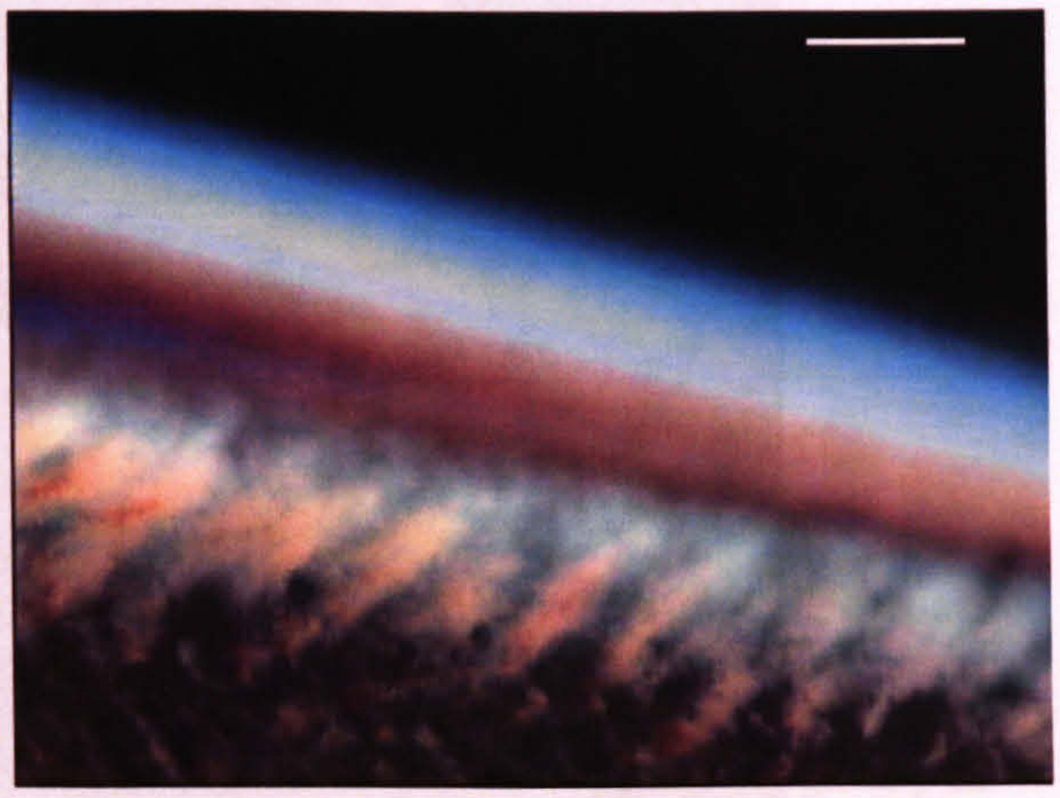

Figure 5.6b. The same area but twisted through 17° showing the disturbed surface layer of the SAP bentonite very clearly and disturbed uniformly.

The scale bars denotes 100 μm.

The thickness of the disturbed surface layer above the sediment was 0.2 mm and tumbling particles were seen as twinkling specks within this layer. Over the course of an hour the layer did not diminish in size or brightness but was not taken as a permanent feature since there was no sign of it when the sample tube was kept upright over a number of days. The thickness of the birefringent stripes seen in the sediment varied from 0.02 to 0.04 mm wide and up to 0.15 mm deep. Below this layer the sediment displayed birefringent domains of around 0.03 × 0.03 mm, characterised by similarly orientated particles surrounded by particles with different orientations.

Near the bottom of the sample holder there were also many features but the colouration was more consistent without dramatic bands of colour and any bright layers. This suggested a more uniformly settled layer and was most clear immediately adjacent to the bottom of the glass cell. The texture shown in this figure indicates that

the platelets in the sediments are ordered into a nematic structure. A detailed survey of the concentration at which the isotropic - nematic transition occurs for SAP bentonite has not yet been carried out. (figure 5.7).

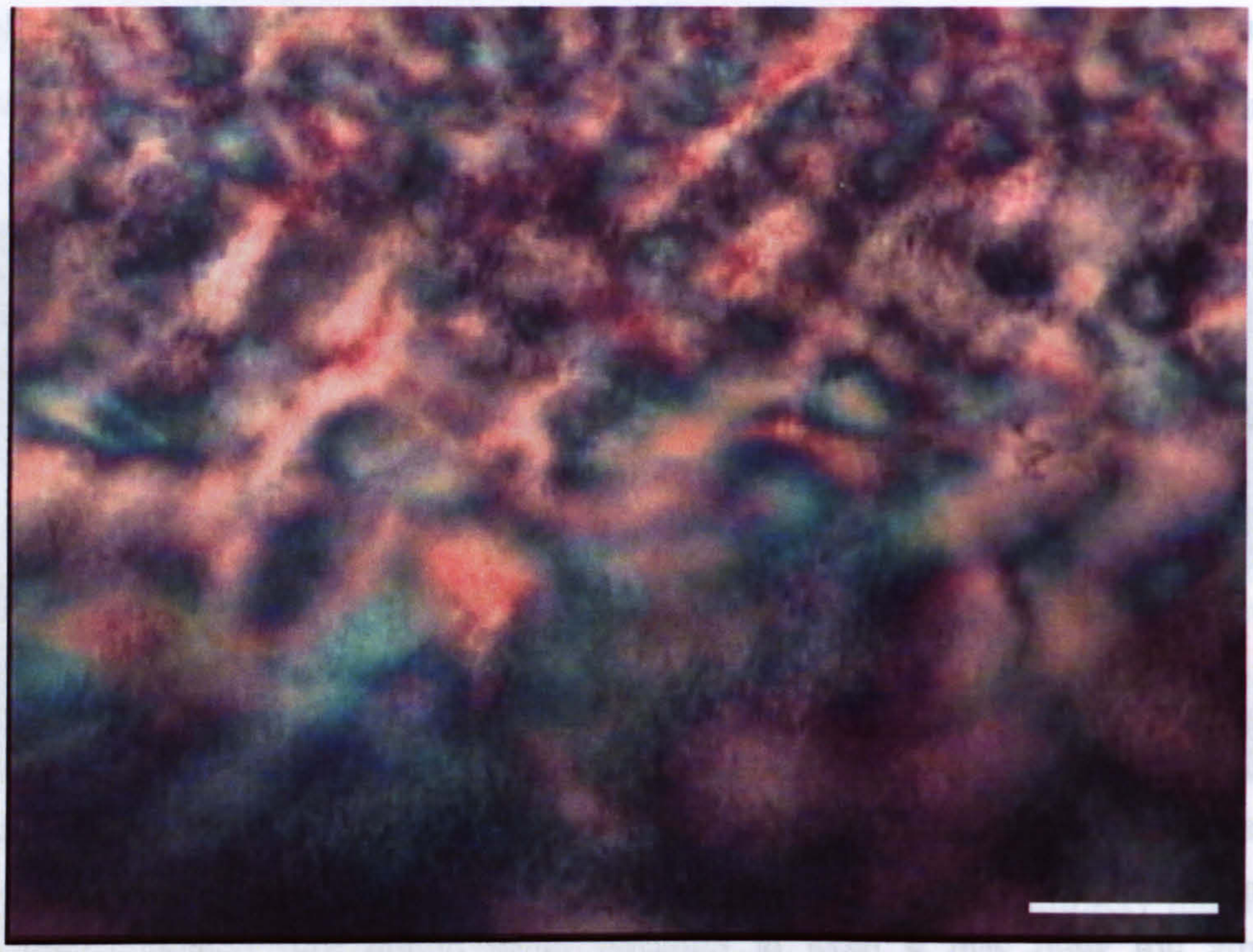

Figure 5.7. SAP bentonite sediment observed through crossed polarisers. These particles settled first and were at the bottom of the sample tube. Scale bar = 100 μm.

5.2.3 SAP Laponite and SAP bentonite in marginal solvent

By marginalising the solvent conditions for the polymeric steric layer of stabilised particles, attractions were induced as the polymer favoured polymer-polymer contact over polymer-solvent interaction [17]. For the SAP-treated clays the solvent was marginalised with the addition of miscible but polar ethanol to the non-polar solvent toluene. The aim of the experiment was to induce attractions between particles and to form a gel. The same overall concentration of the particles was maintained throughout each series for direct comparisons between samples with the ethanol added last (figure 5.8). The SAP Laponite and SAP bentonite were spin mixed and left in the sonic bath for 1 hour, then allowed to stand and settle under gravity for 7 days at room temperature. This dispersing procedure was also carried out on the samples at 40 °C to determine if there were any temperature effects on the sediment height.

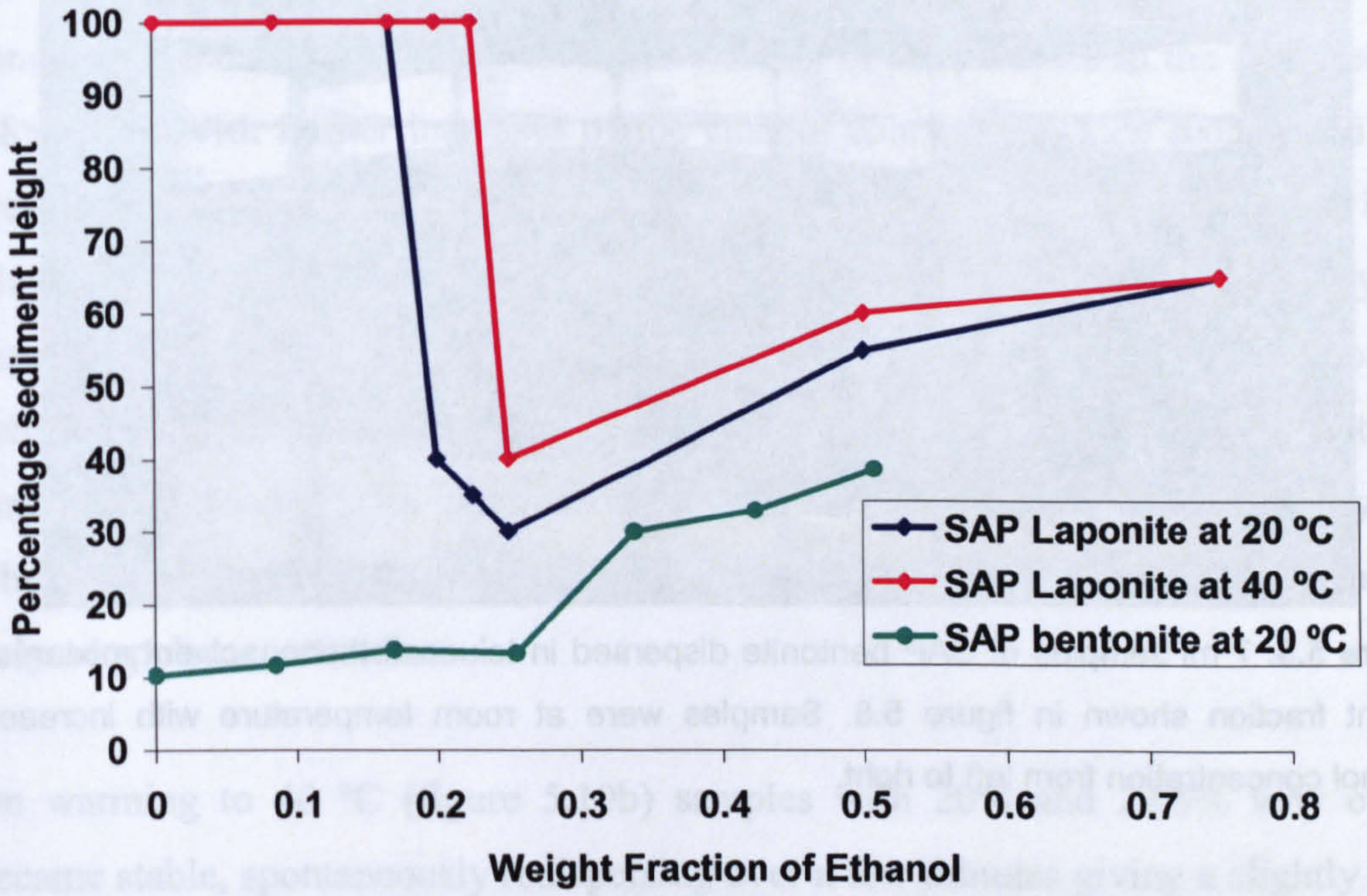

Figure 5.8. Plot of SAP Laponite and SAP bentonite with marginal ethanol/toluene solvent. The concentration of the SAP Laponite was 1.0% w/w and the SAP bentonite was 1.6% w/w. No plot of SAP bentonite is given at 40 °C as the sediment height changed only marginally at raised temperature.

The sample of SAP bentonite was not stable in pure toluene and gave the densest sediment, and with an increasing proportion of ethanol the sediment height became larger due to increased attraction between treated clay particles and them sticking together on contact. The series of samples is shown below (figure 5.9).

Figure 5.9. 7 ml samples of SAP bentonite dispersed in toluene/ethanol solvent mixtures at weight fraction shown in figure 5.8. Samples were at room temperature with increasing ethanol concentration from left to right.

For the SAP bentonite the sediment height changed only slightly until the amount of ethanol reached somewhere between 25% and 33.8% of the total solvent. From observations, however, the marginal samples formed aggregates that could easily be redispersed as a very fine "smoke" with no large flocs seen. This was true over the range of samples including the sample with the highest proportion of ethanol. The sediment height for the SAP bentonite particles remained small for samples containing up to 25% w/w ethanol but then rapidly increased with greater proportions of ethanol. Flow birefringence was evident in the SAP bentonite samples up to an ethanol concentration of 16.9% w/w. At this concentration the sediment height was very similar to the pure toluene sample suggesting that particle-particle attractions were not sufficient to stick the particles together on first contact. The effect of raising the temperature on the sedimentation of the SAP bentonite dispersion in toluene/ethanol was investigated. The samples were dispersed at 40 °C and kept at this temperature whilst being allowed to resettle over 1 week. No observable difference in the final sediment height was found when compared to the samples prepared at 20 °C.

The same marginalisation experiment was carried out with the non-settling SAP Laponite samples, which gave a differing result, showing a temperature-dependent effect. At 20 °C (figure 5.10a), with an increased proportion of ethanol in the solvent, the sample became slightly cloudier but no settling was observed indicating the turbidity may be due to larger flocs and also the refractive index difference between

the mixed solvent and the particles. A sediment was formed with an ethanol concentration of 20% w/w and the concentration of the particles in the sediment was 3.8% w/w. With further increases of the ethanol concentration the sedimented layer grew in thickness and the particle concentration in the sediment decreased to below 2% w/w. The increase in sediment height with decreasing solvent quality was expected since the particles became stuck as their polymer layers touched neighbouring particles. The most compact gel was seen as the solvent quality just turned from good to bad. The reason for this was the particles did not simply stick when they first encountered other particles but instead rearranged due to the low polymer-polymer attraction.

On warming to 40 °C (figure 5.10b) samples with 20% and 22.5% w/w ethanol became stable, spontaneously redispersing over a few minutes giving a slightly turbid dispersion. These samples could be warmed and cooled repeatedly and always dispersed and sedimented with raising and lowering temperatures. At an ethanol proportion of 25% w/w, stability was not detected at 40 °C but the sediment height remained higher than for the same sample at 20 °C. This suggested the interparticle attraction was greater for this sample at higher temperature, a feature not observed for the samples with a lower proportion of ethanol.

On phase separation the lower particle-rich phase did not flow if the sample tube was held at an angle for over a day. Slight shaking also failed to disturb the particles and therefore it was assumed the lower phase was a gel. Unfortunately, when the supernatant was decanted from those lower temperature samples that became stable at high temperatures, they did not form space-filling gels and a colourless supernatant was always observed. The reason for this was not known but an alteration in the solvent composition due to evaporation was strongly suspected.

Figure 5.10a. 4 ml samples of SAP Laponite dispersed in mixed toluene/ethanol solvents at 20 °C. Increasing polarity from left to right.

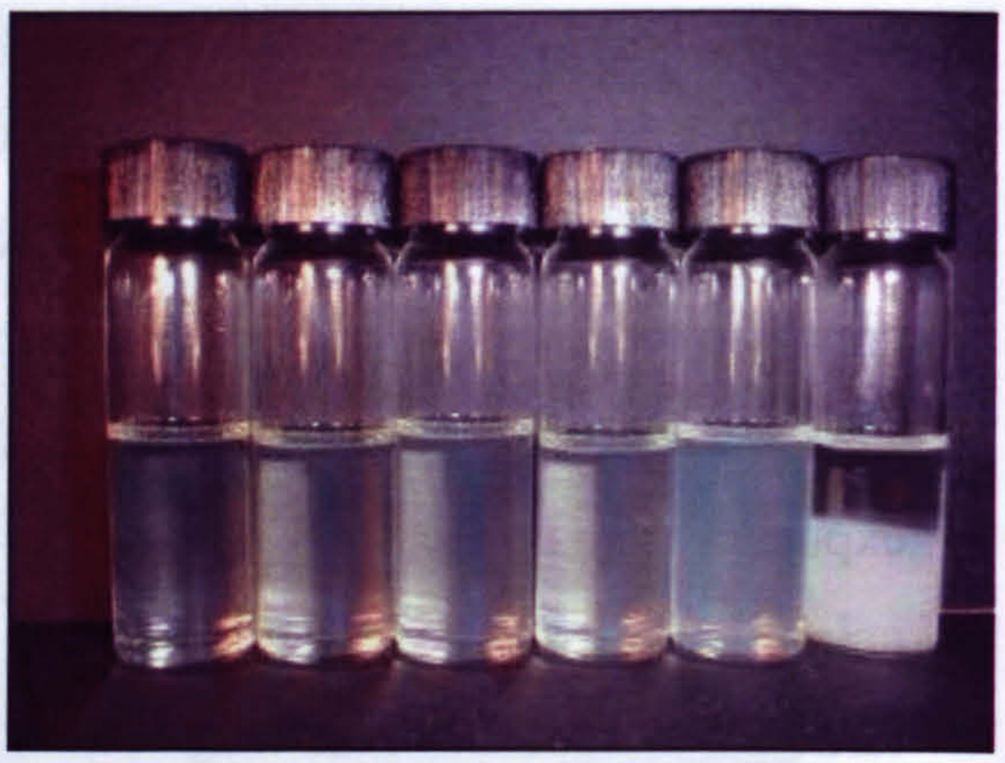

Figure 5.10b. The same mixed solvent SAP Laponite dispersions at 40 °C.

The toluene/ethanol solvent composition is shown in figure 5.8.

5.2.4 SAP Laponite and SAP bentonite Comparisons

Despite undergoing the same treatments, the SAP Laponite and SAP bentonite behaved differently. The clay plates had one large physical difference: their size. The density and surface area of the plates was similar and the reason for the SAP bentonite settling out was due to particle size.

As a result of the very different aspect ratios of the treated clay particles flow and static birefringence was found for the SAP bentonite but not for the SAP Laponite. This was not unexpected since the aspect ratio of the SAP Laponite particles was much lower than that of the SAP bentonite plates.

The untreated bentonite particles had a very high polydispersity and if the sedimentation in pure toluene of the SAP bentonite were due to size alone then a great time range for the sample to settle would be expected. This was not found therefore particle aggregation seemed probable.

As a comparison of the samples in marginal solvents, the SAP bentonite settled and the settled volume was moderately affected by the "quality" of the solvent conditions. The SAP Laponite dispersions showed a much bigger response to the reduction of the quality of the solvent but initially remained as a single-phase. When phase separation

occurred at 20 ºC samples over a narrow range of concentration could be returned to a single-phase fluid by warming to 40 ºC.

5.3 Cationic surfactant treated Clays.

The samples of Dioctadecyl dimethyl ammonium bromide (DODAB) Laponite and DODAB bentonite were prepared as described in section 3.4. After grinding in a pestle and mortar the fine powders were distinctive in colour. DODAB Laponite was a white powder (figure 5.11a), DODAB bentonite was light grey (figure 5.11b), and Claytone AF was beige (figure 5.13c). The Claytone was supplied as a much finer powder than could be produced by grinding in a pestle and mortar and was used as received.

The samples were placed in glass sample tubes with the thread wrapped in a single layer of PTFE tape. This was done to prevent both toluene from evaporating and ultrasonic bath water from contaminating the samples.

Figure 5.11a. Dry powdered DODAB Laponite. The powder was white

Scale bar equals 10 mm

Figure 5.11b. Dry powdered DODAB bentonite. The powder was slightly grey.

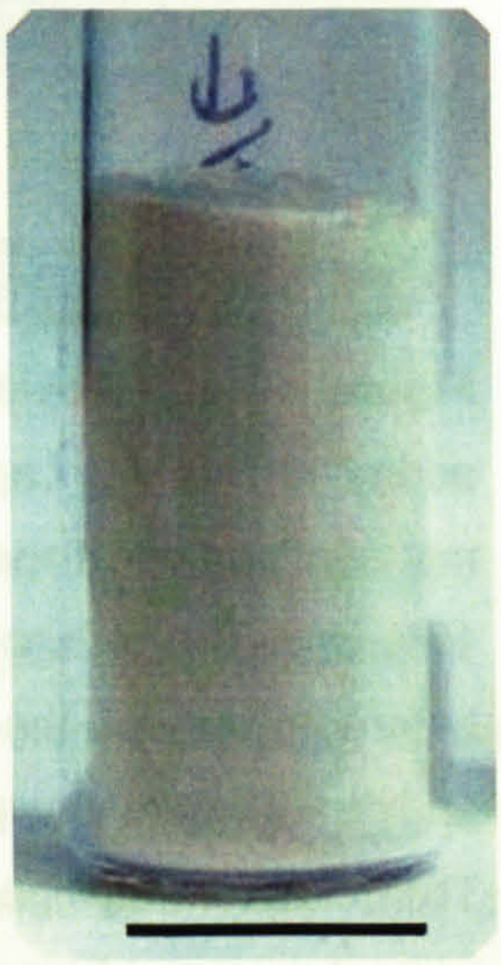

Figure 5.11c. Dry powdered Claytone AF. The particles were finer than the homemade treated clays and beige

Scale bar equals 20 mm

Many samples of DODAB Laponite, Claytone, and DODAB bentonite were prepared in toluene at different concentrations. The highest concentration attempted was 20%

w/w but wetting the clays proved very difficult because the samples gelled rapidly and so firmly that dry patches of clay powder persisted that could not be wet, even by stirring with a spatula and these samples were abandoned. At lower concentrations samples were dispersed using spin mixing, sonication and heating over several hours to form a homogeneous dispersion (figures 5.12).

Figure 5.12a. Toluene was added to DODAB Laponite to make a particle dispersion of 10% w/w. The picture is taken before mixing of the sample and is at room temperature. The toluene wets the powder without the need for agitation

Figure 5.12b. Toluene was added to DODAB bentonite to make a particle dispersion of 7.3% w/w. The picture is taken before mixing of the sample and is at room temperature and no agitation was required to wet the particles.

Figure 5.12c. Toluene was added to Claytone AF to make a particle dispersion of 7.3% w/w. The picture is taken before mixing of the sample and is at room temperature. A large amount of dry Claytone can be seen at the bottom of the sample tube.

Scale bar equals 10 mm

Scale bar equals 20 mm

The Claytone sample, despite having a wide dry layer, showed early signs of dispersal because large loose aggregates could be seen extending into the solvent. The DODAB bentonite and DODAB Laponite samples, on the other hand, despite being wetted by the toluene remained firmly attached to the bottom of the sample tube.

The Claytone required less agitation to disperse than both the homemade surfactant treated clays, which was no surprise, the excess surfactant adsorbed to the surface kept the clay plates further apart reducing the van der Waals forces of attraction [18] and allowed for easier solvent inter-layer penetration. Also, the Claytone powder was finer than the bigger granules of the pestle and mortar-ground DODAB bentonite that were wetted more rapidly.

The samples were spin mixed to break up the clay at the bottom of the tube and then were placed in a beaker of water at 80 ºC and left to stand in an ultrasonic bath for 1 hour. The temperature of the water in the beaker dropped to the ambient temperature of the water bath (35 ºC) within the first 10 minutes. The photographs were taken to show the development of the dispersion (figures 5.13).

Figure 5.13a. 10% w/w DODAB Laponite in toluene after 1 hour of sonication and heating showing yet to be complete dispersion. The sample at room temperature after standing for 15 minutes. Small bubbles fail to rise through the sample indicating the presence of a gel.

Scale bar represents 10 mm

Figure 5.13b. 7.3% w/w DODAB bentonite after agitation and heating for 1 hour. The dispersion developed as a gel but remains incomplete. The picture was taken at room temperature with the sample standing for 15 minutes.

Figure 5.13c. 7.3% w/w Claytone AF dispersion has developed to a point where the particles occupy 100% of the available volume and have gelled. The picture was taken at room temperature with the sample standing for 15 minutes.

Scale bar represents 20 mm

The Claytone sample formed a gel that remained space filling after only a moderate amount of agitation. The DODAB Laponite and DODAB bentonite samples also

formed a gel but they very quickly settled leaving a colourless supernatant. The DODAB bentonite and DODAB Laponite left a grainy solid of large aggregates on the walls of the sample tube if shaken by hand.

On heating and with sonication the Claytone dispersion became less turbid indicating that the remaining aggregates were becoming fewer or smaller.

The complete dispersion was achieved by placing the sample tubes in an ultrasonic bath heated to 60 ºC and every minute for one hour the samples were removed and shaken vigorously by hand. The samples were then left to stand in the hot ultrasonic bath for a further two hours with occasional shaking by hand, and finally the samples were simply left to stand in the ultrasonic bath for another three hours (figures 5.14). This was the most powerful agitation method found that worked without having to resort to a high pressure homogeniser, which would have heated the samples very rapidly to a high temperature, consequently causing the volatile solvent to evaporate [19].

Figure 5.14a. 10% w/w well dispersed DODAB Laponite gel in toluene at room temperature. The space-filling gel was almost colourless.

Scale bar represents 10 mm

Figure 5.14b. 7.3% w/w well dispersed DODAB bentonite gel in toluene at room temperature. The gel was cloudy.

Figure 5.14c. 7.3% w/w well dispersed Claytone AF gel in toluene at room temperature. The sample appears light yellow in colour.

Scale bar represents 20 mm

The samples were allowed to stand at room temperature overnight and did not settle and were inverted as a simple display of the gel strength (figures 5.15). This period of standing was significant because gel strength increased if the samples were left untouched for more than a few hours, which suggests that the samples of cationic surfactant adsorbed clay underwent structural reorganisation [20].

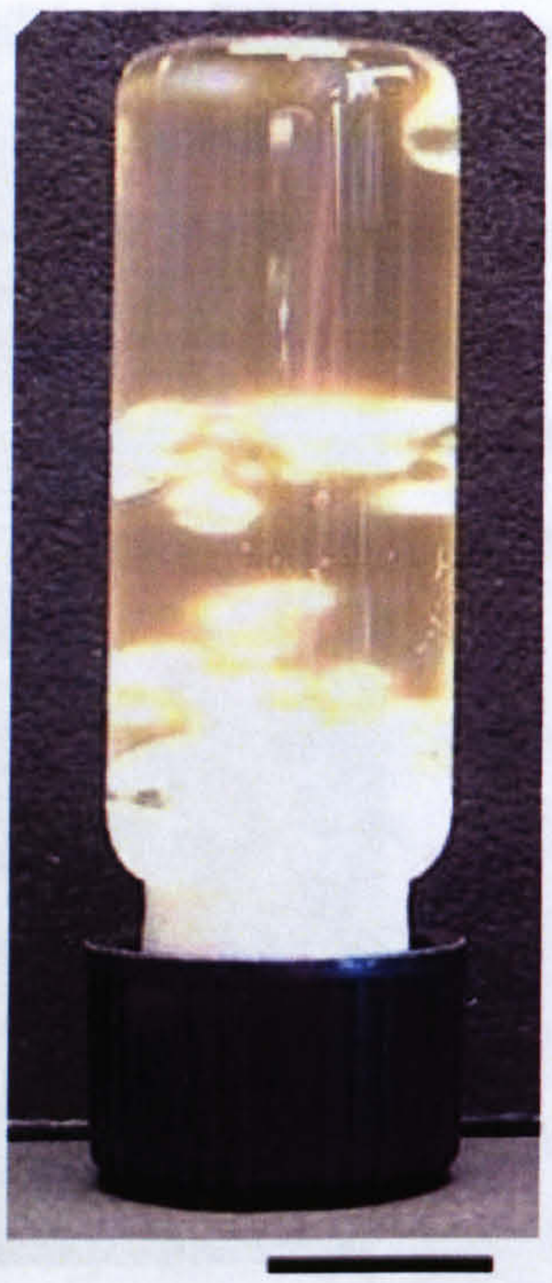

Figure 5.15a. 10% w/w DODAB Laponite in toluene can be inverted without slumping to the bottom of the sample tube.

Scale bar represents 10 mm

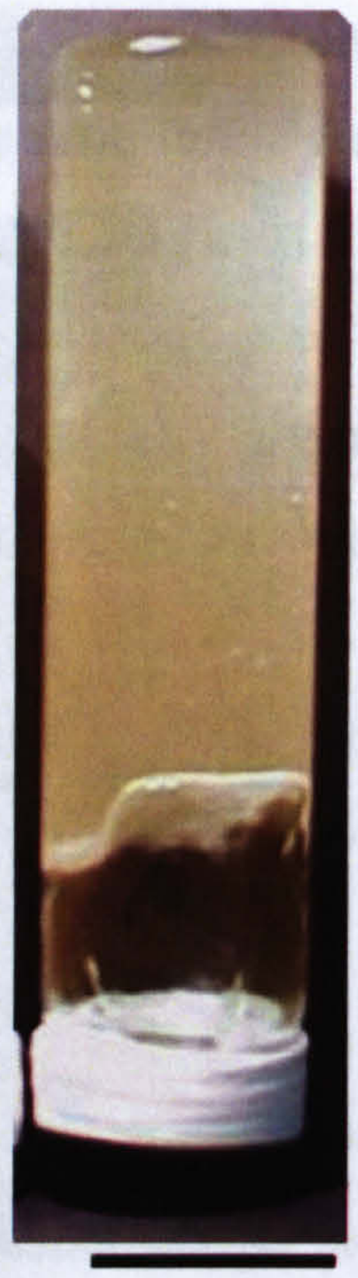

Figure 5.15b. 7.3% w/w DODAB bentonite in toluene can be inverted without the sample falling to the bottom of the tube.

Figure 5.15c. 7.3% w/w Claytone in toluene slid to the bottom of the sample tube upon inversion.

Scale bar represents 20 mm

The samples of surfactant-treated clay were all gels but the Claytone, the most easily dispersed sample, could not be inverted without sliding down the side of the sample holder. However, from these observations alone the gel strengths of Claytone dispersions in toluene compared to DODAB Laponite and DODAB bentonite at the same concentration appeared similar.

All three samples gelled when dispersed in toluene but importantly they required a substantial amount of vigorous shaking and stirring in order to fully disperse (with Claytone requiring the least amount of agitation). This was unsurprising as the Claytone was such a fine powder and supplied with dispersing agents already added [21].

An excess surfactant was added to the Claytone [22] during its manufacture and some of this excess became unattached when the clay was dispersed in toluene and could be

seen as aggregates by the polarising microscope (figure 5.16c). The same was not true for the homemade samples that had a near cationic exchange capacity amount of surfactant used for the treatment (figures 5.16a and 5.16b).

Figure 5.16a. Polarising microscopy image of 10% w/w DODAB Laponite in toluene at 20 °C. The sample was allowed to stand for one week before a small amount was placed on the microscope slide for examination.

Figure 5.16b. Polarising microscopy image of 7.2% w/w DODAB bentonite in toluene at 20 °C and was prepared in the same way as the DODAB Laponite sample.

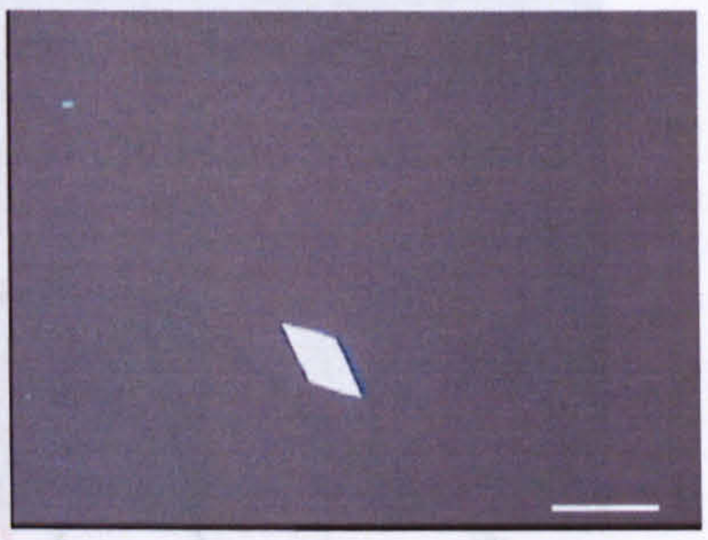

Figure 5.16c. Polarising microscopy image of Claytone AF in toluene under the same magnification and conditions as the previous samples. A diamond shaped surfactant aggregate can be seen.

Scale bar represents 200 μm for all images

5.3.1 Marginalising experiments

One of the first experiments carried out with the surfactant-treated clay samples was to marginalise the solvent with the addition of ethanol but keep the overall concentration constant throughout. The reason for this experiment was to find a solvent mixture that was stable at high temperature but gelled at low temperature. This state was never found with purely surfactant-treated clays and there was little observable temperature dependence of the gelling behaviour (samples remained as gels over a wide temperature range). All the surfactant-treated clays appeared to require a small amount of ethanol in order to form a space-filling gel but as the proportion of ethanol was increased the samples phase separated again.

The samples were prepared at higher concentration in pure toluene and placed in an ultrasonic bath for 1 hour before the addition of toluene and ethanol to keep the particle concentration constant throughout the series. After the toluene and ethanol

addition, the samples were sealed in their tubes, spin mixed for a few seconds and placed for another hour in the ultrasonic bath. The water temperature in the ultrasonic bath, though warmed by the ultrasonic action, was not set by hand and rose to 45 ºC by the end of the hour in the bath.

The toluene and ethanol composition of the samples is given in figure 5.17.

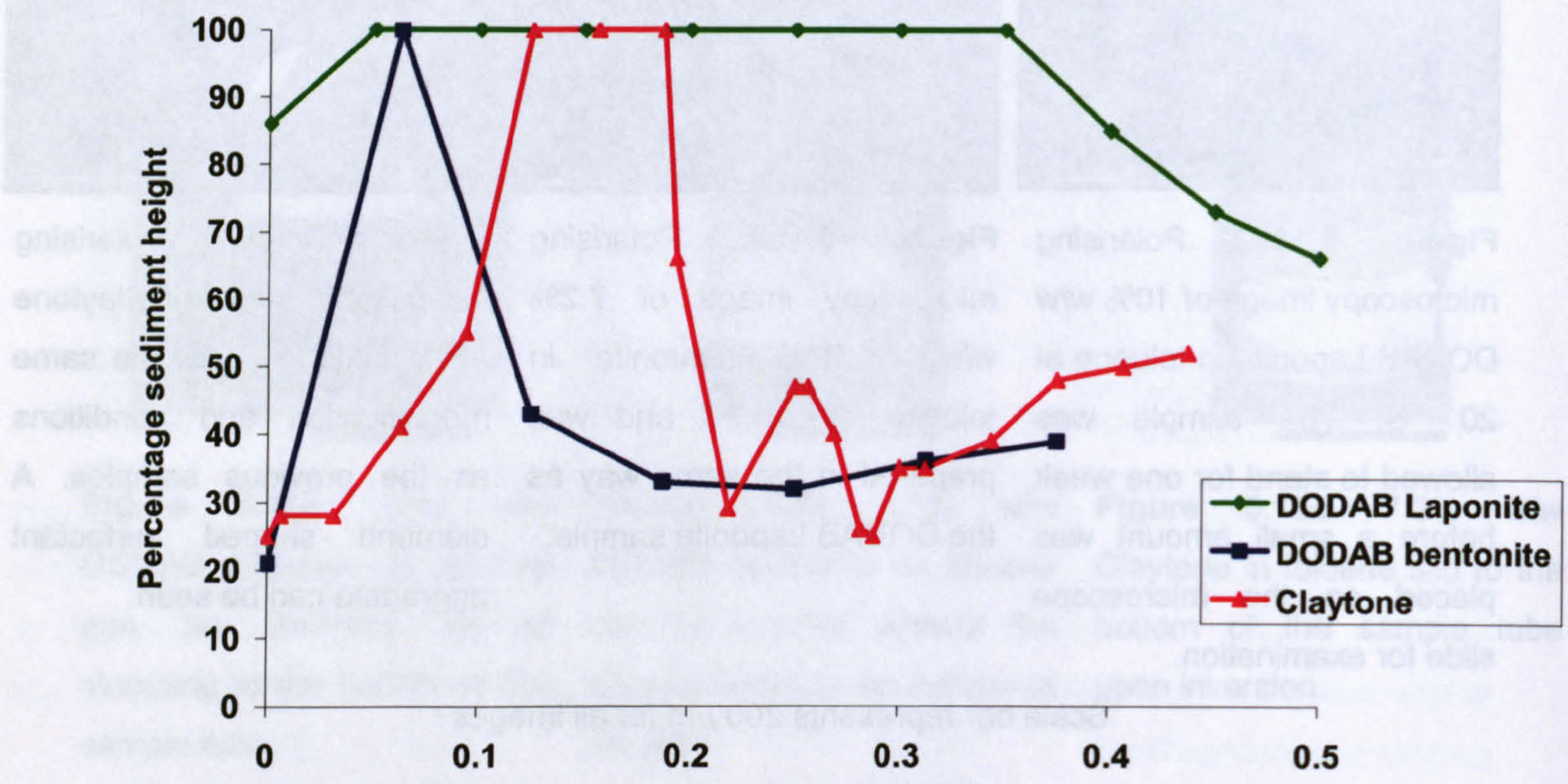

Figure 5.17. Graph of the variation of gel height with solvent composition for DODAB Laponite, DODAB bentonite and Claytone in toluene/ethanol mixed solvents.

Images of the marginalisation experiments of DODAB Laponite, DODAB bentonite and Claytone can be seen in figures 5.18, below.

Figure 5.18a. Series of DODAB Laponite samples, 20 g total solvent mass at 5% w/w in mixed solvent of toluene/ethanol at room temperature after standing for 7 days. Solvent composition given in figure 5.17, above.

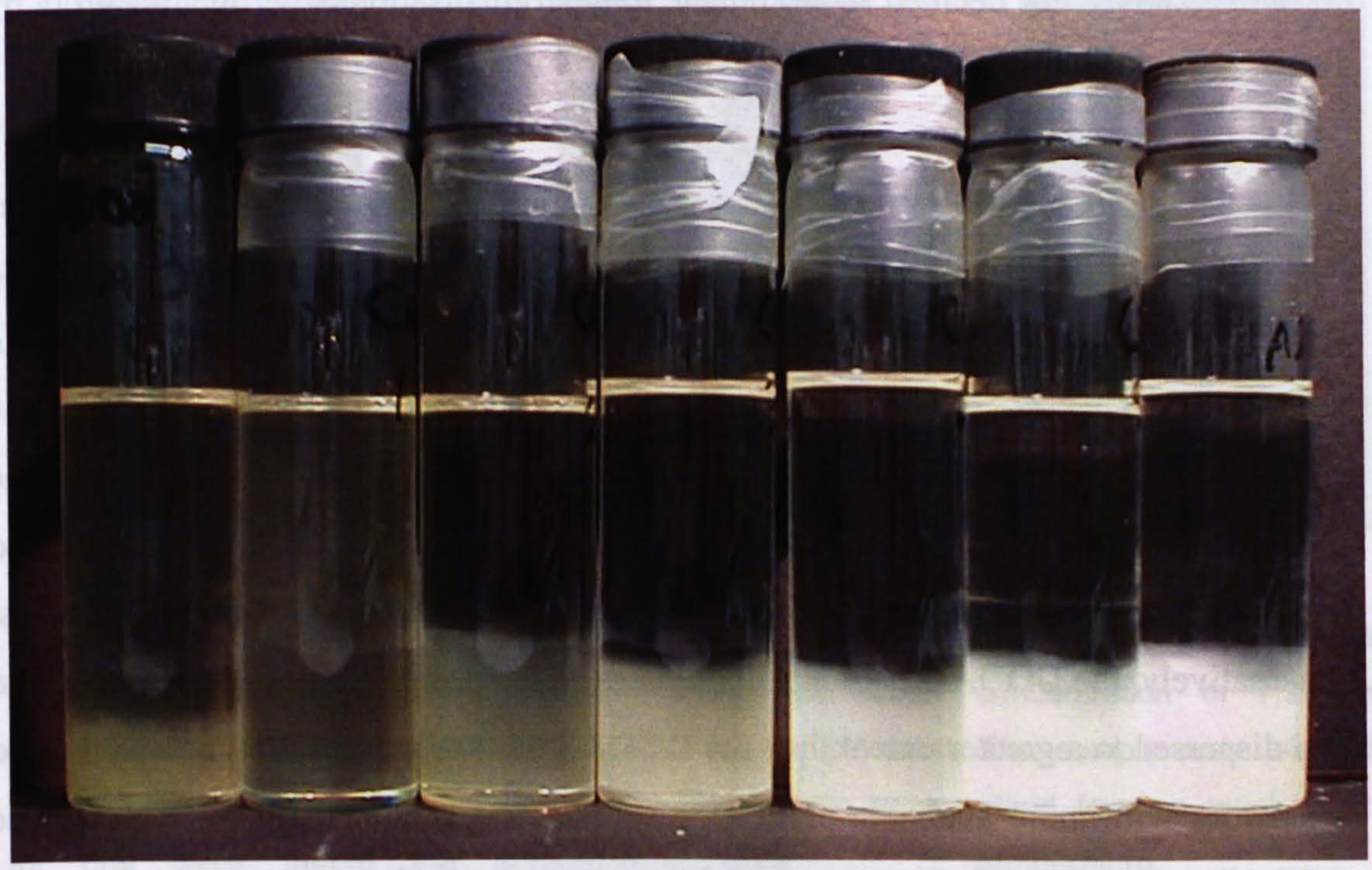

Figure 5.18b. Series of DODAB bentonite samples 16 g total solvent mass at 4% w/w in mixed solvent of toluene/ethanol at room temperature after standing for 7 days. Solvent composition given in figure 5.17, above.

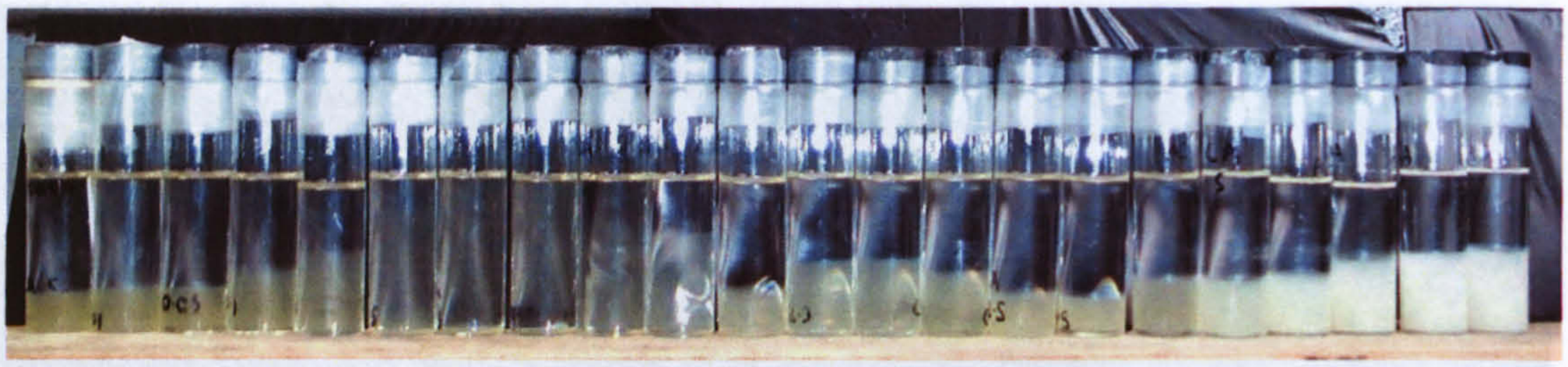

Figure 5.18c. Series of Claytone AF samples 16 g total solvent mass dispersed at 5% w/w in mixed solvent of toluene/ethanol at room temperature after standing for 7 days. Solvent composition given in figure 5.17, above.

Initially it was thought that a small amount of ethanol was needed to stabilise the dispersion but further literature investigation found that the ethanol was acting as a dispersing agent [1, 2]. Sonicating whilst heating the particles for a longer time confirmed this, however because of some ambiguity in the literature regarding the role of the ethanol it was decided not to pursue the marginalisation experiments purely by this method.

The behaviour displayed in figures 5.18 was certainly interesting with all the samples sedimenting without the addition of ethanol. The DODAB bentonite and Claytone formed quite a dense sediment (low sediment volume) and the DODAB Laponite showed a much more open sediment. There were two possible reasons for this; the first was that the DODAB Laponite particles formed an open network due to the greater inter-particle attraction without any ethanol present causing the particles to become stuck fast on first contact with other DODAB Laponite particles. Alternatively, the DODAB Laponite aggregates as the powder may have broken down and dispersed to a greater extent than the DODAB bentonite and Claytone and formed a network with more available particles resulting in a greater network volume. The DODAB bentonite and Claytone may have rearranged after contact and formed a more ordered and dense structure. Beyond a certain limit the solvent mixture became poor for the surfactant-adsorbed particles and they phase separated again. However, for the DODAB Laponite samples, the sediment became denser with increasing ethanol; but for the Claytone and DODAB bentonite the sediment height goes through a minimum and starts to occupy greater volume. It was the increasing sediment height that could be explained by reasoning that the poorer the solvent the greater the interparticle attraction and the more open the sediment structure. Also, the Laponite

particles have a high proportion of plate edge with no surfactant adsorbed and this may play an important role in gel formation.

5.3.2 Cationic Surfactant-treated clays in polydecene

An alternative solvent, polydecene [23, 24] was used to disperse the samples and was selected because of its non polarity, low volatility, and use in many cosmetic formulations. The same dispersing procedure was used to disperse the particles as for the well dispersed toluene samples, i.e. prolonged sonication and heating (figures 5.19).

Figure 5.19a. DODAB Laponite dispersed in polydecene at a concentration of 7.1% w/w. The sample was returned to room temperature for one week before the photograph was taken.

Scale Bar represents 20 mm

Figure 5.19b. DODAB bentonite dispersed in polydecene at a concentration of 7.2% w/w. The sample was allowed to stand for one week at room temperature.

Figure 5.19c. Claytone AF dispersed in polydecene at a concentration of 7.2% w/w. The sample was allowed to stand for one week at room temperature.

Scale Bar represents 10 mm

Only the Claytone could be dispersed in the polydecene using the spin mixing, heating, and sonication method outlined previously. The reason for this was attributed to the excess surfactant added to the surface of the clay during its preparation. With the Claytone surface covered with surfactant molecules the polydecene was able to

penetrate between the layers of clay separating the individual plates thus easing the dispersion.

5.4 SAP and Surfactant Combined Treatment

The SAP-treated samples of surfactant-adsorbed clay showed a number of interesting features. The method used to treat the clays with the SAP polymer was very quick and effortless in comparison with the other treatments. Excess SAP polymer was simply added neat or diluted in toluene to a dispersion of surfactant adsorbed clay particles and shaken by hand.

5.4.1 SAP DODAB Laponite

On addition of SAP to DODAB Laponite the gel rapidly reduced in viscosity and became a fluid yet shaking of the sample revealed large aggregates that settled out within 5 minutes (figure 5.20). Sustained sonication and spin mixing did not break down these aggregates and the excess polymer was removed by allowing the particles to settle and decanting the yellow coloured supernatant before adding fresh toluene. This process was repeated until the supernatant remained colourless. There was no change in the behaviour of the SAP DODAB Laponite particles and the large aggregates were still visible as grains on the walls of the sample tube.

Figure 5.20. SAP DODAB Laponite at 5% w/w in toluene at room temperature with the excess polymer removed. The sample phase separate within a few minutes when left to stand. The scale bar equals 20 mm.

From observing the colour change in the sample it was evident that SAP adsorbed to the surface of the Laponite but unlike the pure SAP treated Laponite, the particles were not stable. It was expected that the addition of SAP to the DODAB Laponite would stabilise a dispersion of the particles in toluene since toluene is a good solvent for the polymer [25]. The addition of DODAB to Laponite occurred over the faces of the plates and not at the edges but the SAP adsorbed over all of the surface [26] and may have disrupted the gelling mechanism where edge charges have been considered important [4, 27]. There is also the possibility of bridging flocculation between the exposed edges of DODAB Laponite from the succinimide head group. This does not fully explain the instability of the SAP DODAB Laponite dispersion in toluene and the cause of the SAP DODAB Laponite flocculation was a mystery, especially when they had adsorbed an appreciable amount of polymer that was designed to stabilise particles in organic media [7].

5.4.1.1 SAP DODAB Laponite Solvent Transfer

The effect of changing the solvent was investigated with the transfer of the SAP DODAB Laponite particles to non-volatile polydecene (section 3.2.6) however, the particles remained unstable (figure 5.21). This was not unexpected, since polydecene is a branched chain alkane and hence is a slightly poorer solvent than toluene.

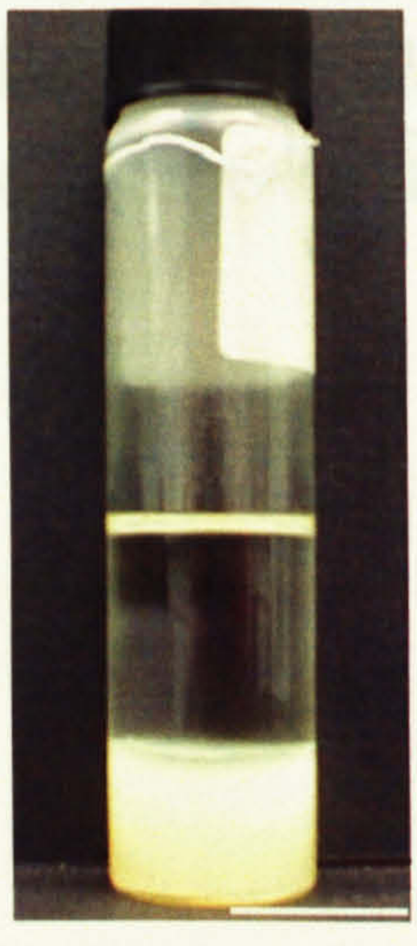

Figure 5.21. SAP DODAB Laponite at 3% w/w dispersed in polydecene at room temperature. The sample phase separated after 5 minutes settling to the height in the picture within 2 hours. The scale bar represents 20 mm.

The concentration of the particles in the sediment where polydecene was the solvent was 8% w/w but 13% w/w for the particles dispersed in toluene. This indicates that toluene was a better solvent for the SAP DODAB Laponite as the particles formed a more dense network since the energy barrier to rearrangement was not too high [28]. If rearrangements can occur then the mechanism for particle aggregation will be a dynamic process and not a chemical process such as bridging flocculation.

5.4.2 SAP DODAB bentonite and SAP Claytone

On addition of SAP to a dispersion of DODAB bentonite or Claytone in toluene the gel broke down very quickly and the sample became a fluid with a low viscosity. If the samples were held between crossed polarisers upon addition of the SAP to the DODAB bentonite and Claytone, flow birefringence was observed suggesting the particles were well stabilised. The excess polymer was removed by centrifugation, the supernatant was removed and after addition of fresh toluene, the particles were redispersed by spin mixing and sonication. This process was repeated 3 times.

The slightly turbid dispersions of DODAB bentonite and Claytone became clearer after treatment with SAP indicating the number and/or size of aggregates was reduced (figures 5.22). However, the value of the refractive index of the treated particles may have approached the value of the refractive index of the solvent causing a reduction of the light scattering contrast. The refractive index of the SAP polymer was 1.5045 [26, 29] and toluene solvent was 1.497 [29].

Figure 5.22a. SAP DODAB bentonite at 5% w/w dispersed in toluene at room temperature without excess SAP removed.

Figure 5.22b. SAP Claytone dispersed at 5% w/w in toluene at room temperature without excess SAP removed

Scale bar represents 20 mm.

Unlike the SAP DODAB Laponite particles dispersed in toluene, the SAP DODAB bentonite and SAP Claytone dispersions did not settle out when left standing for days or even weeks. With toluene as the solvent and over a wide range of concentrations the particles remained as fluids showing no tendency to gel. However, samples of SAP-treated Claytone showed some slow-growing aggregates when observed through crossed polarisers that looked fine and wispy and took a number of days to develop (figure 5.23). The aggregates rapidly disappeared upon warming to 50 °C and were too delicate to remove from the sample intact. They were believed to be surfactant above the cationic exchange capacity adsorbed to the Claytone displaced by the SAP molecules.

Figure 5.23. Aggregation of excess surfactant from a sample of 3% w/w SAP treated Claytone in toluene. No attempt was made to purify the sample and get rid of excess surfactant and polymer. The picture was taken between crossed polarisers. The scale bar represents 20 mm.

Flow birefringence was displayed by the SAP DODAB bentonite and SAP Claytone samples and appeared when gently shaken between crossed polarisers (figure 5.24). The flow birefringent patterns rapidly relaxed at low particle concentration once the flow of the sample ceased.

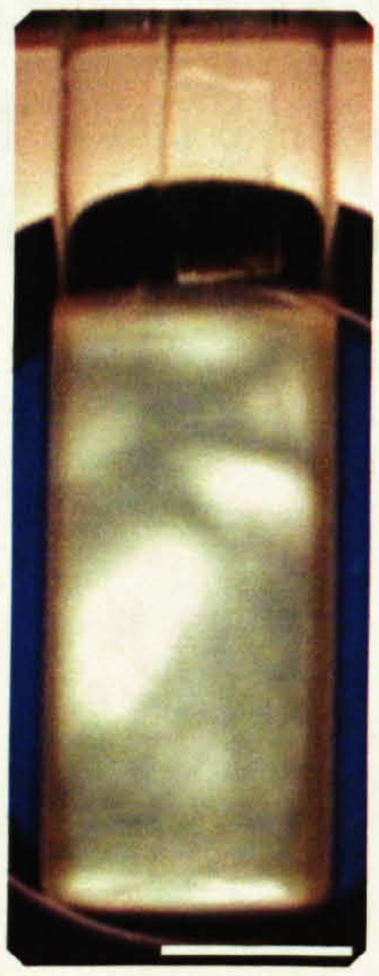

Figure 5.24. Flow birefringence seen for a sample of SAP DODAB bentonite at 2.1% w/w in toluene at room temperature. Scale bar equals 10 mm.

The flow birefringence remained at concentrations above 5% w/w. However, this permanent birefringence was not found to occur spontaneously and was always flow induced (figure 5.25). For these samples the permanent birefringence showed that a very weak gel was formed that was broken down by a small disturbance.

Figure 5.25. Flow induced permanent birefringence seen for a sample of SAP Claytone at 5% w/w in toluene at room temperature. Scale bar denotes 20 mm.

The difference in behaviour between the dispersions of SAP DODAB bentonite and SAP Claytone in toluene, when compared to the SAP DODAB Laponite dispersion, was remarkable especially considering the much smaller size of Laponite particles. Aggregation of the SAP DODAB Laponite clearly occurred but the nature of the strong interparticle attraction was unknown.

5.4.3 SAP Claytone Marginal solvent

The SAP Claytone samples were stable in pure toluene and the solvent was marginalised with the addition of ethanol to induce gelation. A series of samples were made at low but constant SAP Claytone concentrations in toluene and the proportion of ethanol and toluene was altered.

The dispersions in the marginal solvent were prepared (figures 5.26) with the addition of first toluene then ethanol and finally they were spin mixed and allowed to stand. The sample with the greatest amount of ethanol became the most turbid and started to

phase separate rapidly. The turbidity was due not only to large aggregates forming but also the increased difference in the refractive index between the particles and the solvent.

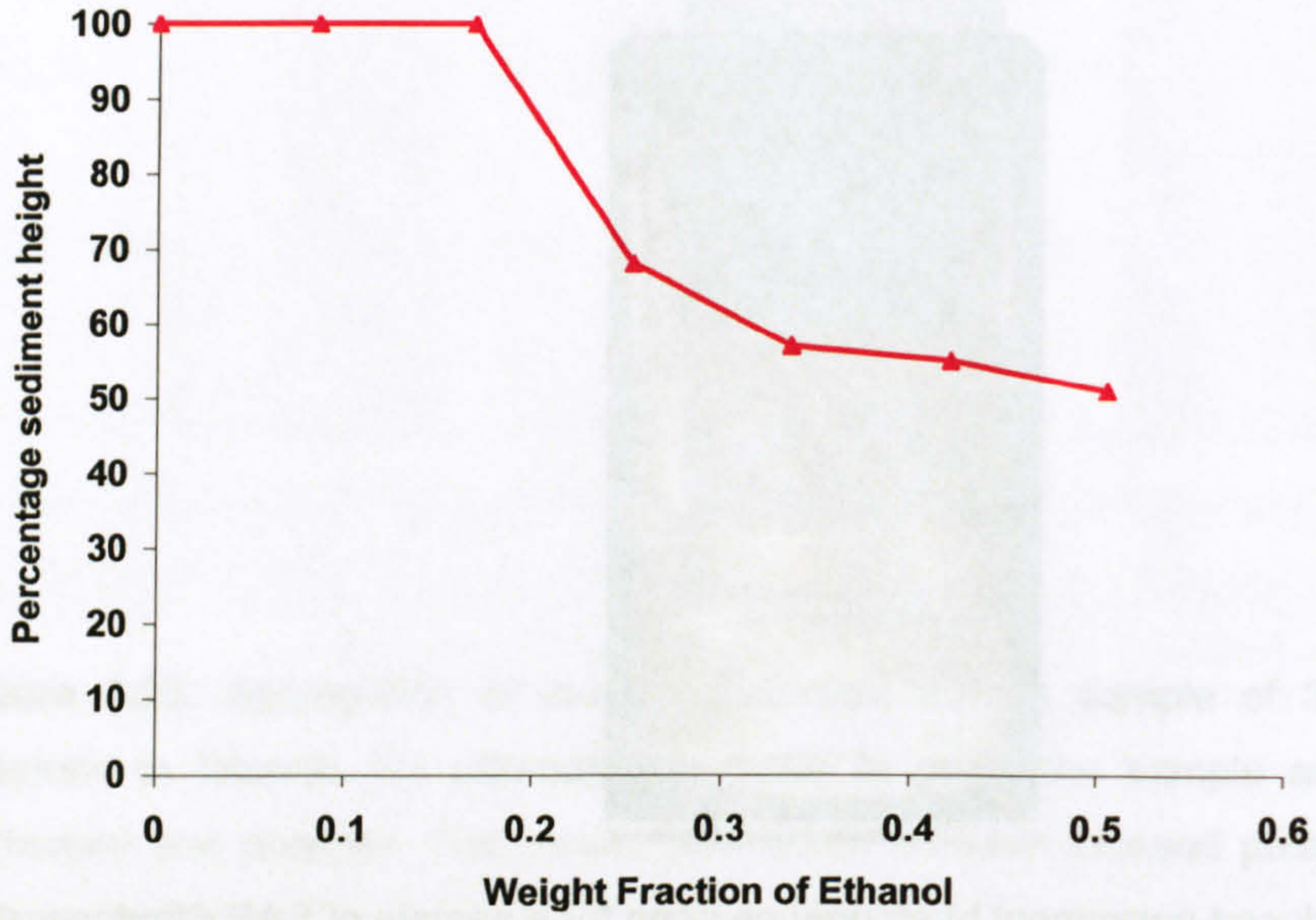

Figure 5.26. 1% w/w SAP Claytone dispersed in mixtures of toluene and ethanol at 20 ºC.

Pictures of the samples are shown below, figure 5.27.

Figure 5.27a. SAP Claytone dispersions in toluene ethanol mixtures with increasing proportion of ethanol at 20 ºC.

Figure 5.27b. The same SAP Claytone mixed solvent dispersions 40 ºC.

Scale bar represents 20 mm.

Phase separation was found as the solvent was increasingly marginalised with the addition of a greater proportion of ethanol (figures 5.27). This phase separation occurred as the total amount of ethanol exceeded 25% w/w with the sample at this concentration not becoming homogeneous when kept at 40 ºC overnight. After shaking by hand the nature of the samples did not alter and they all displayed the

same behaviour as at 20 °C. The sediments of the phase-separated samples were gels since they held their original shape when the sample tubes were placed on a steep slope overnight. Using this method to marginalise the solvent conditions for the SAP-adsorbed particles was not productive. Another problem with this method was the solvent evaporation changing not only the concentration of the particles but also the composition of the solvent mixtures.

5.4.4 Transfer of SAP DODAB bentonite and SAP Claytone into Polydecene

The original aim of the study was to make a dispersion of anisotropic particles that was stable at high temperature but unstable and gel forming at low temperature (figures 5.28). Transferring the SAP Claytone and SAP DODAB bentonite samples from toluene into non-volatile polydecene [24] gave a dispersion that displayed temperature-dependant gelling. This transfer was carried out by placing a known mass of SAP-adsorbed clay in toluene in a round-bottomed flask and adding polydecene to make a dispersion at a known weight concentration. The toluene was removed by rotary evaporation to leave the SAP adsorbed clay dispersed in polydecene alone. Dry weight analysis could not be carried out on the particles in polydecene, because polydecene did not significantly evaporate under vacuum at 100 °C for 24 hours. The weight concentration of the treated clay in the polydecene was based upon knowledge the concentration and mass of the toluene samples.

Figure 5.28a. 5.2% w/w samples of SAP DODAB bentonite, on the left, and SAP Claytone, on the right, dispersed in polydecene at room temperature.

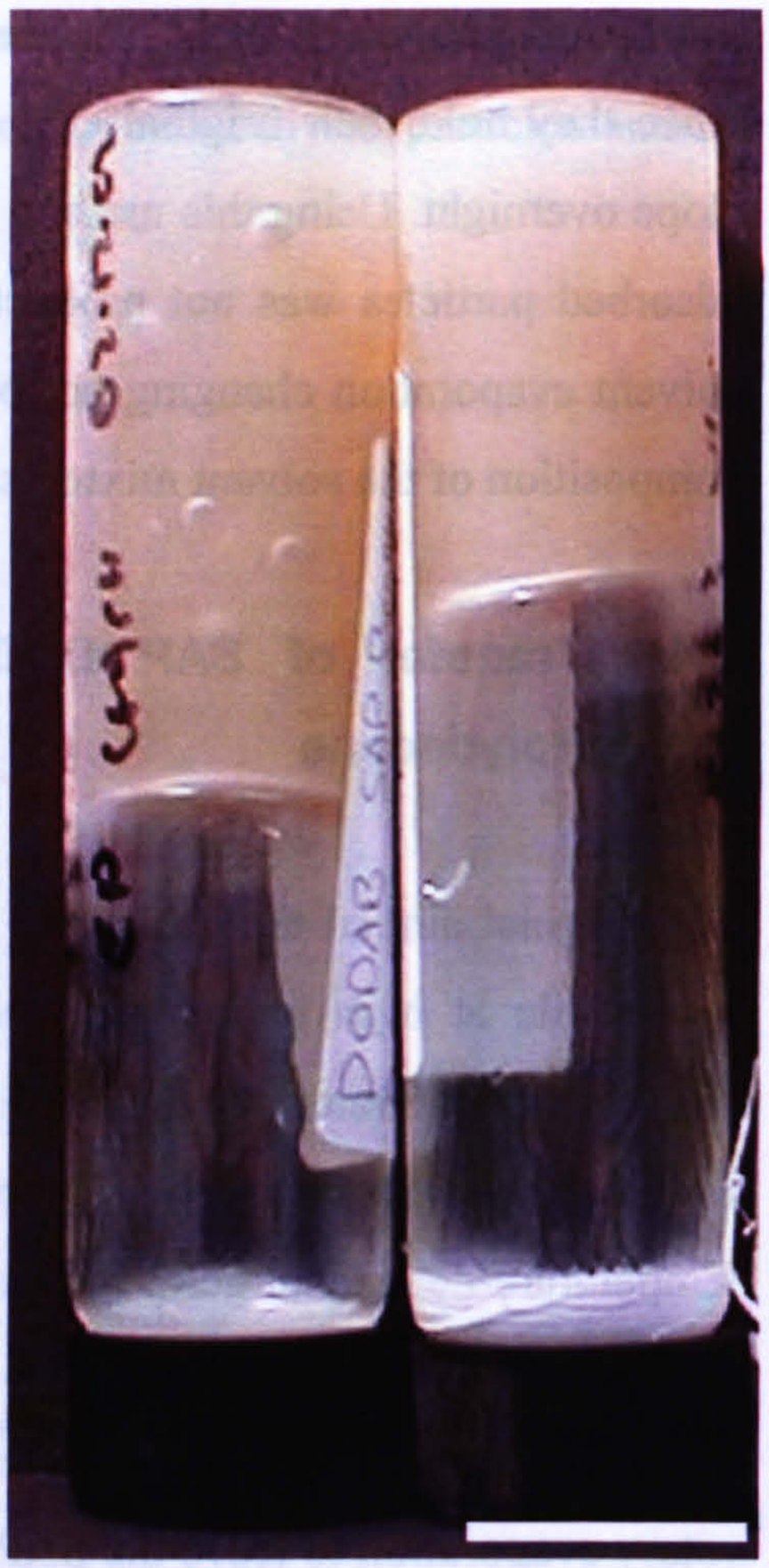

Figure 5.28b. 5.2% w/w SAP DODAB bentonite, on the left, and SAP Claytone, on the right, dispersed in polydecene at –7 °C. The samples form a gel.

Scale bars indicate 20 mm.

The dispersions in polydecene were opaque and fluid but more viscous than dispersions at the same concentration in toluene. Due to the turbidity of the samples, evidence for flow birefringence was not found but particle aggregation did not occur as the samples only started to sediment if left to stand for weeks. Samples were prepared from 3.5% w/w to 10% w/w and all showed highly important temperature-dependant gelling behaviour. The temperature at which the gelling transition occurred was below 0 °C and was found by cooling the samples in a freezer.

This behaviour was not as a result of the polymer and surfactant-rich polydecene freezing; the addition of free SAP and DODAB to the polydecene found in the gelling samples did not form a gel over a range of concentrations (see chapter 7).

Placing the samples in a freezer and noting the temperature at which the samples gelled and then permitting them to warm back up to room temperature and noting the temperature at which they became fluid were the initial experiments carried out with the temperature-dependant gelling samples. Due to the samples' very low volatility and the reversible gelling behaviour displayed a rheological study was undertaken.

5.5 Conclusions

Both Laponite and bentonite were successfully treated at low concentration with a low molecular weight poly (isobutylene) polymer SAP. The particles dispersed in toluene showed very different behaviour with the SAP Laponite remaining stable with a low viscosity but the SAP bentonite sedimented completely within a few days due to particle aggregation.

The highly anisotropic SAP bentonite plates displayed flow birefringence and the sediment was nematic. No liquid crystalline phases were found for the stable SAP Laponite dispersion, however the aspect ratio of these particles was at best 4:1 and the concentration required was never achieved without the particles drying out on the walls of the vessel. A temperature-dependant gelling transition was found for SAP Laponite dispersed in a toluene/ethanol mixed solvent but slight solvent evaporation made quantitative study of the samples difficult.

The behaviour of dispersions in toluene of dioctadecyldimethyl ammonium bromide (DODAB) cationic surfactant-adsorbed clays was investigated but the dispersions always formed gels. However, the treatment was very simple and a commercially available cationic surfactant adsorbed bentonite (Claytone) with a polydisperse version of DODAB was also used. The samples required vigorous stirring and shaking to disperse in toluene making space-filling gels at concentration of a few percent by weight. Marginalisation of these samples with the addition of ethanol was undertaken and revealed that dispersion could be eased with small amounts of polar molecules yet no temperature-dependent gelling could be found. The characteristics of dispersions

of DODAB Laponite, DODAB bentonite, and Claytone were very similar in toluene but Claytone was most easily dispersed in polydecene.

The addition of SAP to Claytone and DODAB bentonite in toluene gave a colloidally stable system that did not form a gel at low concentration. The dispersion was flow birefringent indicating the presence of anisotropic particles and did not settle when left to stand. At a concentration above 5% w/w, permanent birefringence was flow induced but the sample remained low in viscosity. The SAP DODAB Laponite dispersion in toluene aggregated and sedimented very rapidly and was not stable despite sonication and heating. Adding SAP to very dilute dispersions of DODAB Laponite was not tried but would reduce the chance of flocculation as a result of bridging between the particles.

Destabilising the SAP DODAB bentonite and SAP Claytone plates with the addition of ethanol to the 'good' solvent, toluene, caused the particles to aggregate and phase separate but no temperature effect was found.

By exchanging the solvent for polydecene, a saturated and branched chain hydrocarbon, a temperature-dependent gelling transition was found where the SAP DODAB bentonite and SAP Claytone dispersions gelled upon cooling. This behaviour was found over a range of concentrations and was reversible.

5.6 References

1. Theng, B.K.G., *The Chemistry of Clay-Organic Reactions*. 1974, London: Rank Precision Industries.
2. Bongiovanni, R., M. Chiarle, and E. Pelizzetti, *Adsorption of Organic-Molecules onto Montmorillonite - Cationic Surfactants with Different Polar Head Group*. Journal of Dispersion Science and Technology, 1993. **14**(3): p. 255-268.
3. Jones, T.R., *The Properties and Uses of Clays Which Swell in Organic Solvents*. Clay Minerals, 1983. **18**(4): p. 399-410.
4. Damerell, V.R. and E. Milberger, *Organophilic Montmorillonite Gels*. Nature, 1956. **178**: p. 200.
5. Lagaly, G. and R. Malberg, *Disaggregation of Alkylammonium Montmorillonites in Organic- Solvents*. Colloids and Surfaces, 1990. **49**(1-2): p. 11-27.
6. van der Kooij, F.M. and H.N.W. Lekkerkerker, *Formation of nematic liquid crystals in suspensions of hard colloidal platelets*. Journal of Physical Chemistry B, 1998. **102**(40): p. 7829-7832.
7. Smits, C., et al., *Influence of the stabilizing coating on the rate of crystalization of colloidal systems*. Progress in colloidal and polymer science, 1989. **79**: p. 287-292.
8. Ho, D.L., R.M. Briber, and C.J. Glinka, *Characterization of organically modified clays using scattering and microscopy techniques*. Chemistry of Materials, 2001. **13**(5): p. 1923-1931.
9. Imhof, A., A. van Blaaderen, and J.K.G. Dhont, *Shear Melting of Colloidal Crystals of Charged Spheres Studied with Rheology and Polarising Microscopy*. Langmuir, 1994. **10**: p. 3477-3484.
10. Hunter, R.J., *Foundations of Colloid Science*. Second Edition ed. 2001, Oxford: Oxford University Press.
11. Wieland, E., et al., *A Surface Chemical Model of the Bentonite-Water Interface and its Implications for Modelling the Near Field Chemistry in a Repository for Spent Fuel*. 1994, Swedish Nuclear Fuel and Waste Management Company: Stockholm.
12. Grillo, I., P. Levitz, and T. Zemb, *Insertion of small anisotropic clay particles in swollen lamellar or sponge phases of nonionic surfactant*. European Physical Journal E, 2001. **5**(3): p. 377-386.
13. Everett, D.H., *Basic Principles of Colloid Science*. First Edition ed. Royal Society of Chemistry Paperbacks. 1988, London: The Royal Society of Chemistry.
14. van Olphen, H., *An Introduction to Clay Colloid Chemistry: For Clay Technologists, Geologists, and Soil Scientists*. 2nd Edition ed. 1977: John Wiley & Sons, Inc.
15. Shaw, D.J., *Colloid and Surface Chemistry*. Fourth Edition ed. 1992, Oxford: Butterworth-Heinemann.
16. van der Kooij, F.M., K. Kassapidou, and H.N.W. Lekkerkerker, *Liquid crystal phase transitions in suspensions of polydisperse plate-like particles*. Nature, 2000. **406**(6798): p. 868-871.
17. Kiraly, Z., et al., *Van der Waals attraction between Stober silica particles in a binary solvent system*. Colloid and Polymer Science, 1996. **274**(8): p. 779-787.

18. Tabor, D. and R. Winterton, *The direct measurement of Normal and Retarded van der Waals Forces.* Proceedings of the Royal Society A, 1969. **312**: p. 435-450.
19. Lewkowicz, N.M., *An Investigation into the Structuring of an Hydrophobic Clay in Silicone Fluid.* PhD. Thesis. Faculty of Medicine, University of London, London. UK, 2000.
20. Mourchid, A., et al., *On viscoelastic, birefringent, and swelling properties of Laponite clay suspensions: Revisited phase diagram.* Langmuir, 1998. **14**(17): p. 4718-4723.
21. http://www.scprod.com/europe/claytoneseurope.htm, *Claytone AF Safety Data Sheet.* 2002, Southern Clay Products.
22. Ho, D.L. and C.J. Glinka, *Effects of solvent solubility parameters on organoclay dispersions.* Chemistry of Materials, 2003. **15**(6): p. 1309-1312.
23. Lee, C. and W. Kumler, *The dipole moment and Structure of the Imide Group. 1. Five- and Six-membered Cyclic Imides.* Journal of the American Chemical Society, 1961. **83**(22): p. 4586-4590.
24. Lee, B., *The physical properties of polydecene and its use in personal care products.* 1994, Amoco Chemical Company: Chicago.
25. Pathmamanoharan, C., *Preparation of Monodisperse Polyisobutene Grafted Silica Dispersion.* Colloids and Surfaces, 1988. **34**(1): p. 81-88.
26. Buining, P.A., et al., *Preparation of a Nonaqueous Dispersion of Sterically Stabilized Boehmite Rods.* Colloids and Surfaces, 1992. **64**(1): p. 47-55.
27. Granquist, W.T. and J. McAtee, J. L., *The gelation of Hydrocarbons by Montmorillonite organic complexes: The role of the Dispersant.* Journal of Colloid Science, 1963. **18**: p. 409-420.
28. Szanto, F., et al., *Wetting, Swelling and Sediment Volumes of Organophilic Clays.* Colloids and Surfaces, 1986. **18**(2-4): p. 359-371.
29. Lide, D.R., ed. *CRC Handbook of Chemistry and Physics.* 75th ed. 1994, Chemical Rubber Company: Florida, USA.

6 Electron Microscopy and Atomic Force Microscopy

6.1 Introduction

Simple observations and light microscopy revealed much about the macroscopic behaviour of the particles in dispersion. A limiting factor was that only relatively large features were observable. Using scanning electron microscopy and transmission electron microscopy it was possible to see much more detail (section 3.4.1) but the samples were observed dried down under vacuum. Studies into the network structure using SEM have been undertaken to directly observe the make up of montmorillonite gels [1] but careful methods were needed to dry the samples and preserve the structure. For all SEM samples a 15 nm thick conducting layer of gold was applied to prevent the sample charging under the electron beam. The samples examined using the Atomic Force Microscope (AFM) (section 3.4.2) were dried down on to a molecularly flat mica surface. Individual clay particles showed up clearly using the AFM and features such as the thickness of dry treated clay plates were found.

6.2 Untreated Laponite

In the literature many methods have been used to characterise Laponite dispersions and the plates that make them up [2-4] but there exist very few images of Laponite plates. Transmission electron microscopy (TEM) gave little contrast resulting in diffuse images and scanning electron microscopy (SEM) did not possess the resolution to give good images of the Laponite particles.

6.2.1 Untreated Laponite imaged using AFM

The AFM experiments were all carried out in air using the tapping mode under the supervision of Rachel Owen in the department of Physics, University of Bristol. In the tapping mode a silicon nitride tip oscillates at its resonance frequency as it scans the surface of the sample line-by-line and experiences only intermittent contact with the surface [5]. A piezo electric crystal controls the distance of the tip from the surface and the image is built up from the tiny changes in surface height and the

corresponding change in the voltage applied to the piezo electric crystal. All samples examined under the AFM were dried onto freshly exposed molecularly flat mica substrates.

AFM was used to examine untreated Laponite to find out the size and shape of the particles. The AFM samples were prepared from 0.001% w/w aqueous dispersions and dried under vacuum at room temperature on a mica stub (figure 6.1). Keeping the sample in a desiccator and transporting it in a covered petri dish prevented contamination by dust.

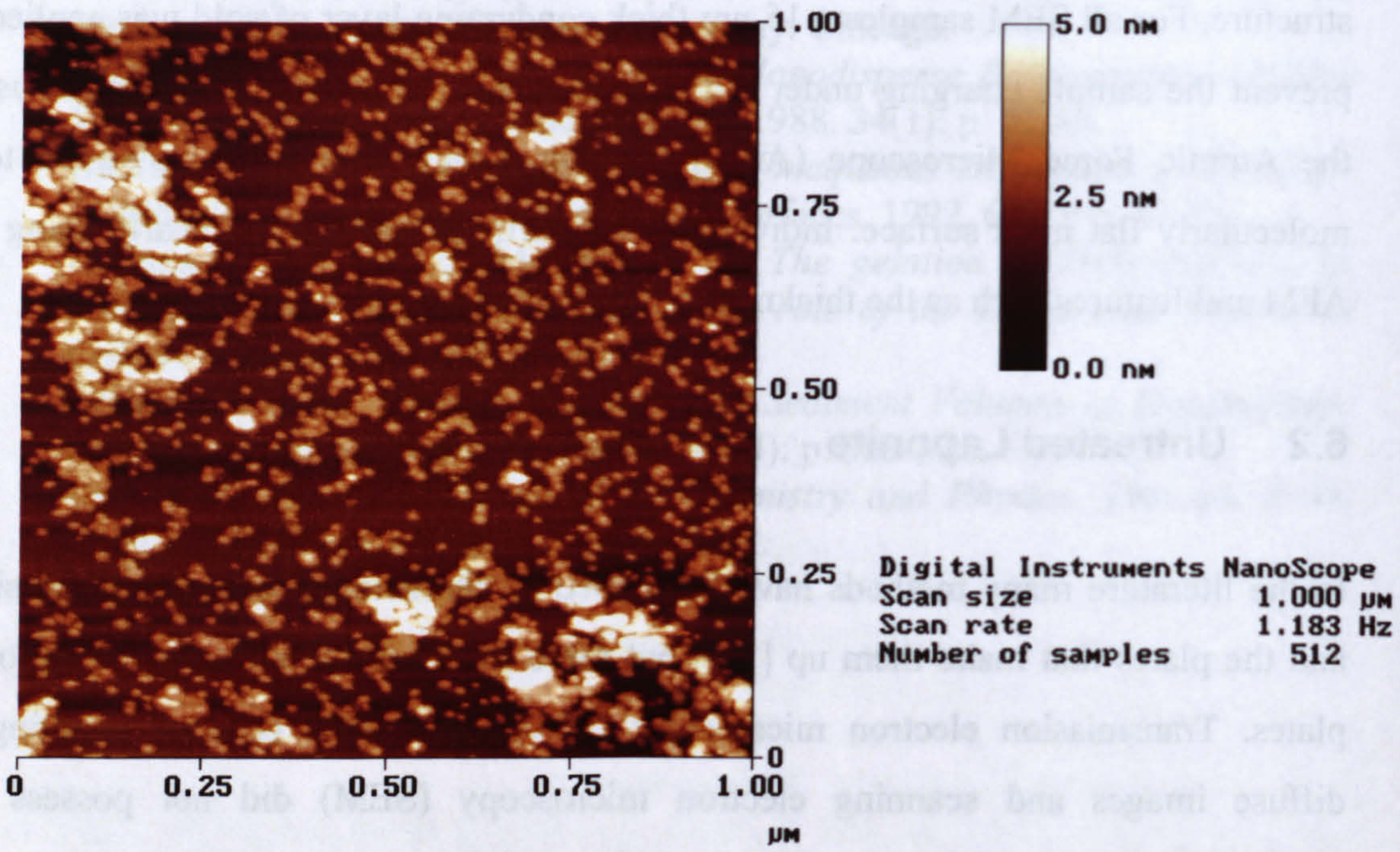

Figure 6.1. A low magnification image of the dried Laponite plates showing single plates and aggregates. The sample was prepared from a 0.001% w/w aqueous dispersion.

The Laponite particles were very easily distinguished from the substrate and many individual particles were seen as well as a number of aggregates. It was not clear if the aggregates were formed as the sample dried to the stub or were present in the dispersion. The shape of the untreated Laponite plates was seen from a close-up image of the particles (figure 6.2).

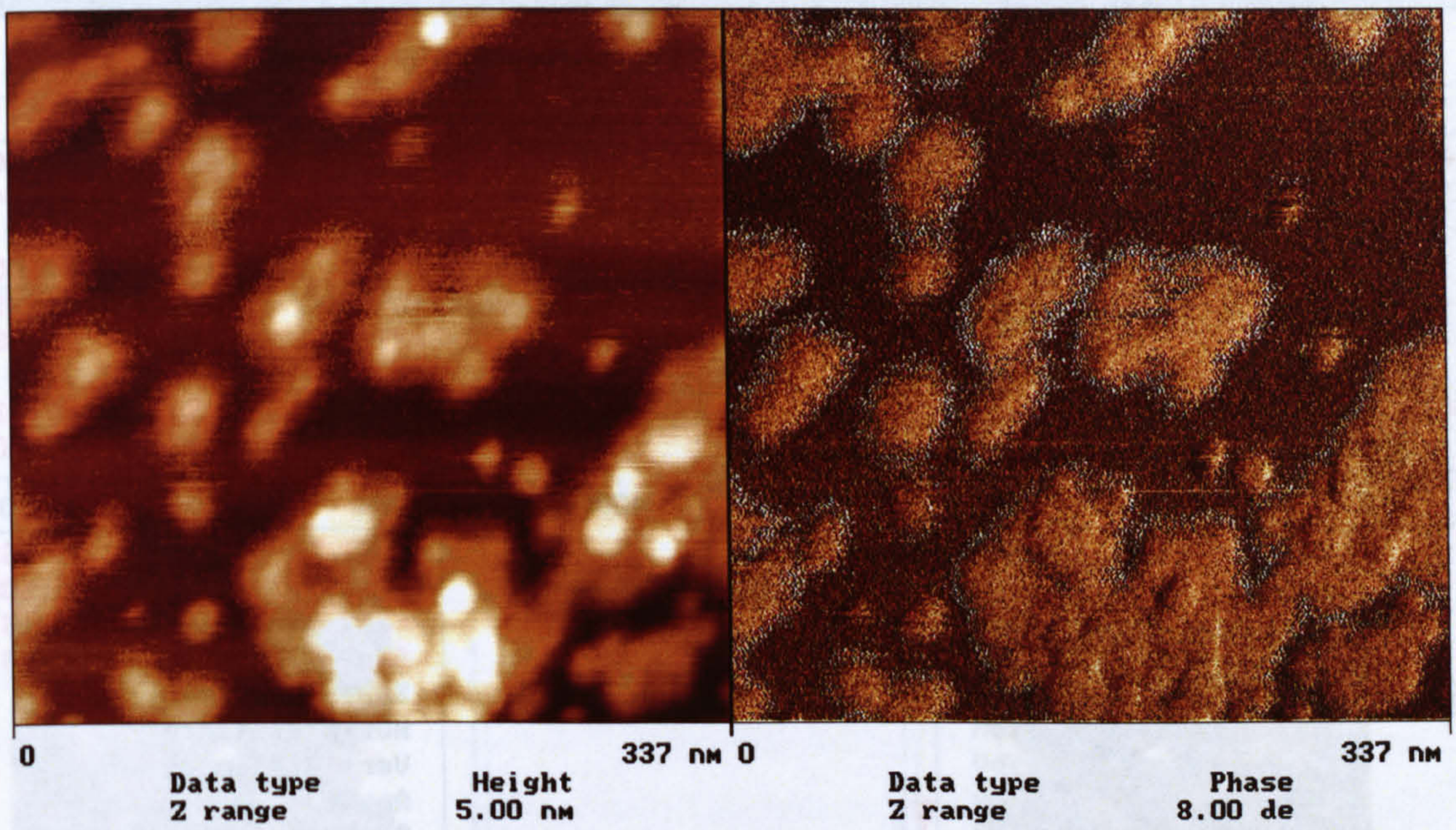

Figure 6.2. Close-up AFM image of untreated Laponite with the amplitude image on the left and the phase image on the right.

The Laponite plates were disc-shaped and fairly uniform in diameter. The light coloured ring around the edges of the plates in the phase image was due to a small attractive force between the positive edges of the plates and the negatively charged silicon nitride tip. This attraction was only found at the edges of particles and not for particles lying on top of the faces of other particles. The thickness and diameter of the Laponite plates were measured by analysis of the image (figure 6.3).

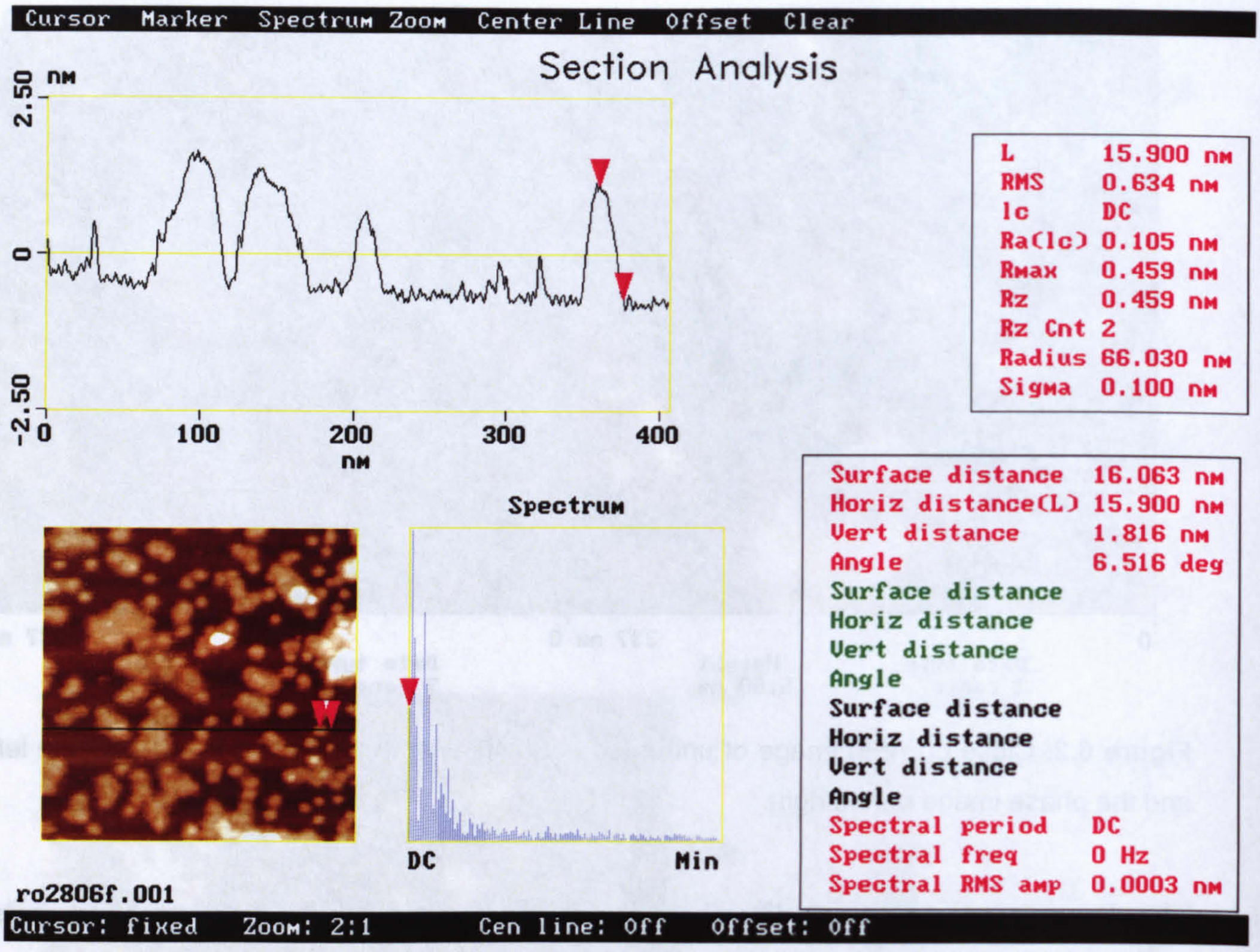

Figure 6.3a. Section analysis of an untreated Laponite plate showing the thickness of a plate at 1.8 nm.

The thickness of a typical Laponite plate was given as 1.8 nm, a value higher than found from scattering experiments [6, 7]. The difference between the literature and the value found in this study may have been due to very short range electrostatic repulsion between the tip of the AFM and the face of the Laponite plates [8, 9].

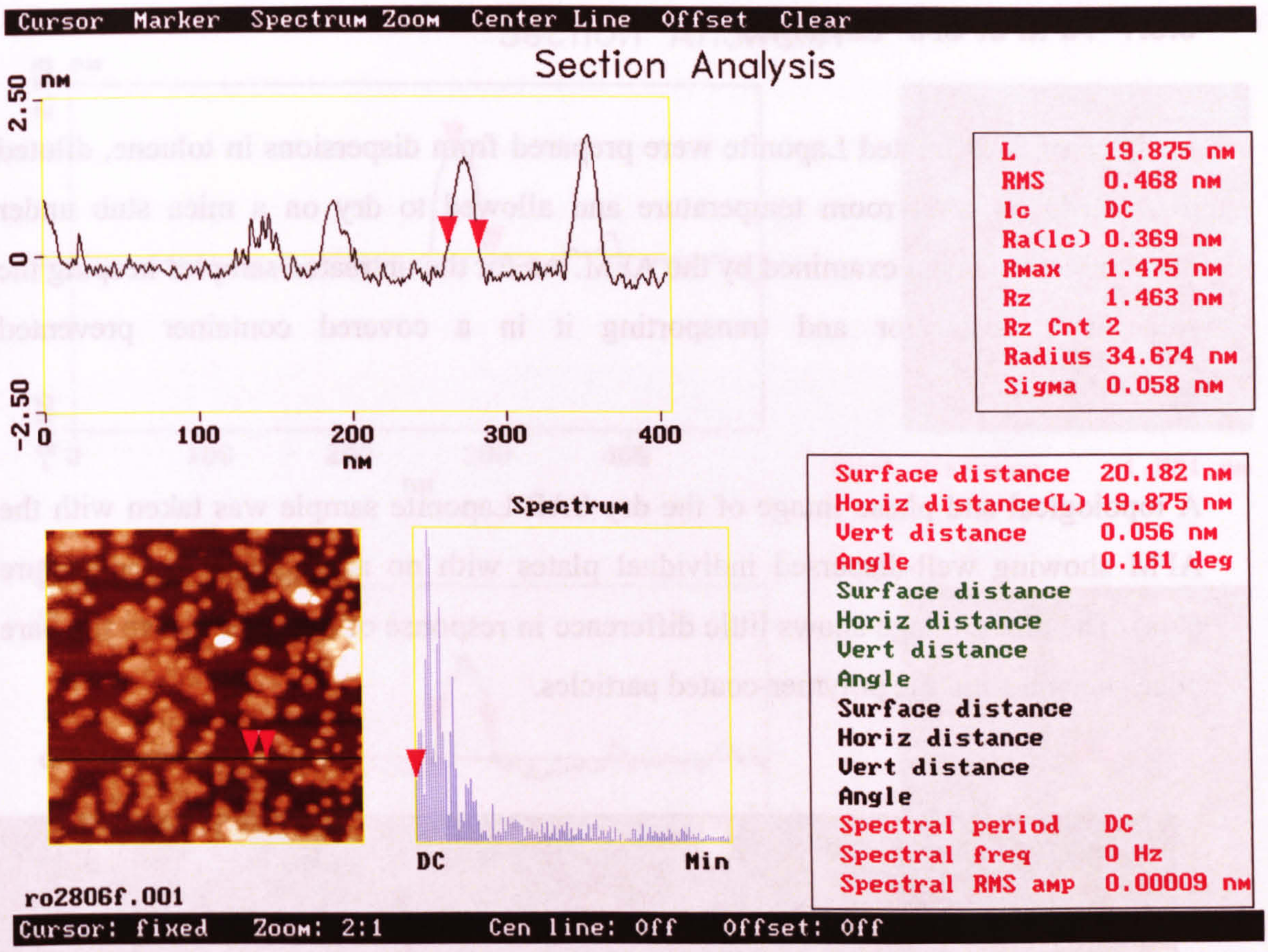

Figure 6.3b. Section analysis of an untreated Laponite plate showing the diameter of a plate at 22 nm.

The diameter of a Laponite plate was given as 22.6 nm a value close to literature values [9-11] but there was quite a wide range of particle diameters in the sample.

Overall, the untreated Laponite particles were found to be disc-shaped with a diameter of between 20-30 nm and a thickness of 1.8 nm. Attractive electrostatic forces between the AFM tip and the edges particles were found and the possibility of repulsive forces existed between the AFM tip and the faces of the plates.

6.3 SAP Laponite

The standard procedure was used to make and clean the SAP treated Laponite in toluene (section 3.2.1). The concentration of the particles was determined by dry weight analysis and a small sample of the treated particles was removed and prepared for microscopic analysis.

6.3.1 AFM of SAP Laponite

Samples of SAP treated Laponite were prepared from dispersions in toluene, diluted to 0.0014% w/w at room temperature and allowed to dry on a mica stub under vacuum before being examined by the AFM. As for the untreated samples keeping the stub in a desiccator and transporting it in a covered container prevented contamination.

A topological and phase image of the dry SAP Laponite sample was taken with the AFM showing well-dispersed individual plates with no aggregation found (figure 6.4a). The phase image shows little difference in response of the tip between the bare mica substrate and the polymer-coated particles.

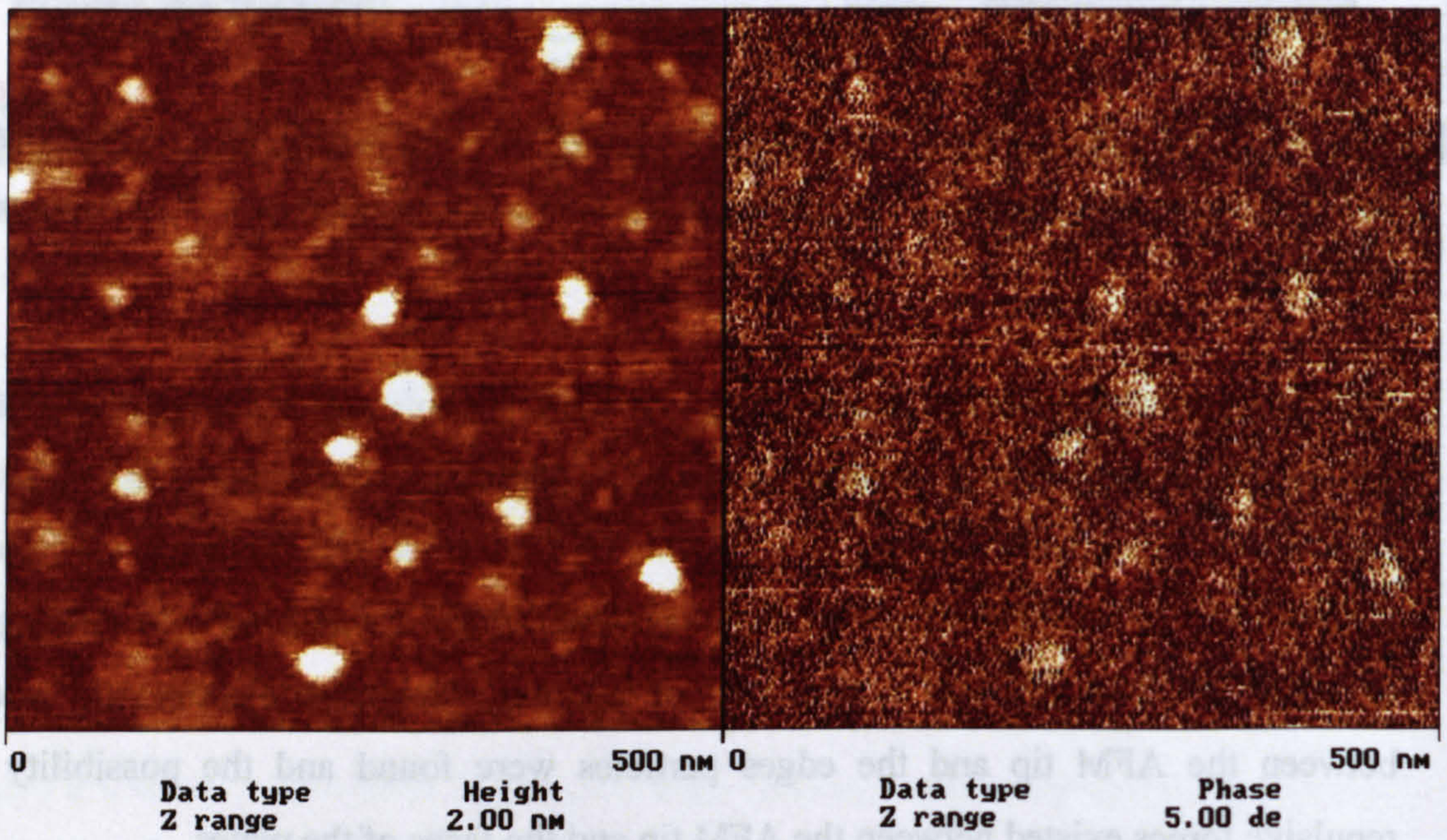

Figure 6.4a. AFM topological image of SAP Laponite dried from a solution in toluene at 0.0014% w/w. The topological image on the left shows the plates clearly.

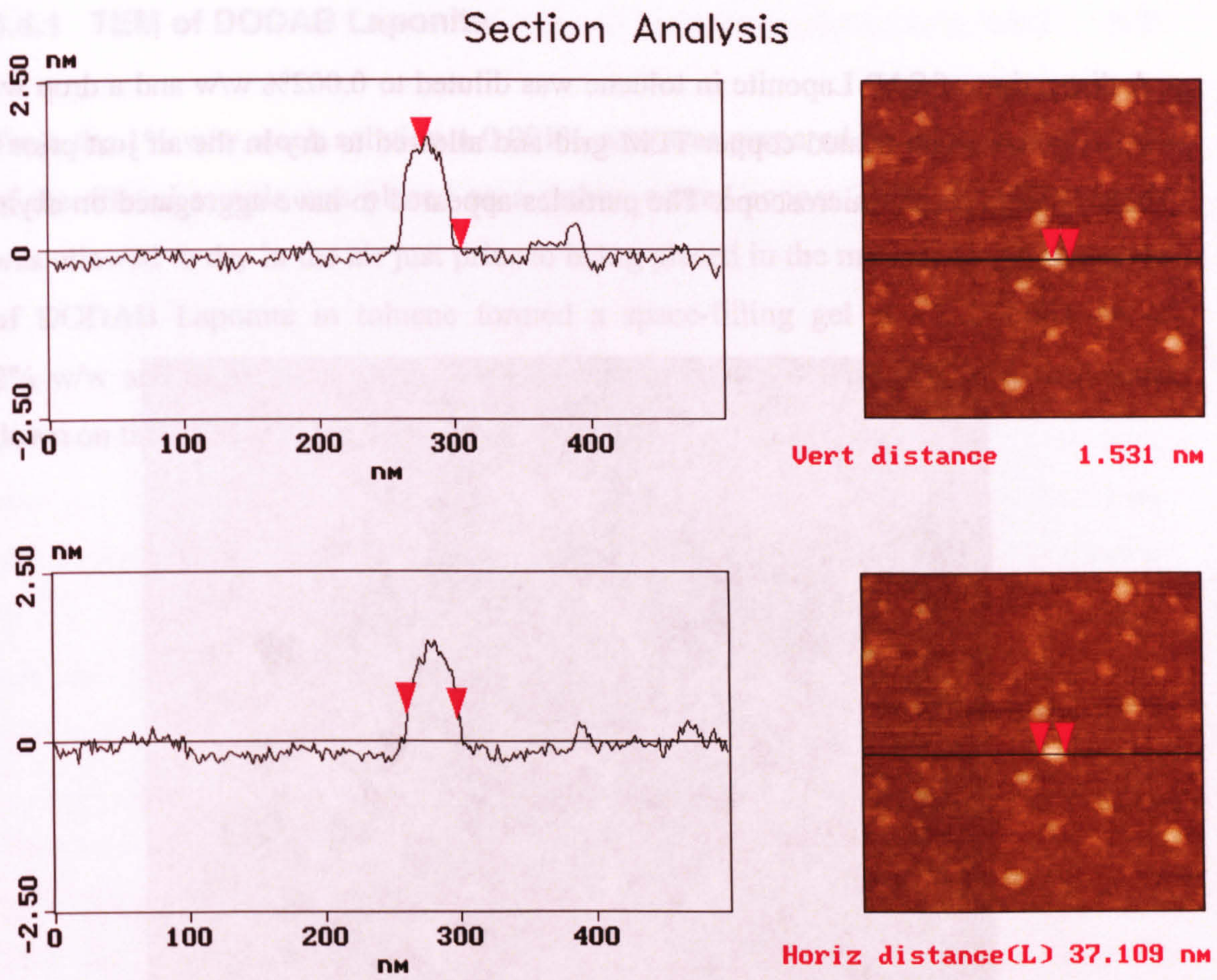

Figure 6.4b. AFM section analysis of SAP Laponite dried from the same solution of SAP Laponite in toluene as before.

The vertical height of a typical plate was 1.5 nm with a diameter of 37 nm. The particle was assumed to be an individual with a dried polymer coating that made it thicker than the literature value for the thickness. Interestingly, the particle was not as thick as the bare Laponite plate as measured by the AFM. This was possibly due to reduced electrostatic repulsion as result of the polymer layer. The diameter was higher than for the untreated Laponite plate but was still in the acceptable range of particle sizes.

6.3.2 Transmission electron microscopy of SAP Laponite

TEM was used to view SAP Laponite particles. It was expected the polymer coating on the surface of the Laponite plates would enhance the contrast and show the particles clearly.

A dispersion of SAP Laponite in toluene was diluted to 0.002% w/w and a drop was added to a carbon coated copper TEM grid and allowed to dry in the air just prior to being placed in the microscope. The particles appeared to have aggregated on drying (figure 6.5).

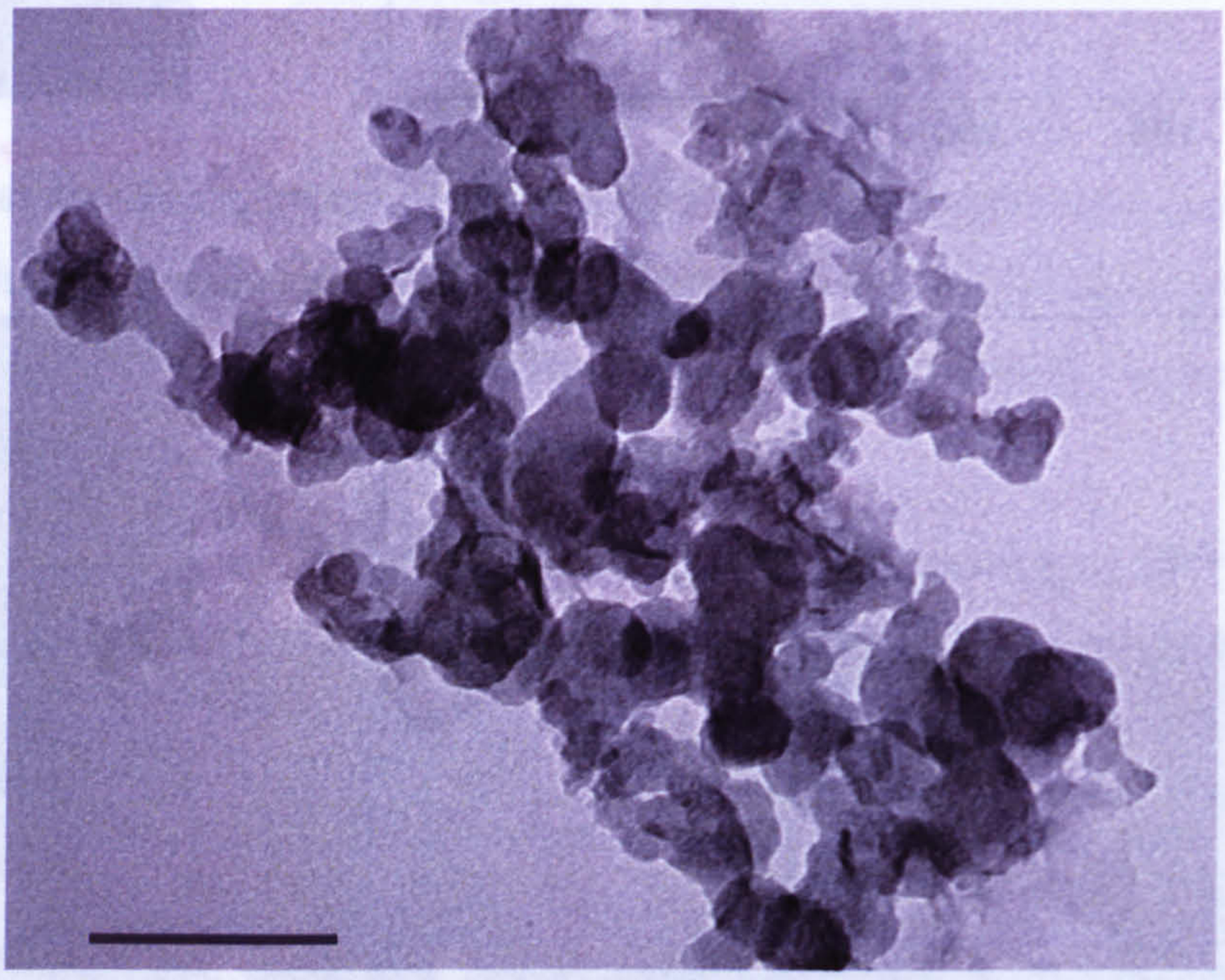

Figure 6.5. A TEM of SAP Laponite particles dried in air at room temperature from 0.002% w/w dispersion in toluene. The accelerating voltage was 100 kV. Scale bar represents 100 nm.

The SAP Laponite particles have a wide size range and some appear quite dense. Edge-to-edge aggregation has occurred and possibly face-to-face aggregation too. In the top right corner of the image the wispy material consists of broken parts of the carbon grid that came apart with the addition of the sample in toluene. The TEM image is quite different to the AFM image but was prepared at a higher concentration on a different substrate.

6.4 DODAB Laponite

A 1% w/w dispersion of DODAB Laponite in toluene was prepared (section 3.2.4) and used as a stock solution for much more dilute samples.

6.4.1 TEM of DODAB Laponite

From the 1% w/w stock solution a 0.001% w/w was prepared by dilution and a drop of the diluted sample was placed on a carbon coated copper TEM grid. The sample was allowed to dry in the air just prior to being placed in the microscope. Dispersions of DODAB Laponite in toluene formed a space-filling gel at a concentration of 2% w/w and aggregation of the low concentration sample was expected as it dried down on the TEM grid (figure 6.6).

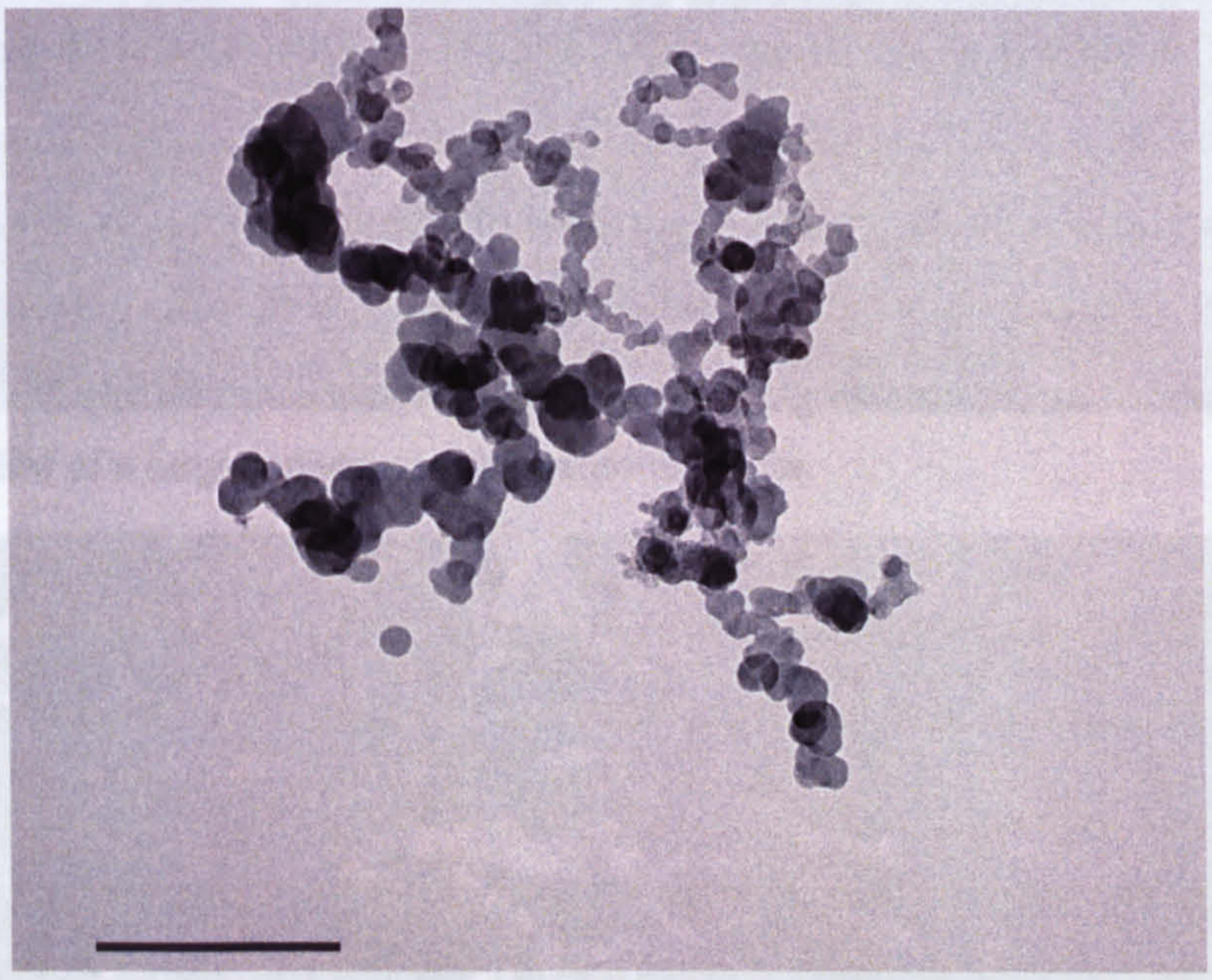

Figure 6.6. TEM of DODAB Laponite dried at room temperature from 0.001% w/w dispersion in toluene. The accelerating voltage was 100 kV. The scale bar represents 200 nm.

The sample of DODAB Laponite dried on the carbon grid had aggregated with a large number of the particles being joined together by the edges forming a looping chain and appearing flat. A range of diameters of the Laponite plates was found from 15 nm to 40 nm. This does not include the large dark objects that were suspected to be two or more particles stacked on top of each other with individuals ill defined.

6.5 SAP Bentonite particles

After preparation of the SAP bentonite particles in toluene (section 3.2.1) the concentration was measured by dry weight analysis. A small sample was then removed and prepared for microscopic analysis.

The diameter of untreated bentonite plates can be as high as 1000 nm [12] but electron micrographs show a wide variation of the size and shape of the particles [13, 14]. The size and shape of SAP bentonite particles were expected to be similar and were investigated using the SEM (figure 6.7). A drop of a 0.1% w/w dispersion of SAP bentonite particles in toluene was placed on a small glass microscope slide and the solvent was allowed to evaporate in air at room temperature. The sample was then coated under vacuum with a thin conducting layer of gold before examination under the microscope. The accelerating voltage of the electrons was 10 kV.

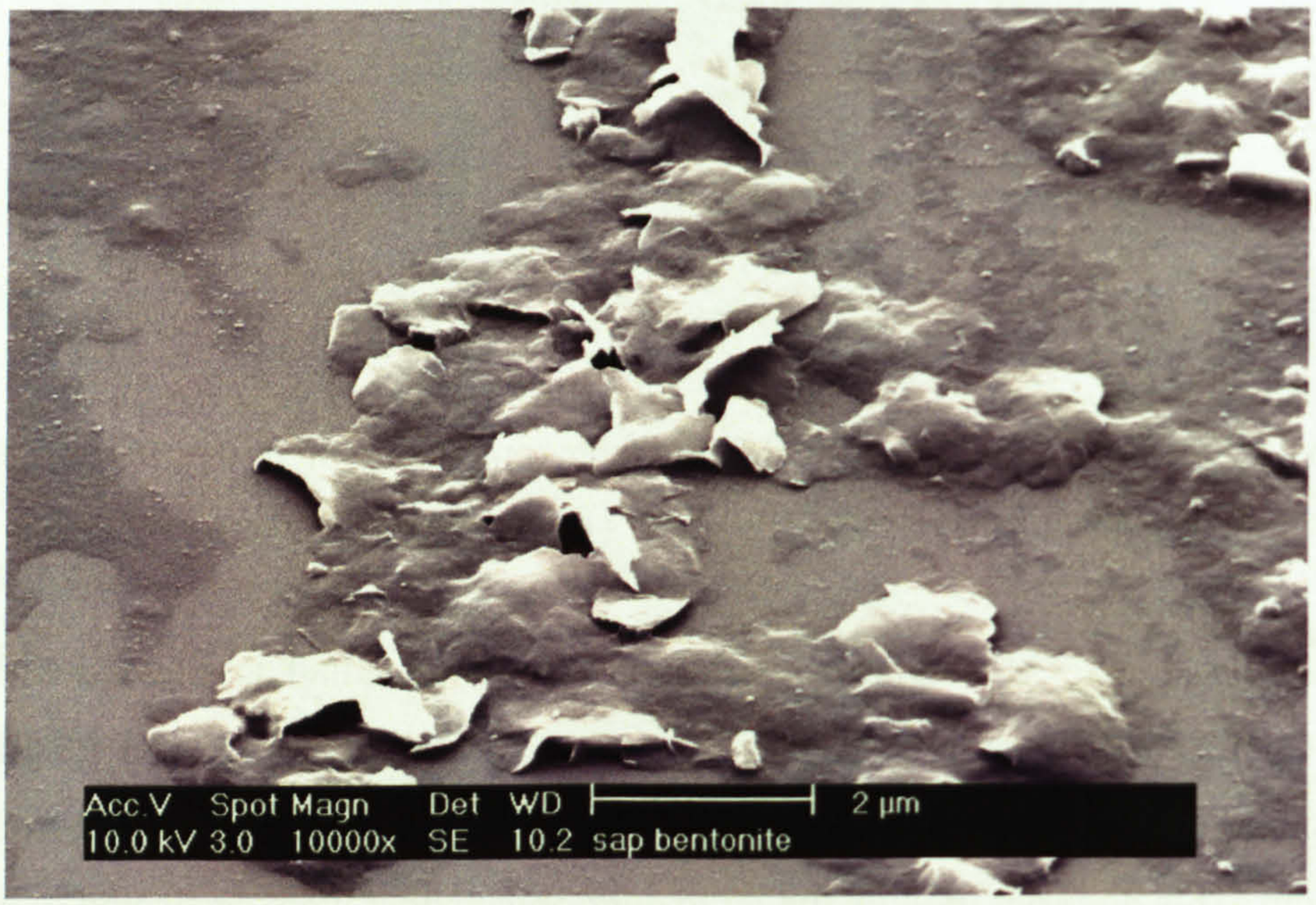

Figure 6.7. SEM micrograph of SAP adsorbed bentonite plates showing individual plates of over 1 µm in diameter.

The dried SAP bentonite particles appear bent and twisted and some over a micron in size. There was no evidence of a wide size distribution as no very small particles can be seen. There was also quite a large amount of non-clay material of unknown origin

covering some of the particles. A close up of a single bentonite plate showed it was rectangular and quite large at about 1.5 μm by 0.7 μm (figure 6.8).

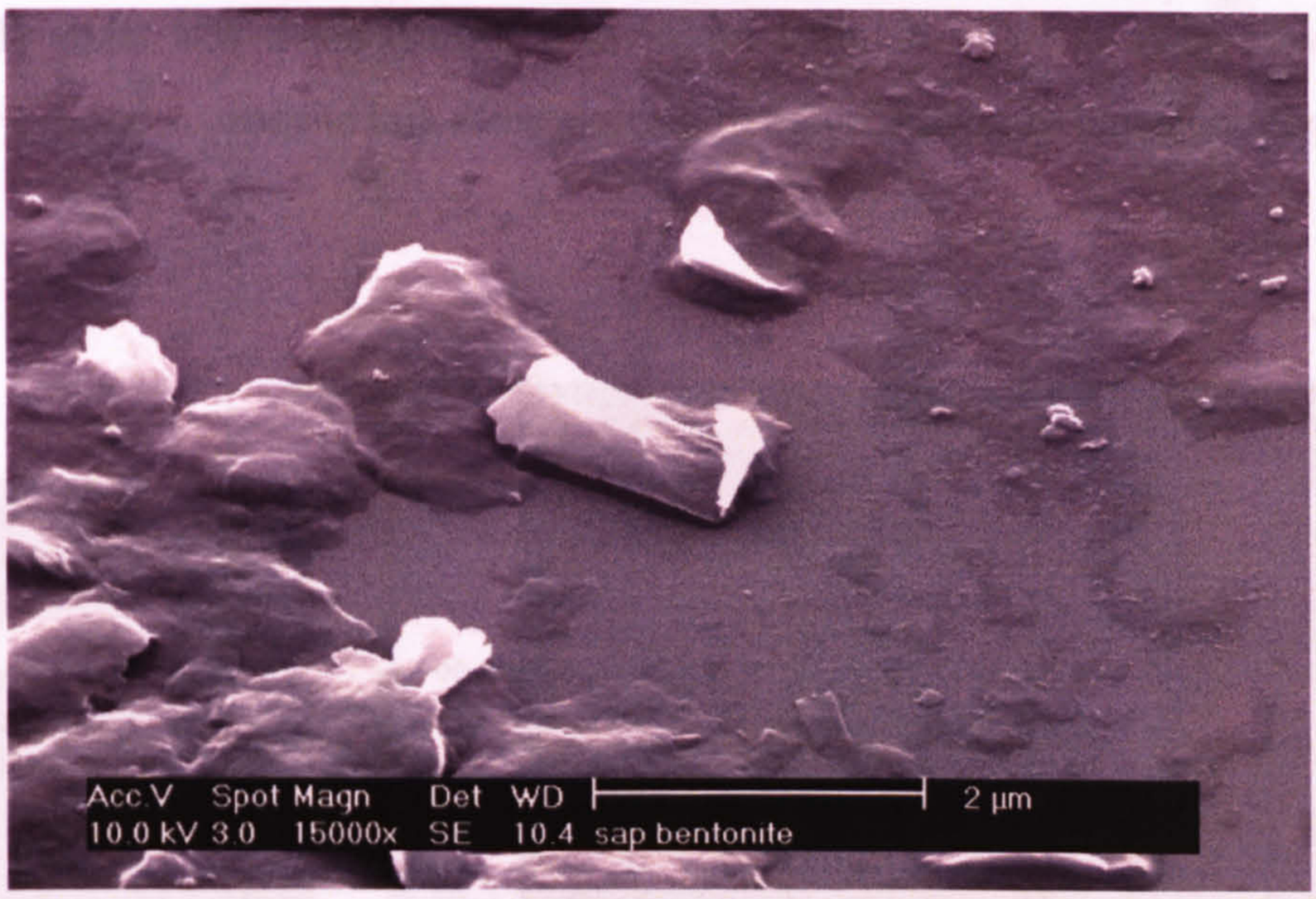

Figure 6.8. SEM of a large individual SAP bentonite plate.

From the SEM it was impossible to tell if the plates were stuck together face-to-face or dispersed individually, however the diameter of the plates can be estimated at between 1 and 2 μm. The material on their surface was unknown but seen over a large proportion of the plates, but only where there were high concentrations of particles and could have been an artefact from the dried polymer. The polymer coated bentonite plates appeared quite thick. The reason for this was possibly due to the 15 nm thick conducting gold layer on all surfaces of the plates or the material contaminant on the surface of the particles.

6.6 DODAB bentonite and Claytone

Samples of DODAB bentonite and Claytone were dispersed in toluene (section 3.2.4) and diluted to 0.001% w/w. A drop of the dispersion was added to a freshly exposed molecularly flat mica substrate dried at room temperature in air and examined using the AFM.

6.6.1 DODAB bentonite

A large area scan was taken of the sample of DODAB bentonite and many stacks of plates were seen. A more detailed image of a typical stack was taken (figure 6.9) showing it consisted of a wide range of particle sizes and shapes.

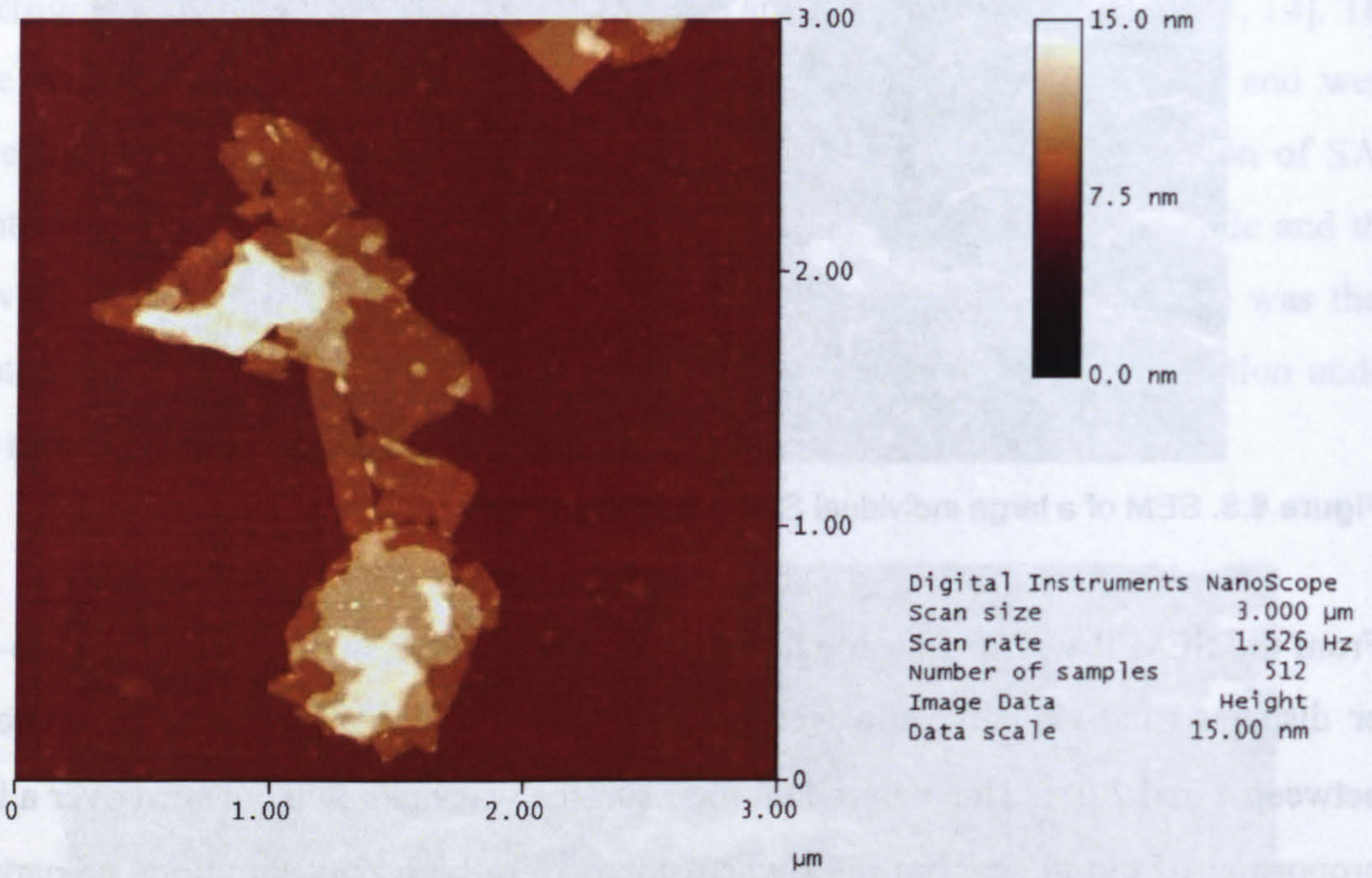

Figure 6.9. Topological AFM image of DODAB bentonite on a mica stub. The sample was dried in air from a dilute suspension in toluene and shows an aggregate with particles lying in stacks.

Aggregation of the DODAB bentonite particles was found with the plates lying in a face-to-face arrangement. It was not known if the aggregation was a result of the drying of the sample on the stub or if the aggregates were present in the dispersion. The particles were polydisperse with a diameter from 100 nm to 1000 nm. Not many completely isolated single plates were found but sections of plates not covered by other plates were seen and used to measure the thickness of the individual DODAB bentonite plates (figure 6.10).

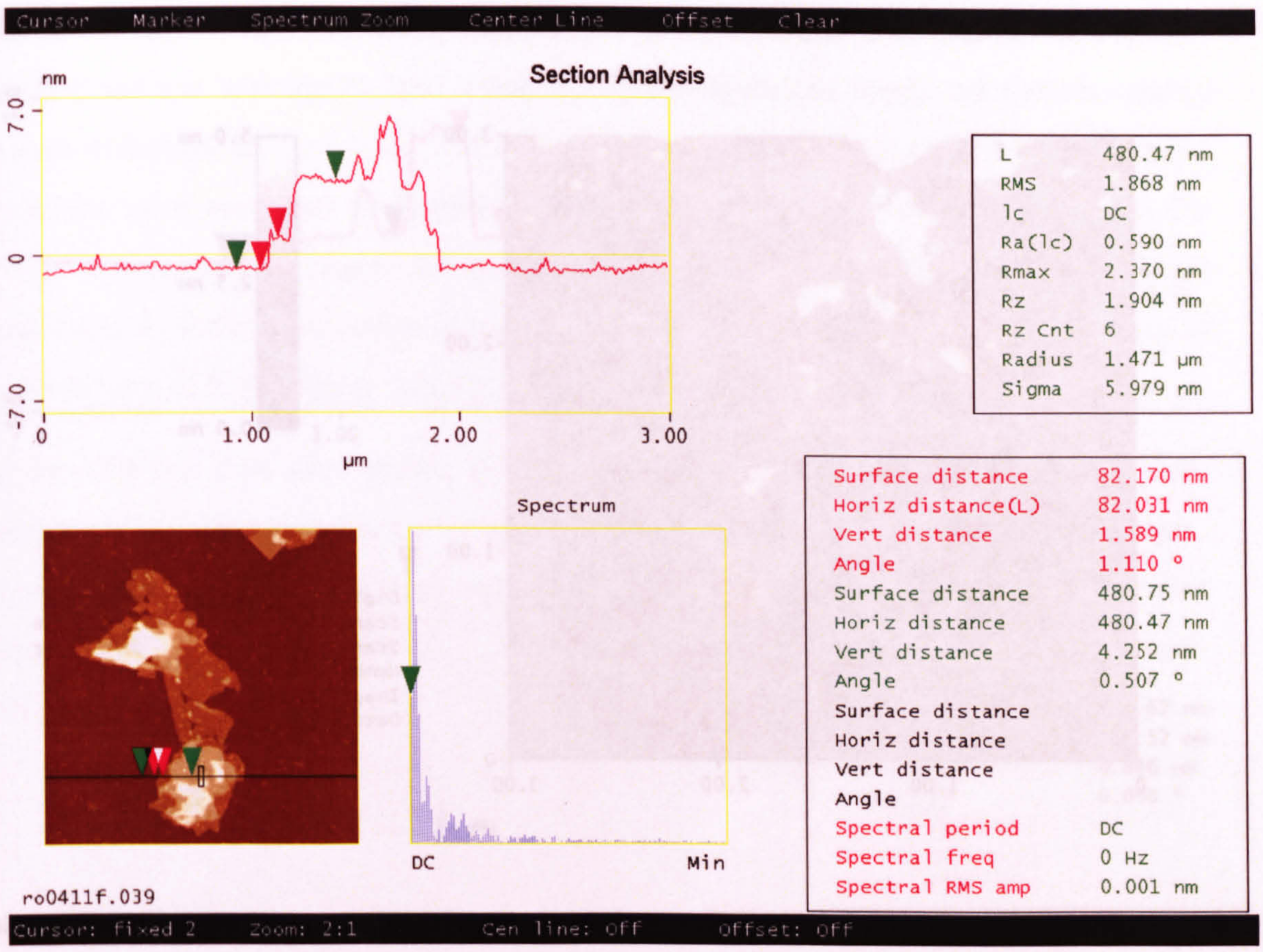

Figure 6.10. Section analysis from the AFM data for DODAB bentonite showing the vertical height of a DODAB bentonite plate was 1.5nm.

The thickness of an individual DODAB bentonite plate was measured at 1.6 nm and the thickness of a short stack was measured at 4.3 nm. On inspection of the image the stack actually appears to be two plates high but more than twice the thickness of one plate. The reason for this was not known but toluene solvent may have been trapped between the layers of clay. From small angle X-ray scattering (section 8.3) the plate separation was found to be 2.7 nm for dispersed samples in toluene suggesting the stack found using the AFM was indeed two plates. This distance is a little larger than the separation found by AFM but not remarkably so.

The excess surfactant was not removed from the dispersion of Claytone in toluene before the sample was dried to the mica substrate at 0.001% w/w. No free surfactant aggregates were found by the AFM from the dried Claytone sample. This may be due to the speed of the drying process not giving the surfactant time to crystallise. The AFM image of Claytone was typical showing plates lying next to and on top of each other (figure 6.11).

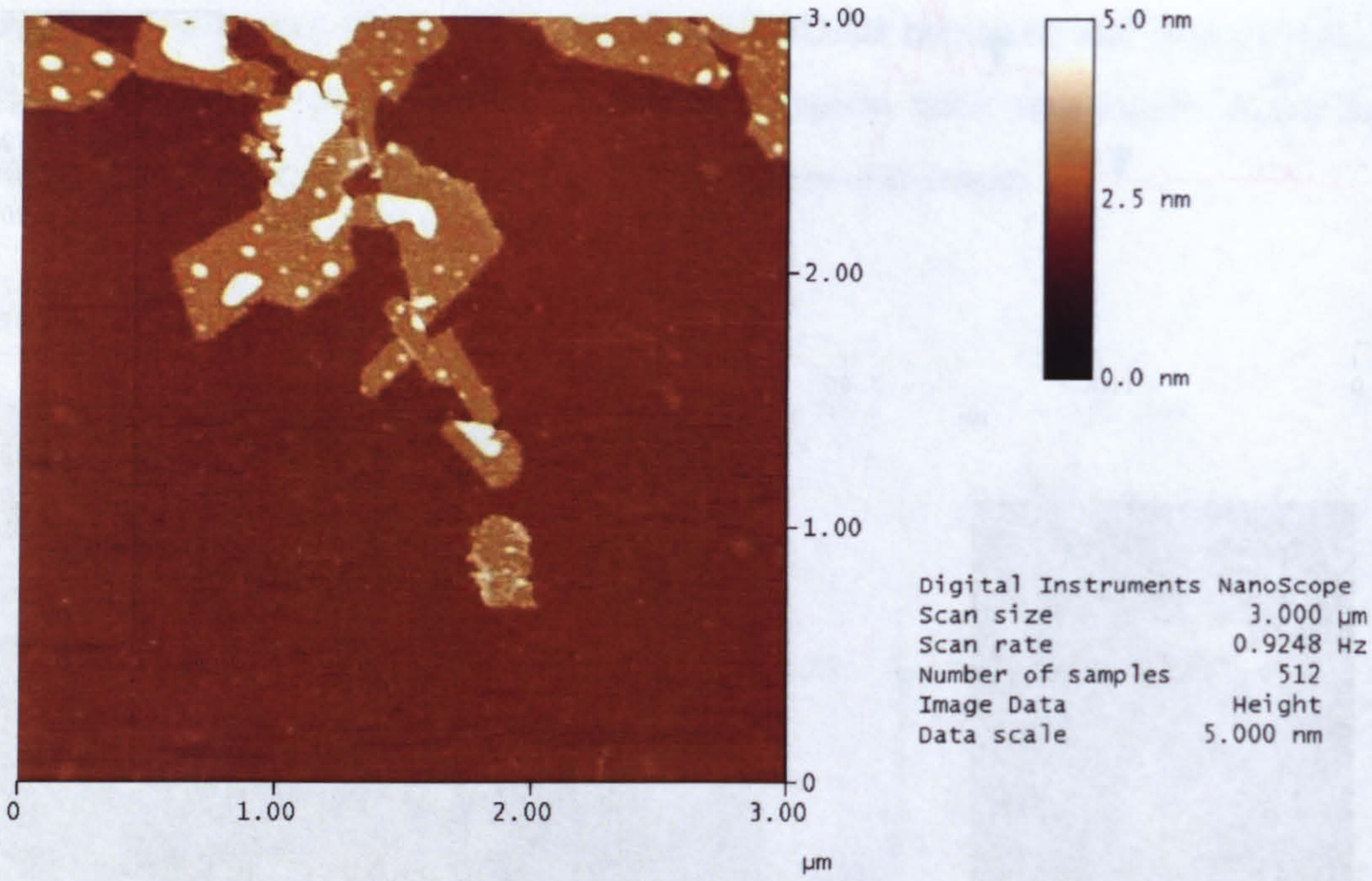

Figure 6.11. Topological AFM of Claytone AF on a mica stub. The sample was dried in air from a 0.001% w/w suspension in toluene.

The AFM image of the sample of Claytone was similar to the DODAB bentonite sample with the size and shape of individual Claytone plates being obvious with a size range of 100 nm to 1000 nm in a wide variety of shapes. Extensive aggregation was not found in the dried sample but the plates were usually touching the edge of neighbouring plates and lying on top of each other but very few stacks were found to be higher than 5 nm. On top of a number of plates there were very much smaller plates stuck to their face. Where plates were laying on top of other plates the shape of the bottom plate was still very clearly identifiable underneath showing the plates were deformable as they dried. The thickness of a Claytone plate was determined from analysis of the AFM image (figure 6.12).

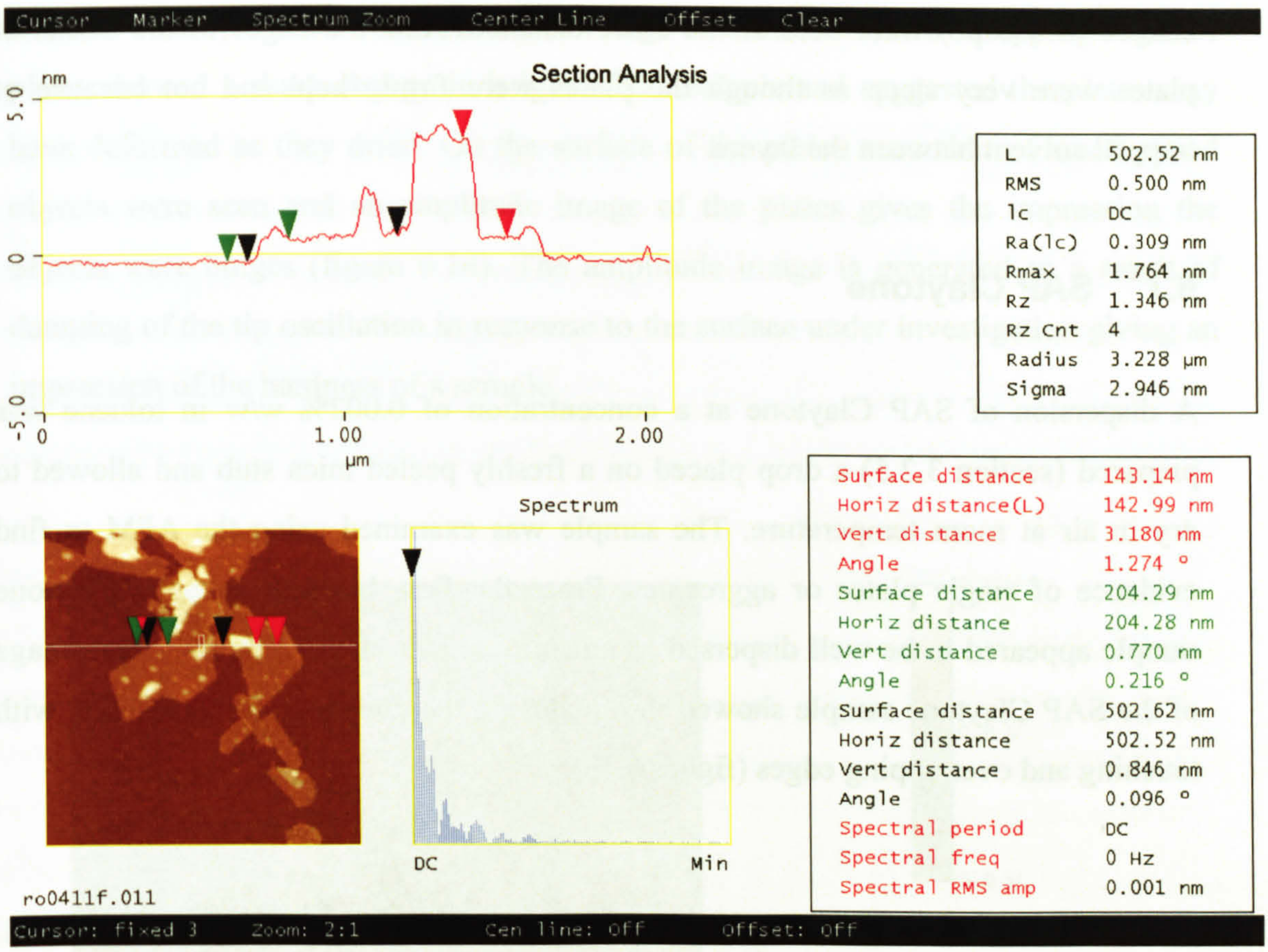

Figure 6.12. Section analysis of the AFM image for Claytone.

The thickness of a Claytone plate was measured from two different positions but gave similar results of 0.8 nm thick. The first position of measurement was from the mica substrate to the top of a single Claytone plate. The second measurement was from the mica substrate to a plate that was either suspended between two plates or had two plates lying over its edges. It gave a very similar result to the first measurement at 0.8 nm thick. This value was half the measured thickness of the DODAB bentonite plate and thinner than the crystallographic thickness of a plate [14]. Clearly the value was not correct and the difference was assumed to be as a result of reduced interaction between the AFM tip and the Claytone plate [8] but this was not found with the DODAB bentonite sample. The thickness of a Claytone plate stacked on top of another was measured at 3.2 nm. From the image it appeared this was a single particle on top of another and this was supported by the fact no thinner stacks were found. It appears the Claytone plates lie on top of each other as at a distance greater than twice the thickness of the plates. The reason for this may be trapped solvent between the layers but even small plates (where trapped solvent molecules should have more

chance of escape) were held at the same distance. Also the edges of the stacks of plates were very steep as though the plates were firmly held and not because of trapped solvent between the layers.

6.7 SAP Claytone

A dispersion of SAP Claytone at a concentration of 0.002% w/w in toluene was prepared (section 3.2.5) a drop placed on a freshly peeled mica stub and allowed to dry in air at room temperature. The sample was examined using the AFM to find evidence of single plates or aggregates. From the flow birefringence the Claytone sample appeared to be well dispersed as anisotropic particles. The topological image of the SAP Claytone sample showed thin plates on the mica stub lying together with touching and overlapping edges (figure 6.13).

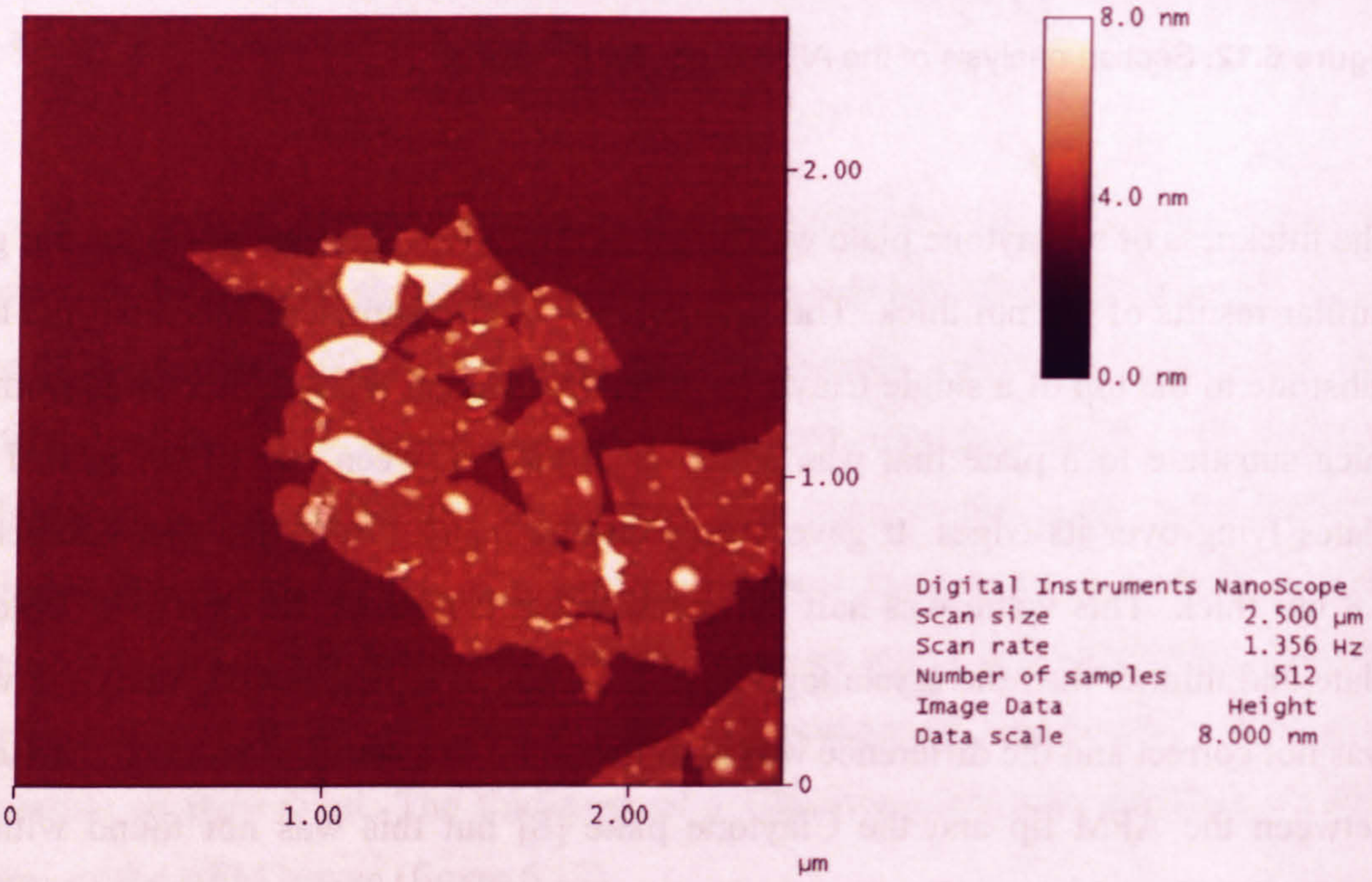

Figure 6.13. AFM topological image of the SAP Claytone sample showing plates partially lying on top of each other.

The SAP Claytone plates did not lie as stacks and had very little material on the surface such as smaller plate fragments. The AFM images of SAP Claytone the shape

and size of the particles was varied with a large distribution. The overlapping edges of plates showed a sharp change in height of the sample and suggested the plates may have deformed as they dried. On the surface of the plates a number of small round objects were seen and an amplitude image of the plates gives the impression the objects were bulges (figure 6.14). The amplitude image is generated as a result of damping of the tip oscillation in response to the surface under investigation giving an impression of the hardness of a sample.

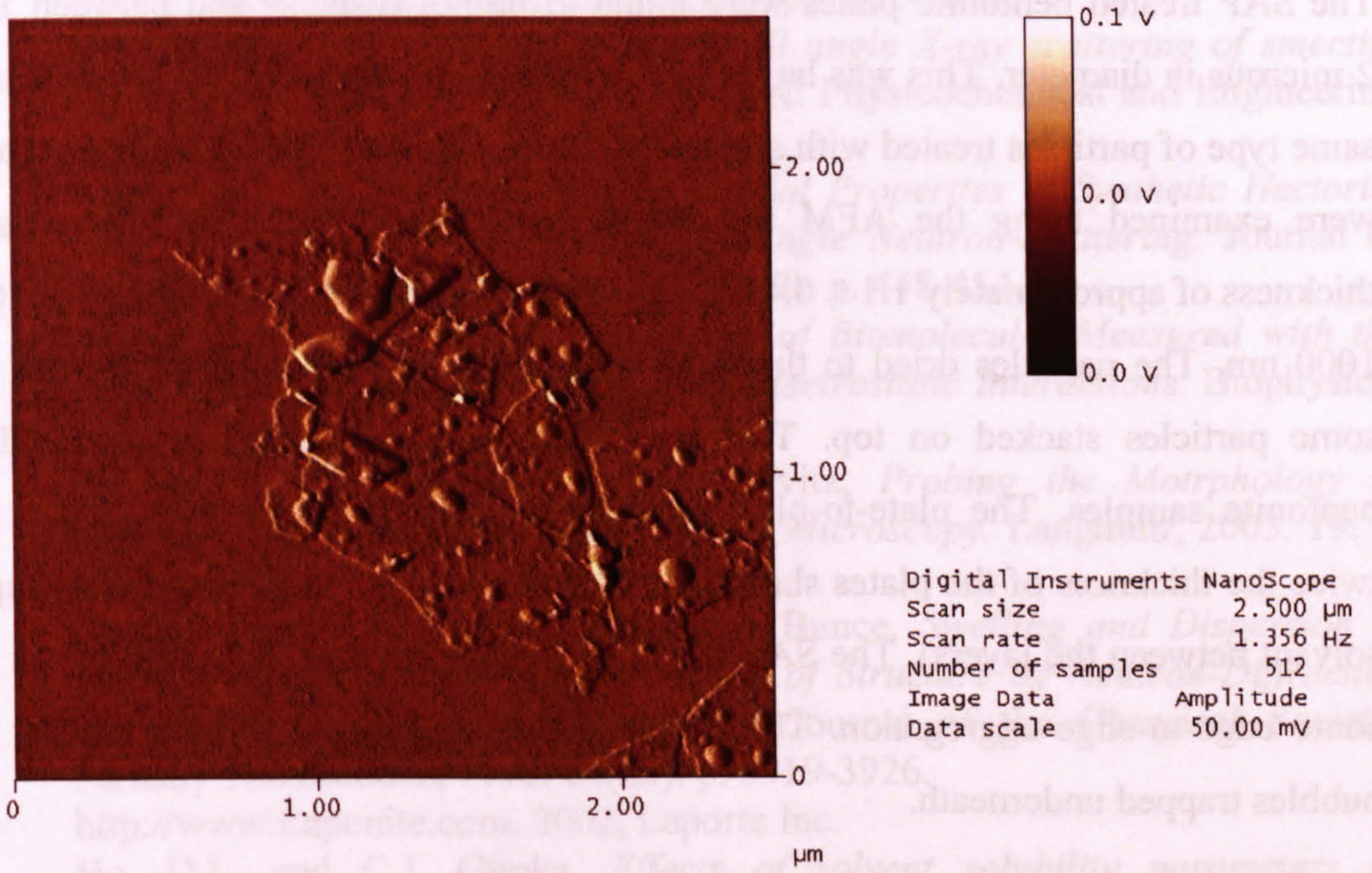

Figure 6.14. Amplitude AFM image of the SAP Claytone.

The amplitude image clearly shows the SAP Claytone stuck to the mica surface but gives the appearance of bubbles trapped under each plate. The areas where plates overlapped each other also showed their own amplitude response giving the impression of a raised area.

6.8 Conclusions

The images obtained from the microscopy techniques used have given information regarding the size and shape of the clay plates. The AFM has given values for the thickness of the dried plates of around one nanometer. Interactions between the AFM tip and the clay play a large role as the untreated Laponite was apparently thicker than the SAP treated version. The Laponite plates imaged using AFM and TEM had a diameter between 20 to 40 nm a size range that did not differ as a result of treatment with a polymer or surfactant.

The SAP treated bentonite plates were found to be polydisperse and between 1 and 2 microns in diameter. This was larger than expected and considerably larger than the same type of particles treated with surfactant. Claytone and DODAB treated bentonite were examined using the AFM and were polydisperse plates with a measured thickness of approximately 1.1 ± 0.4 nanometers but a polydisperse diameter of 100 to 1000 nm. The particles dried to the mica substrate as edge-to-edge aggregates with some particles stacked on top. This was found predominantly for the DODAB bentonite samples. The plate-to-plate distance for these samples was greater than twice the thickness of the plates showing something was holding them apart (trapped solvent between the layers). The SAP Claytone sample dried as individual plates with some edge-to-edge aggregation. The Claytone plates appeared to have settled with bubbles trapped underneath.

6.9 References

1. Zou, J. and A.C. Pierre, *Scanning electron microscopy observations of "card-house" structures in montmorillonite gels.* Journal of Materials Science Letters, 1992. **11**: p. 664-665.
2. Bonn, D., et al., *Laponite: What is the difference between a gel and a glass?* Langmuir, 1999. **15**(22): p. 7534-7536.
3. Kroon, M., W.L. Vos, and G.H. Wegdam, *Structure and formation of a gel of colloidal disks.* Physical Review E, 1998. **57**(2): p. 1962-1970.
4. Thompson, D.W. and J.T. Butterworth, *The Nature of Laponite and Its Aqueous Dispersions.* Journal of Colloid and Interface Science, 1992. **151**(1): p. 236-243.
5. Round, A.N., et al., *Heterogeneity and persistence length in human ocular mucins.* Biophysical Journal, 2002. **83**(3): p. 1661-1670.
6. Morvan, M., et al., *Ultrasmall and Small angle X-ray scattering of smectite clay suspensions.* Colloids and Surfaces A: Physicochemical and Engineering Aspects, 1994. **82**: p. 193-203.
7. Avery, R.G. and J.D.F. Ramsay, *Colloidal Properties of Synthetic Hectorite Clay Dispersions .2. Light and Small-Angle Neutron-Scattering.* Journal of Colloid and Interface Science, 1986. **109**(2): p. 448-454.
8. Muller, D.J. and A. Engel, *The Height of Biomolecules Measured with the Atomic Force Microscope Depends on Electrostatic Interactions.* Biophysical Journal, 1997. **73**: p. 1633-1644.
9. Balnois, E., Durand-Vidal, and P. Levitz, *Probing the Motrphology of Laponite Clay Colloids by Atomic Force Microscopy.* Langmuir, 2003. **19**: p. 6633-6637.
10. Ramsay, J.D.F., S.W. Swanton, and J. Bunce, *Swelling and Dispersion of Smectite Clay Colloids - Determination of Structure by Neutron-Diffraction and Small- Angle Neutron-Scattering.* Journal of the Chemical Society-Faraday Transactions, 1990. **86**(23): p. 3919-3926.
11. http://www.Laponite.com. 2002, Laporte Inc.
12. Ho, D.L. and C.J. Glinka, *Effects of solvent solubility parameters on organoclay dispersions.* Chemistry of Materials, 2003. **15**(6): p. 1309-1312.
13. Bongiovanni, R., *Small Angle Neutron Studies on Clay Systems.* PhD. Thesis. School of Chemistry University of Bristol, Bristol. UK, 1997.
14. van Olphen, H., *An Introduction to Clay Colloid Chemistry: For Clay Technologists, Geologists, and Soil Scientists.* 2nd Edition ed. 1977: John Wiley & Sons, Inc.

7 Thermoreversible Gelation

7.1 Introduction

The simple observation of thermoreversible gelling for the SAP DODAB bentonite and SAP Claytone samples (figures 5.28) was investigated more closely using rheological methods and the magnitude and temperature of the transition was measured using DSC. The terms and theory are introduced in section 3.4.5 and section 3.4.12.

The rheology of aqueous and non-aqueous clay dispersions is a subject that has been studied extensively [1-6] and is often motivated by the numerous industrial applications. In general, the rheological properties of dispersed systems depend on a number of factors including the size and shape of the suspended particles and their forces of interaction. [7]. As a result understanding the rheological behaviour of polydisperse clay dispersions is not easy [8, 9].

The rheological behaviour of samples is effectively a well-controlled measure of the "feel" of a sample. For the experiments carried out during this study the sample under examination was placed on a fixed base with a frictionless spindle above, (cone and plate). The computer-controlled spindle was oscillated and the response of the sample to the oscillation was measured. From this details about the structure of the sample were built up. One of the primary pieces of information concerned the thermoreversible gelling nature of the sample.

7.2 Protocol for the rheology experiments

The protocol for carrying out the rheological experiments was very simple and followed throughout the study to enable direct comparisons between samples (table 7.1). This minimised errors that were possible due to differences in the samples treatment before undergoing the rheological analysis.

1.	A solvent trap was placed around the geometry and a much larger plastic guard was placed around the machine, to stop condensation on the sample. Within the plastic guard next to the solvent trap a Petri dish filled with anhydrous calcium chloride was added to dry the atmosphere.
2.	For the first measurement, the temperature of the stage was set to 30 °C and lowered for the temperature sweeps in increments of 5 °C until -15 °C then the temperature was raised by 5 °C each time up to 30 °C
3.	The cooling water bath for the Peltier stage was kept at -10 °C throughout the experiments as this made for the most accurate temperature control over the full range.
4.	A compromise pre-shear of 50 Pa was applied for 60 seconds as any greater pre-shear expelled the fluid samples from the geometry but for the high concentration samples at low temperature the samples were not sheared. However for all samples at high temperature this applied pre-shear was enough to let the geometry move.
5.	After the pre-shear the sample was allowed to stand for 5 minutes until the rate of change in the moduli became constant.
6.	For each sample the order of experiments was time sweep followed by a test frequency sweep from low to high frequency, then frequency sweep from 30 °C down to -15 °C.

Table 7.1. Protocol used for all rheological experiments.

7.3 Rheological samples

A range of concentrations of clays treated with SAP were prepared for rheological investigation as well as a sample of surfactant and polymer without clay to serve as a control.

Sample	Description	Solvent
A	Free 2% w/w DODAB and 1% w/w SAP	Polydecene 364NF
B	3.6% w/w SAP treated Claytone	Polydecene 364NF
C	9.7% w/w SAP treated Claytone	Polydecene 364NF
D	9.8% w/w SAP DODAB bentonite	Polydecene 364NF
E	7.1% w/w Claytone alone	Polydecene 364NF

Table 7.2. Samples chosen for the rheological study.

The samples chosen for the rheological study were all prepared dispersed in polydecene because these samples were found to display thermoreversible gelling behaviour. Polydecene was non-volatile and therefore not prone to evaporation, which helped reproducibility.

The rheological experiments undertaken were all oscillatory, carried out using a cone and plate geometry, either at a single frequency or over a range of frequencies starting with the lowest frequency first.

7.3.1 Control sample

The first experiment carried out was a control sample A (figure 7.1). The sample consisted of the solvent, polymer and surfactant at a concentration that was typical of the concentration of the clay sample. This was undertaken to show the gelation was not due to the solvent freezing or aggregation of the surfactant or polymer.

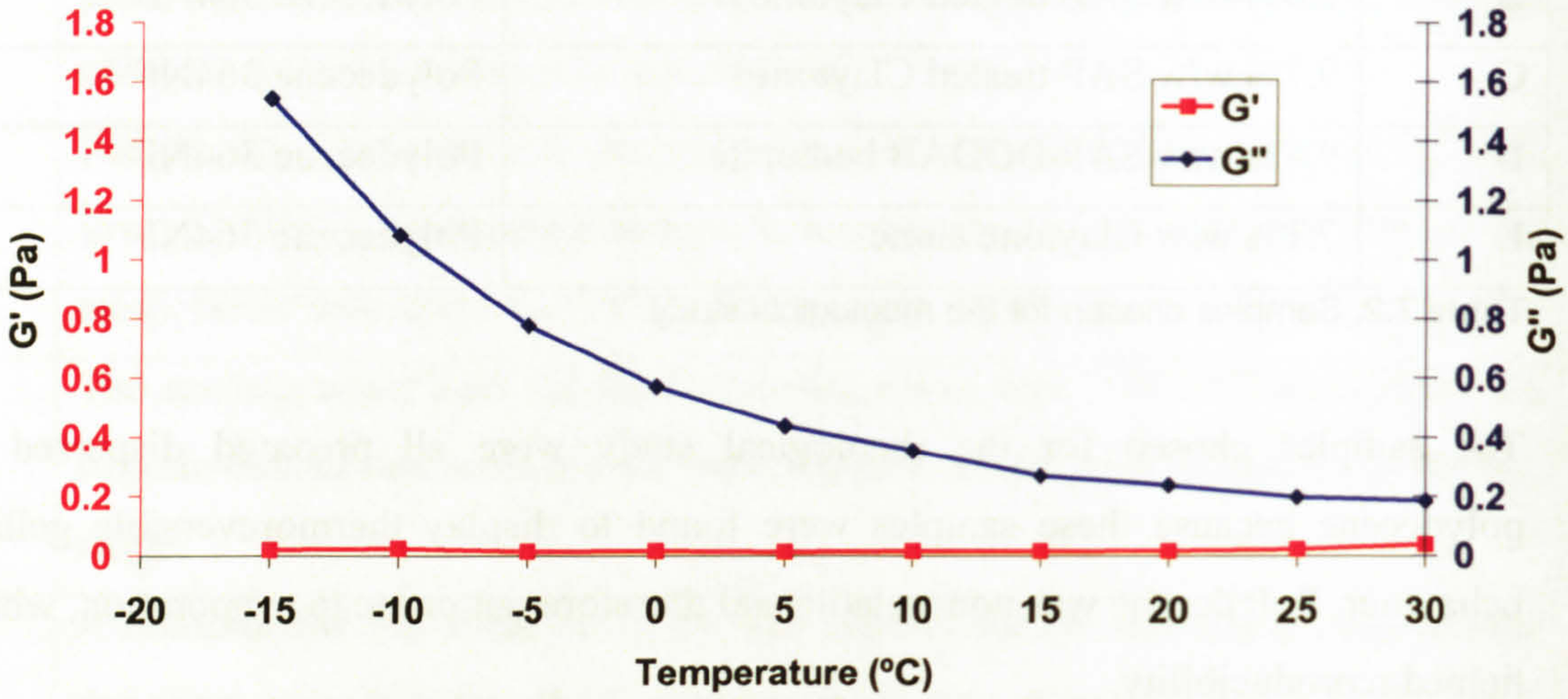

Figure 7.1. The variation of G' and G" with temperature for sample A, measured at an oscillatory frequency of 4.995 radians per second.

The control (sample A) increased in viscosity as the temperature decreased but always remained a fluid over the experimental temperature range. This control showed the gelling found in the treated clay samples was not due to solvent freezing or polymer and solvent forming aggregates. The presence of the clay was essential for gelation.

7.3.2 Low concentration SAP Claytone samples

A sample of 3.6% w/w SAP treated Claytone in polydecene (Sample B) was taken and a time sweep was performed to measure the rate at which the structure rebuilt (figure 7.2). A pre-shear of 50 Pa was applied for 1 minute and measurements were taken immediately after at a controlled strain of amplitude 5×10^{-3}. The choice of strain amplitude was made at a value that was deemed low but without undertaking a strain amplitude sweep that would have shown the strain at which the sample started to break down.

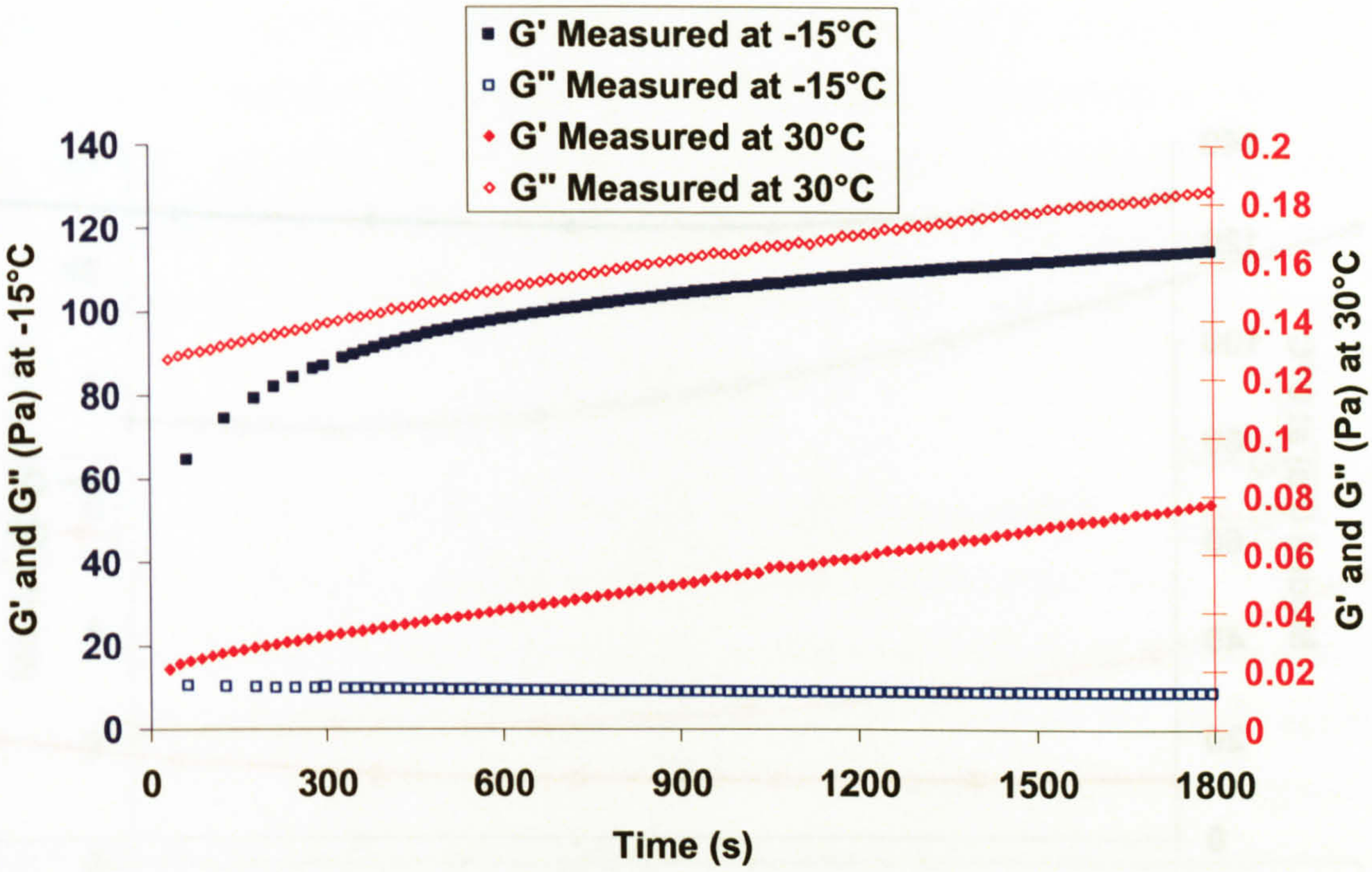

Figure 7.2. Time sweep for 3.6% w/w SAP Claytone dispersion at -15 ºC and 30 ºC. The samples were pre-sheared at 50 Pa for 1 minute then measured at constant strain of 5 x 10^{-3} over 1800 seconds. Note the difference in scale for the samples at low and high temperature.

It is known that clay dispersions often take a very long time for the structure to rebuild after a perturbation [1, 8]. The results showed that a time of at least 300 seconds was needed to allow the samples to rebuild after the pre-shear had ceased as the rate of change of G' was then linear with time. But it was clear to see the structure was still rebuilding as G' and G" did not reach a plateau value. After 1800 seconds the rate of change of the structural rebuild showed no sign of slowing down.

The relaxation time of the sample was measured over a wide temperature range, three of which are plotted below (figures 7.3). The relaxation time of a sample is the ratio of the viscosity to the elasticity measured [10, 11] and is approximately the reciprocal of the frequency at which G' = G" equivalent to a phase angle of 45º [12]. By convention the frequency is measured in radians per seconds, not Hertz.

The frequency sweep measurements were made starting from the lowest frequency and ending with the highest frequency to reduce disturbance of the sample.

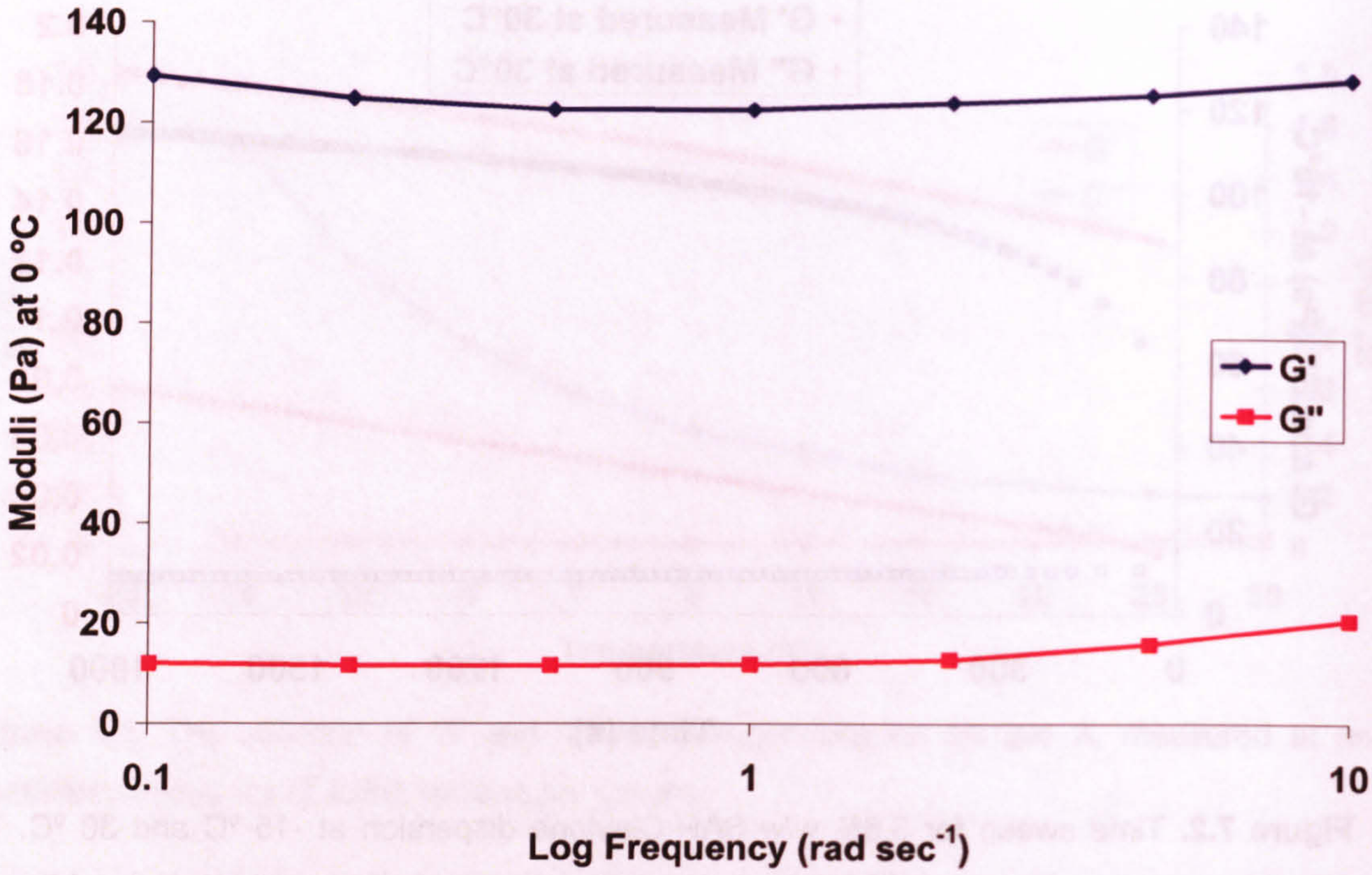

Figure 7.3a. Plot of the Log of a range of frequency against G' and G" at 0 °C for a 3.6% w/w SAP Claytone dispersion in polydecene (sample B).

At the temperature of 0 °C (figure 7.3a) the elastic modulus was greater than the viscosity modulus over the full range of frequencies and therefore at this temperature the relaxation time (τ_r) was much greater than 10 seconds.

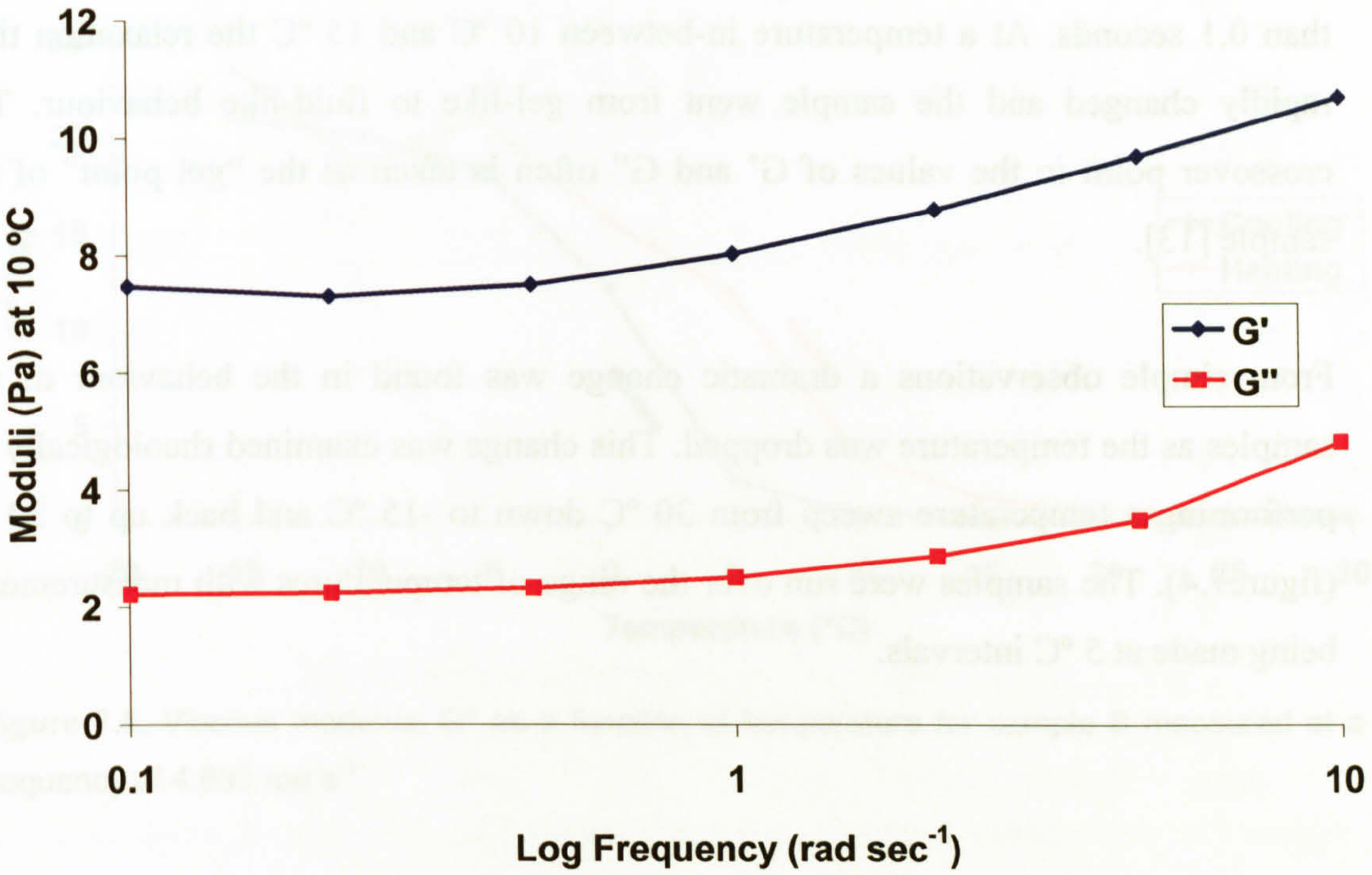

Figure 7.3b. Plot of the Log of a range of frequency against G' and G" at 10 ºC for sample B.

At 10 ºC (figure 7.3b) the relaxation time was still greater than 10 seconds but the values for the elastic and viscous moduli were of similar magnitude.

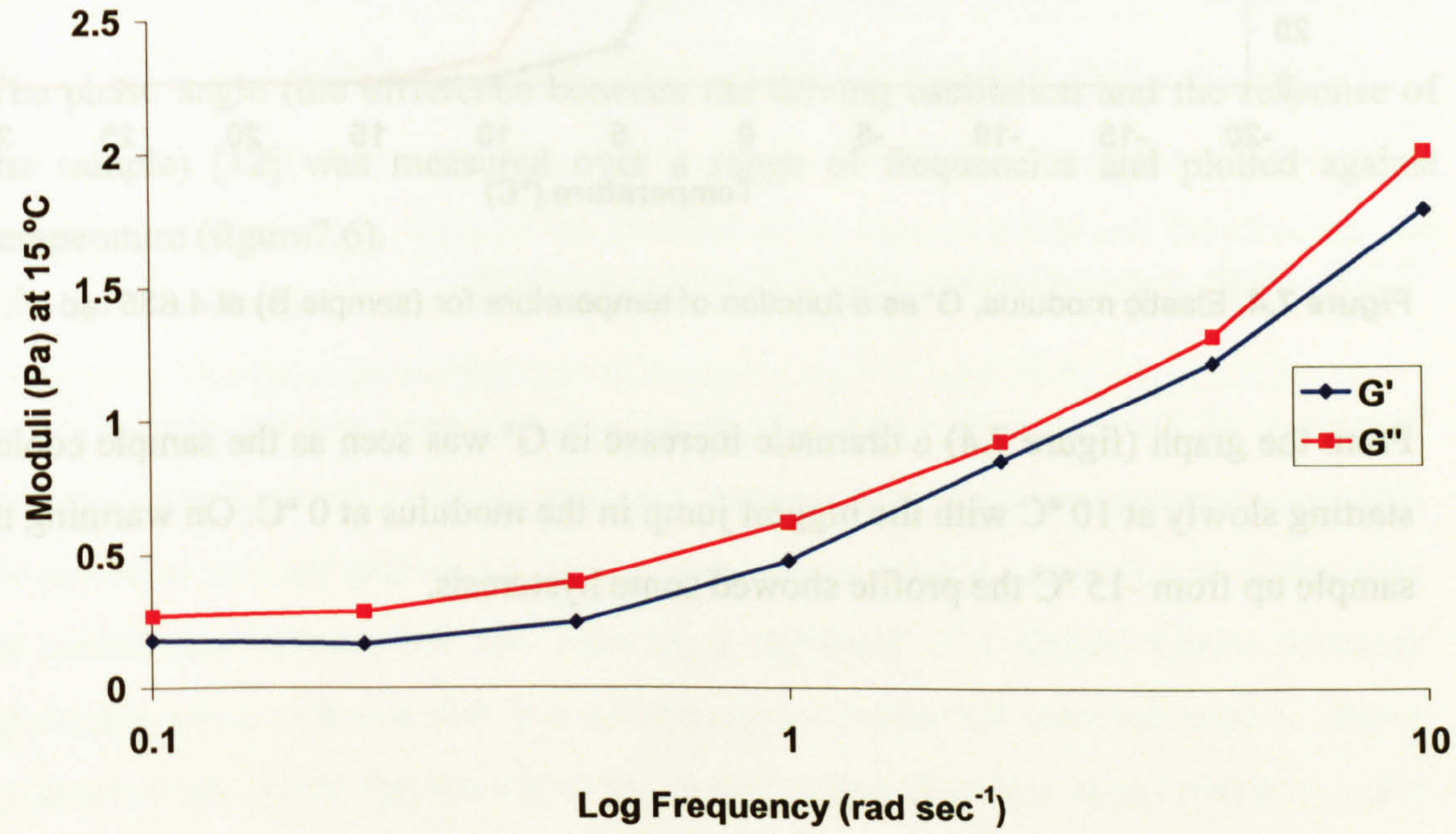

Figure 7.3c. Plot of the Log of a range of frequency against G' and G" at 15 ºC for sample B.

For the sample at 15 ºC (figure 7.3c) the viscous modulus was larger than the elastic modulus over the entire range of frequencies therefore the relaxation time was less than 0.1 seconds. At a temperature in-between 10 ºC and 15 ºC the relaxation time rapidly changed and the sample went from gel-like to fluid-like behaviour. The crossover point in the values of G' and G" often is taken as the "gel point" of the sample [13].

From simple observations a dramatic change was found in the behaviour of the samples as the temperature was dropped. This change was examined rheologically by performing a temperature sweep from 30 ºC down to -15 ºC and back up to 30 ºC (figure7.4). The samples were run over the range of temperatures with measurements being made at 5 ºC intervals.

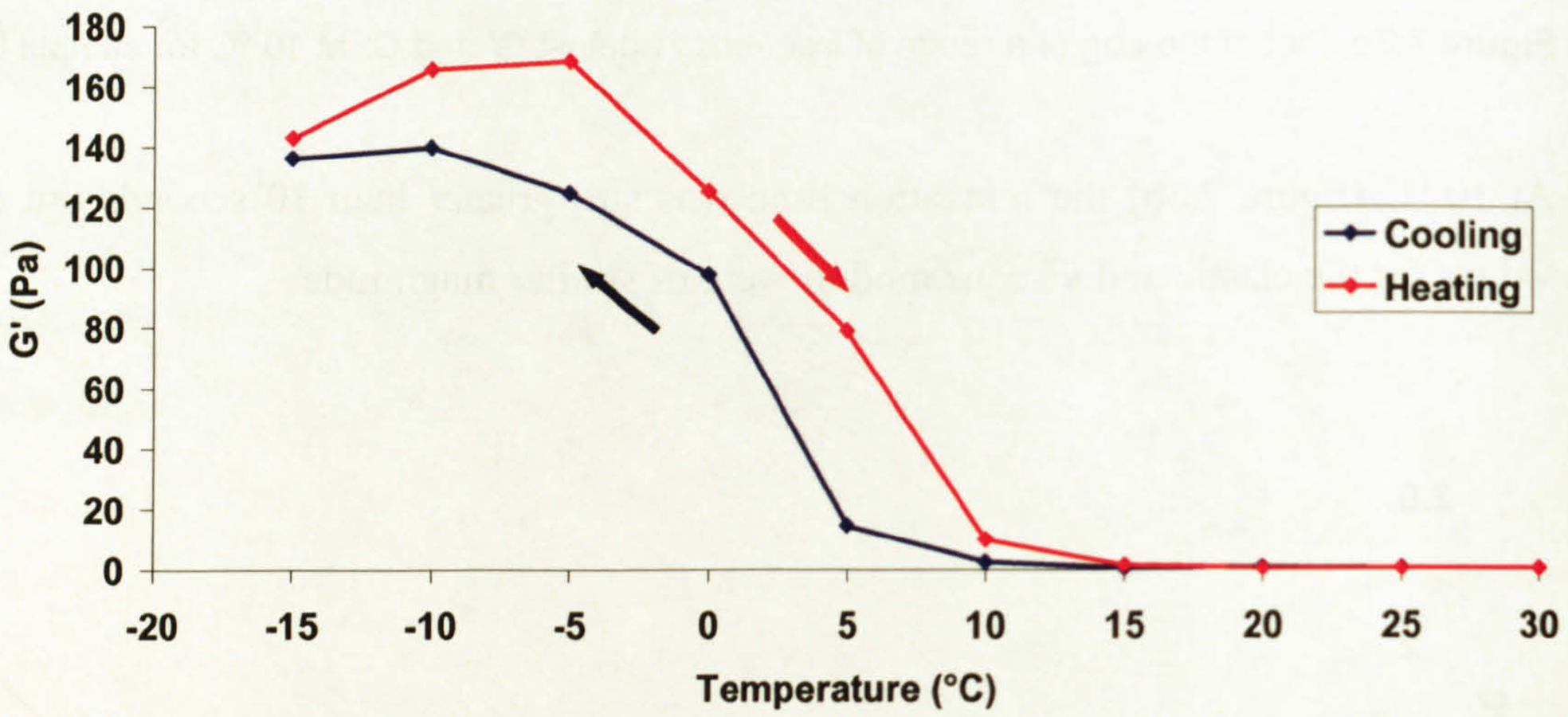

Figure 7.4. Elastic modulus, G' as a function of temperature for (sample B) at 4.635 rad s^{-1}.

From the graph (figure 7.4) a dramatic increase in G' was seen as the sample cooled, starting slowly at 10 ºC with the biggest jump in the modulus at 0 ºC. On warming the sample up from -15 ºC the profile showed some hysteresis.

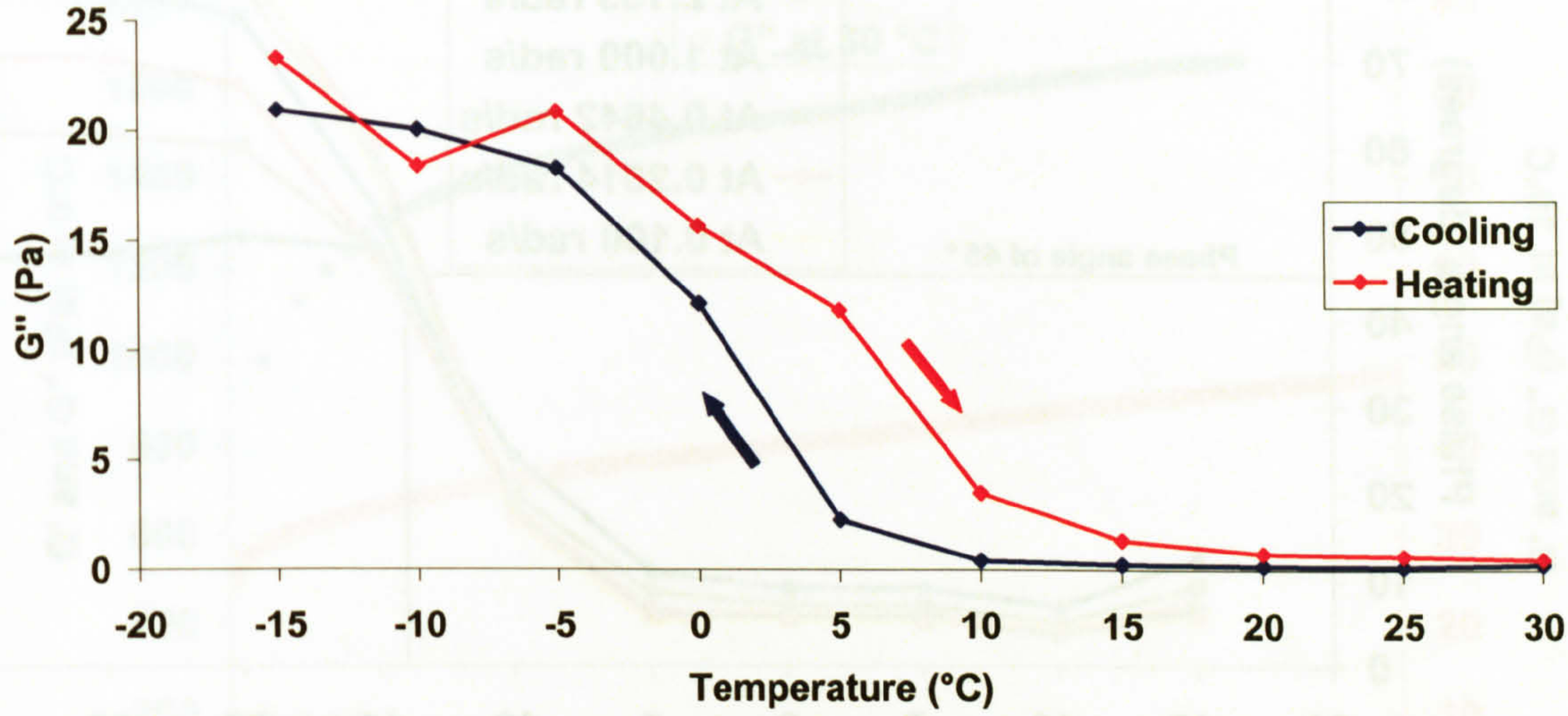

Figure 7.5. Viscous modulus, G" as a function of temperature for sample B measured at a frequency of 4.635 rad s^{-1}

The values for G" (figure 7.5) show a dramatic increase in the modulus of the sample as it cooled which was most rapid from 5 °C to 0 °C. The overall shape of the curves for G' and G" was very similar but the G' values changed by a larger amount. The cause of the hysteresis found for both G' and G" was possibly due to thermal lag in the rheology experiment but 300 seconds was allowed for the structure to rebuild which also allowed the samples a chance to thermally equilibrate.

The phase angle (the difference between the driving oscillation and the response of the sample) [12] was measured over a range of frequencies and plotted against temperature (figure7.6).

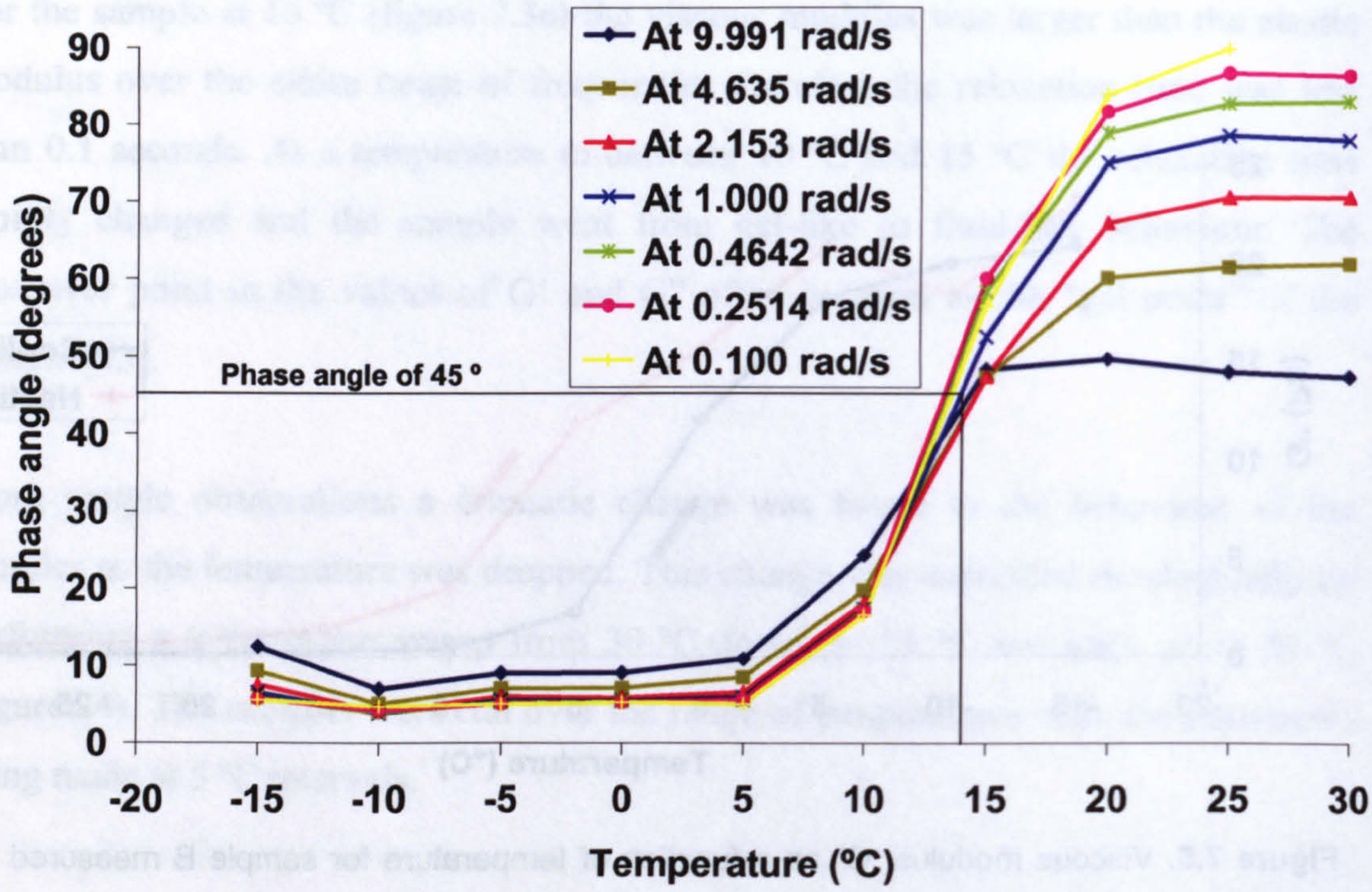

Figure 7.6. The gelation temperature found from the crossover point of phase angle and frequency for sample B measured as the temperature was decreased.

The phase angle for all the frequencies tested dropped with decreasing temperature and at around 12 °C the response of the sample became much less frequency dependent indicating the formation of a gel. However, the gel-point was not at a phase angle of 45 ° (the point where the elastic and viscous moduli are equal). As expected, the temperature at which the frequency dependence was lost was within the range where the relaxation time reduced from 10 seconds to less than 0.1 seconds (figures 7.3).

7.3.3 High concentration SAP Claytone samples

Sample C (9.7% w/w SAP treated Claytone) was examined and the main observed difference between sample B and sample C was that sample C became very solid-like on cooling in a freezer. A time sweep was carried out to find the rate at which the structure rebuilt (figure 7.7). However a problem was encountered concerning the length of time between the initial measurements and this was due to the rheometer being in strain mode and took some time to reach the correct strain. As a result the time sweeps were carried out at 30 °C and 0 °C.

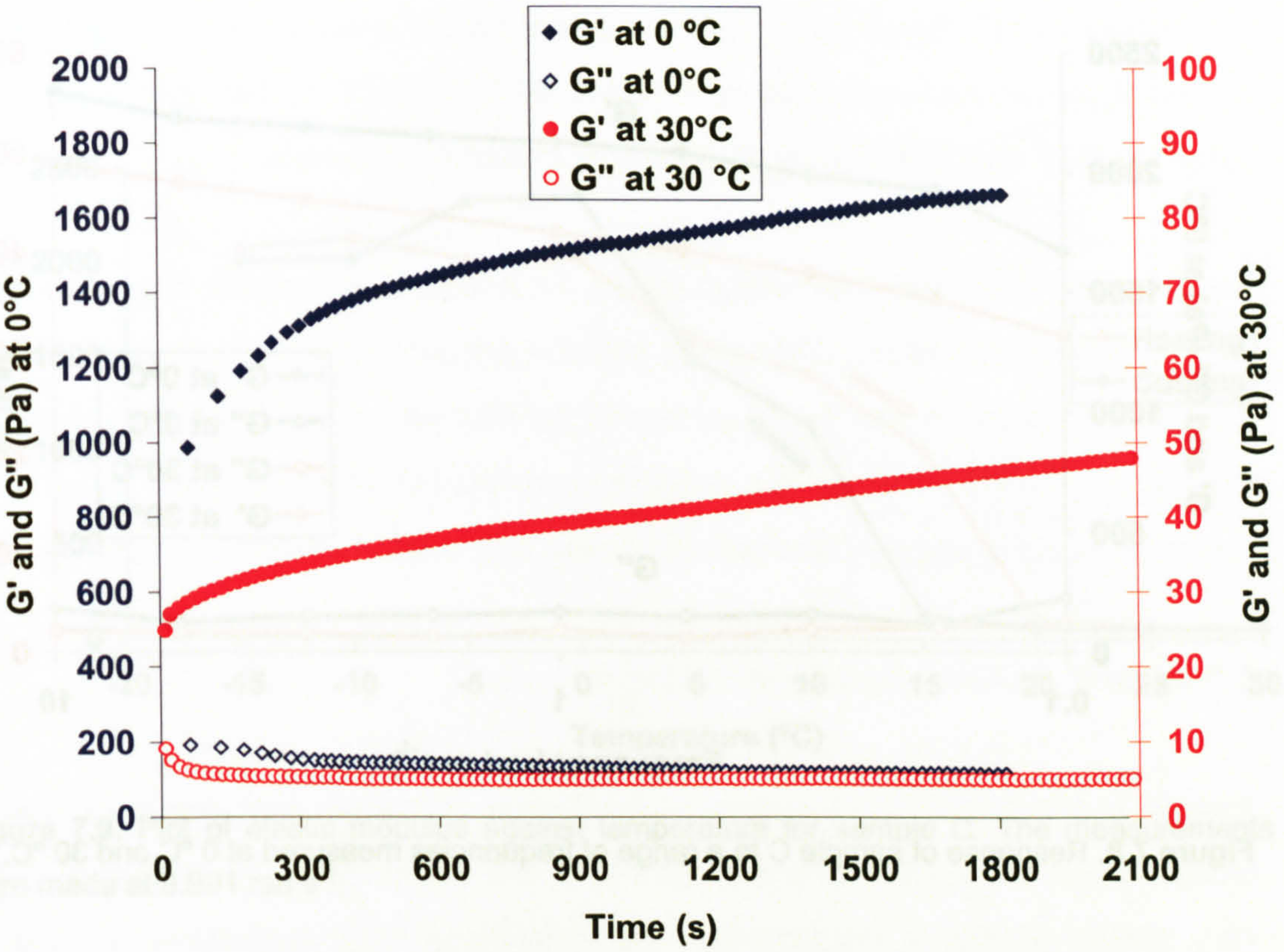

Figure 7.7. Time sweep for 9.72% w/w SAP Claytone in polydecene (sample C) at 0 °C and 30 °C. The samples were pre-sheared at 50 Pa for 1 minute then measured at constant strain of 5×10^{-3} over 30 minutes.

The time taken for structural reorganisation for sample C was in excess of 1800 seconds, but the time for the moduli to increase at a constant rate was 300 seconds, the same time as sample A. However, there was a difference between the measurements in that the geometry did not move when a preshear of 50 Pa was applied. If the preshear was increased to much beyond this point the geometry just slipped over the sample. Despite the problem there was an effect and the structure did rapidly rebuild after the pre-shear as the graph indicates.

Frequency sweeps were carried out on sample C at 0 °C and 30 °C (figure 7.8).

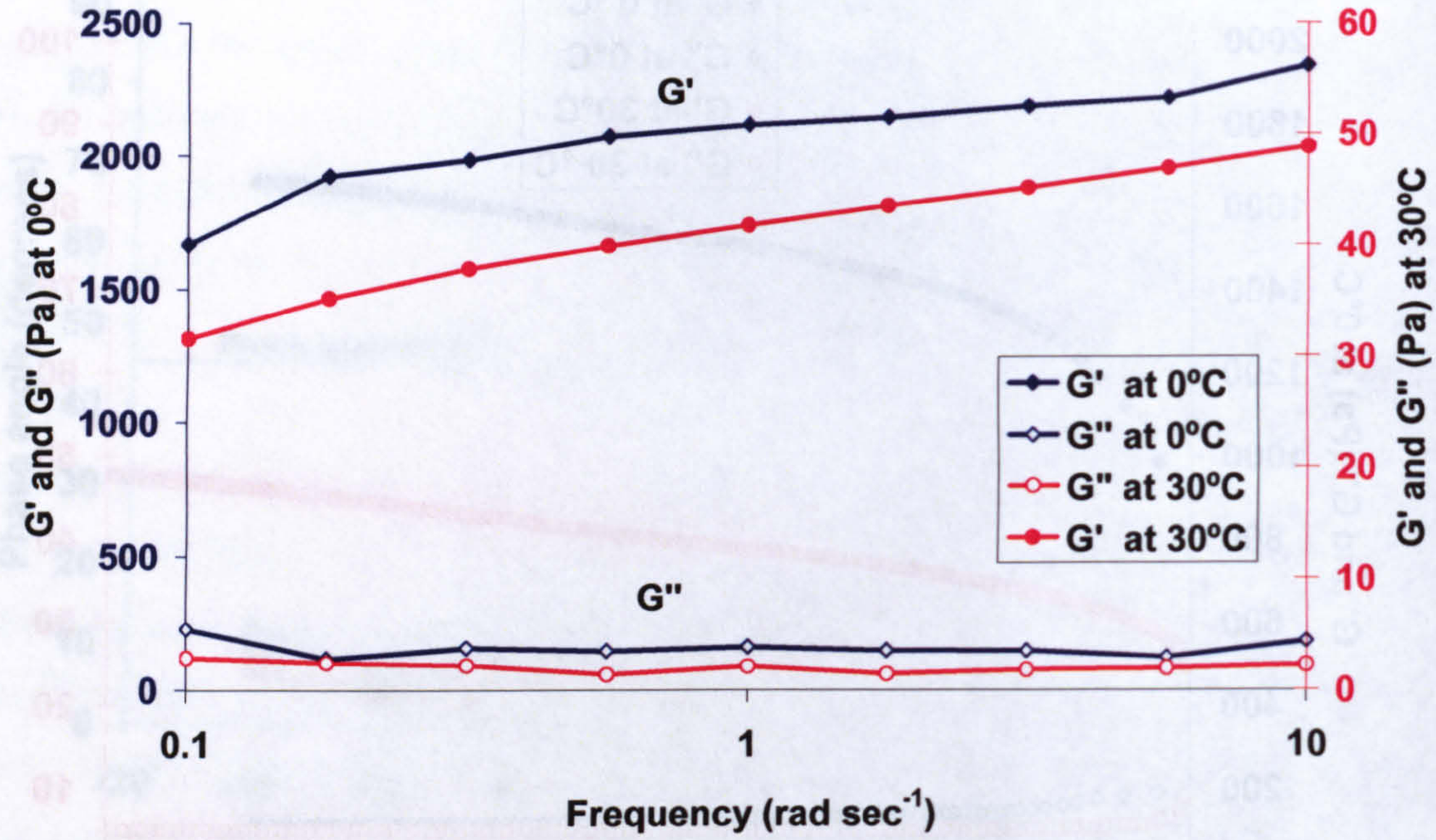

Figure 7.8. Response of sample C to a range of frequencies measured at 0 °C and 30 °C.

Over the range of frequencies measured little frequency dependence was found. Unlike the low concentration (sample B) the relaxation time remained greater than 10 seconds at both low and high temperature. This showed that over the time of the experiment the sample was a gel.

A temperature sweep was performed with the high concentration sample to show how the values of the moduli changed with temperature. The response of the elastic modulus with temperature is plotted below (figure 7.9).

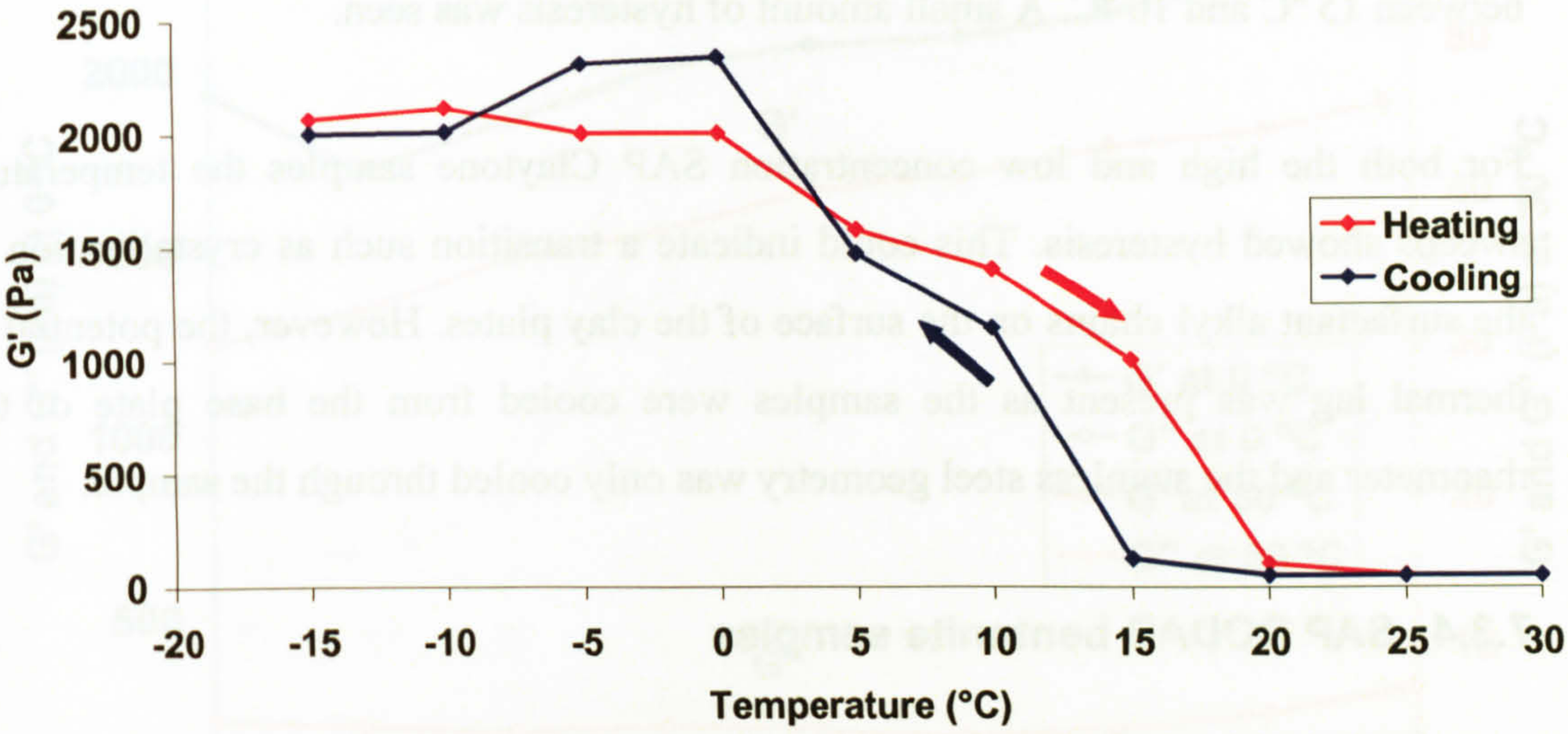

Figure 7.9. Plot of elastic modulus against temperature for sample C. The measurements were made at 9.991 rad s^{-1}.

A large increase in the value of G' was found on reduction of the temperature. The increase in G' started to occur between 10 °C and 15 °C. On raising temperature G' did not return to the very low values until a temperature of 20 °C. The hysteresis was similar but at a higher temperature to the low concentration sample.

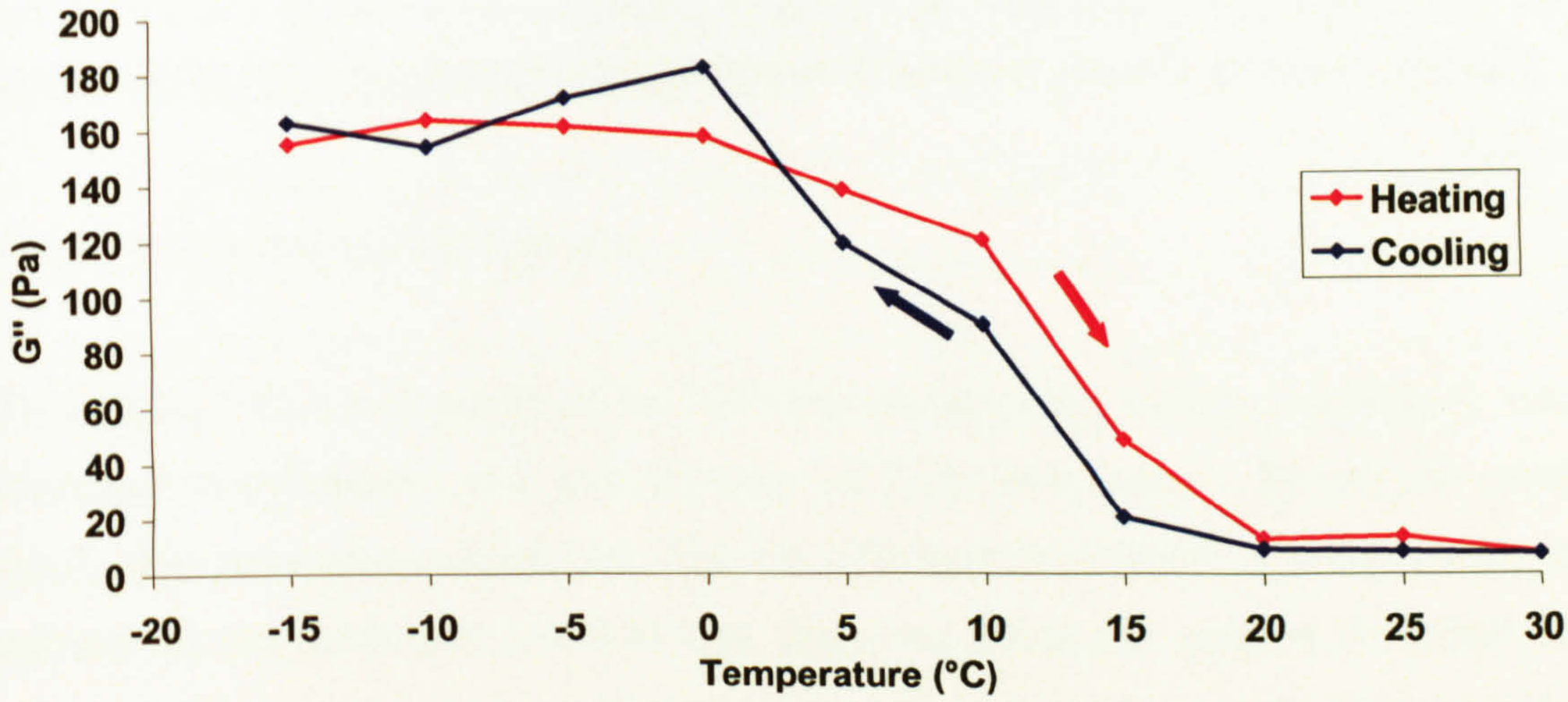

Figure 7.10. Plot of viscous modulus against temperature for sample C. The measurements were made at 9.991 rad s^{-1}.

The values for G" (figure 7.10) followed a very similar trend as the G' values with an the onset of the increases starting between 20 °C and 15 °C but with a rapid rise between 15 °C and 10 °C. A small amount of hysteresis was seen.

For both the high and low concentration SAP Claytone samples the temperature sweeps showed hysteresis. This could indicate a transition such as crystallisation of the surfactant alkyl chains on the surface of the clay plates. However, the potential of thermal lag was present as the samples were cooled from the base plate of the rheometer and the stainless steel geometry was only cooled through the sample.

7.3.4 SAP DODAB bentonite samples

Sample D (SAP DODAB bentonite at 9.8% w/w in polydecene) was very close in concentration to the SAP Claytone sample C and a time sweep (not plotted) gave a very similar profile. A frequency sweep at low and high temperature showed the sample had a relaxation time of greater than 10 seconds over the temperatures tested (figure7.11).

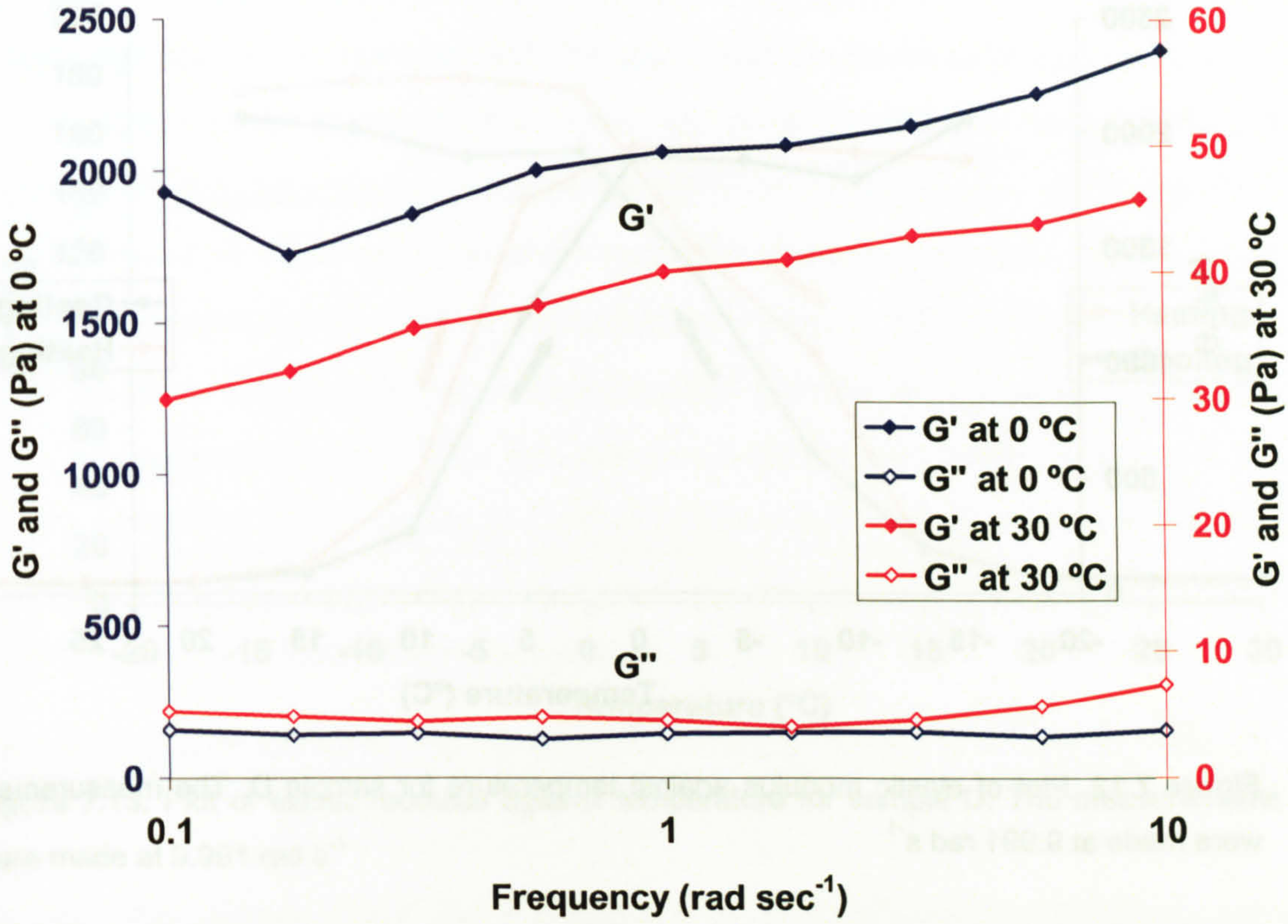

Figure 7.11. Plot of elastic modulus against temperature for sample D. The measurements were made at 9.991 rad s^{-1}

The samples were run through the same temperature cycle as the SAP Claytone samples as a comparison with the less well-characterised Claytone dispersions. The sample D values for G' are shown below (figure 7.12).

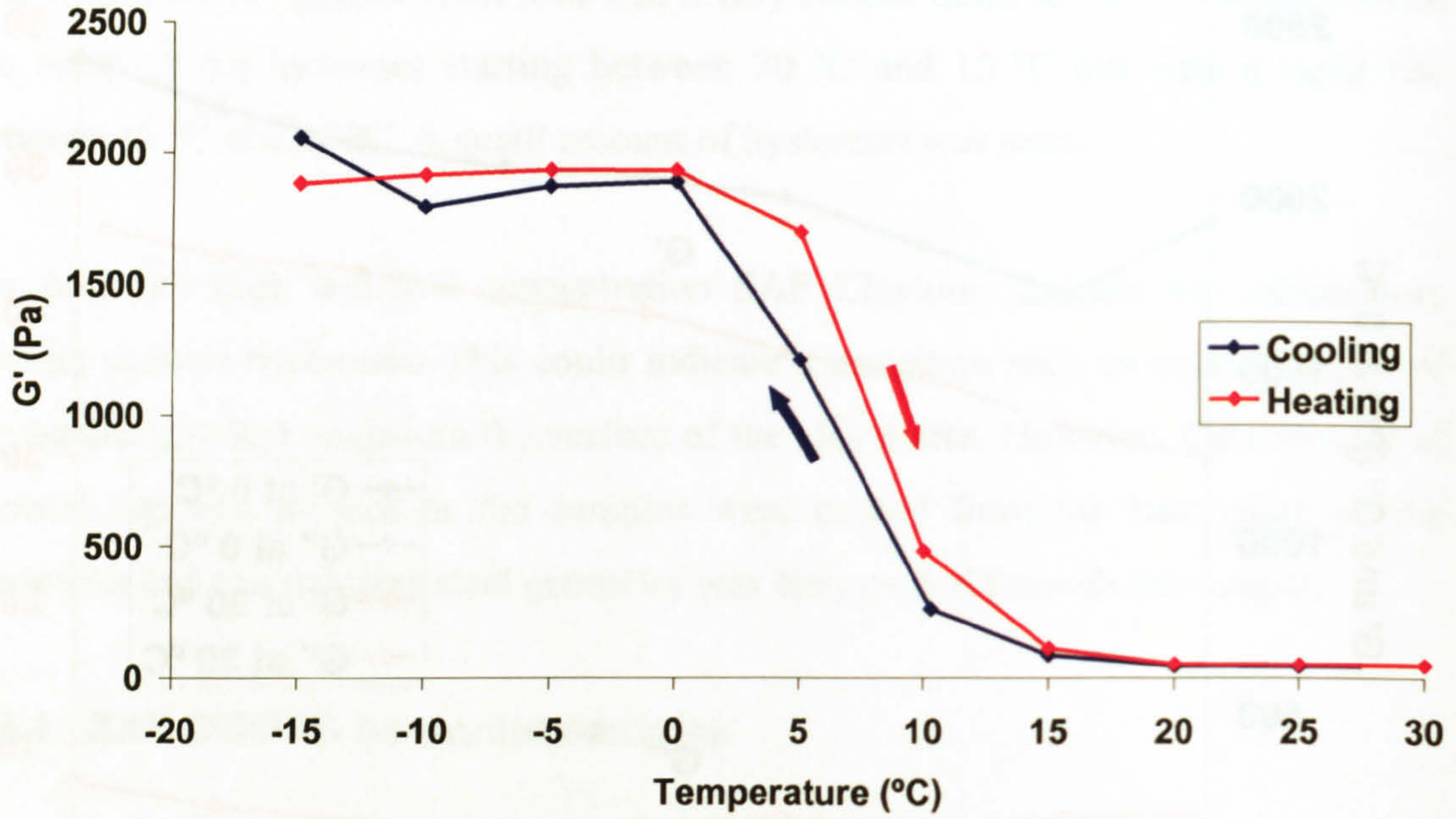

Figure 7.12. Plot of elastic modulus against temperature for sample D. The measurements were made at 9.991 rad s^{-1}

The same behaviour was shown for the DODAB bentonite sample with the elastic moduli becoming much larger as the temperature dropped below 10 °C. There appears to be less hysteresis than for the SAP Claytone samples with the structure reducing at the same temperature, not dependent on the temperature history of the sample. The magnitude of the moduli was also very similar between the high concentration samples of SAP DODAB bentonite and SAP Claytone.

The profile for the viscous modulus with temperature was recorded and plotted (figure 7.13).

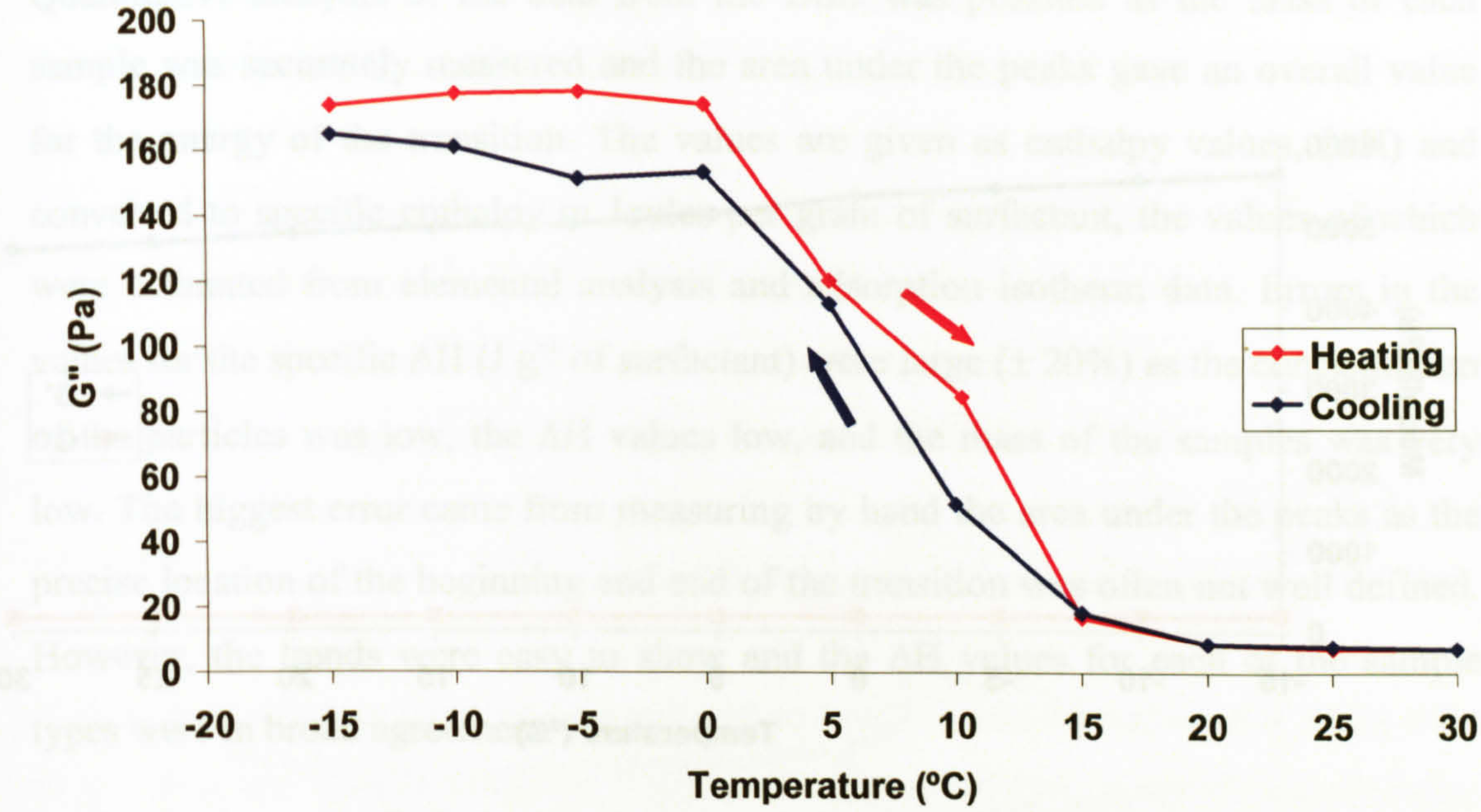

Figure 7.13. Plot of elastic modulus against temperature for sample D. The measurements were made at 9.991 rad s^{-1}

Like the previous figure the sample showed a small difference in the values of G" between the cooling and warming stages of the measurement with the values converging as the sample temperature was raised above 10 ºC. In comparison with the SAP Claytone sample little difference could be found.

From the comparison between the SAP Claytone and SAP DODAB bentonite samples the differences in the way the samples behaved was small and the overall values for elastic and viscous moduli were close.

7.3.5 Claytone in Polydecene

To contrast with the rheology of the SAP treated samples a sample of Claytone was dispersed in polydecene at a concentration of 7.2% w/w (sample E) and the same rheological tests were carried out. The dry Claytone was added to the polydecene without excess surfactant removed and dispersed using the method described in section 3.2.4. A temperature cycle was not performed as the sample showed little response as the temperature was dropped from 30 ºC to -15 ºC (figure 7.14).

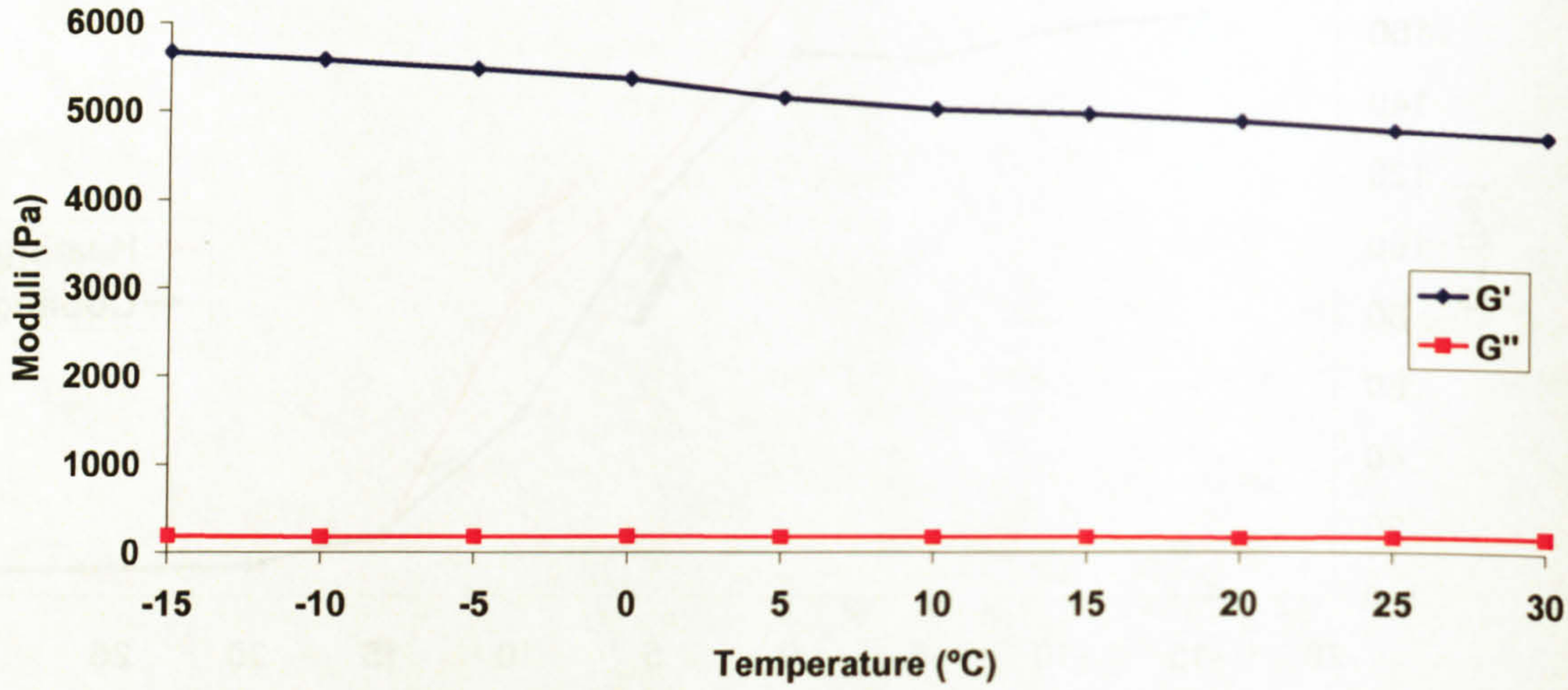

Figure 7.14. Plot of G' and G" against temperature for sample E. The measurements were made at 9.991 rad s^{-1}

The sample of Claytone without adsorbed SAP was a gel and starting at 30 °C and decreasing in 5 °C steps little temperature dependence on the values for the elastic and viscous moduli was found. However, the values for the storage modulus were 3 times as large as the higher concentration SAP Claytone and SAP DODAB bentonite samples.

7.4 Differential Scanning Calorimetry (DSC)

When a sample of a dispersion changes phase there is either a release or absorption of energy and this could be measured using DSC. For this experiment the individual samples were heated up at a constant rate and the amount of energy taken to keep that the change in temperature constant was plotted against the temperature of the sample [14]. For samples such as thermoreversible clay dispersions the peaks found were over a wide temperature range and were of a small value due to the large temperature range of the transition and small energy difference. To reduce thermal lag in the samples under analysis only 20 to 30 mg of the dispersions were weighed into the aluminium sample holders before being sealed.

Quantitative analysis of the data from the DSC was possible as the mass of each sample was accurately measured and the area under the peaks gave an overall value for the energy of the transition. The values are given as enthalpy values, (ΔH) and converted to specific enthalpy in Joules per gram of surfactant, the values of which were estimated from elemental analysis and adsorption isotherm data. Errors in the values for the specific ΔH (J g^{-1} of surfactant) were large ($\pm$ 20%) as the concentration of the particles was low, the ΔH values low, and the mass of the samples was very low. The biggest error came from measuring by hand the area under the peaks as the precise location of the beginning and end of the transition was often not well defined. However, the trends were easy to show and the ΔH values for each of the sample types were in broad agreement.

7.4.1 DSC protocol

To make the comparison of the dispersions more straightforward the samples were analysed using the same protocol (Table 7.3).

1.	Cool samples to -30 °C and hold for 5 minutes
2.	Heat samples at 10° $Cmin^{-1}$ up to 110 °C and hold for 2 minutes
3.	Cool samples at 20° C min^{-1} to -30 °C.

Table 7.3. The protocol followed for the DSC measurements.

Note: When carrying out the experiments the cooling curve was never a straight line and no definite sample peak could be identified making repeated cycled temperature scans difficult to interpret.

7.4.2 DSC samples

The DSC experiments were rapid and relatively simple to undertake and a number of sample concentrations and types were examined (table 7.4).

Sample	Description	Solvent
DSC.A	Free 2% w/w DODAB and 1% w/w SAP	Polydecene 364NF
DSC.B	3.6% w/w SAP treated Claytone	Polydecene 364NF
DSC.C	9.7% w/w SAP treated Claytone	Polydecene 364NF
DSC.D	10.2% w/w SAP treated Claytone	Polydecene 364NF
DSC.E	9.8% w/w SAP DODAB bentonite	Polydecene 364NF
DSC.F	7.2% w/w Claytone	Polydecene 364NF

Table 7.4. Codes for the samples submitted for DSC analysis.

For small transition energies a rapid heating rate was required to make the transition obvious on the graph but by heating the sample up more rapidly the onset of the transition occurred at a higher temperature. A calibration plot was carried out using the melting point of an Indium metal sample with a known melting point of 156.6 °C [15] to show how the thermal lag was related to the rate of change in temperature (figure 7.15).

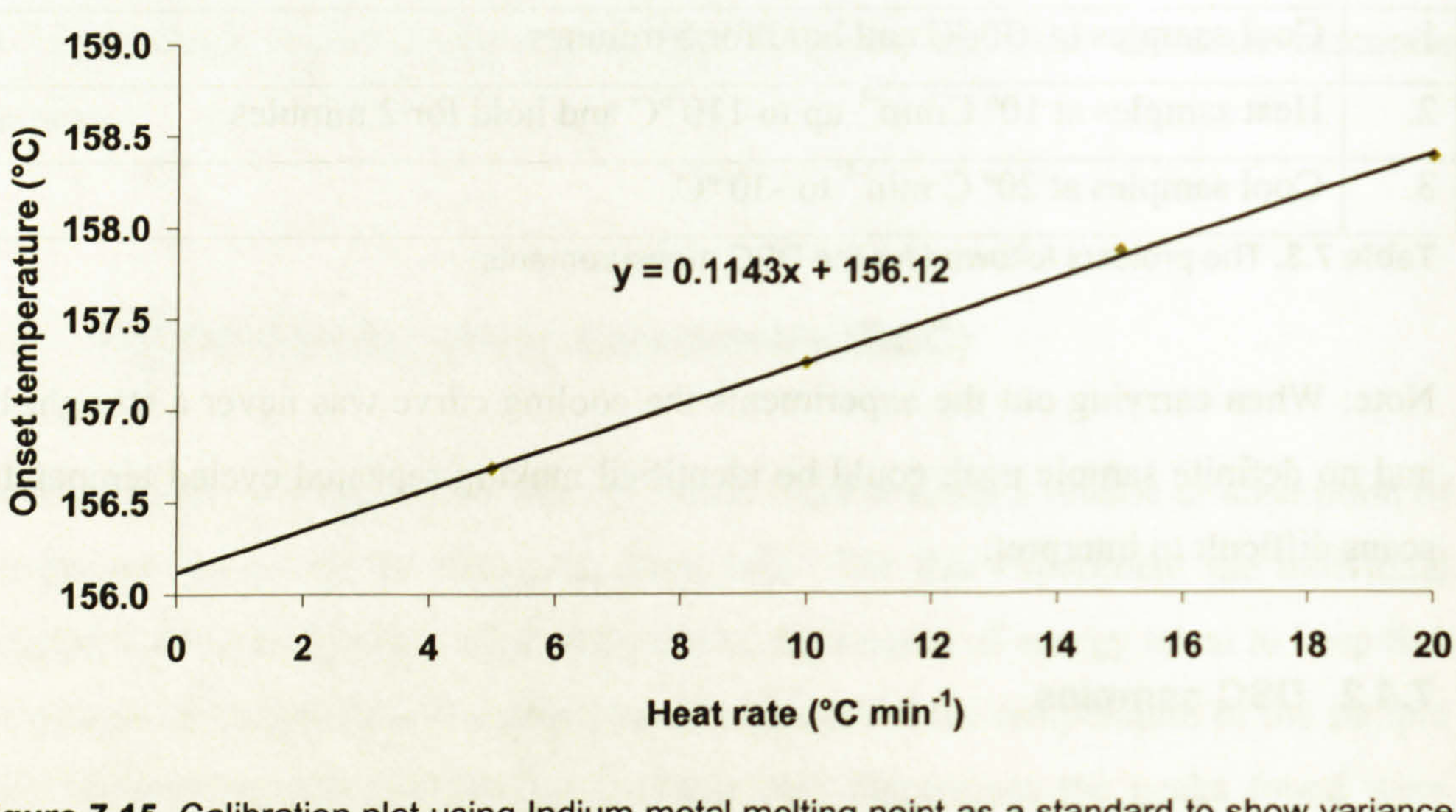

Figure 7.15. Calibration plot using Indium metal melting point as a standard to show variance of heat rate with onset temperature.

The calibration plot showed that the onset temperature at a heat rate of 10 °C min^{-1} was 1 °C above the temperature of the transition if measured at 0 °C min^{-1}. The melting temperature of Indium metal is 156.6 °C and therefore the predicted

temperature of melting at zero heat rate was 0.5 °C below this temperature. The error for the samples in the onset temperature was taken as less than 1 degree.

The first samples to be analysed were made up of DODAB and SAP dispersed in polydecene without clay to act as controls (figure 7.16).

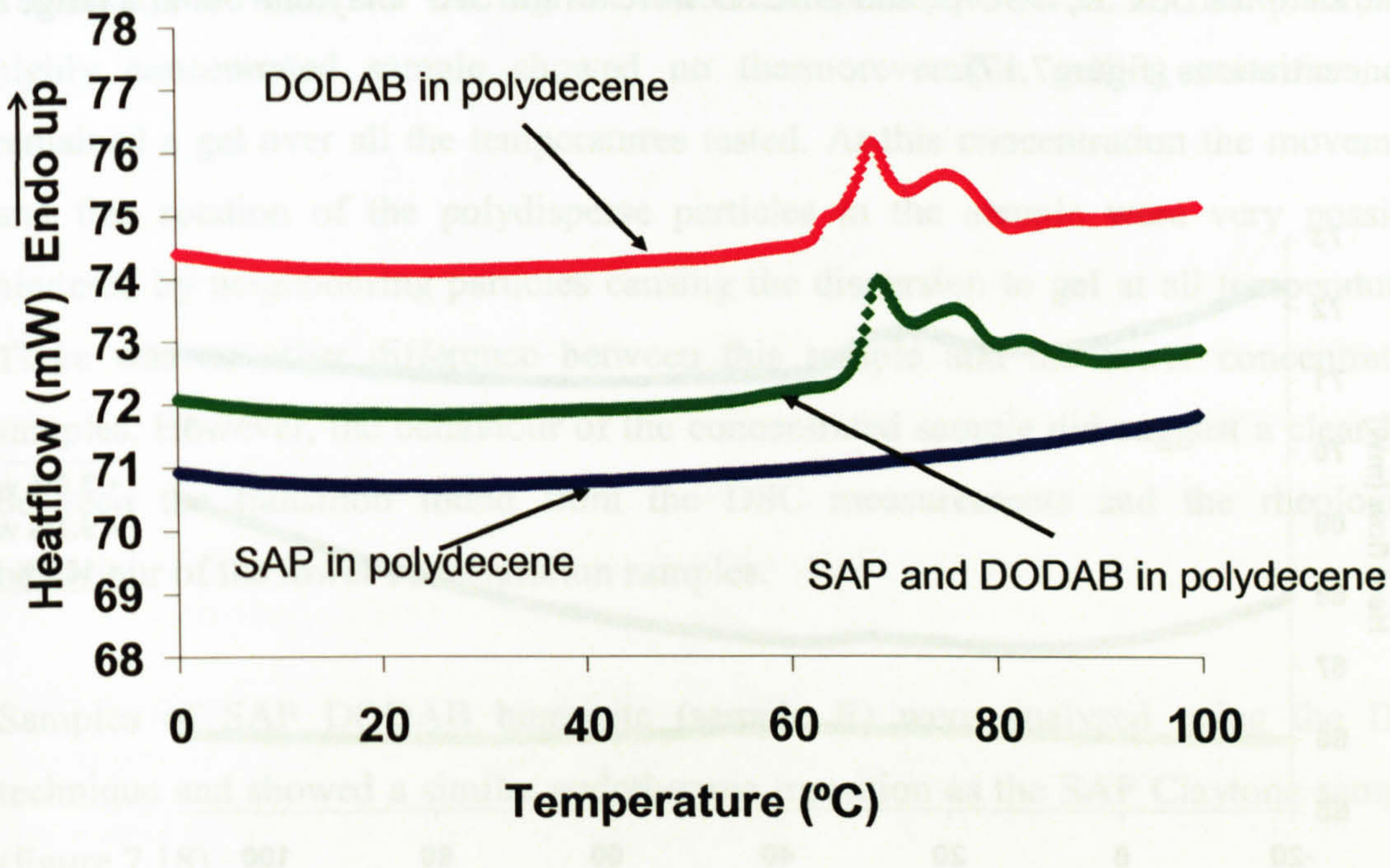

Figure 7.16. Control samples of SAP, DODAB and both dispersed in polydecene (samples A, B, and C).

For the sample of free SAP in polydecene no peak in the DSC data was found from 0 °C to 100 °C but for the DODAB sample an endothermic peak due to the surfactant dispersing was seen at 64 °C to 74 °C. A peak of the same shape and at almost exactly the same point was found for the sample that contained both SAP and surfactant. The magnitude of the endothermic change was given (table 7.5).

Percentage mass of DODAB	Peak onset (°C)	Peak end (°C)	Peak top (°C).	ΔH values (J g^{-1})	Specific ΔH (J g^{-1} of surfactant)
DODAB alone					
2.3	64.9	72.3	68.1	2.85	145.0
DODAB and SAP					
2.5	66.2	73.5	68. 7	2.55	118.9

Table 7.5. Enthalpy values for the endothermic transition found for DODAB dispersing in polydecene.

The transition of the DODAB dispersing in the polydecene was highly visible as the dispersion became colourless as the sample was warmed above 65 °C. SAP polymer alone showed no such transition and rapidly dispersed in the solvent at all temperatures.

The samples DSC.B, DSC.C, and DSC. D were all the SAP Claytone but at a range of concentrations (figure7.17).

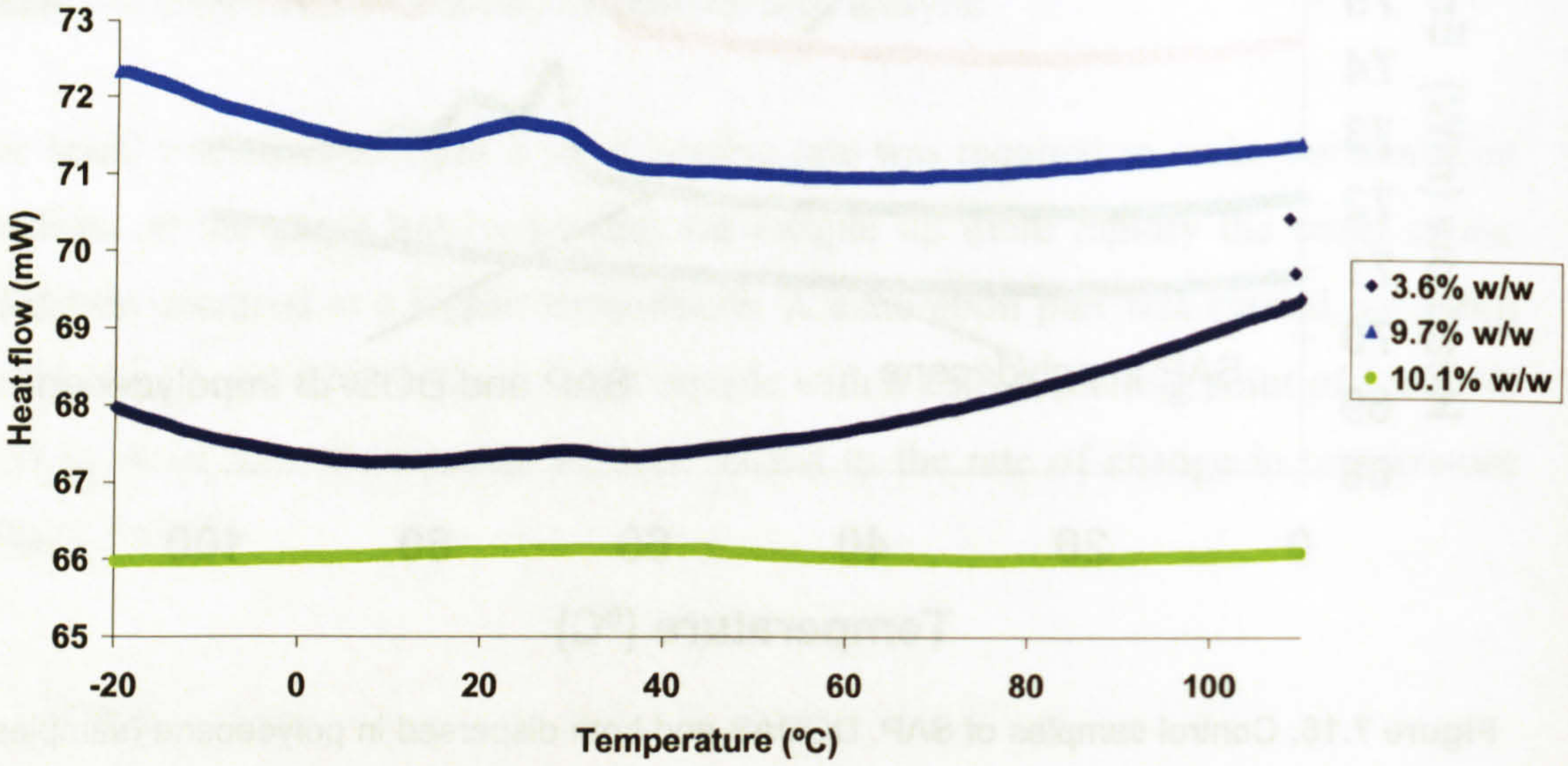

Figure 7.17. DSC for SAP Claytone samples with an endothermic transition. The scale for the Y-axis is over a smaller range than for the control samples to make the peaks visible.

The full range of SAP Claytone concentrations examined using DSC consisted of a number of intermediate concentrations of samples giving similar results (table 7.6).

SAP Claytone samples					
Percentage mass of particles	Peak onset (°C)	Peak end (°C)	Peak top (°C).	ΔH values (J g^{-1})	Specific ΔH (J g^{-1} of surfactant)
3.6	12.6	34.2	29.4	0.23	21.6
5.2	12.7	34. 9	24.7	0.36	23.0
7.2	15.3	32.5	23.4	0.43	19.9
9.7	13.9	34.8	34.8	1.01	34.6

Table 7.6. Enthalpy values for the endothermic transitions found for all SAP Claytone samples submitted for DSC.

For DSC.B and DSC.C an endothermic transition was found with the onset temperature from 12 ºC to 15º C. The magnitude of the transition was much smaller than the free surfactant values but this was not surprising as the surfactant molecules attached to the surface of the clay were held further apart than free surfactant molecules in the solvent and were not able to closely aggregate. No endothermic transition was found for the highest concentration sample (DSC.D). However, this highly concentrated sample showed no thermoreversible gelling transition and remained a gel over all the temperatures tested. At this concentration the movement and free rotation of the polydisperse particles in the sample were very possibly hindered by neighbouring particles causing the dispersion to gel at all temperatures. There was no other difference between this sample and the lower concentration samples. However, the behaviour of the concentrated sample did suggest a clear link between the transition found from the DSC measurements and the rheological behaviour of the lower concentration samples.

Samples of SAP DODAB bentonite (sample E) were analysed using the DSC technique and showed a similar endothermic transition as the SAP Claytone samples (figure 7.18).

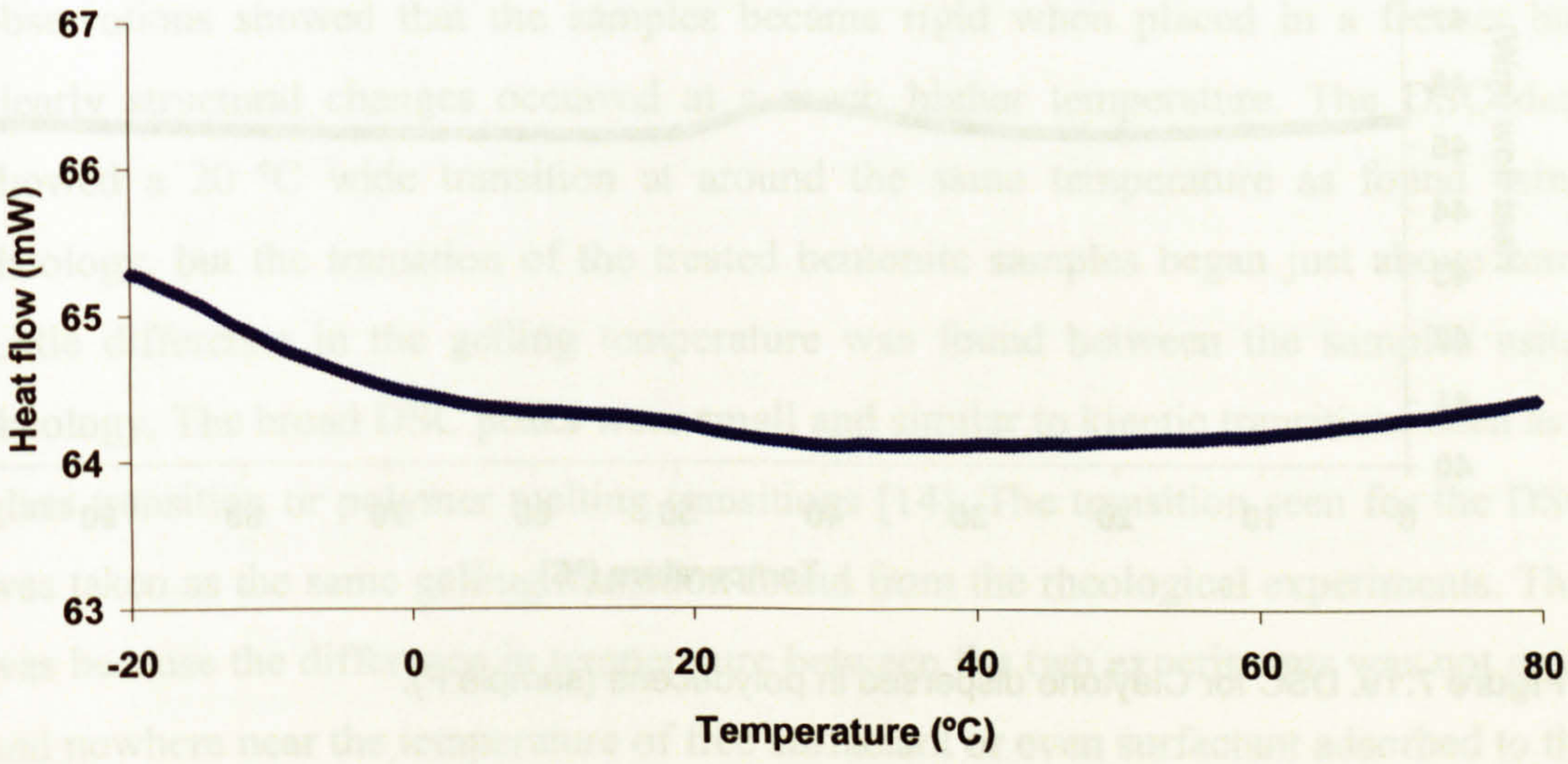

Figure 7.18. DSC for SAP DODAB bentonite sample E. The scale for the Y-axis is over a smaller range than for the SAP Claytone samples to make the peak visible.

The energy of the transition was measured over a range of concentrations of SAP DODAB bentonite in polydecene (table7.7).

SAP DODAB bentonite					
Percentage mass of particles	Peak onset (°C)	Peak end (°C)	Peak top (°C).	ΔH values (J g^{-1})	Specific ΔH (J g^{-1} of surfactant)
5.2	5.4	26.0	17.7	0.31	19.7
7.1	4.2	24.1	18.9	0.60	28.0
9.8	5.7	17.7	11.7	0.71	30.0

Table 7.7. Enthalpy values for the endothermic transitions found for all SAP DODAB bentonite samples submitted for DSC

The size of the peak for the SAP DODAB bentonite was comparable to the SAP Claytone samples but the onset of the transition was consistently at a lower temperature than the SAP Claytone. The reason for this was the DODAB surfactant adsorbed to the bentonite samples was of slightly longer chain length and of lower polydispersity giving it a lower "freezing" temperature on the surface of the clay.

A sample of Claytone dispersed in polydecene without further treatment (sample F) was analysed using DSC (figure 7.19).

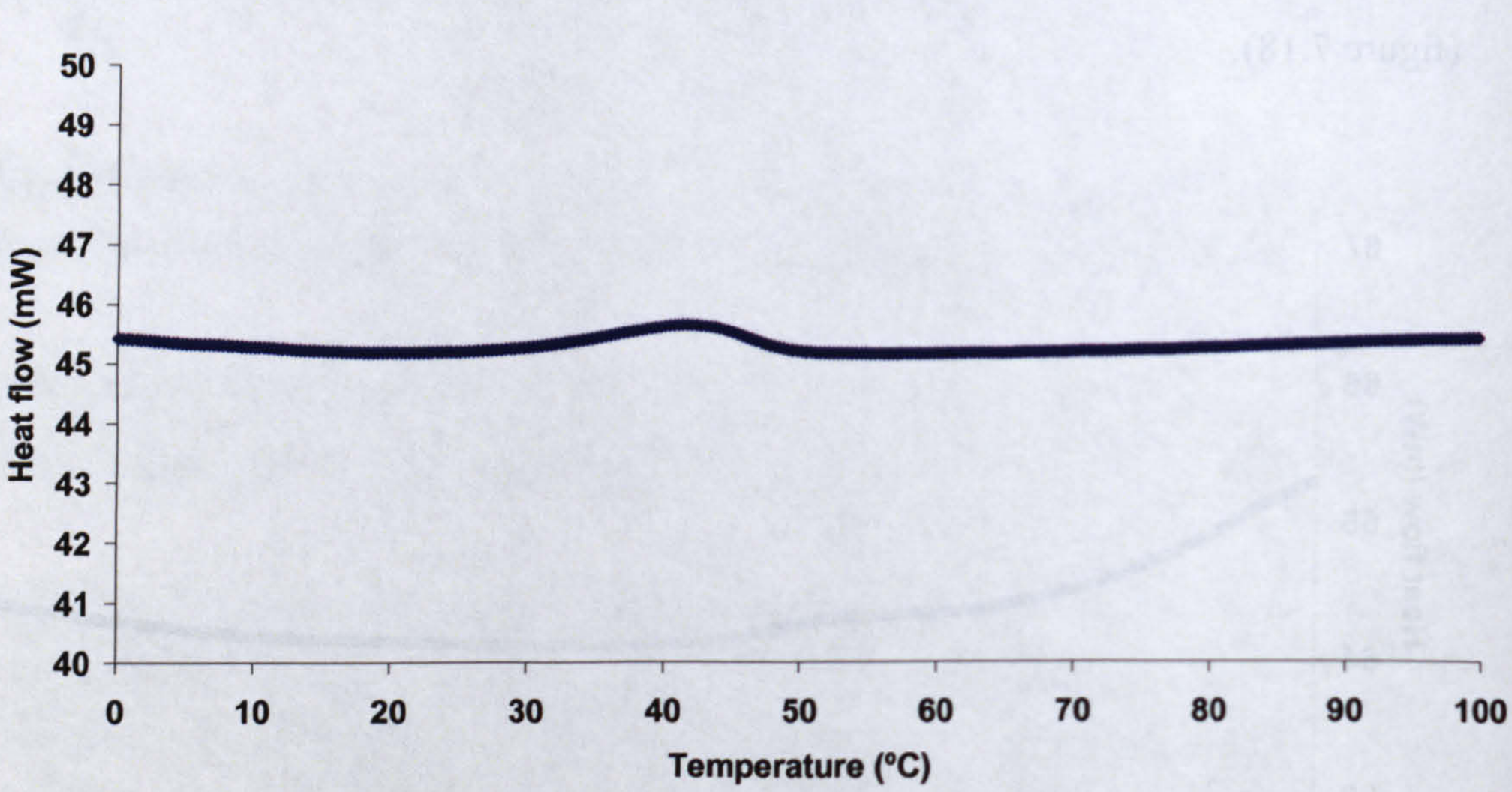

Figure 7.19. DSC for Claytone dispersed in polydecene (sample F).

The transition for the Claytone dispersion occurred at a higher temperature than for the SAP Claytone and SAP DODAB bentonite samples and the specific energy was also larger (table7.8).

Claytone					
Percentage mass of particles	Peak onset (°C)	Peak end (°C)	Peak top (°C).	ΔH values (J g^{-1})	Specific ΔH (J g^{-1} of surfactant)
7.2	29.4	49.0	41.4	1.26	58.2

Table 7.8. Enthalpy values for the endothermic transitions found for Claytone samples dispersed in polydecene (sample F).

The dispersion of Claytone in polydecene showed an onset temperature of a peak at 29 °C. The transition was thought to be due to desorbed surfactant from the Claytone sample dispersing and the transition was 30 °C lower than the free DODAB surfactant value but the 2HT surfactant adsorbed to the Claytone was expected to have a lower transition temperature.

7.5 Discussion

From the rheological data it was found that all SAP and surfactant treated samples, apart from the lowest concentration, were gels over the entire temperature range investigated. All the SAP treated samples showed a dramatic increase in the value of the elastic modulus and viscosity modulus below 10 °C to 15°C. The size and shape of the moduli profile for the SAP treated Claytone and DODAB bentonite samples was very similar despite the differences in their surface treatment. The initial simple observations showed that the samples became rigid when placed in a freezer but clearly structural changes occurred at a much higher temperature. The DSC data showed a 20 °C wide transition at around the same temperature as found using rheology, but the transition of the treated bentonite samples began just above zero. Little difference in the gelling temperature was found between the samples using rheology. The broad DSC peaks were small and similar to kinetic transitions such as a glass transition or polymer melting transitions [14]. The transition seen for the DSC was taken as the same gelling transition found from the rheological experiments. This was because the difference in temperature between the two experiments was not great and nowhere near the temperature of free surfactant or even surfactant adsorbed to the surface of the untreated Claytone sample. Also the very high concentration SAP Claytone sample that was rigid at all temperatures showed no DSC peak as further evidence of a gelling transition for the lower concentration samples but this sample

was not examined rheologically because it was a stiff gel at all temperatures and thought to be of less interest.

7.6 The role of polydecene

The DSC vividly showed how free surfactant went into solution at a temperature of 64 °C to 66 °C and the well dispersed sample of free SAP in polydecene showed no transition from 0 °C to 100 °C (figure 7.16). The SAP molecules consisting of poly (isobutylene) chains were not expected to aggregate over any temperature range. The stability of the SAP Claytone and SAP DODAB bentonite particles dispersed in polydecene was governed by the stability of both SAP and surfactant. It was assumed at low temperatures the surfactant molecules adsorbed to the surface of the plates either aggregated or froze on the surface of the plates, destabilising and gelling the dispersion. The thermoreversibility of the dispersion and the small magnitude of the transition showed the interaction between destabilised particles was physical and not chemical in nature and the hysteresis found in the rheology experiments was very possibly due to a nucleated transition such as "crystallisation" of the alkyl chains. Conformation of this was possible with DSC but the experiment was not carried out as there were problems with cooling temperature control on the instrument.

7.7 References

1. Ramsay, J.D.F., *Colloidal Properties of Synthetic Hectorite Clay Dispersions .1. Rheology.* Journal of Colloid and Interface Science, 1986. **109**(2): p. 441-447.
2. Rand, B., et al., *Investigation into the Existence of Edge-Face Coagulated Structures in Na-Montmorillonite Suspensions.* Journal of the Chemical Society-Faraday 1, 1980. **76**: p. 225-235.
3. Rossi, S., et al., *Influence of low molecular weight polymers on the rheology of bentonite suspensions.* Revue De L Institut Francais Du Petrole, 1997. **52**(2): p. 199-206.
4. Schmidt, G., A.I. Nakatani, and C.C. Han, *Rheology and flow-birefringence from viscoelastic polymer-clay solutions.* Rheologica Acta, 2002. **41**(1-2): p. 45-54.
5. Saunders, J., *An investigation of the Structure and Interactions in Aqueous Dispersions of Novel Laponite Clays.* PhD Thesis. School of Chemistry, University of Bristol, Bristol, UK, 1998.
6. van der Kooij, F.M., E.S. Boek, and A.P. Philipse, *Rheology of dilute suspensions of hard platelike colloids.* Journal of Colloid and Interface Science, 2001. **235**(2): p. 344-349.
7. van Olphen, H., *An Introduction to Clay Colloid Chemistry: For Clay Technologists, Geologists, and Soil Scientists.* 2nd Edition ed. 1977: John Wiley & Sons, Inc.
8. Kroon, M., W.L. Vos, and G.H. Wegdam, *Structure and formation of a gel of colloidal disks.* Physical Review E, 1998. **57**(2): p. 1962-1970.
9. Luckham, P.F. and S. Rossi, *The colloidal and rheological properties of bentonite suspensions.* Advances in Colloid and Interface Science, 1999. **82**(1-3): p. 43-92.
10. Jones, R.A.L., *Soft Condensed Matter.* First ed. 2002, Oxford: Oxford University Press.
11. Horigorne, M. and Y. Otsubo, *Long-Time Relaxation of Suspensions Flocculated by Association Polymers.* Langmuir, 2002. **18**(6): p. 1968-1973.
12. Goodwin, J.W. and R.W. Hughes, *Rheology for Chemists.* 2000, Cambridge: The Royal Society of Chemistry. 290.
13. Winter, H.H., P. Morganelli, and F. Chambon, *Stoichiometry Effects on Rheology of Model Polyurethanes at the Gel Point.* Macromolecules, 1988. **21**: p. 532-535.
14. Larson, R.G., ed. *The structure and rheology of complex fluids.* Topics in Chemical Engineering, ed. K.E. Gubbins. 1999, Oxford University Press: New York.
15. Lide, D.R., ed. *CRC Handbook of Chemistry and Physics.* 75th ed. 1994, Chemical Rubber Company: Florida, USA.

8 Small Angle X-ray scattering

8.1 Introduction

Small angle X-ray scattering (SAXS) is a very powerful and widely used technique available for the study of colloidal suspensions [1, 2]. For SAXS, as with all scattering methods, the change in direction of the propagated radiation due to interactions with inhomogeneities within the sample provides the basis of the method [2]. X-rays are scattered by electrons so the pattern is as a result of the electron density distribution in the sample. Only the elastically scattered radiation (the wavelength of the incoming and outgoing wave the same) contributes to the scattering pattern detected.

The scattering from dispersions of treated clays in organic solvents using SAXS can show periodic structures in the sample such as stacks of clay plates and the separation between the layers of clay in a stack [4, 5]. The size range accessible by the equipment used was from 10 Å to 150 Å. The thickness of individual clay plates was not reliably accessible because the signal generated at a value of 10 Å was at the very limits of the range of q ($q = 0.61 Å^{-1}$) and the data was noisy and inconclusive. The diameter of Laponite plates was not found using SAXS as only a few points probed this size range and the diameters of Claytone and bentonite plates were well out of range. Scattering from the periodic interlayer distance of the clay samples was easily identified (figure 8.1). This information was very useful as it showed how well dispersed the particles were in the sample.

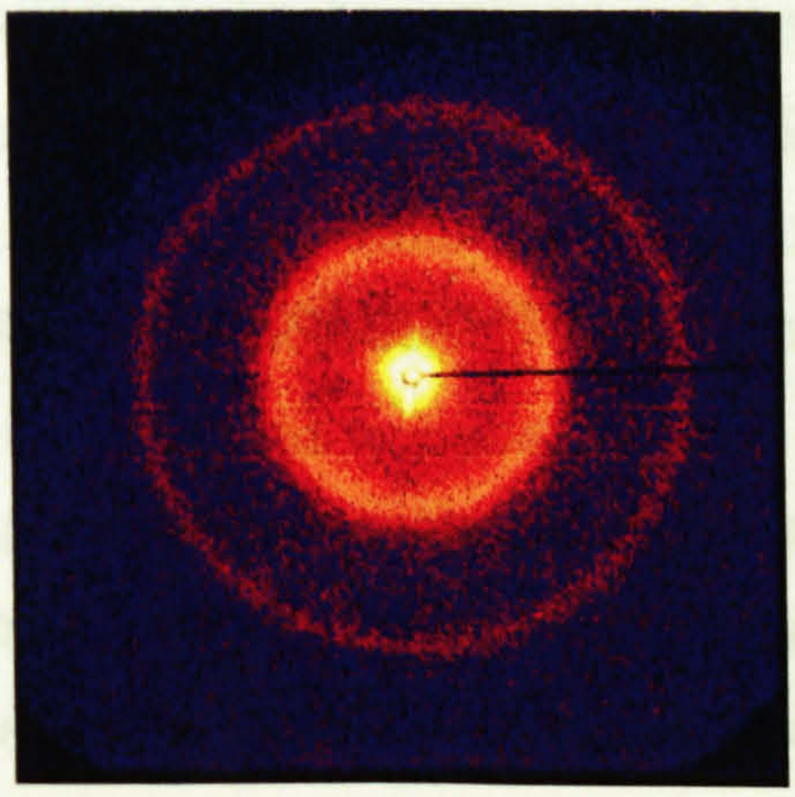

Figure 8.1. The intensity of scattered X-rays on the position sensitive detector (brighter colours indicate higher intensity).

When the Laponite was treated with cationic surfactant dioctacecyl dimethyl ammonium bromide (DODAB), and dried under vacuum small but broad peaks appeared in the SAXS data (figure 8.4). This was evidence of a periodic structure in the powder and showed the plates were not randomly orientated anymore but organised with respect to each other.

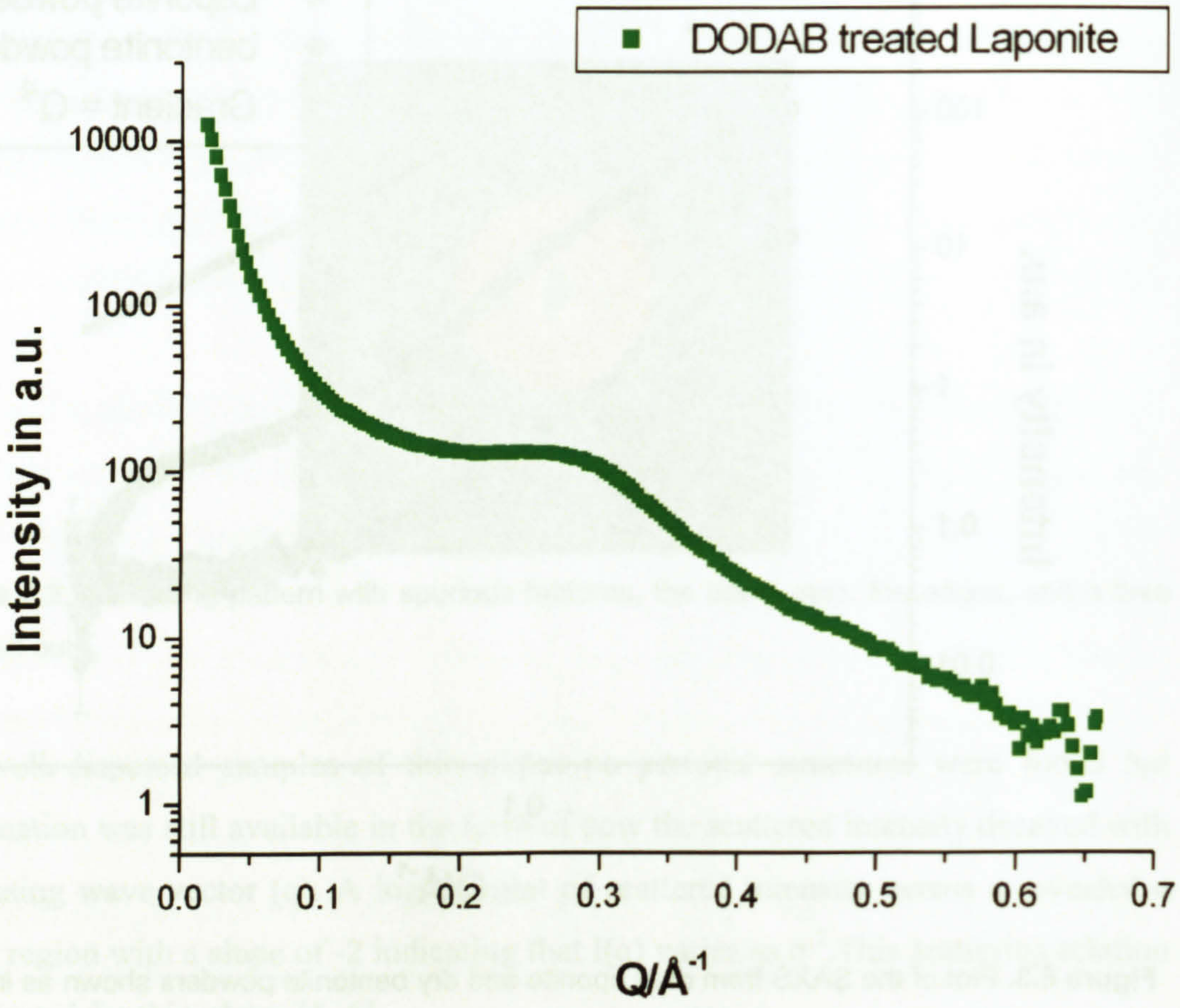

Figure 8.4. Scattering from DODAB treated Laponite powder. The intensity is plotted as a function of the wave-vector. The plotted error bars are very small.

The shoulder at $Q = 0.29$ Å^{-1} in the sample of DODAB treated Laponite is equivalent to a 21 Å interlayer spacing. The plate separation is 11 Å assuming that Laponite has a thickness of 10 Å as given by the manufacturer [7] and determined from the crystal structure [8].

The peaks for the sample of DODAB bentonite and Claytone were not at the same positions (figure 8.5) and this was due to the differing surface treatments. The Claytone surface comprised of an industrial grade of DODAB made from animal fat

called 2HT (di-hydrogenated tallow) [6]. Also the Claytone has been shown from elemental analysis to have a greater amount of surfactant adsorbed to the surface than DODAB bentonite thus swelling the Claytone layers [9, 10].

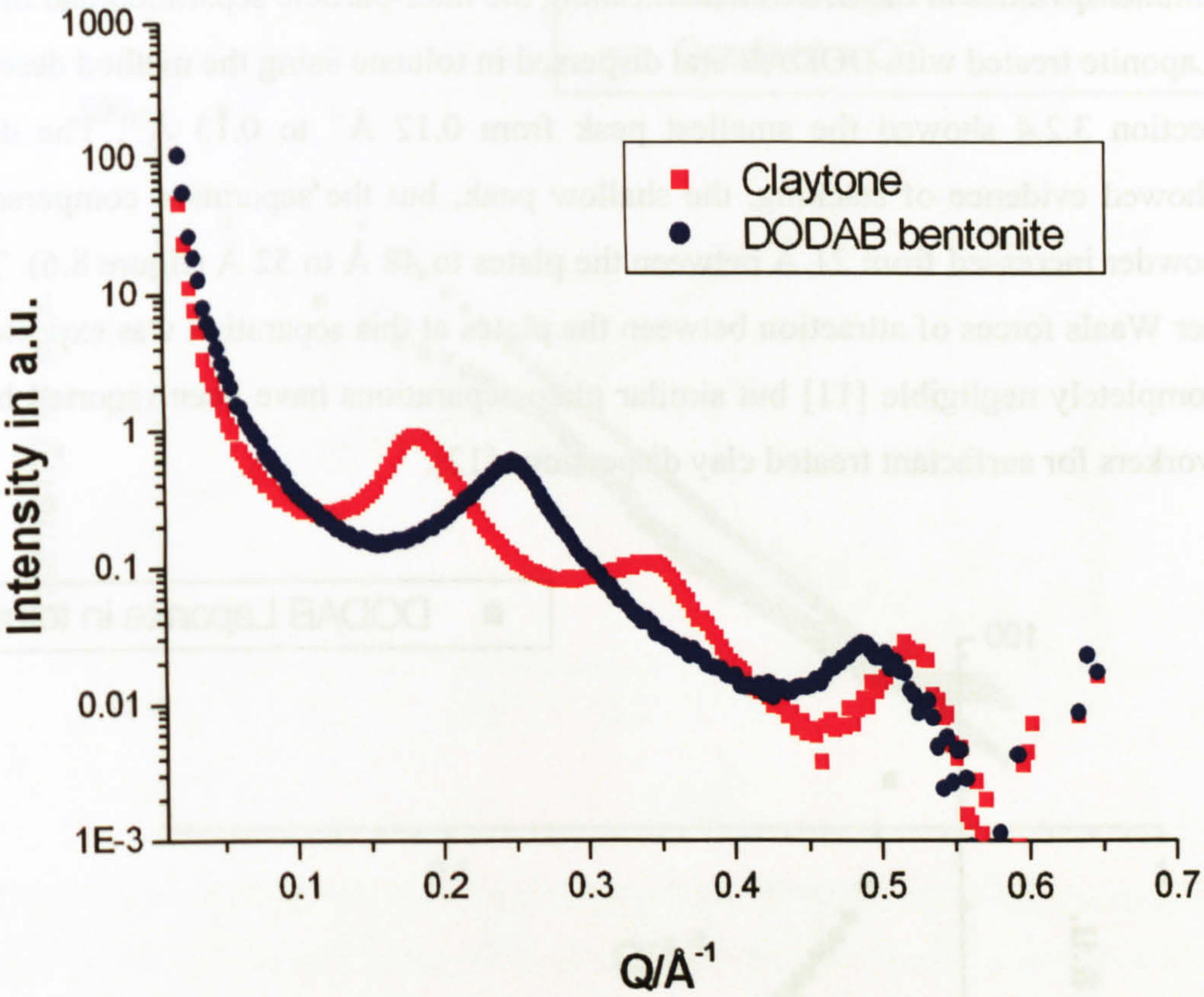

Figure 8.5. Scattering from DODAB treated bentonite and Claytone powders. The intensity is plotted as a function of the wave-vector. Error bars are plotted but are very small.

The DODAB treated bentonite and Claytone showed higher peaks than the DODAB Laponite, i.e. more ordering with the higher plate radius appearing to favour stack formation (figure 8.5). Claytone showed three peaks which is a sign of extremely low polydispersity in the periodicity within the stacks. Compared to DODAB Laponite the first peak is shifted to lower q and with a value of 0.18 $Å^{-1}$ giving an interlayer spacing of 35 Å (distance from midpoint to midpoint) again assuming a plate thickness of 10 Å. The second peak is a second order peak with q = 0.34 $Å^{-1}$ equivalent to 18 Å and the third order is found at q = 0.52 $Å^{-1}$ equivalent to 12 Å. The peaks of DODAB treated bentonite shift back towards the DODAB treated Laponite peaks. With q = 0.25 $Å^{-1}$ and q = 0.5 $Å^{-1}$ they result in roughly the same interlayer spacing of 25 Å.

8.3 Small angle X-ray scattering from suspensions in organic solvents

Suspending the clays in an organic solvent produced a clear shift of the peaks to smaller q values in the SAXS data meaning the inter-particle separation had increased. Laponite treated with DODAB and dispersed in toluene using the method described in section 3.2.4 showed the smallest peak from 0.12 $Å^{-1}$ to 0.13 $Å^{-1}$. The data still showed evidence of stacking, the shallow peak, but the separation compared to the powder increased from 21 Å between the plates to 48 Å to 52 Å (figure 8.6). The van der Waals forces of attraction between the plates at this separation was expected to be completely negligible [11] but similar plate separations have been reported by other workers for surfactant treated clay dispersions [12].

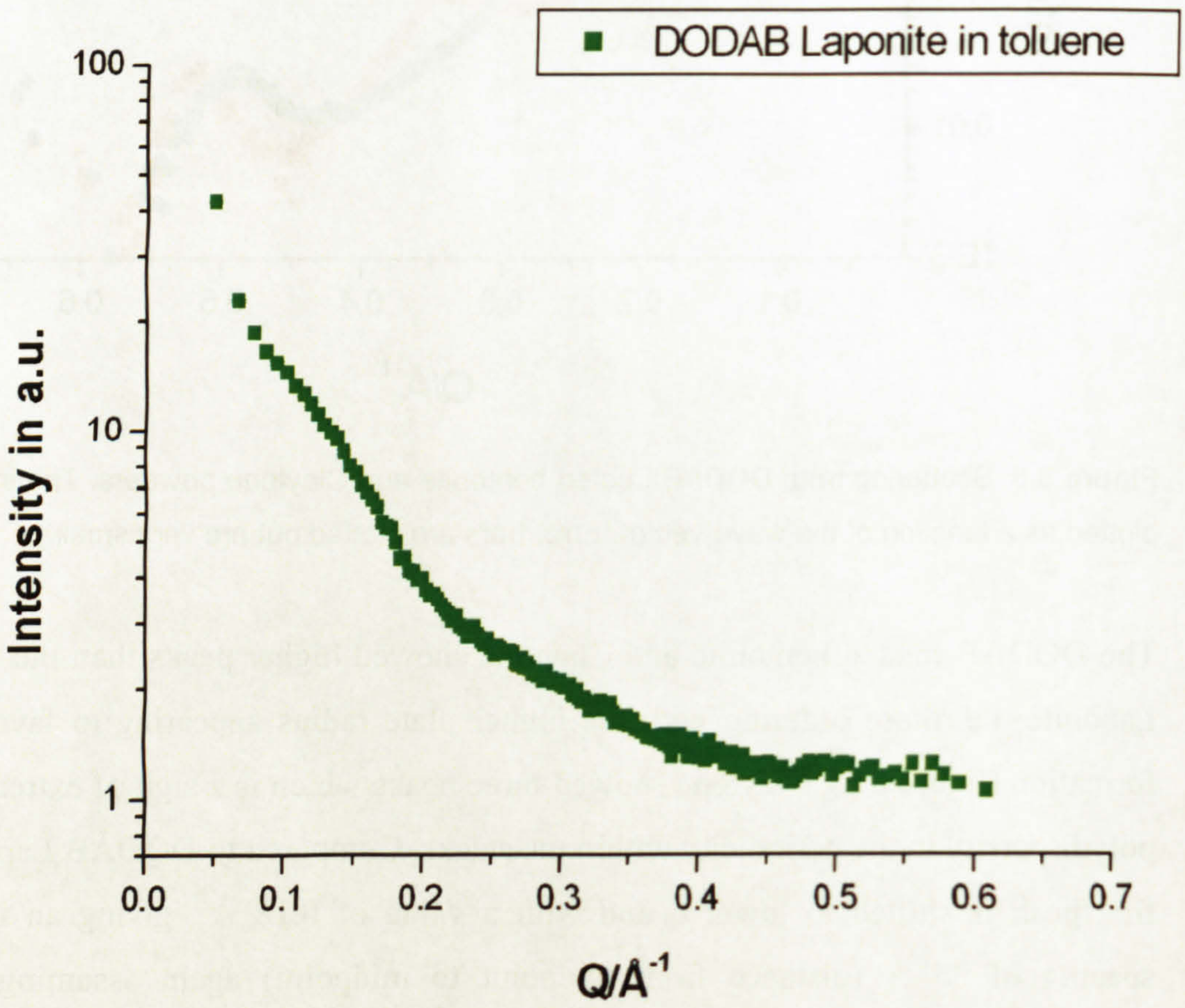

Figure 8.6. Scattering from 3% w/w DODAB treated Laponite dispersed in toluene. The intensity is plotted as a function of the wave-vector. Error bars are plotted but tiny.

The overall shape of the scattering curves was that expected for free tumbling plates but like the powders the orientation of the particles was random with a gradient close to -2. (figure 8.7).

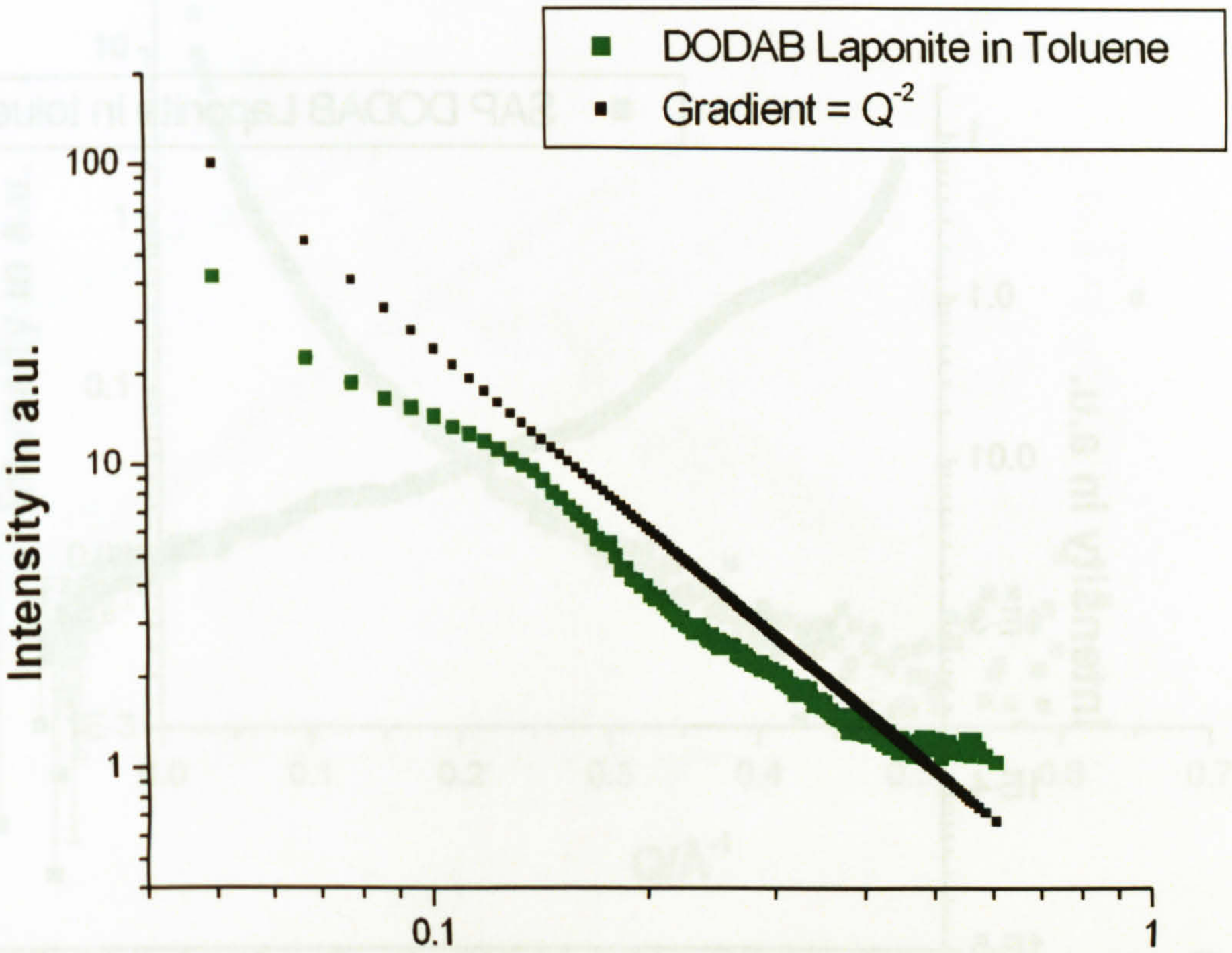

Figure 8.7. Intensity verses wave-vector plot of the scattering from 3% w/w DODAB treated Laponite dispersed in toluene. The overall orientation of the plates was random.

The sample of SAP DODAB Laponite dispersed in toluene settled very rapidly and clearly aggregated. The nature of the aggregates was investigated using SAXS but the sample showed less periodic structure than anticipated. A peak was found at q of 0.12 Å to 0.13 $Å^{-1}$ representing a distance of 48 Å to 52 Å (figure 8.8). This separation was the same as the pure DODAB treated sample but the scattering intensity tailed off more slowly at higher q. This could be indicative of a very wide range of separations between plates. It was found from simple observations that the SAP DODAB Laponite sample in toluene formed huge flocs that phase separated after approximately 5 minutes. The peak at q = 0.13 $Å^{-1}$ (distance of 48 Å) showed the plates were still separated by a layer of solvent but did not give information regarding the nature of the aggregates.

During the course of the SAXS experiment the SAP DODAB Laponite aggregates settled to the bottom of the Lindemann tube below the X-ray beam. This process took more than 1 hour to complete and did not affect the shape of the scattering curve.

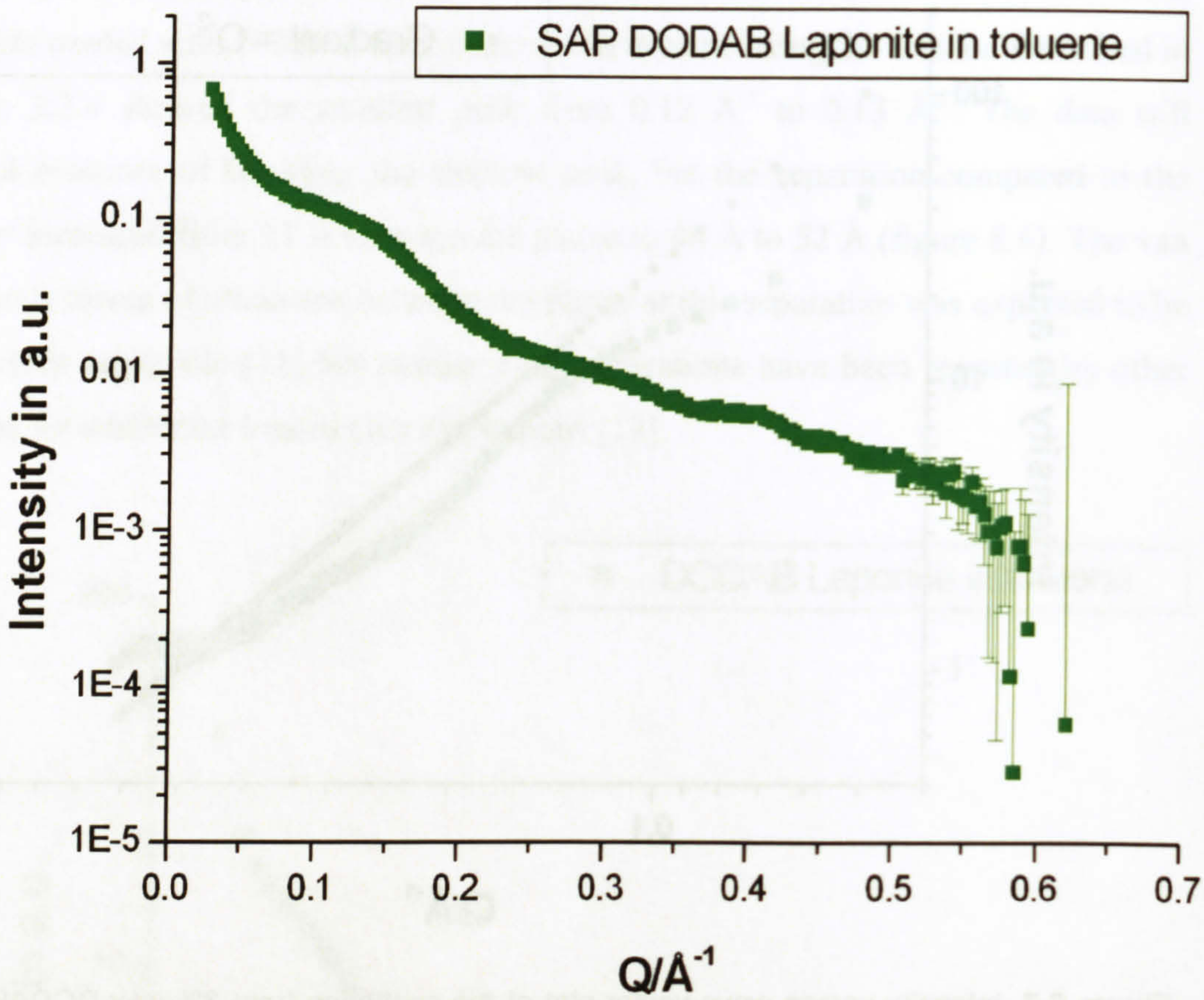

Figure 8.8. Scattering from 5% w/w SAP DODAB treated Laponite dispersed in toluene. The intensity is plotted as a function of the wave-vector.

The original sample made was Laponite treated with SAP alone suspended in toluene. This sample did not settle or aggregate over a number of months. Similarly, a dispersion of SAP Laponite in polydecene was expected to behave as free tumbling discs. The scattering pattern showed no peaks at any q value (figure 8.9) indicating the particles were well dispersed.

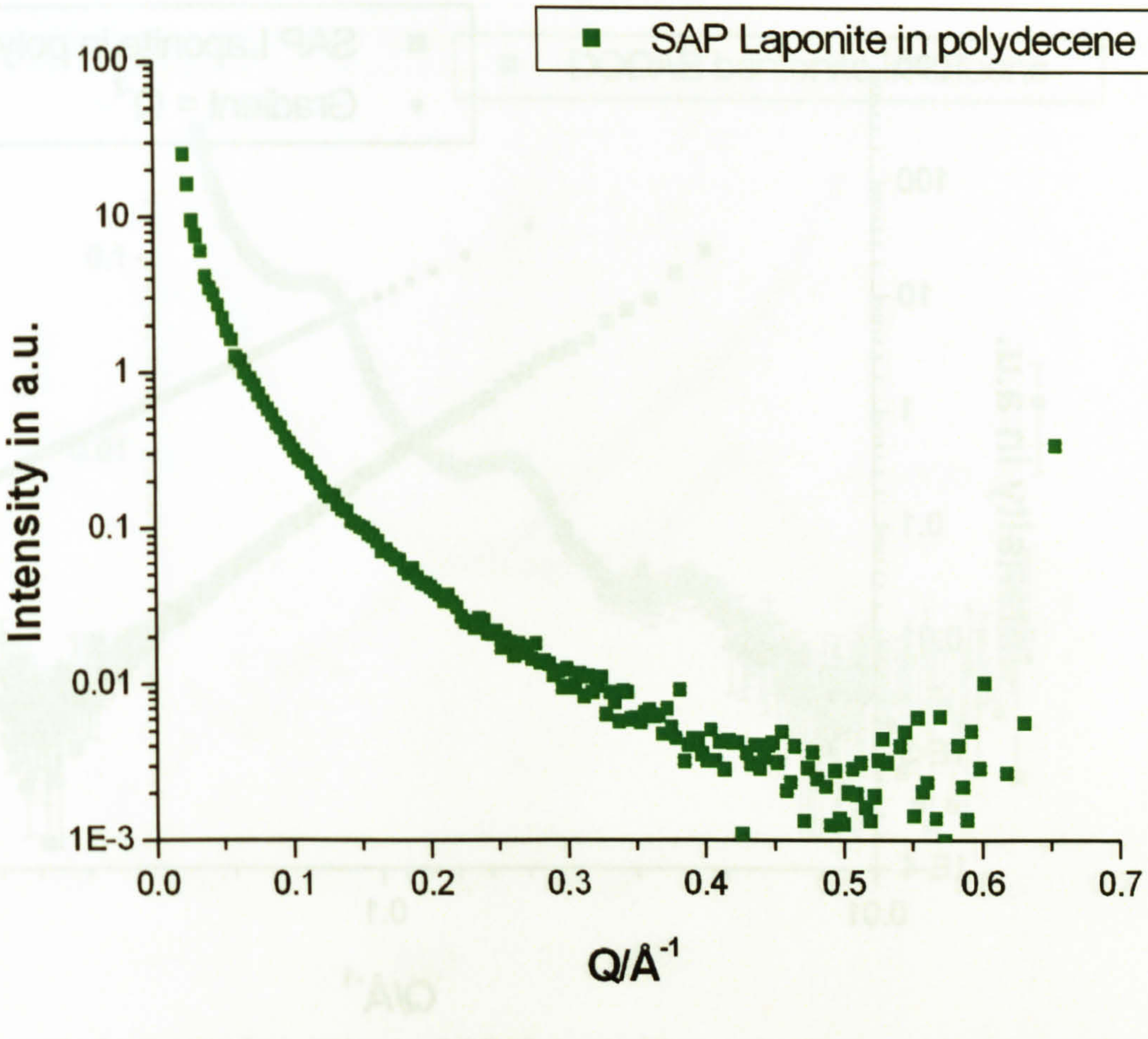

Figure 8.9. Scattering from 6% w/w SAP treated Laponite dispersed in polydecene. The intensity is plotted as a function of the wave-vector. No peaks were visible. Error bars are tiny.

The log-log plot for the scattering intensity of SAP treated Laponite in polydecene showed roughly an overall q^{-2} dependence (figure 8.10).

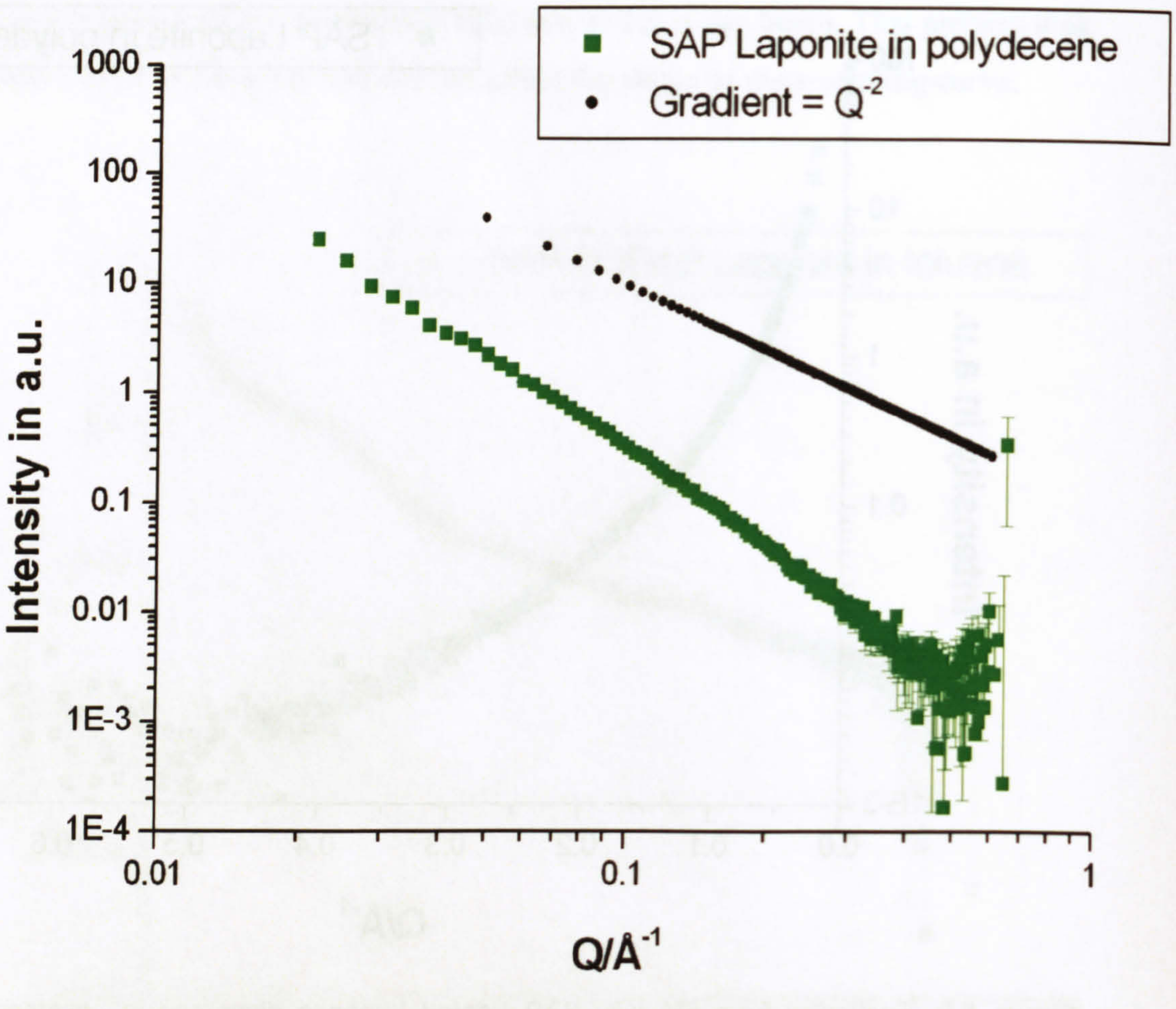

Figure 8.10. Intensity verses wave-vector plot of the scattering from 6% w/w SAP treated Laponite dispersed in polydecene. The overall orientation of the plates was random.

The plate separation of DODAB treated bentonite suspended in toluene was similar to DODAB treated Laponite suspended in toluene, but three prominent peaks can be seen (figure 8.11). Their positions were at $q = 0.13$ Å^{-1}, $q = 0.26$ Å^{-1} and $q = 0.39$ Å^{-1}. The distance between the plates is therefore 38 Å as the peaks at higher q are harmonics. A number of plates organise in stacks since the three peaks were very well defined. The sharpness of the peaks and their number also indicate that the distance between the plates and the plate thickness is of low polydispersity. This behaviour seems to match the powder samples of DODAB bentonite (figure 8.5) and indicates the difficulty in breaking down aggregates of DODAB bentonite when dispersing in toluene. However the spacing increases so solvent does penetrate between the layers.

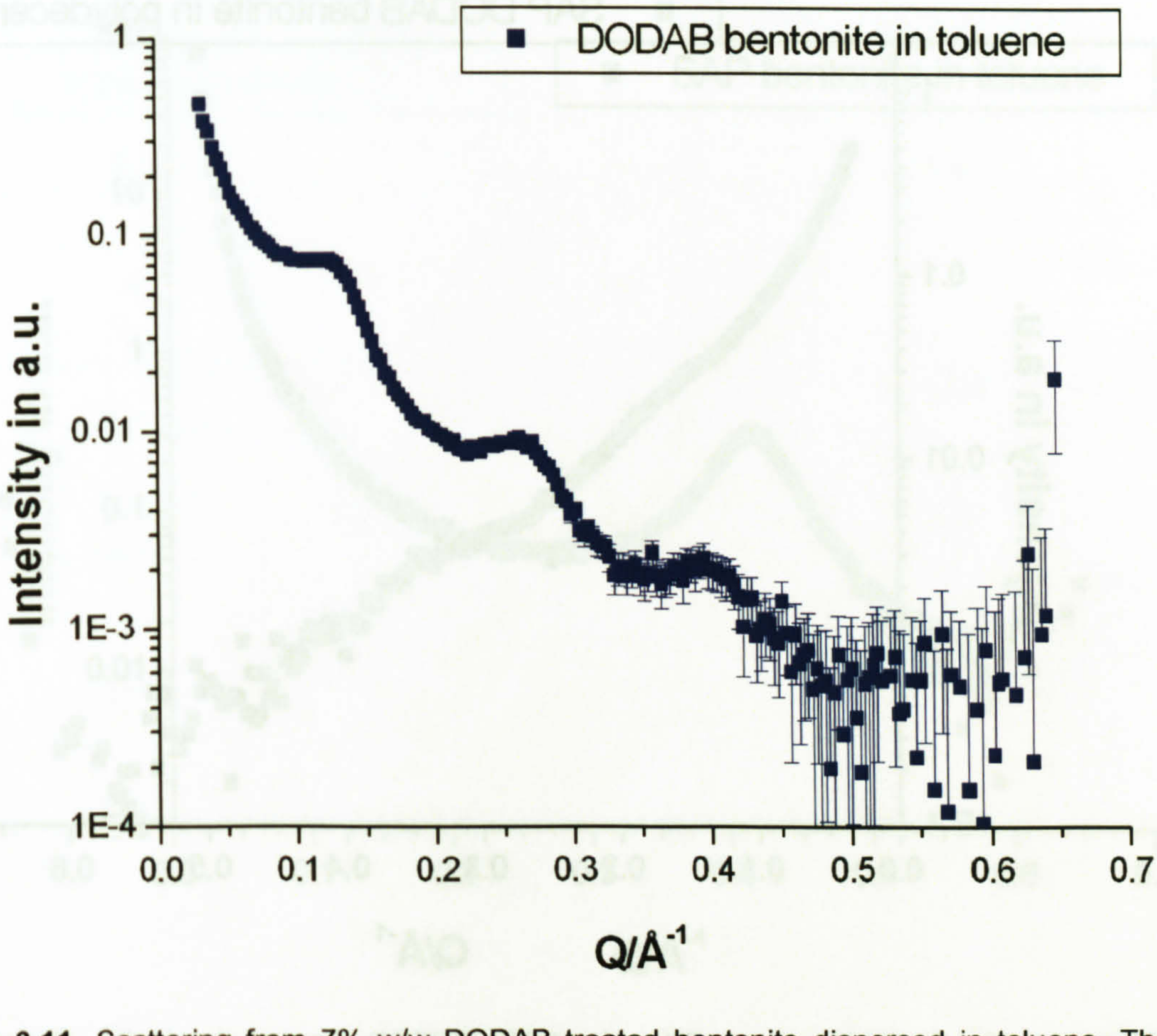

Figure 8.11. Scattering from 7% w/w DODAB treated bentonite dispersed in toluene. The intensity is plotted as a function of the wave-vector.

The dispersion of SAP DODAB treated bentonite in polydecene showed a small shoulder at q = 0.17 $Å^{-1}$ equivalent to an inter platelet separation of 38 Å (figure 8.12). The small peak was well-defined and shallow indicating the clay behaved mostly as a free tumbling particle and only a few plate aggregates were present.

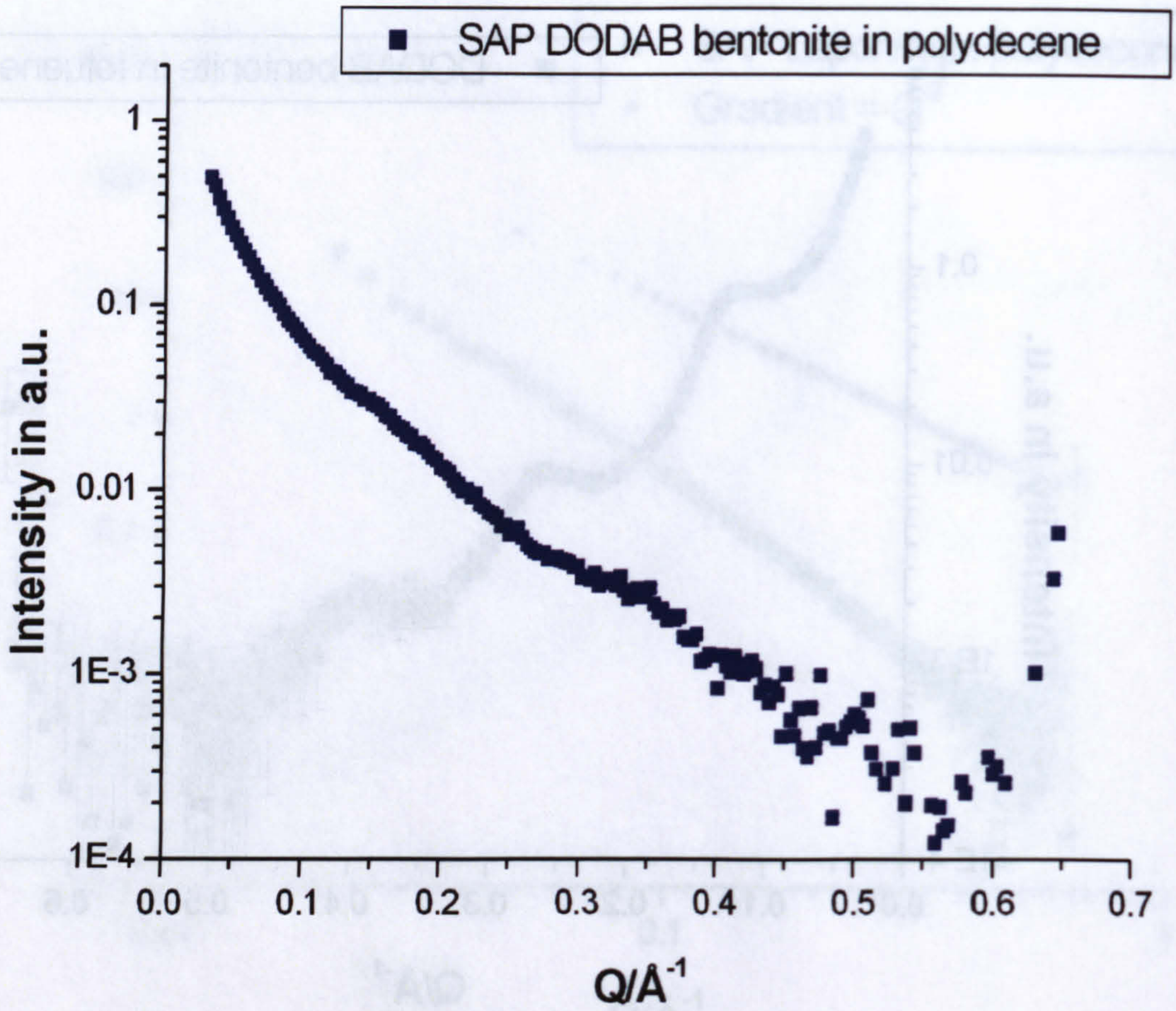

Figure 8.12. Scattering from 7% w/w SAP DODAB treated bentonite dispersed in polydecene. The intensity is plotted as a function of the wave-vector and only a small peak is visible.

SAP bentonite particles dispersed in toluene showed a huge but broad peak at $q = 0.42$ $Å^{-1}$ corresponding to an interlayer spacing of 15 Å (figure 8.13). This is a very small distance and is strong evidence that the particles aggregated face-to-face during the grafting procedure despite the low concentration during preparation (section 3.2.1). The fact the peak was broad showed that a distribution of particle layer spacing was evident. The plate-to-plate distance of 5 Å was too small for polymer chains to occupy so the aggregation almost certainly occurred as the solvent was transferred from water to propan-1-ol. However once the polymer was adsorbed to the exposed surface of the bentonite the aggregates were well stabilised but too large to remain suspended.

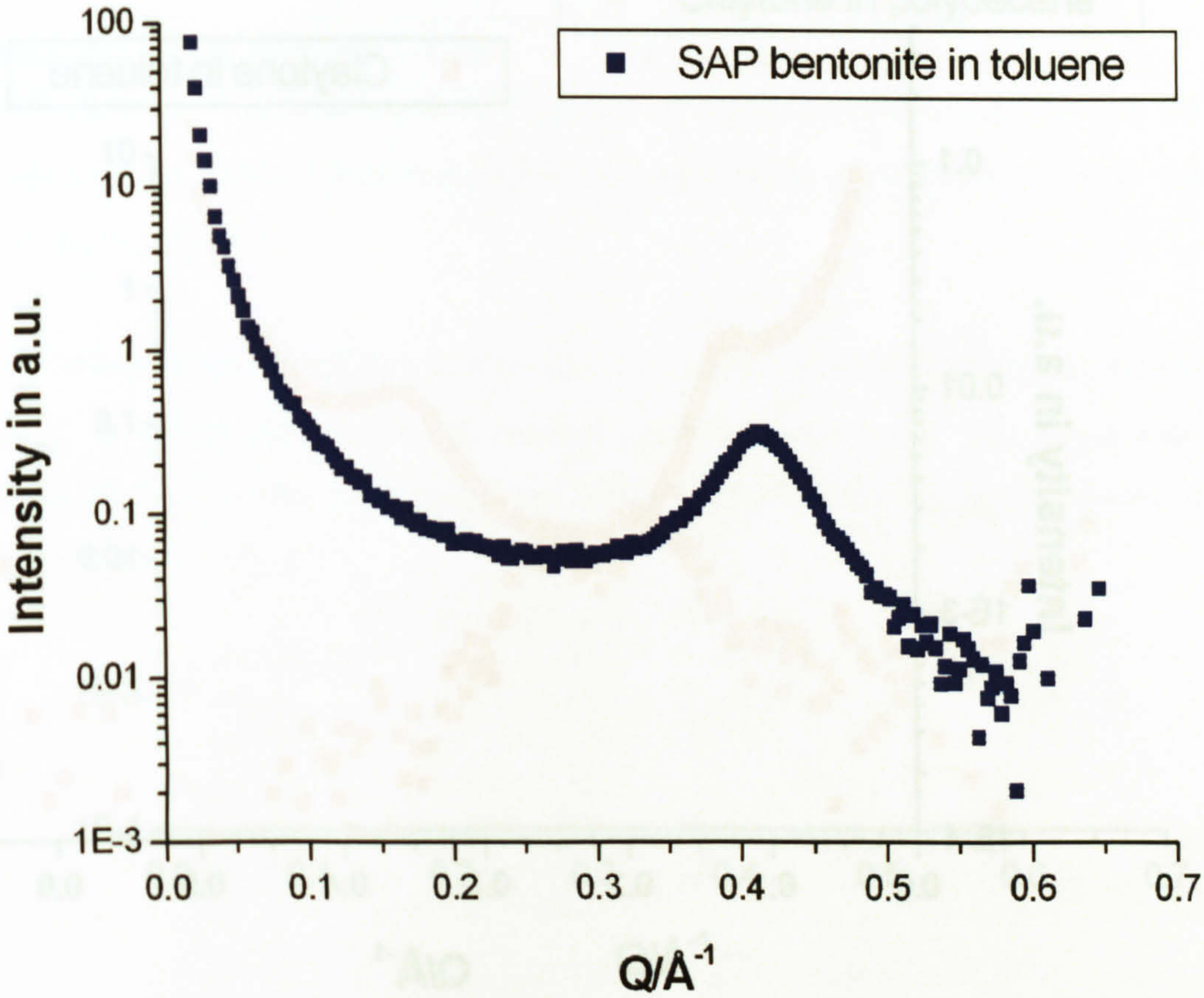

Figure 8.13. Scattering pattern from SAP treated bentonite dispersed in toluene at 10% w/w. The intensity is plotted as a function of the wave-vector.

A suspension of Claytone in toluene (figure 8.14) showed very similar peaks as DODAB bentonite suspended in toluene (figure 8.11). A third peak was no longer visible, but the first two peaks appeared at a value of $q = 0.13$ Å^{-1} and $q = 0.26$ Å^{-1}. It showed that toluene as a solvent for 2HT and DODAB gave a inter platelet spacing of 38 Å.

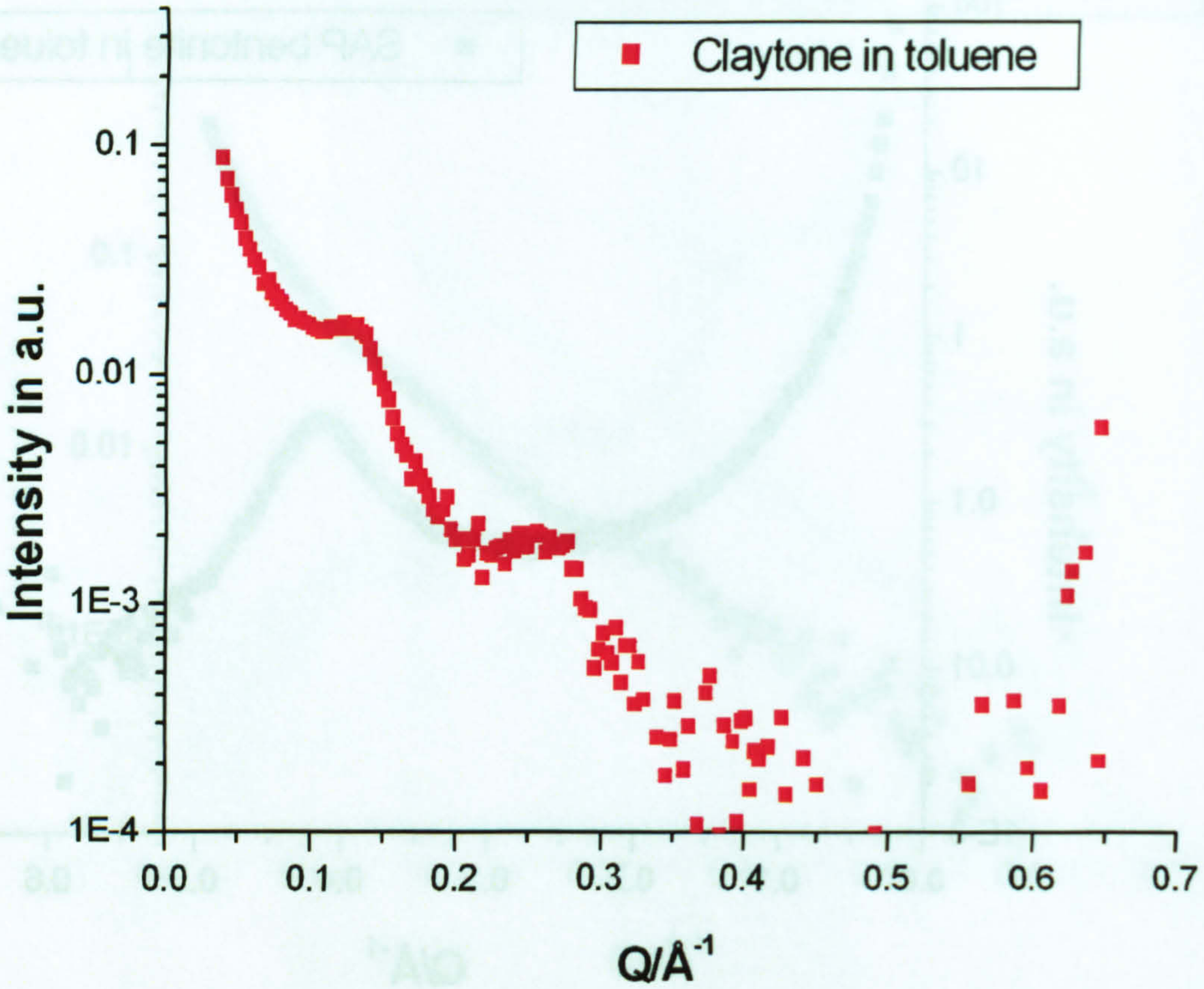

Figure 8.14. Scattering from 4% w/w Claytone dispersed in toluene. The log of intensity is plotted as a function of the wave-vector with a peak visible at q = 0.13 $Å^{-1}$ and a much smaller one at q = 0.26 $Å^{-1}$

It seemed that polydecene was not as successful at extending the alkyl chains of the 2HT and DODAB molecules. The Claytone in polydecene peak is at Q =0.17 $Å^{-1}$ and Q = 0.34 $Å^{-1}$ which meant the plates were separated by 27 Å only, i.e. 10 Å less than in the case of toluene (figure 8.15).

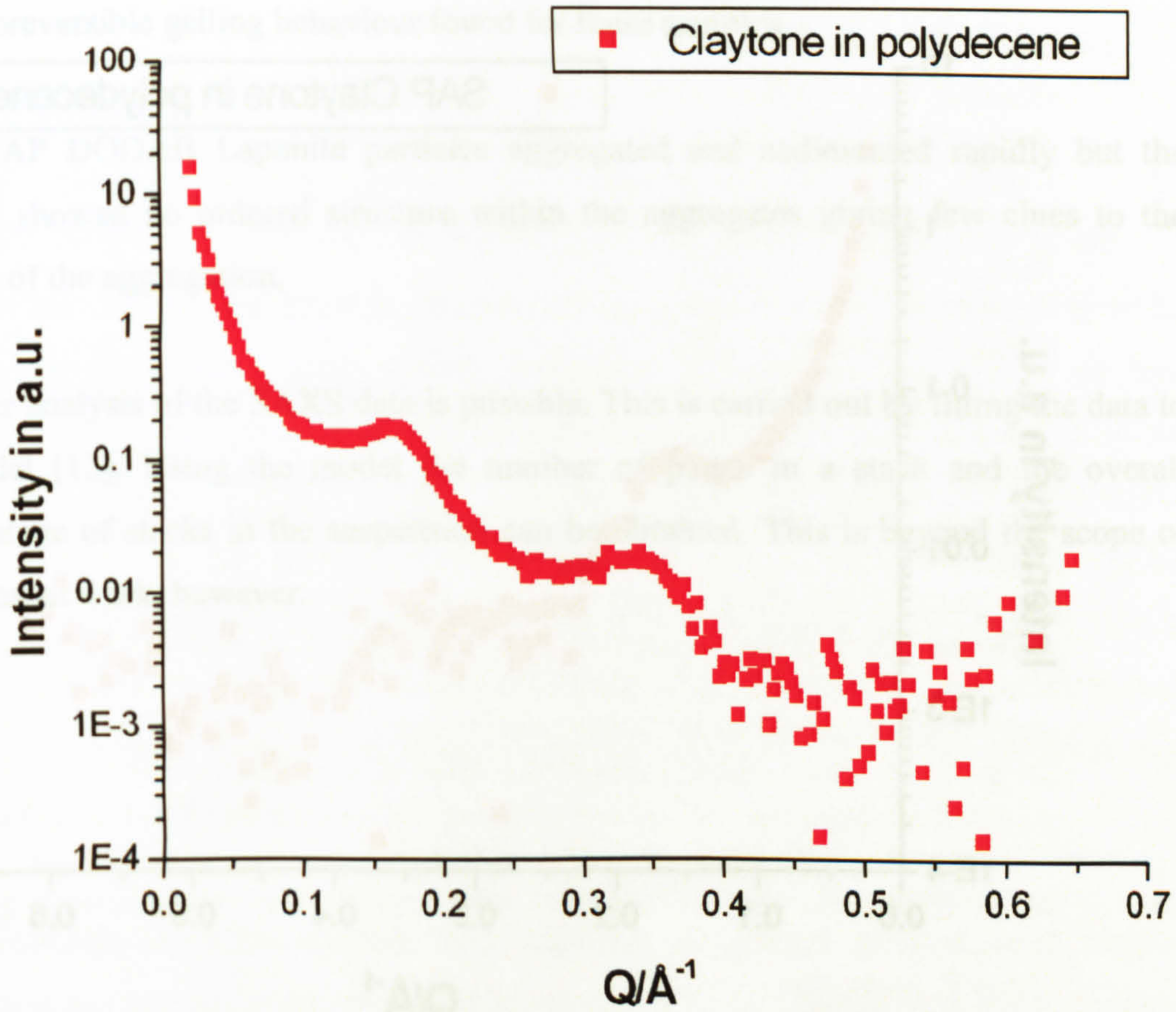

Figure 8.15. Scattering from 7% w/w Claytone dispersed in polydecene. The intensity is plotted as a function of the wave-vector.

Addition of the SAP molecule to the surface of Claytone seemed to break up the stack of the particles in polydecene (figure 8.16) but did not shift the peak position of the remaining first peak. The main repeated distance remained at 37 Å but the spacing between the clay plates varied in polydecene much more when the additional stabiliser was present.

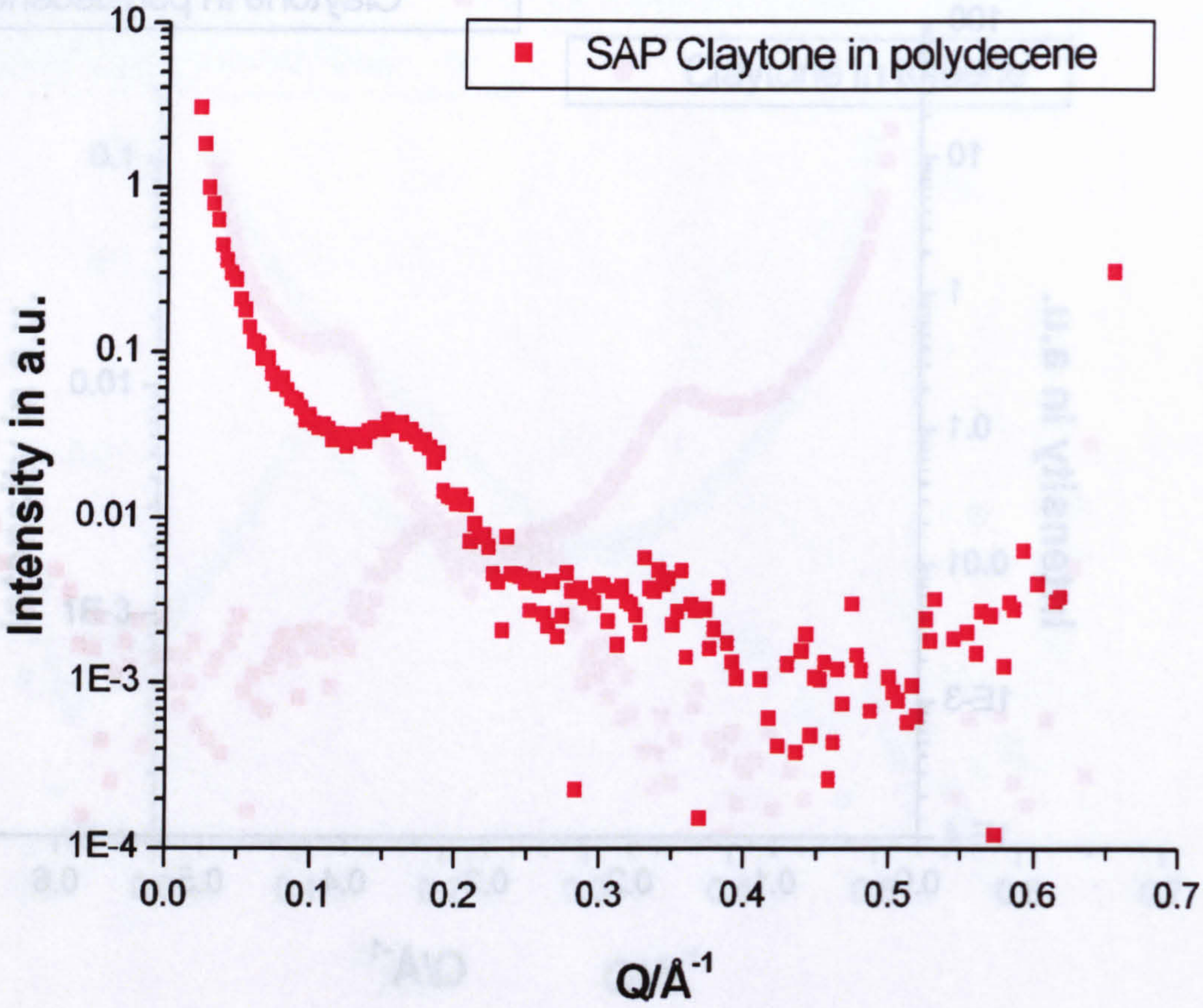

Figure 8.16. Scattering from 5% w/w SAP Claytone dispersed in polydecene. The log of intensity is plotted as a function of the wave-vector.

8.4 Conclusions

SAP treated Laponite dispersed in polydecene was a well-stabilised colloidal dispersion showing no periodic structure. The surfactant treated samples showed plates were held as highly ordered stacks and the ordering was not completely removed when the particles were dispersed. Combination of the stabilisers DODAB and SAP with the solvent polydecene gave good results with only a small peak due to particle stacks. Interestingly, there was greater evidence for particle stacks for the samples dispersed in toluene. The plate separation was reduced for SAP Claytone dispersed in polydecene indicating the surfactant chains did not extend very well in to the polydecene solvent. The behaviour of the surfactant chains was believed to be the cause of the thermoreversible gelation found for the SAP Claytone and SAP DODAB

bentonite. The SAXS data confirms this assumption and is directly related to the thermoreversible gelling behaviour found for these samples.

The SAP DODAB Laponite particles aggregated and sedimented rapidly but the SAXS showed no ordered structure within the aggregates giving few clues to the nature of the aggregation.

Further analysis of the SAXS data is possible. This is carried out by fitting the data to a model [13]. Using the model the number of plates in a stack and the overall percentage of stacks in the suspension can be obtained. This is beyond the scope of the present work, however.

8.5 References

1. Guinier, A., *X-Ray Diffraction In Crystals, Imperfect Crystals, and Amorphous Bodies*. 1994, New York: Dover Publcations, Inc.
2. Larson, R.G., ed. *The structure and rheology of complex fluids*. Topics in Chemical Engineering, ed. K.E. Gubbins. 1999, Oxford University Press: New York.
3. Norrish, K., *The Swelling of Montmorillonite.* Discussions of the Faraday Society, 1954. **18**: p. 120.
4. Jones, T.R., *The Properties and Uses of Clays Which Swell in Organic Solvents.* Clay Minerals, 1983. **18**(4): p. 399-410.
5. Nelson, A.J.R., *Neutron and Light Scattering Studies of Polymer Adsorbed on Laponite. PhD Thesis.* School of Chemistry, University of Bristol, Bristol, UK, 2002.
6. Ho, D.L., R.M. Briber, and C.J. Glinka, *Characterization of organically modified clays using scattering and microscopy techniques.* Chemistry of Materials, 2001. **13**(5): p. 1923-1931.
7. http://www.Laponite.com. 2002, Laporte Inc.
8. Grillo, I., P. Levitz, and T. Zemb, *Insertion of small anisotropic clay particles in swollen lamellar or sponge phases of nonionic surfactant.* European Physical Journal E, 2001. **5**(3): p. 377-386.
9. van Olphen, H., *An Introduction to Clay Colloid Chemistry: For Clay Technologists, Geologists, and Soil Scientists*. 2nd Edition ed. 1977: John Wiley & Sons, Inc.
10. Lagaly, G., *Characterization of Clays by Organic-Compounds.* Clay Minerals, 1981. **16**(1): p. 1-21.
11. Tabor, D. and R. Winterton, *The direct measurement of normal and Retarded van der Waals Forces.* Proceedings of the royal Society A, 1969. **312**: p. 435-450.
12. Hanley, H.J.M., C.D. Muzny, and B.D. Butler, *Surfactant adsorption on a clay mineral: Application of radiation scattering.* Langmuir, 1997. **13**(20): p. 5276-5282.
13. Pizzey, C., S. Klein, E.S.H. Leach, J.S. van Duijneveldt, R.M. Richardson, *Suspension of Colloidal Plates in a nematic Liquid Crystal: A Small Angle X-ray Scattering Study.* Journal of Physics: Condensed Matter, 2003. Submitted.

9 Conclusions and Further Work

9.1 Conclusions

The aim of this project was to make novel particles stable in an organic solvent at high temperature but unstable at low temperature. Laponite and bentonite clay were selected as they show good gelling behaviour in aqueous suspensions at low concentration due to particle anisotropy. It was expected for well dispersed stable particles a thermoreversible gelling transition could be induced with the right combination of solvent, surface treatment, and clay. Gels in organic solvents can be produced using cationic surfactant adsorbed bentonite and a commercial product, Claytone. Claytone made from montmorillonite clay is available as a rheological modifier in organic solvents but with a large concentration of polydisperse surfactant adsorbed to the surface.

Laponite and bentonite treated with DODAB surfactant showed very similar behaviour to Claytone when dispersed forming gels at all temperatures. By increasing the polarity of the solvent the samples went, as expected, from gelling to forming large flocs but crucially no region of stability was found. A stable dispersion was needed in the first place that subsequently could be destabilised.

Colloidally stable dispersions of clay have been produced by treatment with a short chain poly (isobutylene) polymer acting as a steric stabiliser. Treatment in this way for the bentonite produced a sample that sedimented under gravity but colloidal stability was achieved for the polymer treatment of the Laponite plates. The difference between the treated clays was size of the particles and the amount of polymer adsorbed with the bentonite being bigger but with a lower density of polymer. However the bentonite sediment displayed vivid flow birefringence when stirred and settled as a nematic phase. For the polymer treated Laponite a reversible temperature dependent gelling transition was induced by careful marginalisation of the solvent. The gels were not space filling even when concentrated and the samples were difficult to make in any quantity. Also, partial evaporation of the mixed solvent made a systematic rheological investigation impossible.

A surfactant and polymer treated Laponite sample was not stable under any conditions and sedimented rapidly, however the same treatment applied to bentonite and Claytone produced stable dispersions that showed flow birefringence at low concentration and flow induced permanent birefringence at higher concentrations. Temperature controlled destabilisation was achieved by transferring to a medium weight, low volatility organic solvent, polydecene, used for commercial cosmetic applications. The relatively low concentration particles were stable at room temperature characterised by their low viscosity and lack of phase separation but formed a space filling gel on cooling that could be returned to a more fluid state by re-warming. Due to the low volatility of the solvent the samples were ideally suited for low temperature rheological studies and their properties were also investigated using differential scanning calorimetry to find the temperature of the transition, and small angle X-ray scattering to find evidence of particle aggregation.

9.2 Future Work

The temperature dependent gelling transition occurred at a low temperature and may be raised by making the particles more stable. From our observations it appears this could be achieved by adsorbing a longer chain surfactant or polymer to the surface of the clay; or by reducing the molecular weight of the solvent thus making the stable dispersion entropically more favourable. Choosing slightly different clay particles that adsorbed more surfactant or polymer may give a higher gelation temperature, however the interaction is complex and better stabilisation is not guaranteed.

Alternatively, optimising the gelling transition for the polymer and surfactant treated bentonite samples could be achieved by examining the factors that govern the gelling transition. It is known the samples are not fully dispersed and in other types of dispersion this leads to slow sedimentation and though not observed for these samples undoubtedly there is an effect.

The crystallisation of the surfactant alkyl chains on the surface of the plates could be investigated using low temperature SAXS experiments to find the variation of the

interparticle separation and interparticle association. Also investigations into the crystallisation of the surfactant alkyl chains could be undertaken using cycled temperature scans with DSC showing the freezing transition as well as the melting transition for these chains.

Appendix I

Calculation of the Cationic Exchange Capacity and Area per Surfactant Molecule from the Elemental Analysis results.

The elemental analysis results were given in percentage mass of the sample. The errors in the values were ±0.3% w/w but each sample was tested at least twice to reduce the errors. The clay samples were assumed to contain no nitrogen, carbon, or hydrogen in their elemental make up. In actual fact about 0.5% of the mass of the clay in the sample was hydrogen from the interlayer hydroxyl groups. The elemental analysis results for untreated Laponite particles is given below (table A1).

Sample	% Nitrogen	% Carbon	% Hydrogen
Untreated Laponite	0.00	0.08	1.50

Table A1.1. Elemental analysis results for untreated vacuum oven dried Laponite. Only nitrogen was completely absent from the samples.

The untreated Laponite sample showed no nitrogen adsorption to the surface, a trace of carbon and a small amount of hydrogen (mostly from adsorbed water). After adding Laponite and the short-chain cationic surfactant together the washed and dried sample was submitted again for elemental analysis (table A2).

Sample	% Nitrogen	% Carbon	% Hydrogen
Laponite average	0.73	11.28	2.84
Elemental mass ratio	1.00	15.45	3.89

Table A1.2. The amount of tetrabutyl ammonium adsorbed to the surface of the Laponite

The nitrogen, carbon, and hydrogen were all assumed to come from the adsorbed surfactant or contaminants making up 14.85% of the mass of the sample. The Laponite plates were assumed to make up the rest of the mass (85.15%). As a check for contaminants adsorbed to the surface of the Laponite the elemental mass ratio was compared to the pure surfactant (table A3). The elemental mass ratio was obtained by dividing all the percentage mass values by the value for nitrogen and was not dependent on the actual mass of the element present in the sample.

Sample	% Nitrogen	% Carbon	% Hydrogen
Stochiometric mass value for tetrabutyl ammonium hydroxide.	5.79	79.34	14.88
Elemental mass ratio	1.00	13.70	2.57

Table A1.3. The expected elemental analysis for tetrabutyl ammonium ion. Expected results and elemental mass ratio.

From the elemental mass ratios of the stoichiometric formula of the surfactant compared to the actual surfactant adsorbed to the Laponite it was clear excess carbon and hydrogen were present. The origin of the hydrogen was assumed to be from adsorbed water and the carbon was assumed to be from longer chain surfactant molecules. For this reason the nitrogen values alone were taken for the CEC calculation.

In order to transform these values to molar amounts it was assumed there was 100 g of sample and therefore the value for the percentage mass was equivalent to the mass of the element in grams. The number of moles of surfactant was assumed to be the same as the number of moles of nitrogen adsorbed as all surfactant molecules possessed only 1 nitrogen atom. From the Laponite average (table A2) 0.73 g of nitrogen was spread over 85.15 g of Laponite. The number of moles of nitrogen was 0.73/14 = 0.052 moles. The CEC is given in meq/100g of clay where meq is equal to millimoles. The amount of surfactant adsorbed to 100 g of clay is therefore

$$0.052 \times \frac{100}{85.15} = 0.061 \text{ moles or } 61 \text{ meq/100 g of clay.}$$

This simple calculation can be taken a stage further and the number of surfactant molecules per meter^2 can be found. The area of the clay plates was taken from crystallographic data and for Laponite this was $800 m^2 g^{-1}$. The amount of clay in 100 g of sample was 85.15 g. The total surface area was 68120 m^2. The number of surfactant molecules spread over this surface was $0.052 \times 6.02 \times 10^{23} = 3.14 \times 10^{22}$. The number of molecules per meter^2 was $\frac{3.14 \times 10^{22}}{68120} = 4.61 \times 10^{18}$. The area per molecule was 2.17×10^{-18} m^2 or 2.17 nm^2 per molecule.

Appendix II

SAP adsorption to Laponite and bentonite

The amount of SAP adsorbed to the clay particles was determined from the elemental analysis results. The percentage mass values for nitrogen were taken for the calculations as the polymer was known to be polydisperse and the carbon and hydrogen values were unreliable as a method for determining the number of molecules adsorbed. It was assumed that the adsorbing molecule possessed 4 nitrogen atoms in the head group. A sample of free polymer was submitted for elemental analysis and compared to the expected elemental analysis results from the molecule formula of SAP (figure A2.1).

Sample	% Nitrogen	% Carbon	% Hydrogen
Average Pure SAP mass values	2.25	82.38	15.09
Pure SAP Mass ratio	1.00	36.61	6.71
Stoichiometric mass values	2.41	81.58	13.26
Stoichiometric Mass ratio	1.00	33.85	5.50

Table A2.1. Elemental analysis result for pure SAP polymer and the expected mass values for the stoichiometric formula.

The mass ratio was obtained from dividing all the elemental analysis results by the value for nitrogen for ease of comparison between samples. The elemental analysis for SAP Laponite and SAP bentonite is given below (figure A2.2)

Sample	% Nitrogen	% Carbon	% Hydrogen
Average SAP Laponite	2.90	41.48	7.24
Average SAP Laponite Elemental ratio	1.00	14.30	2.50
Average SAP bentonite	2.45	28.78	5.14
Average SAP bentonite Elemental ratio	1.00	11.75	2.10

Figure A2.2. Elemental analysis results for SAP Laponite and SAP bentonite

The mass ratios of SAP adsorbed to Laponite and bentonite are very different to the ratio found for the pure sample of SAP and the expected values from the stoichiometric formula. This was evidence that low molecular weight polymer molecules adsorbed preferentially.

It was assumed that all the nitrogen, carbon, and hydrogen mass did not come from the clay sample. For a 100 g sample of SAP Laponite 51.62 g was from adsorbed polymer and 48.68 g was from Laponite with an area of 39840 m^2 (800 m^2g^{-1} [1]). The number of moles of SAP adsorbed was calculated as $\frac{2.90}{56} = 0.0518$ moles of N_4 head group. The number of molecules was $0.0518 \times 6.02 \times 10^{23} = 3.12 \times 10^{22}$ and the number per square meter was 3.83×10^{17}. The area per molecule of SAP adsorbed to the Laponite was 1.3×10^{-18} m^2 or 1.3 nm^2 per molecule.

For a 100 g sample of SAP bentonite 63.63 g was due to the clay and 36.37 g of the sample was due to SAP. The surface area of the bentonite in this sample was 47850 m^2 (752 m^2g^{-1} [2]). The number of moles of polymer (from the nitrogen values) was $\frac{2.45}{56} = 0.0438$. The number of polymer molecules was $0.0438 \times 6.02 \times 10^{23} = 2.64 \times 10^{22}$ The number of molecules per square metre was 5.5×10^{17} and the area per molecule was 1.8×10^{-18} m^2 or 1.8 nm^2 per molecule.

References

1. Grillo, I., P. Levitz, and T. Zemb, *Insertion of small anisotropic clay particles in swollen lamellar or sponge phases of nonionic surfactant.* European Physical Journal E, 2001. 5(3): p. 377-386.
2. van Olphen, H. *Determination of Surface Areas of Clays-Evaluation of Methods*. in *The International Symposium on Surface Area Determination.* 1969. IUPAC. Held at the School of Chemistry, University of Bristol, UK: Butterworths.

Appendix III

Adsorption Isotherm Calculations

The measurement made for the adsorption isotherms was a measurement by depletion from the absorbance of light from the unadsorbed SAP polymer at left in the supernatant at a wavelength of 284 nm.

The ratio of the transmitted intensity, I, to the incident intensity, I_0, at a given frequency is called the transmittance, T, of the sample at that frequency:

$$T = \frac{I}{I_0} \qquad \text{A3.1}$$

It is found empirically that the transmitted intensity varies with the length, l, of the sample and the molar concentration, $[J]$, of the absorbing species J in accordance with the Beer-Lambert Law:

$$I = I_0 10^{-\varepsilon[J]l} \qquad \text{A3.2}$$

The quantity ϵ is called the molar absorption coefficient and depends on the frequency of the incident radiation and is greatest where the absorption is most intense. Its dimensions are 1/(concentration x length), and it is normally convenient to express it in litres per mole per centimetre, (L mol^{-1} cm^{-1}). Alternative units are square centimetres per mole (cm^2mol^{-1}). This change of units demonstrates that ϵ may be regarded as a molar cross-section for absorption and the greater the cross-sectional area of the molecule for absorption, the greater its ability to absorb incident radiation [1].

The form of equation 2 suggests that it is sensible to introduce the absorbance, A, of the sample at a given wavelength as

$$A = \log\frac{I_0}{I} \qquad \text{or} \qquad A = -\log T \qquad \text{A3.3}$$

Then the Beer-Lambert Law becomes

$$A = \varepsilon[J]l \qquad \text{A3.4}$$

The product $\varepsilon[J]^{l}$ was known formerly as the optical density of the sample and for a set path length and chemical the absorbance increases linearly with molar concentration [J] [1].

The sample of SAP was found to have an absorbance peak at a wavelength of 284 nm. (figure 2.5) and a calibration plot of the concentration of the SAP versus the absorbance was made (figure A3.1)

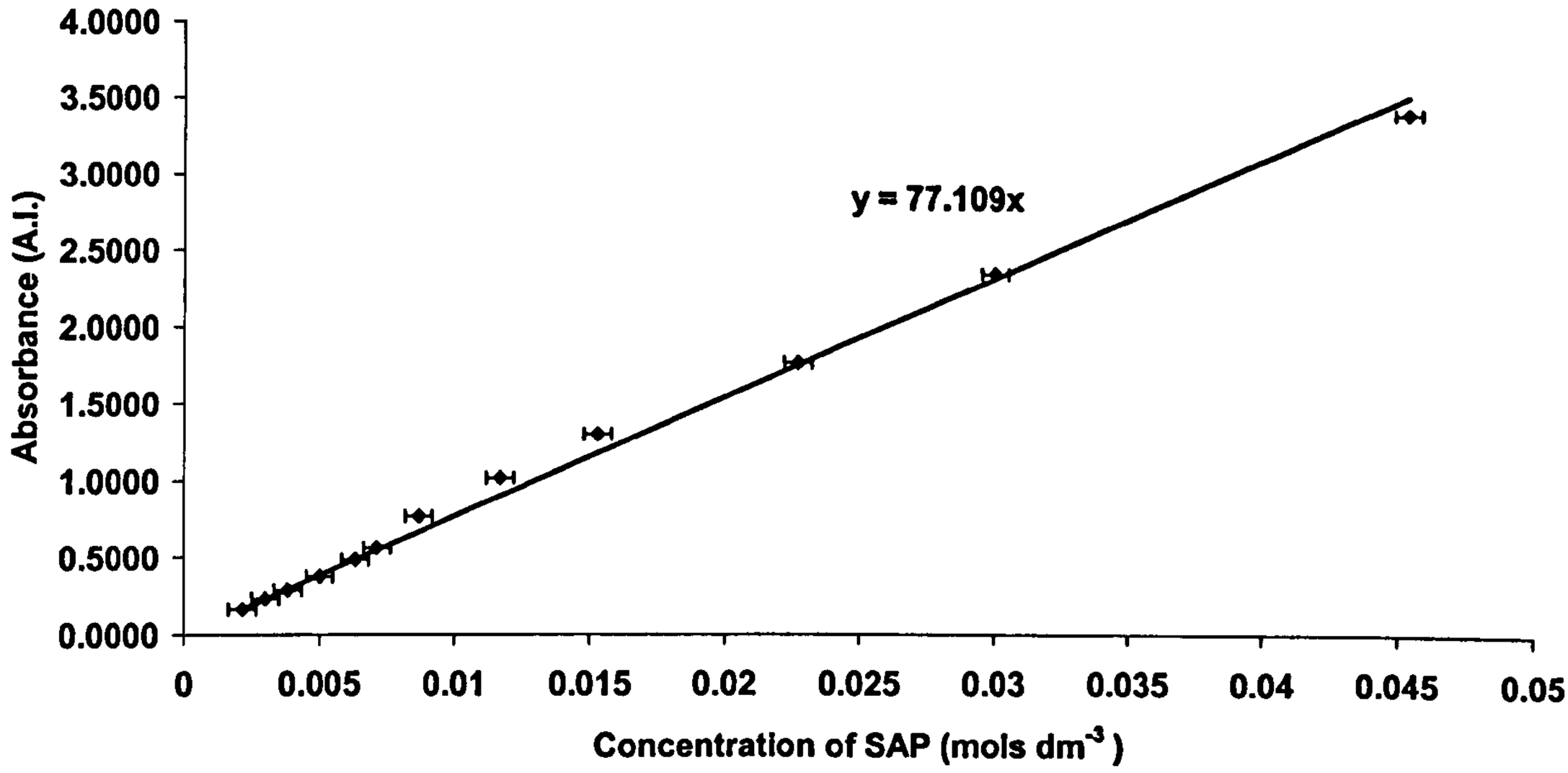

Figure A3.1. Concentration of SAP dispersed in toluene versus absorbance measured at a wavelength of 284 nm.

The graph demonstrates how absorbance depends linearly on the concentration of the absorbing species. During the absorption isotherm work the concentration of the unadsorbed SAP polymer was found by measuring the absorption of SAP in the supernatant.

The procedure for the preparation of the samples for the adsorption isotherm can be found in section 3.4.7

The precise amount of clay in each sample was noted and the total surface area was calculated from published crystallographic data [2]. The mass of SAP added to the samples was noted as was the mass of toluene. The density of SAP was taken as 0.9

gcm^3 and toluene as 0.867 gcm^3 [3]. The total volume of the sample was then calculated and the concentration of the SAP in the solution was obtained.

The supernatant of the centrifuged samples was collected and the UV-Vis analysis was carried out using a quartz glass 1.0 cm path length sample cell. The absorption measurements were repeated to reduce errors and the results were collected and analysed.

The concentration of the SAP in the supernatant was calculated from the gradient of the calibration graph using the equation of a straight line. The number of moles of SAP was then obtained from knowing the total volume of the solution. This value was compared to the number of moles of SAP added at the beginning of the experiment to give the number of moles of SAP adsorbed. From knowing the surface area of the clay the number of moles of SAP per m^2 was found and from the molecular mass of the SAP the mass per m^2 was reached.

The actual mass of the SAP adsorbed to the clay was an over-estimate as it was assumed that lower molecular weight SAP molecules preferentially adsorbed. However the absorption peak in the UV was due to the succinimide group on the molecule so the molar amount of SAP adsorbed was correct.

An example of data handling.

Mass of Claytone	= 0.5020 g
Surface area of sample	= 377.5 m^2
Mass of toluene	= 19.9305 g
Volume of toluene	= 0.02299 dm^3
Mass of SAP added	= 0.0699 g
Volume of added SAP	= 7.769x10^{-5} dm^3
Total volume of sample	= 0.02307 dm^3
Measured absorption	= 0.0153
Conc. of SAP in supernatant	= 0.00019842 mols dm^{-3}
No. of moles of SAP in supernatant	= 4.5777x10^{-6}
Mass of SAP in supernatant	= 0.0105 g
Mass of SAP adsorbed	= 0.0594 g

No. of moles of SAP adsorbed $= 2.587 \times 10^{-5}$ mols

Adsorbed amount in moles m^{-2} $= 6.854 \times 10^{-8}$ mols m^{-2}

Adsorbed amount in mg m^{-2} $= 0.157$ mg m^2.

References

1. Atkins, P.W. and J. de Paula, *Atkins' Physical Chemistry*. Seventh Edition ed. 2002, Oxford: Oxford University Press.
2. van Olphen, H. *Determination of Surface Areas of Clays-Evaluation of Methods*. in *The International Symposium on Surface Area Determination*. 1969. IUPAC. Held at the School of Chemistry, University of Bristol, UK: Butterworths.
3. Lide, D.R., ed. *CRC Handbook of Chemistry and Physics*. 75th ed. 1994, Chemical Rubber Company: Florida, USA.

Appendix IV

Mysterious particle aggregation

During the course of the study a number of different cationic surfactant and solvent types were attempted in the search for particle stability. A strong candidate was cetyl trimethyl ammonium bromide $C_{16}H_{33}(CH_3)_3N^+Br^-$ (CTAB) adsorbed to Laponite and dispersed in benzyl alcohol (made and dispersed in the same manner as the DODAB clay samples in toluene). The dispersions formed gels and were transparent but the system was never adopted as the benzyl alcohol was very hygroscopic and the particles always settled slightly when the samples were left to stand for any length of time despite prolonged sonication. Out of all the samples produced two high concentration samples formed aggregates that were initially thought to be desorbed surfactant. The aggregates were highly birefringent thin plates, the biggest being 4 mm by 5 mm and remarkably robust withstanding heat treatment and sonication, unlike surfactant aggregates that quickly redispersed after heating. One of the aggregates was removed using tweezers and washed in acetone and ethanol to remove all gel coating the plate and studied under the polarising microscope (figure A4.1).

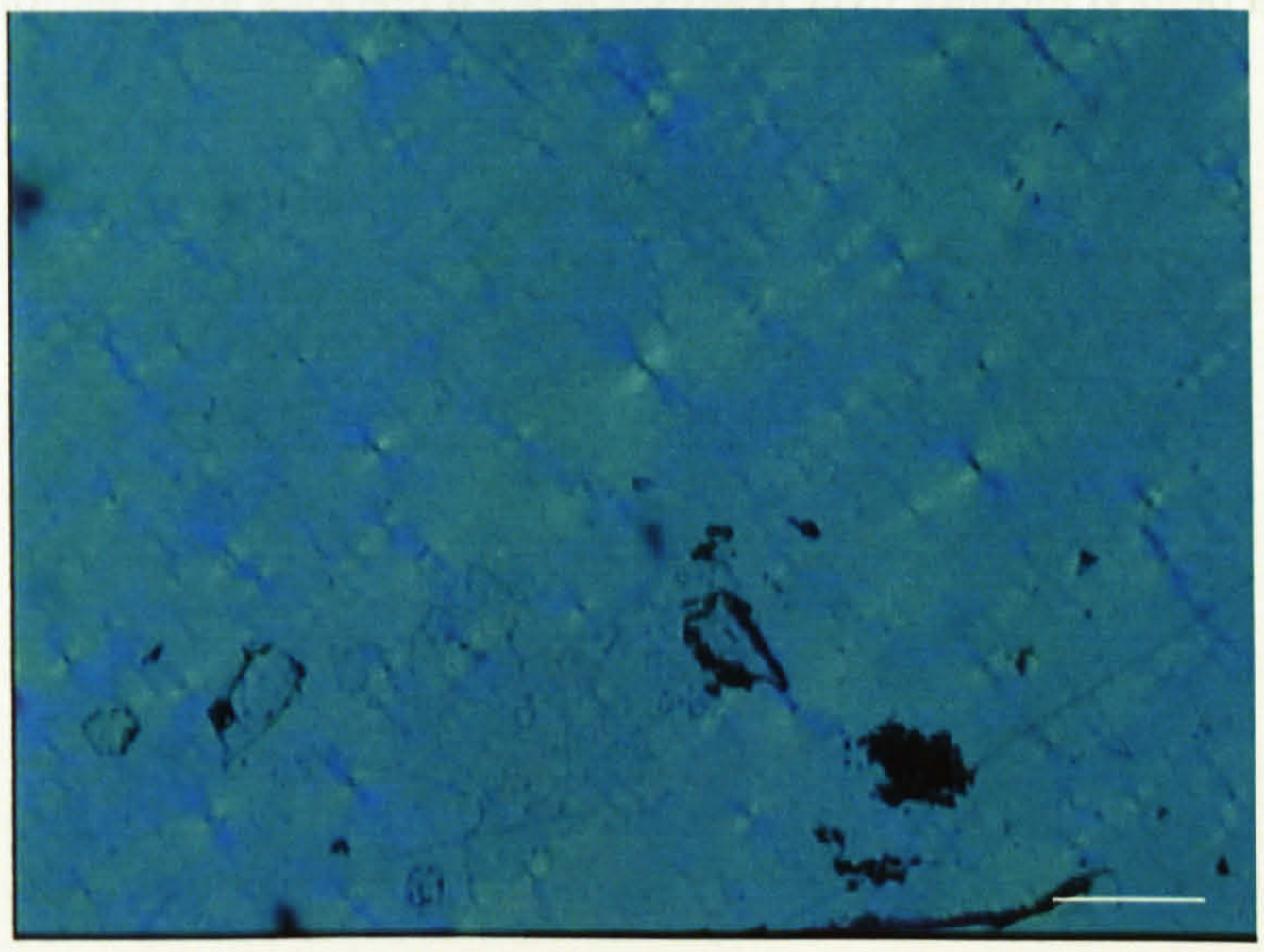

Figure A4.1 Polarising microscope image of CTAB Laponite aggregate in benzyl alcohol solvent observed through crossed polarisers. The scale bar represents 200 μm.

The elemental content of the particle was assessed using the EDAX spectrometer attached to the scanning electron microscope and found carbon, silicon, magnesium, and oxygen present in the scan area suggesting the presence of CTAB Laponite plates (figure A4.2).

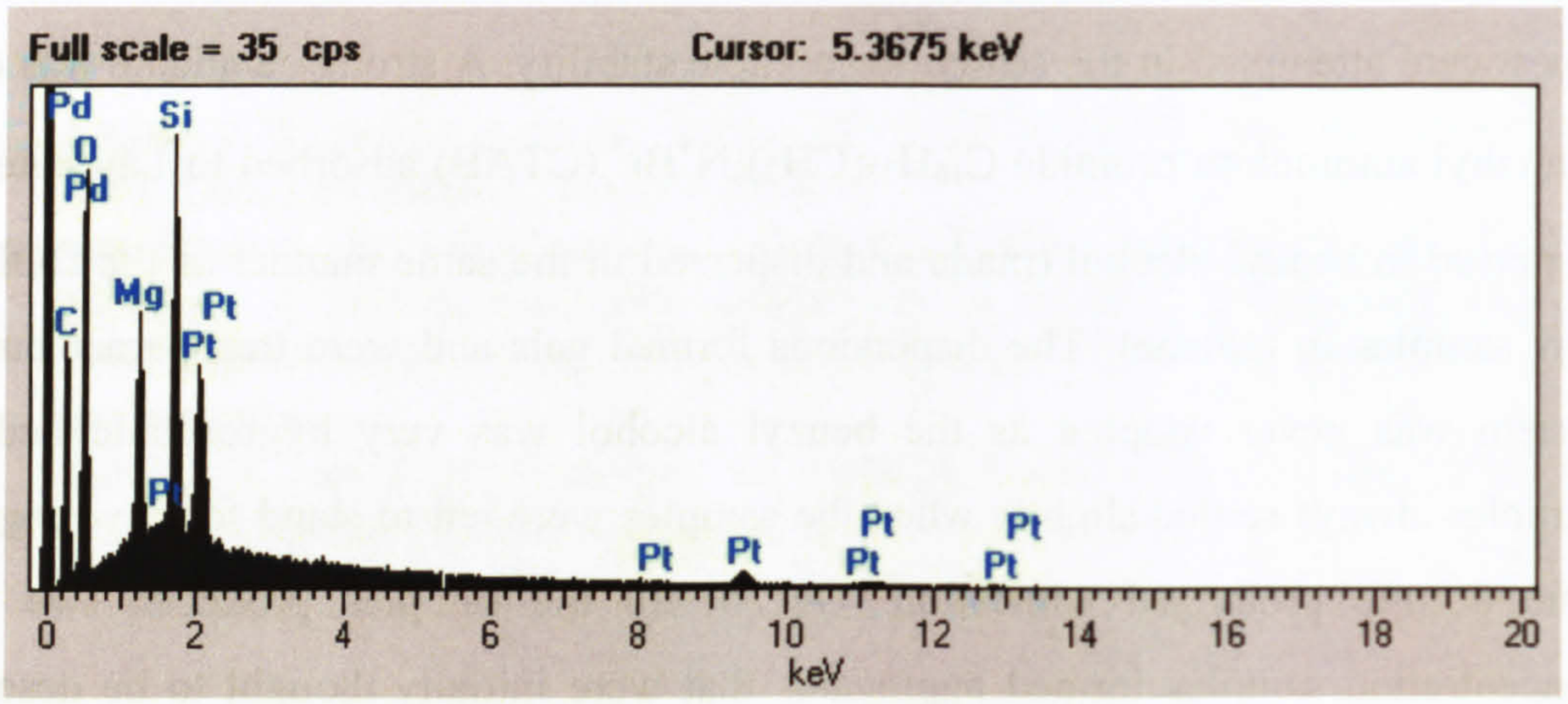

Figure A4.2. EDAX scan of aggregate found in the CTAB Laponite in benzyl alcohol dispersion.

The exact composition of the aggregate was unknown and electron diffraction was attempted but the particle proved too thick for the electron beam to penetrate. All attempts to reproduce the result failed and no other CTAB adsorbed Laponite dispersions in benzyl alcohol ever resulted in such obvious aggregation.